The effects of paternal exposure to cyclophosphamide on the development of cleavage stage embryos

Lisanne Grenier

Department of Pharmacology and Therapeutics

McGill University, Montreal

April 2012

A thesis submitted to McGill University in partial fulfillment for the requirements of the degree of Doctor of Philosophy

Cette thèse est dédicacée à...

… Ma grand-mère, que je regarde comme un modèle, dont j'ose espérer un jour avoir sa volonté d'apprendre et sa persévérance comme inspiration et qui m'a appris à ne jamais laisser tomber et à toujours foncer la tête haute à travers toutes les épreuves

…. Mes parents, que je dois remercier pour m'avoir permis de devenir la personne que je suis présentement et de m'avoir donné les plus beaux des cadeaux, celui de l'amour inconditionnel et d'une éducation universitaire des plus renommées. De plus, je m'engage à garder cette lueur de fierté dans leurs yeux à tout jamais.

… Ma sœur, un modèle de réussite académique ayant tout nouvellement conquis le milieu professionnel. Je te remercie de m'avoir soutenue lorsque j'en avais le plus besoin.

This thesis is dedicated to...

... My grandmother, whom I look up to as a great model and whose thirst for knowledge and perseverance inspired me to never give up and always thrive to the next challenge.

... My parents, whom I must thank for supporting my development into the person that I am now and for giving me the greatest gifts: unconditional love and the greatest university education. I promise to make you proud every step of the way.

... My sister, whom I look up to as a successful academic and professional model. I thank you for being there for me when I needed you the most.

ABSTRACT

Abnormal embryonic development can arise from maternal or paternal exposure to therapeutic agents, environmental toxicants or social habits. Such exposures prior to conception may damage the gametes and have detrimental effects on the developing embryo. When male rats are exposed to the chemotherapeutic agent, cyclophosphamide, the genomic integrity of the male germ cells is altered. The goals of these studies were to determine the impact of paternal preconceptional exposure to cyclophosphamide on embryonic development and to elucidate how cleavage stage embryos respond to DNA damage in the male genome. Paternal exposure to cyclophosphamide induces sperm DNA damage and leads to the alteration of chromatin compaction during spermiogenesis. Exposure to cyclophosphamide alters the rate of sperm decondensation, as manifested by the difference in the number of zygotes within each sperm decondensation stage compared to controls. DNA double strand breaks, detected by γH2AX small and large foci, are enhanced during sperm decondensation, indicative of chromatin remodelling and DNA damage recognition, respectively. The damaged male genome leads to the formation of micronuclei during the first zygotic division and to a gradual developmental delay in cleavage stage embryos. The capacity of cleavage stage embryos to mount an efficient DNA damage response against the damaged male genome prevents the propagation of DNA damage to all blastomeres in subsequent cellular divisions. The activation of DNA damage responses was inappropriate, as indicated by a decrease in PARylation, in the presence of an accumulation of DNA damage in the form of large γH2AX foci in eight-cell embryos sired by cyclophosphamide exposed males. Thus, DNA damage induced by paternal cyclophosphamide exposure is transmitted to the early embryo, altering the progression of developmental events and activating DNA damage responses that are likely to determine embryonic fate. Furthermore, the assessment of the quality of cleavage stage embryos and developmental competence with biomarkers of the DNA damage response, such as γH2AX foci and PAR polymers, may be useful in developmental medicine and infertility clinics.

RÉSUMÉ

Un développement embryonnaire anormal peut être induit par l'exposition maternelle ou paternelle à des produits thérapeutiques, à des produits toxiques présents dans l'environnement ou à des habitudes sociales néfastes. De telles expositions peuvent endommager les gamètes mâtures et avoir des conséquences néfastes sur le développement embryonnaire. Lorsque des rats mâles sont exposés à un agent anticancéreux, la cyclophosphamide, l'intégrité des cellules germinales mâles est modifiée. Le but de ces études était de déterminer les conséquences d'un génome mâle endommagé par la cyclophosphamide sur le développement et les mécanismes de reconnaissance de l'ADN modifié dans des embryons au stade de division cellulaire rapide. L'exposition paternelle à la cyclophosphamide altère l'ADN et la condensation de la chromatine du spermatozoïde durant la spermatogénèse. Par conséquent la progression du spermatozoïde suivant la fertilisation durant les différents stades de la décondensation de la chromatine est affectée puisque les nombres de zygotes observés à chaque stade de décondensation étaient différents entre le groupe contrôle et celui soumis au traitement. Le nombre de cassures de l'ADN double-brin détectées par la méthode de comptage des petits et grands focis γH2AX est augmenté dans le groupe traité aussitôt que la chromatine commence à être décondensée dans les spermatozoïdes, démontrant ainsi un remodelage chromatinien et une altération de l'ADN, respectivement. Lors de la première division du zygote, nous avons observé la formation de micro-noyaux provoquant un retard du développement embryonnaire au stade de division cellulaire rapide. La capacité des embryons à induire une réponse appropriée aux dommages causés à l'ADN des spermatozoïdes durant ces stades de divisions rapides prévient la propagation des dommages à l'ADN d'un blastomère à un autre durant les subséquentes divisions. Les mécanismes de défense normalement activés dans les embryons sont inefficaces puisque le niveau de PARylation ne refléte pas la quantité des dommages causés à l'ADN des spermatozoïdes, tels que démontré par l'accumulation de grands focis γH2AX, dans les embryons à huit cellules fertilisés par des mâles exposés à la cyclophosphamide. Ces résultats démontrent que les

dommages à l'ADN causés par l'exposition paternelle à la cyclophosphamide sont transmis aux embryons ayant des conséquences néfastes sur la progression du développement embryonnaire et l'activation des mécanismes de défenses affectant ainsi leur survie. L'analyse d'embryons au stade de division rapide ainsi que l'utilisation des marqueurs γH2AX et PAR polymère comme marqueurs de qualité embryonnaire et compétence du développement s'avèrent potentiellement utiles dans le domaine de la médecine du développement et en cliniques de fertilité.

TABLE OF CONTENTS

Abstract 3

Résumé 4

Table of Contents 6

List of Figures 13

List of Tables 16

List of Supplementary Figures 17

Format of the Thesis 18

Contributions of Authors 18

Abbreviations 19

Acknowledgements 21

CHAPTER 1: **Introduction**

1.1 Mature Gametes 24

1.1.1 Spermatozoa 24

1.1.1.1 Chromatin Remodeling during Spermiogenesis 24

1.1.1.2 Spermatozoal Epigenetic Programming 25

1.1.1.3 Contribution of the Spermatozoon to the Zygote 26

1.1.2 Oocyte 28

1.1.2.1 Oocyte Epigenetic Programming 28

1.1.2.2 Contribution of the Oocyte to the Zygote 29

1.2 Fertilization 30

1.2.1 Sperm-Egg Binding 30

1.2.1.1 Capacitation 30

1.2.1.2 Acrosome Reaction 31

1.2.1.3 Cortical Reaction 31

1.2.2 Pre-Pronuclear Zygote 32

1.2.2.1 Oocyte Activation 32

1.2.2.2 Spermatozoal Chromatin Decondensation and Remodeling 32

1.2.3 Pronuclear Zygote 36

1.2.3.1 DNA replication 36

1.2.3.2 Transcription 37

1.2.4 Zygotic Epigenetic Reprogramming 40

1.3 Cleavage Stage Embryos 41

1.3.1 The Two-Cell Embryo 41

1.3.1.1 DNA Replication and Transcription 42

1.3.1.2 Roles of the Major Zygotic Genome Activation 42

1.3.2 Four- to Eight-Cell Embryos 43

1.3.3 Epigenetic Reprogramming in Cleavage Stage Embryos 43

1.4 Paternal Exposure to Toxicants 44

1.4.1 Environmental and Occupational Exposures 45

1.4.1.1 Metal Exposure 45

1.4.1.2 Air Pollution 46

1.4.1.3 Endocrine Disruptors 46

1.4.2 Lifestyle Factors 48

1.4.2.1 Alcohol Consumption 48

1.4.2.2 Food Consumption 49

1.4.2.3 Cigarette Smoking 49

1.4.2.4 Recreational Use of Illicit Drugs 50

1.4.3 Therapeutic and Chemotherapeutic Exposures 51

1.5 Cyclophosphamide 53

1.5.1 Pharmacokinetics 53

1.5.2 Human Relevance 58

1.5.3 Spermatozoal Toxicities 58

1.5.4 Male-Mediated Developmental Toxicities of CPA 62

1.6 DNA Damage Responses, DDR 63

1.6.1 DNA Damage 64

1.6.1.1 Micronuclei 64

1.6.1.1.1 Mechanisms of Formation 64

1.6.1.1.2 Impact on Cellular Fate 65

1.6.2 Chromatin Relaxation 68

1.6.3 DNA Repair Pathways 69

1.6.3.1 Phosphorylation of H2AX, γH2AX 69

1.6.3.2 Poly (ADP-ribose) Polymerase 1, PARP1 72

1.6.3.3 P53 Binding Protein 1, 53BP1 76

1.6.4 Spermatozoon DNA Damage Responses, DDR 76

1.6.5 Oocyte DNA Damage Responses, DDR 82

1.6.6 Embryo DNA Damage Responses, DDR 82

1.6.6.1 DNA Repair 82

1.6.6.2 Mitochondrial Activity 84

1.7 Rationale for Thesis Studies 85

1.8 Formulation of the Project 86

REFERENCES 88

CHAPTER II: Paternal Exposure to Cyclophosphamide Affects the Progression of Sperm Chromatin Decondensation and Activates a DNA Damage Response in the Prepronuclear Rat Zygote

Abstract 116

Introduction 117

Materials and Methods 119

Results 124

Discussion 131

Acknowledgements.....135

References 136

Connecting Text from Chapter II to III 160

CHAPTER III: Paternal cyclophosphamide exposure induces the formation of functional micronuclei during the first zygotic division

Abstract 162

Introduction 163

Materials and Methods 164

Results 169

Discussion 173

Acknowledgements 177

References 178

Connecting Text from Chapter III to IV 198

CHAPTER IV: The Activation of DNA Damage Detection and Repair Responses in Cleavage Stage Rat Embryos by a Damaged Paternal Genome

Abstract 200

Introduction 201

Materials and Methods 204

Results 210

Discussion 215

Acknowledgements 220

References 221

CHAPTER V: Discussion

5.1 A DNA Damaged Paternal Genome and its Contribution to the Zygote 246

5.2 The Acquisition and Activation of DNA Damage Responses during the Development of Cleavage Stage Embryos 246

5.3 The Incidence of Micronuclei in Cleavage Stage Embryos; a Cell Death Sentence? 249

5.4 Assisted Reproduction Techniques, ARTs 253

5.4.1 Increased Use of ARTs and their Safety 253

5.4.2 Sperm Selection Methods 254

5.4.3 Preimplantation Genetic Diagnosis, PGD 259

5.4.3.1 Embryo Biopsy 259

5.4.3.2 Embryo Selection Methods 261

5.5 Significance, Implication and Relevance of the Project to ARTs Outcomes 262

5.6 The Possible Existence of a Block to Apoptosis in Cleavage Stage Embryos 263

5.6.1 Apoptotic Block at the level of Mitochondria 264

5.6.2 Apoptotic Block at the Epigenetic Level 265

5.7 Future Directions 266

ORIGINAL CONTRIBUTIONS 268

REFERENCES 271

LIST OF FIGURES

Chapter 1:

Figure 1.1 Pre-pronuclear developmental events following fertilization …..34

Figure 1.2 DNA replication and transcription in cleavage stage embryos 38

Figure 1.3 Cyclophosphamide activation and detoxification pathways 56

Figure 1.4 Cyclophosphamide as a model for male-mediated developmental toxicity studies ……..60

Figure 1.5 DNA damage responses 66

Figure 1.6 The detection of DNA double strand breaks by γH2AX 70

Figure 1.7 PARP activity is a measure of DNA damage, repair and energy status 74

Figure 1.8 P53 binding protein 1 as a mediator of DNA DSB damage 78

Chapter 2:

Figure 2.1 Types of paternal nuclei observed in early postfertilization zygotes 140

Figure 2.2 The distribution of types of paternal nuclei in early pre-PN zygotes 142

Figure 2.3 Quantitative analysis of the initial appearance, progression, and pattern of H4K12ac staining intensity on the paternal chromatin for all sperm decondensation stages of pre-PN zygotes 144

Figure 2.4 Quantitative analysis of the initial appearance, progression, and pattern of histone H3 phosphorylated at serine 10, H3S10ph, on the decondensing paternal nuclei in pre-PN zygotes 146

Figure 2.5 The appearance and distribution of γH2AX foci on the decondensing sperm chromatin is altered in decondensing sperm nuclei after CPA exposure 148

Figure 2.6 Quantitative analysis of the average number of small (Top panel) and large (Bottom panel) γH2AX foci per sperm per male for all sperm decondensation stages 150

Chapter 3:

Figure 3.1 In vitro timing of the first zygotic division …….184

Figure 3.2 In vivo progression of early cell cleavage stage embryos ……..186

Figure 3.3 The incidence of micronuclei in cell cleavage embryos ……188

Figure 3.4 Nuclear and micronuclear (MN) chromatin compaction in early cleavage stage embryos ……..190

Figure 3.5 Parental origin of micronuclear chromatin in early cell cleavage embryos fertilized by CPA exposed males …….192

Figure 3.6 Micronuclear membrane characterization in early cell cleavage embryos fertilized by CPA exposed spermatozoa ……..194

Figure 3.7 DNA replication in the micronuclei of CPA sired embryos 196

Chapter 4:

Figure 4.1 Distribution of MitoTracker probes in cleavage stage embryos .226

Figure 4.2 γH2AX detection of DNA double strand breaks in cleavage stage embryos 228

Figure 4.3 Large γH2AX foci as sites of DNA damage in cyclophosphamide-sired 8-cell embryos 230

Figure 4.4 53BP1 reactivity in cleavage stage embryos ……..232

Figure 4.5 Poly(ADP-ribose) (PAR) polymer reactivity in cleavage stage embryos ……..234

Chapter 5:

Figure 5.1 Reproductive medicine relevance of the CPA male-mediated developmental toxicity model 256

LIST OF TABLES

Chapter 2:

Table 2.1 Quantification of the pattern of deposition of modified histones H4K12ac and H3S10ph in all sperm decondensation stages 152

SUPPLEMENTAL FIGURES

Chapter 2:

Suppl. Figure 2.1 The pattern of H4k12ac staining on the maternal nucleus and polar body of pre-pronuclear zygotes 154

Suppl. Figure 2.2 The pattern of H3S10ph staining on the maternal nucleus and polar body of pre-pronuclear zygotes 156

Suppl. Figure 2.3 The pattern of γH2AX staining on the maternal nucleus and polar body of pre-pronuclear zygotes 158

Chapter 4:

Suppl. Figure 4.1 Quantification of mitochondrial selective MitoSox probes in cleavage stage embryos 236

Suppl. Figure 4.2 The presence of micronuclei (MN) and the rate of embryonic development had no impact on the detection of δH2AX foci, marking DNA double strand breaks 238

Suppl. Figure 4.3 The presence of micronuclei (MN) and the rate of embryonic development had no impact on the nuclear localization of 53BP1 240

Suppl. Figure 4.4 The presence of micronuclei (MN) and the rate of embryonic development had no impact on the nuclear localization of Poly(ADP-ribose) polymers (PAR) 242

FORMAT OF THE THESIS

This thesis is composed of five chapters. The first chapter is the introduction in which subjects such as developmental events, epigenetic and DNA damage responses are reviewed for mature spermatozoa, oocytes and cleavage stage embryos. It also contains a section on the different types of paternal exposures, including the model drug cyclophosphamide, and their effects on spermatozoa and their consequences to early embryos. Chapter 1 concludes with the rationale, objectives, experimental model, protocols and principal findings of this work. The next three chapters are in the format of the manuscripts that were submitted for publication. Chapter II is available in *Biology of Reproduction*; 83(2): 195-204, 2010. Chapter III is available in *PLoS One*; the advance access paper was published on November 16, 2011 (doi:10.1371/journal.pone.0027600: PMID: 22110683). Chapter IV is available in *Toxicological Science*; the advance access paper was published on March 27, 2012 (doi:10.1093/toxsci/kfs120: PMID: 22454429). Between each chapter there is a connecting text linking every section for better understanding of the research progression, in accordance with the Thesis Preparation and Submission Guidelines for a Manuscript-based thesis. Chapter V is the discussion of the significance, implications and relevance of this research work to the fields of developmental toxicology and reproductive medicine, followed by a list of original contributions.

CONTRIBUTIONS OF AUTHORS

For chapters II, III and IV, all the experiments were done by the candidate under the supervision of Dr. Barbara Hales and Dr. Bernard Robaire.

ABBREVIATIONS

53BP1	p53 binding protein 1
ADP	Adenosine diphosphate
ART	Assisted reproduction technique
ATM	Ataxia telangiectasia mutated
ATP	Adenosine triphosphate
BER	Base excision repair
BRCA1	Breast cancer type 1 susceptibility protein
BrUTP	5-Bromouridine 5'-triphosphate
COMET	Single cell gel electrophoresis assay
CPA	Cyclophosphamide
DEHP	Bis(2-ethylhexyl)phthalate
DDR	DNA damage response
DNA	Deoxyribonucleic acid
DNMT1	DNA methyl transferase 1
DSB	Double strand break
EdU	5-ethynyl-2´-deoxyuridine
GSH	Glutathione
Gy	Gray unit
ICSI	Intra-cytoplasmic sperm injection
IVF	*In vitro* fertilization

MDM2	Murine double minute 2
MDMX	Murine double minute X
MMR	Mismatch repair
MRN	Mre11, Rad50, Nsb1 complex (Meiotic recombination 11, Recombinational DNA repair 50, Nibrin 1)
NADH	Nicotinamide adenine dinucleotide
NER	Nucleotide excision repair
MII	Meiosis II
MN	Micronucleus
PAR	Poly(ADP-ribose)
PARG	Poly(ADP-ribose) glycosylase
PARP-1	Poly(ADP-ribose) polymerase 1
PGD	Preimplantation genetic diagnosis
PGS	Preimplantation genetic screening
PN	Pronucleus
Pre-PN	Pre-pronucleus
RNF8	RING finger protein 8
SSB	Single strand break
ZGA	Zygotic genome activation

ACKNOWLEDGEMENTS

I should thank my supervisors, **Dr. Barbara Hales** and **Dr. Bernard Robaire,** for giving me the opportunity to become a scientist and for always believing in me. On a more personal note, I would like to thank Dr. Hales for her valuable guidance and constant presence and Dr. Robaire for his challenging vision and motivational discussion.

I would like to thank the members of my committee, my advisors', **Dr. Derek Bowie** and **Dr. Daniel Bernard**, for keeping me on track and focusing on the relevance of my work, i.e. the big picture, to **Dr. Hugh Clarke** for his specialized discussion on early embryonic development, and to **Dr. Asangla Ao** for her helpful discussion on the impact of micronuclei and clinical implications of my work. Thank you all for broadening my research perspectives.

I would like to thank the staff of the Department of Pharmacology and Therapeutics, **Tina Tremblay, Hélène Duplessis and Chantal Gagnon** for your guidance and mental support throughout the years. Thank you for all the work and effort you put every year into the organization of events: we appreciate it!

To **Chunwei Huang**, you are the heartbeat of the lab. The warmness of your presence and smile is comforting and reassuring to us.

To **Dr. Tara Barton** and **Dr. Alexis Codrington** for being my embryo and sperm mentors. My experimental successes were greatly influenced by your individual expertise. I am forever grateful for your dedication.

To **Anne-Marie Downey** for sharing the burden of chronic rat treatment and for helping me with some of my animal work. I really appreciated it!

To **Serena Banh** for helping me with some of my animal work and allowing me to have a day of rest per week, I am forever thankful! You are one hard working student. I wish you good luck in all your endeavours!

To my dearest friends: **Ava Schlisser** and **Dr. Michelle Carroll**. Ava, for your perfectionism and for all the helpful discussion about work and life related issues. I will always remember us playing tricks on April Fools, and celebrating birthdays and Christmas parties. Michelle, for your strong personality, laughter and joy to be around; you are one of the most loving and caring person I know. Thank you both for your great moral support and, most importantly, for all the good times we spent together.

To **Dr. Géraldine Delbès**, **Dr. Sheila Ernest** and **Dr. Claudia Lalancette** for being great friends, for all the laughter, snowboarding trips, walks to the train and football games. Thank you for your specialized advice and helpful discussions throughout the years.

To all the past and present lab members, Huge, Caroline, Victoria, France-Hélène, Thomas, Elise, Catriona, Maselli, Rob, Pavine, Elsa, Nazem, and Trang. Ground floor scientists, you guys rock!

CHAPTER 1

INTRODUCTION

1.1 Mature Gametes

1.1.1 Spermatozoa

Spermatogenesis is a highly specialized process leading to the formation of mature male gametes, spermatozoa, in the testes. Spermatogenesis starts at the basement membrane of the seminiferous tubules where spermatogonia, the most immature sperm cells, undergo multiple mitotic divisions; this is called the proliferative phase or the pre-meiotic phase (Huckins, 1971). During the pre-meiotic proliferative phase, spermatogonia divide and become spermatocytes, moving from the basement membrane towards the lumen of the seminiferous tubules of the testes. Spermatocytes duplicate their genome and undergo two meiotic divisions, becoming haploid spermatids (Handel et al., 1999). During the post-meiotic spermiogenesis phase, haploid spermatids undergo complex nuclear chromatin remodeling and cytoplasmic reorganization events, leading to the formation and the release of flagellated spermatozoa in the lumen of seminiferous tubules of the testes (D'Occhio et al., 2007). Spermiation is the release of immotile flagellated spermatozoa into the lumen of seminiferous tubules of the testes (Fawcett, 1975). Spermatozoa acquire motility and the ability to fertilize oocytes during their passage through the epididymis and the male and female reproductive tract.

1.1.1.1 Chromatin Remodeling during Spermiogenesis

During spermatogenesis the chromatin packaging of spermatozoa must undergo numerous nuclear changes and chromatin remodelling steps to be able to fertilize an oocyte. From the most immature spermatogonia to the round spermatids, the chromatin is wrapped around nucleosomes formed by histone octamers of protein dimers of H2A and H2B, H3 and H4, linked with H1 and associated with histone variants (D'Occhio et al 2007). During spermiogenesis, these histones are post-translationally modified, forming elongating spermatids; during this process the chromatin structure is opened up, allowing the replacement of the majority of histones with transition proteins. These transition proteins are

then removed and replaced with highly basic protamines. These protamines condense the chromatin structure of mature spermatozoa into a doughnut structure or toroid conformation (Balhorn et al., 1977; Ward, 2010). Protamines constitute the principal protein in nuclei of spermatozoa; core histones, sperm specific histone variants and noncoding RNAs are also present (D'Occhio et al 2007). The extent of histone replacement by protamines is species specific; mouse spermatozoa retain 1% of their histones (Balhorn et al., 1977) while human spermatozoa retain an average of 15% (Gatewood et al., 1990). Following the completion of spermatogenesis and the release of spermatozoa into the lumen of the testis, the maturation of spermatozoa continues in the epididymis. Spermatozoa complete their chromatin compaction with the formation of disulfide cross-links between cysteine residues in protamine.

1.1.1.2 Spermatozoal Epigenetic Programming

DNA methylation and post-translational histone modifications, including acetylation, methylation, phosphorylation, ubiquitination, and PARylation on the N-terminal tails of histones, dictate the chromatin compaction state. This combination of epigenetic marks regulates gene expression, DNA synthesis, transcription, DNA damage responses and embryonic developmental progression. Chromatin in a transcriptionally active open structure called euchromatin is enriched with lysine acetylation marks on histones H3 and H4 and methylation marks on lysine 4 of histone H3 and hypomethylated DNA (Barski et al., 2007; Guenther et al., 2007). Alternatively, chromatin can be condensed in a transcriptionally repressive structure called heterochromatin, enriched with methylation marks on histone H3 lysine 9 and hypermethylated DNA (Pokholok et al., 2005; Vakoc et al., 2006; Barski et al., 2007; Peng & Karpen 2008). Epigenetic 'mistakes' in DNA methylation and histone post-translational modifications can have great impact on the normal development of the embryo (Hales et al., 2011).

The genome of spermatozoa is heavily methylated in repeated regions and in paternally imprinted genes (Adams et al., 1983) while promoter regions

involved in embryo development, such as the HOX genes, are hypomethylated. Hypomethylated DNA regions are usually associated with histone rich chromatin regions in the nuclei of spermatozoa (Hammoud et al., 2009), while key promoter regulators of pluripotency, such as Sprouty and Nanog, are hypermethylated (Farthing et al., 2008).

The retained, modified, active histone H3K4me3 mark is localized to paternally expressed imprinted loci, micro RNA clusters, and HOX genes, whereas the repressive histone H3K27me3 mark is localized to promoter regions repressed in early embryos (Hammoud et al., 2009; Hales et al., 2011). In addition to the presence of post-translationally modified histones in nuclei of spermatozoa, all core histones, H2A, H2B, H3 and H4, are detected in murine and human spermatozoa (Gatewood et al., 1987; Pittoggi et al., 1999). Histone variants, H2AX, H3.3 and H2Az (Rangasamy et al., 2003; Li et al., 2006; van der Heijden et al., 2008), as well as sperm specific histone variants, tH2B, H2AL1, H2AL2, and H2BL1 (Churikov et al., 2004b; Govin et al., 2007), are all essential contributors to the spermatozoal epigenome (Santenard and Torres-Padilla, 2009).

1.1.1.3 Contribution of the Spermatozoon to the Zygote

The contributions of the mammalian spermatozoon to the zygote include the paternal haploid genome, the sperm centriole essential for the zygotic organization of the mitotic spindle, a phospholipase activating factor critical for the sperm entry into the ooplasm and egg activation, and sperm specific mRNA as well as non coding RNAs.

In addition to the DNA itself, the spermatozoal haploid genome contains three essential structural components (Ward, 2010). The first and most abundant chromatin structural components of the spermatozoon are the protamines (Hud et al., 1995). Two properties of protamines confer to the spermatozoon a unique, highly compacted toroid structure: the positively charged arginine residues neutralize the negatively charged DNA (Balhorn, 1982) and the addition of disulfide cross-links between cysteine residues as the spermatozoon travels

through the epididymis (Perreault and Zirkin, 1982). Chromatin compaction with protamines protects the spermatozoon during fertilization (Ogura et al., 1994; Kuretake et al., 1996).

The second structural chromatin components of the spermatozoon are the histones (Adenot et al., 1997; Pittoggi et al., 1999; Gineitis et al., 2000; Churikov et al., 2004a; Hammoud et al., 2009). Spermatozoal histones are distributed throughout the sperm genome and associated with the promoters regulating gene expression during spermiogenesis (Martins and Krawetz, 2005; Ostermeier et al., 2005) and early embryonic development (Arpanachi et al., 2009; Hammoud et al., 2009). Following fertilization, these sperm specific histones are transmitted to the newly fertilized oocyte, providing a paternal epigenetic signature to the early embryo (van der Heijden et al., 2006; van der Heijden et al., 2008). Upon the completion of spermatogenesis and the early development of the embryo, the histone enriched chromatin regions of the spermatozoon are more susceptible to DNA damage since they are less condensed than protamine-bound DNA.

The third mammalian chromatin structural components are the matrix attachment regions distributed throughout the male genome (Nadel et al., 1995; Martins et al., 2004). The matrix attachment regions organize the spermatozoon chromatin into functional loops of DNA that are attached to the sperm nuclear matrix. These spermatozoal matrix attachment regions are histone-bound chromatin enriched regions (Arpanachi et al., 2009) required for paternal pronuclear DNA replication and important for the regulation of gene expression during preimplantation development (Shaman et al., 2007; Yamauchi et al., 2007a; 2007b; Arpanachi et al., 2009; Hammoud et al., 2009).

Recent findings have reported the spermatozoal contribution of mRNAs and non-coding RNAs in addition to protamines, histones and matrix attachment regions to the zygote. There are at least 3500 individual mRNA species, fully processed in ejaculated spermatozoa. The absence of rRNA and the rest of the translational machinery in spermatozoa prevent mRNA translation de novo in male germ cells (Miller et al., 2007). These spermatozoal mRNAs may function to

regulate the retention and location of sperm specific histones and chromatin remodelling during spermiogenesis. Once inside the fertilized oocyte, spermatozoa mRNA may regulate the remodelling of the paternal genome and epigenetic reprogramming. The mRNAs and non-coding RNAs of ejaculated spermatozoa may provide us with important information on sperm quality and motility as a molecular resource for infertility. A loss of motility appears to correlate with a change in the relative quantity of particular mRNA species (Miller et al., 2007). In addition, the expression profile of these mRNAs may provide us with crucial information on the potential toxic effects of chemicals or environmental agents on spermatogenesis.

1.1.2 Oocyte

Before birth, the female primordial germ cells undergo a few mitotic cycles and become arrested at prophase I of meiosis I as diploid primary oocytes. Upon stimulation, the diploid primary oocyte reinitiates and completes meiosis I, expulses the first polar body and becomes the diploid secondary oocyte. The secondary oocyte initiates meiosis II and is arrested at metaphase II until fertilization. During ovulation, the arrested secondary oocyte is released from the ovary and fertilized by a mature spermatozoon. Fertilization leads to the expulsion of the second polar body and the formation of the mature haploid ovum (Borum, 1967).

1.1.2.1 Oocyte Epigenetic Programming

Information on the methylation status of promoters in mature oocytes is more limited. Similar to spermatozoa, maternally imprinted genes and repeat elements are heavily methylated (Rivera, 2010). The promoter regions of pluripotent-related genes are generally methylated to a lesser extent in mature oocytes than in spermatozoa (Lan et al., 2010).

The mature oocyte expresses all four core histones, H2A, H2B, H3, and H4; most post-translationally modified histones and histone variants are stored as maternal mRNAs in the ooplasm and translated when required in the embryo

(Arnold et al., 2008). Stem loop binding protein is responsible for the regulation of histone H3 and H4 mRNA accumulation during oocyte maturation and is responsible for histone mRNA translation following fertilization (Allard et al., 2005; Arnold et al., 2008). The presence of transcriptionally repressive histone H3K9me in mature oocytes protects the maternal genome in early embryos against histone demethylation (Morgan et al., 2005; Santos et al., 2005). Enzymes involved in the post-translational modification of histones, such as histone deacetylase and histone methyltransferases, are expressed in a time regulated fashion to reset the epigenome during oogenesis and early embryonic development (Akiyama et al., 2004; Sarmento et al., 2004; De la Fuente, 2006).

The incorporation of histone variant H3.3 into the mature oocyte chromatin occurs in transcriptionally active regions during oogenesis and is strictly a maternally inherited histone mark in the early zygote (Akiyama et al., 2011). The presence of histone variant macroH2A (Chang et al., 2005) and oocyte specific histone variant H1fOO (Tanaka et al., 2003; Gao et al., 2004) is also important in the normal development of the early embryo up to the two-cell stage.

The epigenome of mature male and female gametes contains extensive epigenetic asymmetries that are essential for the establishment of gender specific imprinting marks and gene expression during early embryonic development.

1.1.2.2 Contribution of the Oocyte to the Zygote

The ultimate "goal" of the oocyte during maturation is to become a highly differentiated mature metaphase II oocyte capable of supporting normal embryonic development until the zygotic genome activation (ZGA). During the oocyte growth phase, numerous morphological and biochemical changes must occur in both the cytoplasm and the nucleus for the fully grown oocyte to respond to hormonal signals and mature to metaphase II (Fulka et al., 1998).

As the oocyte grows, the cytoplasmic structural changes consist of the accumulation of mitochondria and ribosomes, and growth of the Golgi complex. The nuclear structural changes consist of nucleolar compaction (Chouinard 1975),

an intense period of synthesis of RNAs, chromatin modification (Albertini, 1992), and the preparation of centrosome/microtubule organizing centres. In addition, hormonal influences from gonadotrophins, growth factors, estrogen and leptin, lead to nuclear and cytoplasmic morphological changes promoting oocyte maturation (Assey et al., 1994; Cioffi et al., 1997).

Simultaneously, during the growth phase of the oocyte, biochemical changes consist of the storage of specific mRNAs as ribonucleo-protein particles in the cytoplasm to protect against degradation until the completion of oogenesis or fertilization events (Spirin, 1994). The second important biochemical change is the acquisition of meiotic competence by the synthesis and accumulation of central cell cycle regulatory molecules, $p34^{cdc2}$ and cyclin B, both necessary for the induction of germinal vesicle breakdown (de Vantery et al. 1997).

1.2 Fertilization

Fertilization is the fusion of a mature male gamete, the spermatozoon, with a mature female gamete, the oocyte, giving rise to the development of an embryo. Fertilization is comprised of a chain of molecular events preparing the spermatozoon for efficient sperm-egg binding and penetration.

1.2.1 Sperm-Egg Binding

The sequential events leading to successful fertilization are the spermatozoal capacitation and the acrosome reaction followed by the oocyte cortical reaction and polyspermic block. For successful sperm-egg binding to occur, multiple receptor-ligands interactions are required.

1.2.1.1 Capacitation

For successful fertilization to occur a mature spermatozoon must first acquire motility and competence to fertilize an oocyte in the epididymis, a process called capacitation, as reported in Iwamatsu and Chang, 1970 and reviewed in de Lamirande & O'Flaherty, 2008. The plasma membrane of the spermatozoon is

reorganized by the fertilization promoting peptide produced by the prostate and released into the seminal fluid during ejaculation. In addition, enzymes secreted in the uterus, such as sterol binding albumin, lipoproteins, proteolytic and glycosidase enzymes, further reorganize the plasma membrane of the spermatozoon. The changes in the spermatozoal plasma membrane activate pathways leading to loss of cholesterol and changes in the phosphorylation of numerous proteins, making the spermatozoal acrosomal membrane permeable to Ca^{2+} influx. The reorganization of the spermatozoal plasma membrane hyperactivates the spermatozoon and increases the spermatozoal binding efficacy to oocyte zona pellucida glycoproteins.

1.2.1.2 Acrosome Reaction

The sperm-egg recognition depends on the binding and cleavage status of ZP2 and ZP3 glycoproteins on the zona pellucida to initiate the acrosome reaction, as reported in Gahlay et al., 2010 and reviewed in Gupta and Bhandari, 2011 and Yanagimachi, 2011. The binding of the spermatozoon to the glycoprotein receptor ZP3 leads to the fusion of the sperm membrane with the outer acrosomal membrane, releasing the enzymatic content of the acrosome on the surrounding of the oocyte extracellular matrix. The release of the sperm acrosome enzymes leads to the digestion of the zona pellucida, allowing the penetration of a single spermatozoon into the perivitelline space.

1.2.1.3 Cortical Reaction

Following the fusion of the spermatozoon and the oocyte, the spermatozoal cytoplasmic phospholipase C zeta content is released inside the oocyte and initiates the cortical reaction. The cortical reaction consists of the activation of the inositol phosphate cascade, which promotes the movement of cortical granules into the oocyte perivitelline space (Sun, 2003). The movement of cortical granules is mediated by GTP-binding protein, activating inositol 1,4,5 triphosphate, causing the release of Ca^{2+} and diacylglycerol activating protein kinase C from intracellular stores. Cortical granules release proteases and

peroxidases which cleave the terminal sugars of glycoprotein receptors on the zona pellucida, removing other bound spermatozoa (Burkart et al., 2012). The cortical reaction modifies the sperm egg binding receptor and hardens the zona pellucida, thus activating the polyspermic block. The polyspermic block is a safety mechanism preventing the penetration and fertilization of the oocyte by multiple spermatozoa, thus preventing embryonic death.

1.2.2 Pre-Pronuclear Zygote

The pre-pronuclear zygotic development is a very short event during which major spermatozoal and oocyte chromatin remodeling events occur.

1.2.2.1 Oocyte Activation

The entry of the spermatozoon triggers a calcium influx inside the fertilized oocyte, activating protein kinase C to reactivate the mature oocyte arrested at metaphase II to complete its second meiotic division (Akabane et al., 2007; Yu et al., 2008). The completion of the second meiotic division leads to the expulsion of the second polar body. Early post-fertilization events are governed by maternally accumulated and stored proteins during oogenesis.

1.2.2.2 Spermatozoal Chromatin Decondensation and Remodeling

Major chromatin reorganization and reprogramming events occur in both the maternal and paternal genomes following fertilization, during zygotic pre-pronuclear formation (Figure 1.1) (Van der Heijden et al., 2006). The spermatozoal chromatin structure is tightly compacted by protamines cross-linked by disulphide bonds and sperm specific histones, surrounded by the peri-nuclear theca membrane. Once the spermatozoal nuclear membrane is degraded, the spermatozoal chromatin undergoes major chromatin decondensation and remodelling, starting with the reduction of inter-protamine sulfhydryl bonds by glutathione (Perreault et al., 1988). Simultaneously, cysteine protease degrades sperm-specific protamines while histone cell cycle regulation defective homolog

A and nucleoplasmin chaperone proteins assemble nucleosomes onto the remodeling paternal chromatin (Leno et al., 1996; Loppin et al., 2005). Noncoding RNAs are also thought to play a role during spermatozoal chromatin remodelling as regulators of epigenetic deposition marks (Mattick et al., 2009; Hales et al., 2011).

In pre-pronuclear zygotes, there are four sequential stages of mouse sperm chromatin decondensation (Figure 1.1) (van der Heijden et al., 2005). As the spermatozoon chromatin decondenses, it acquires maternally provided post-translationally modified histones. The first stage of mouse sperm decondensation is the condensed sperm nuclei enriched with protamines. Protamines are gradually replaced with maternal histones in the partially decondensed type *a* sperm nucleus. Totally decondensed type *b* and recondensing type *c* sperm nuclei are the third and fourth stages of sperm decondensation, enriched with maternally provided histones. Simultaneously, the fertilized oocyte completes its second meiotic division. The equivalent developmental stage of the oocyte to the type *a* sperm nucleus is metaphase II, while type *b* and *c* sperm nuclei are anaphase II and telophase II, respectively. Sperm chromatin is re-packaged into somatic cell like chromatin by replacing all sperm-specific protamines with somatic histones, forming the male pronucleus (PN).

Figure 1.1. Pre-pronuclear developmental events following fertilization. Fertilization reactivates meiosis II in mature arrested oocytes. The maternal stored proteins first decondense the paternal chromatin by replacing all sperm specific protamines, except sperm histone variants, with maternally provided histones. These events are called spermatozoon chromatin decondensation and remodeling. Following the completion of the protein exchange, the paternal chromatin recondenses into the pronucleus followed by the formation of the maternal pronucleus. Adapted from McLay and Clarke, (2003) Reproduction 125:625-633 and Hales et al., (2011). Birth Defects Research A Clin Mol Teratol. 91, 652-665.

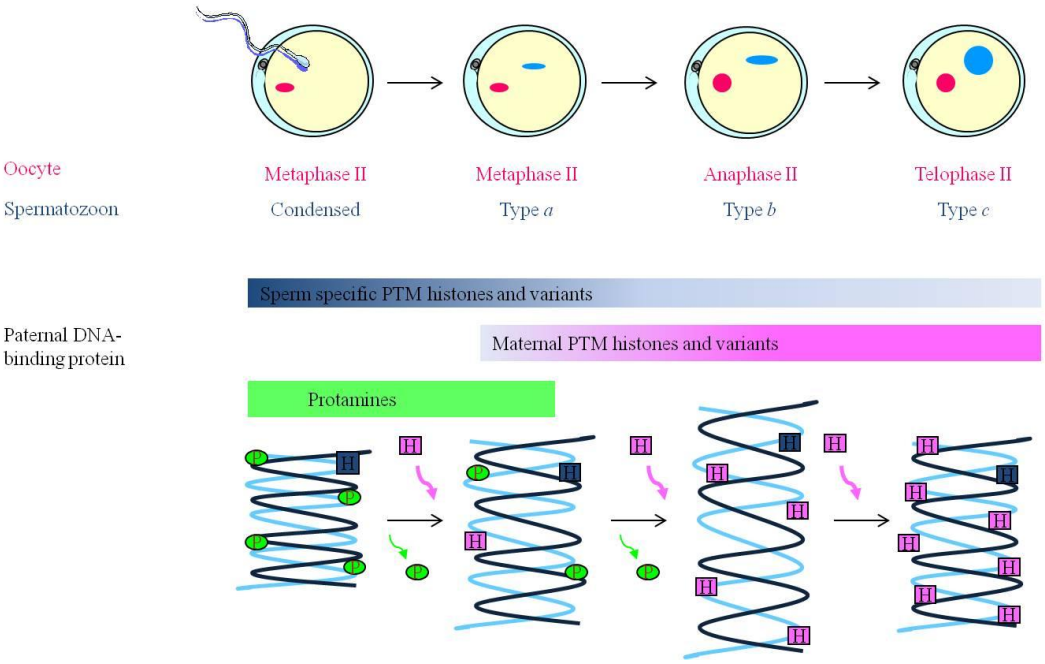
Oocyte
Spermatozoon
Metaphase II
Condensed
Metaphase II
Type a
Anaphase II
Type b
Telophase II
Type c
Paternal DNA-binding protein
Sperm specific PTM histones and variants
Maternal PTM histones and variants
Protamines
H
P

1.2.3 Pronuclear Zygote

The classification of pronuclear stages is based on the cytoplasmic distance between the parental pronuclei (PNs) and on the morphology of the paternal PN (Zollner et al., 2003). Microtubule networks organized by the egg cytoplasmic asters pull both parental PNs toward each other as they progress from PN1 through PN5, regulating the distance between them (Schatten et al., 1985; Schatten et al., 1986). Microtubule networks are also important in the trafficking of nuclear proteins between the two parental genomes, known as pronuclear cross-talk (Sun et al., 1999). Small parental PNs with a large nucleolus within the paternal PN correspond to PN1 and PN2. Parental PNs with double the PN1 pronuclear size, 1 large nucleolus and a few smaller nucleoli within the paternal PN correspond to PN3. Parental PNs with three to four times the PN1 pronuclear size and multiple nucleoli within the paternal PN correspond to PN4 and PN5. The male PN can be easily differentiated from the female PN by its larger pronuclear size and the occasional presence of the flagellum near or still attached to the male PN (Adenot et al., 1997; Santos et al., 2002; Barton et al., 2005). The enriched presence of chromatin remodelling activity on the pre-PN paternal recondensing chromatin leads to the formation of the paternal PN prior to the maternal PN. At the end of the pronuclear stages, the parental pronuclear envelope breaks down (Osada et al., 2010) and the male and female genomes mingle at syngamy before the first zygotic division.

1.2.3.1 DNA Replication

The pronuclear zygote at PN1 and PN2 represents the G1 phase of mitosis during which the parental chromatin condenses and prepares for the first wave of DNA synthesis during the S phase of the PN3 zygote (Figure 1.2). The paternal PN starts synthesizing DNA earlier compared to the maternal PN, probably due to the enriched presence of chromatin remodeling activity and epigenetic marks on the paternal PN. PN4 and PN5 zygotes correspond to the G2 phase of mitosis, which represents the longest phase of the first zygotic division. At the mitotic M phase of syngamy, the zygote divides to the two-cell stage (Adenot et al., 1997).

In rodents, the first cycle of mitosis takes approximately 20 hours following fertilization. The first round of DNA replication is essential for the initial reprogramming of gene expression, allowing maternally-derived transcription factors to gain access to their DNA binding sequences before the formation of transcriptionally repressive nucleosomes in subsequent embryonic developmental stages (Wolffe, 1991; Felsenfeld, 1992).

1.2.3.2 Transcription

At the pronuclear phase, numerous factors account for the preferential binding of maternal mRNA transcripts and the initiation of transcription in the male PN before the female PN (Worrad et al., 1994; Bouniol et al., 1995; Schultz, 2002). The principal factor is the difference in parental PN chromatin structure: the chromatin remodelling (der Heijden et al., 2005) and hyperacetylation of histone H4 on the paternal chromatin (Adenot et al., 1997). The second factor is the relaxation of nucleosome structure on the paternal PN prior to that of maternal PN from the initiation of DNA replication and unwinding of DNA strands by the removal of transcriptional inhibition (Aoki et al., 1997; Wolffe and Hayes, 1999).

The pronuclear transcriptional activity catalyzed by RNA polymerase I, II and III (Ram and Schultz, 1993; Nothias et al., 1996) activates the minor wave of zygotic genome activation (ZGA), a switch from maternal to zygotic transcriptional regulation of gene expression (Figure 1.2). As a mechanism of protection against gene dysregulation and unique to this stage, the activation of transcription is uncoupled from translation (Matsumoto et al., 1994; Nothias et al., 1996; Christova and Oelgeschlager, 2002; Schultz, 2002). The retention of transcription factors without the formation of functional transcripts may provide a mechanism marking promoters for earlier detection and enhanced transcription in two-cell embryos.

Figure 1.2. DNA replication and transcription in cleavage stage embryos. DNA replication and transcription are tightly dependent upon each other in pronuclear zygotes and two-cell embryos. DNA replication is initiated first and is more active in the male pronucleus than in the female pronucleus and gradually increases in the next cleavage stage. In pronuclear zygotes, there is a minor zygotic genome activation that necessitates the recruitment and translation of maternal mRNA. The second and major wave of transcriptional activation occurs in late two-cell embryos when the transcriptional switch between the maternal and the zygotic control is activated. Maternal mRNAs are degraded and replaced by newly transcribed zygotic mRNAs. Subsequent to this maternal to zygotic switch, the cleavage stage embryos adopt a repressive epigenome. Adapted from Schultz, (2002). Human Reprod. 8, 323-331.

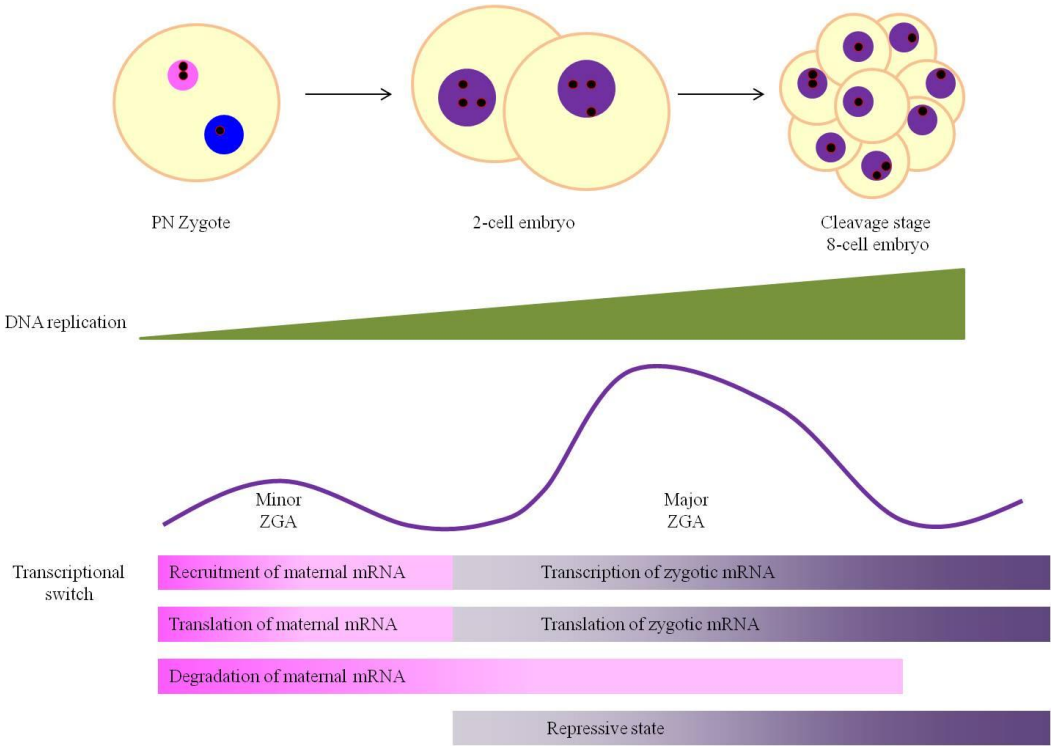
PN Zygote
2-cell embryo
Cleavage stage
8-cell embryo
DNA replication
Minor
ZGA
Major
ZGA
Transcriptional
switch
Recruitment of maternal mRNA
Transcription of zygotic mRNA
Translation of maternal mRNA
Translation of zygotic mRNA
Degradation of maternal mRNA
Repressive state

1.2.4 Zygotic Epigenetic Reprogramming

Following fertilization, the zygote undergoes extensive epigenetic reprogramming; the paternal genome is stripped of its DNA binding proteins and acquires maternally stored epigenetic marks. The paternal genome is globally demethylated (Tokoro et al., 2010) by enzymes (La Salle & Trasler 2006; Chan et al., 2010) and DNA repair proteins (Wossidlo et al., 2010). In contrast the maternal genome remains methylated (Abdalla et al., 2009) due to the presence of murine PGC7/Stella (Nakamura et al., 2007) and methylated histone marks (H3K9me2, H3K9me3, H3K27me3) (Hajkova, 2010). At the two-cell stage, DNA demethylation is initiated in the maternal genome in a replication dependent manner (Haaf, 2006).

The epigenome of the zygote is reprogrammed very early following fertilization and it is thought that the hyperacetylation of histone H4 and histone variants left on the spermatozoon chromatin are involved in zygotic epigenetic reprogramming (Adenot et al., 1997; Santos et al., 2002). The paternal chromatin is remodelled with maternally derived histone H4 and H3 acetylation marks and histone H3 phosphorylated at serine 10 in the pre-pronuclear zygote (van der Heijden et al., 2006). During the zygotic progression through pronuclear stages, the paternal chromatin gradually loses its acetylation marks for monomethyl groups on H3K4me1, H3K9me1, H3K27me1, and H4K20me (Kourmouli et al., 2004; Lepikhov and Walter 2004; van der Heijden et al., 2006) to which di- and tri-methylation groups are added (Santos et al., 2005). The preferential incorporation of open chromatin marks on the paternal PN reflects their roles as regulators of transcriptional activation (Eberharter and Becker, 2002).

Clear epigenetic asymmetry exists between the parental chromatin in the pronuclear zygote; the maternal genome is hypermethylated while the paternal genome is hypomethylated (Lepikhov and Walter, 2004; van der Heijden et al., 2006). The epigenome of the maternal chromatin contains both active acetylated lysine H4 and repressive methylated histone chromatin marks. Histone H3K27me3 and H3K9 methylation are two maternal specific epigenetic marks

until PN3 and the two-cell stage, respectively (Lepikhov and Walter, 2004; Puschendorf et al., 2008). The origin of parental chromatin can be distinguish in two cell embryos since H3K9me3 and H4K20me3 are maternal specific epigenetic marks, absent from the paternal chromatin (Kourmouli et al., 2004; Santenard et al., 2010).

Histone H2A.X variant is present on the paternal decondensing chromatin following fertilization and throughout preimplantation development in both parental epigenomes. Histone H2A.X modulates epigenetic remodelling and regulates cell cycle division events (Barton et al., 2007; Ziegler-Birling et al., 2009). Epigenetic asymmetry between parental genomes also exists with the histone H3.3 variant. Following fertilization, H3.3 is strictly a paternal epigenetic mark while H3.1/2 is predominantly a maternal specific pronuclear epigenetic mark (van der Heijden et al., 2006; Torres-Padilla et al., 2006). The transient disappearance of maternal pronuclear H3.3 is highly suggestive of erasure of the oocyte-specific modifications carried by H3.3 and most likely participates in the generation of totipotency in early two-cell embryos (Akiyama et al., 2011). After the two-cell stage, H3.1 and H3.3 variants resume their usual respective locations on heterochromatin and euchromatin.

At the pronuclear stage, the epigenetic asymmetry between the two parental genomes is crucial to reset the genetic material of the gametes in the zygote, to regulate the zygotic transcriptional gene expression and the progression of early embryonic development (Worrad et al., 1995; Stein et al., 1997).

1.3 Cleavage Stage Embryos

Cleavage stage embryos are two- to sixteen-cell embryos, rapidly dividing with asynchronous DNA synthesis and division between blastomeres.

1.3.1 The Two-Cell Embryo

The two-cell embryo travels from the ampullae to the upper region of the oviduct. The most critical event of early mammalian development is the transition

of the highly differentiated oocyte and spermatozoon into the totipotent blastomeres by the two-cell stage. The acquisition of totipotency is the result of the successful execution of the maternal to zygotic transcriptional switch.

1.3.1.1 DNA replication and Transcription

The maternal genomic control is switched to the zygotic control in two-cell embryos, constituting the major transition in gene expression reprogramming following fertilization, zygotic genome activation (ZGA) or embryonic genome activation (Figure 1.2) (Schultz, 1993).

1.3.1.2 Roles of the Major Zygotic Genome Activation

ZGA has three major functions (Figure 1.2). The first function is the non-specific degradation of the maternal pool of mRNAs following fertilization until the formation of two-cell embryos. The degradation of maternal mRNAs is mediated by the breakdown of the RNA binding protein MSY2, known to regulate maternal mRNA stability in the growing oocyte (Yu et al., 2001). The second function of the major ZGA is to replace all the maternal transcripts with zygotic transcripts setting the zygotic genomic expression (Latham et al., 1991). Lastly, the third function of the major ZGA is the transformation of the differentiated oocyte into totipotent blastomeres in two-cell embryos (Schultz, 2002).

During the ZGA of two-cell embryos, major changes are required in the promoter regions for efficient transcription. The first requirement is the presence of enhancers and maternally derived mRNA co-activators at transcription start sites. The enhancer recruits RNA polymerases to promoters and relieves the transcriptionally repressive state developed during the two- and four-cell stages (Delouis et al., 1992; Christian et al., 1994).The second requirement for efficient zygotic genomic reprogramming is the more efficient use of TATA-less promoters for the transcription of house-keeping genes and genes associated with preimplantation development, such as Oct-4 (Bird, 1986). Transcription of Oct-4 is required for the maintenance of totipotent blastomeres in two-cell embryos

(Nichols et al., 1998). The differential TATA box utilization ensures the appropriate zygotic gene expression during development.

The persistence of the transcriptional repressive state past the two-cell stage is thought to be partially mediated and relieved by changes in histones hyperacetylation (Wiekowski et al., 1993; Aoki et al., 1997). A second factor influencing the persistence of the transcriptional repressive state is the second round of DNA replication, indirectly pausing transcription in two-cell embryos by displacing functional transcription complexes and preventing their reassembly on promoters (Aoki et al., 1997; Schultz, 2002). The embryonic developmental importance of this transcriptional repression is to prevent the transcription of undesired genes and to promote the transcription of genes regulated by strong promoters/enhancers and chromatin accessible structures critical for the progression of embryos during cell cleavage divisions (Schultz, 2002).

1.3.2 Four- to Eight-Cell Embryos

DNA replication and proliferation are asynchronous and extremely rapid during cell cycle cleavage, as embryos travel further down the oviduct. From the two-cell stage, the cleavage stage embryo bypasses the mitotic cellular growth phase and divides into smaller daughter cells called blastomeres. There are two important processes occurring in cleavage stage embryos. The first event involves cell-cell communication between polarized epithelial cells and is called compaction. The second important cleavage stage event is the decision of cellular lineage, influenced by the blastomere plane of division and cell orientation.

1.3.3 Epigenetic Reprogramming in Cleavage Stage Embryos

DNA methylation of the maternal genome decreases further as the embryo divides due to the cytoplasmic sequestration of DNA methyltransferase 1 (DNMT1) (Haaf, 2006). At the morula stage, the methylation status of the maternal genome is indistinguishable from the paternal hypomethylated genome, with the exception of imprinting genes.

Histone H3 variants, H3.1, H3.2 and H3.3, are incorporated into transcriptionally active and repressive regions in all nuclei throughout preimplantation development, from the four-cell stage to the blastocyst stage (Akiyama et al 2011). Deregulation of H3 variant deposition is associated with changes in the level and distribution of post-translational modified histones, such as H3K9me2 and H3K9ac, causing abnormal regulation of important preimplantation developmental events (Akiyama et al., 2011). Histone epigenetic programming of the cleavage stage embryo is important in the regulation of cell cycle division and cell lineage decisions.

The timing of blastomere differentiation and commitment to inner cell mass or trophectoderm cell lineages is ambiguous but seems to be predetermined by the plane of division and the order of the second mitosis cycle during the development of cleavage stage embryos (Chen et al., 2010). Elevated histone H3R26me expression is observed in blastomeres of four-cell embryos predisposed to form the inner cell mass, while lower expression is associated with a trophectoderm cellular fate (Torres-Padilla et al., 2007).

All of the above experiments on DNA replication, transcription and epigenetic reprogramming in cleavage stage embryos were performed in the mouse model. As opposed to the mouse model, very limited data exist on the epigenetic chromatin remodeling and developmental regulation in the rat model.

1.4 Paternal Exposure to Toxicants

Major concerns associated with paternal exposure to toxicants include the risk of spermatogonial stem cell mutations due to exposure to chemicals such as anti-cancer drugs, transmission of genetic disease from the emergence of assisted reproduction techniques, and the epigenetic transgenerational actions of certain chemicals through the male germ line (Curley et al., 2011). The induction of sperm heritable damage from paternal exposures may lead to developmental defects, childhood abnormalities, or adult diseases in the next generation. Due to sample sizes and ethical considerations, there are very limited human data on the

effects of paternal exposure to environmental, occupational or social toxicants on the male reproductive system and on the development of the progeny.

1.4.1 Environmental and Occupational Exposures

A wide range of evidence exists on the potential effects of occupational exposures and environmental catastrophes on the male reproductive system.

1.4.1.1 Metal Exposure

Paternal exposure to metals (B, Ca, Mg, P, Cr, Cu, Sr, Zn and Se) represent one type of occupational exposure with a potential toxic effect on male fertility and on changes in human sperm DNA that may be transmissible to offspring as reviewed in Robbins et al., 2007. The effects of paternal metal exposure on male fertility has been assessed across five different occupational categories: agricultural workers, mechanics and truck drivers, factory workers, professional and office workers and raw ore workers from marble and coal mines. Normal blood and semen levels of metals and unaltered X: Y sperm ratios were obtained in all work categories. Potential caveats to this study were: the low number of men examined to detect a significant change in the X to Y sperm ratio, the widespread exposure to metals in modern society, and the limited sperm quality parameters analyzed, making the assessment of the relationship between metal exposures and outcome difficult to establish.

A retrospective study on paternal occupational exposure to chronic low levels of lead in the battery manufacturing and smelting industries found no correlation between blood lead level and time to pregnancy as the variable to measure fertility (Joffe et al., 2003).

As opposed to lead exposures, results obtained from occupational exposure of men to mercury vapour prior to conception suggested a link between the rate of spontaneous abortion and the concentration of mercury in the urine (Cordier et al., 1991). The reproductive toxicity of mercury is mediated by the damaged male germ cells, affecting the survival of the early embryo.

Preconceptional paternal exposure to depleted uranium, a metal used in military applications and now found in great concentration in some areas, raised concerns regarding its implication in childhood cancers such as leukemia. Data showed that the F1 progeny fathered by male mice exposed to depleted uranium prior to conception had a higher mutation frequency in bone marrow samples. These results suggested a predisposition to cancer transmitted through the male germ cells exposed to depleted uranium (Miller et al., 2010).

1.4.1.2 Air Pollution

A detailed analysis of the effects of exposure to high levels of air pollutants, such as polycyclic aromatic hydrocarbons and sulphur dioxide, on sperm quality was done in the Czech Republic as reviewed in Sram and Rubes, 2007. These data suggest that exposure to a high concentration of air pollutants is associated with increases in DNA fragmentation in sperm, as detected by the sperm chromatin structure assay (SCSA). No association was found between air pollution and other biomarkers of sperm injury such as abnormal sperm morphology and motility determined by computarized assisted semen analysis (CASA). The impact of air pollution on human sperm DNA fragmentation is considerable but seems to be reversible once the pollution is lowered (Rubes et al., 1998; 2002; 2005).

The ambient air in close proximity to steel mills in the Great Lakes is polluted with chemical compounds known to induce genetic damage in animal models (Somers et al., 2002). The frequency of male germline heritable mutations is elevated in mice housed 1 km downwind compared to mice located 30 km downwind from two integrated steel mills. These results indicate a male mediated toxicity effect from the inhalation of airborne chemical mutagens.

1.4.1.3 Endocrine Disruptors

The third example of human environmental and occupational exposure with an impact on sperm quality is the existing relationship between exposure to high concentrations of endocrine disrupting agents, such as pesticides, and the

high incidence of poor semen quality in the agricultural area of Missouri (Swan et al., 2003). Exposure of males to oestrogenic compounds, such as diethylstilboestrol and phytoestrogens, causes the generation of reactive oxygen species, inducing oxidative stress and DNA damage in spermatozoa as reviewed in Anderson et al., 2007. Furthermore, agricultural exposures to the toxic metabolites of organophosphorous pesticides, oxons, alter sperm chromatin structure and induce DNA damage (Salazar-Arredondo et al., 2008). Oxidative stress seems to be the mechanism responsible for the decrease in sperm fertilizing capacity observed after exposures to organophosphorous pesticides (Piña-Guzmán et al., 2009).

The decline in semen and sperm quality observed in men exposed to endocrine disruptors has two major caveats; the first one is due to methodological issues from sperm collection between centres and within-person biological variation over time, and from the low participation of the population as reviewed in Joffe, 2007. Only men in agricultural areas participated in the study, therefore, only they were exposed to a high concentration of oestrogenic compounds. Another caveat is the misdiagnosis of testicular dysgenesis syndrome in baby boys from exposures to endocrine disruptors. Nevertheless, levels of human environmental exposure are insignificant compared to levels required to induce testicular cancer, infertility and abnormal male reproductive organs in animal models (Joffe, 2007). Furthermore, the spectrum of effects from endocrine-disrupting agents, including hormone sensitive cancers, growth and development, secondary sexual characteristics and timing of puberty, is not observed in boys and young adults (Joffe, 2001). Genetic damage could potentially explain the various impairments of the male reproductive system and poor semen quality from exposures to endocrine disruptors (Joffe, 2007).

Contrary to the human data on exposures to endocrine disruptors, animal exposures lead to a range of detrimental effects on sperm quality. Alterations of the methylation pattern of male germ cells and paternal imprinted genes were observed following exposure to endocrine disruptors, such as the fungicide

vinclozolin and the pesticide methoxychlor, during the differentiation of the reproductive tract. Paternal exposure to endocrine disruptors induced an epigenetic transgenerational disease lasting four generations through the male germ-line as reviewed in Skinner, 2007 (Anway et al., 2005). Furthermore, alterations in DNA methylation promoted the development of cancer and tumors in adults, making the identification of these genes as potential diagnostic markers and therapeutic targets for these adult diseases (Feinberg and Tycko, 2004).

The widely used plasticizer, di(2-ethylhexyl)phthalate (DEHP) a well known reproductive and developmental toxicant, is also an endocrine disruptor with antiandrogenic effects (Kavlock et al., 2002). Male mice exposed to di(2-ethylhexyl)phthalate have reduced levels of testosterone, sperm production and other testicular toxicities as reviewed in Dobrzyńska et al., 2007. Male offspring of fathers exposed to a low dose of di(2-ethylhexyl)phthalate (1/16 LD50, 2000mg/kg) are growth retarded and have undescended testes. Male offspring of fathers exposed to a high dose of di(2-ethylhexyl)phthalate (1/4 LD50, 8000mg/kg) showed extensive DNA damage and altered male germ cell and Sertoli cell morphology. Exposure to a high dose of di(2-ethylhexyl)phthalate led to pre- and post-implantation death in offspring of exposed fathers. Most of the data on animal exposures to endocrine disruptors and their effects on the male reproductive system and progeny outcome were done using much higher doses than those relevant for human exposures (Mruk and Cheng, 2011). Nevertheless, these results are considered as important information for extrapolation to humans.

1.4.2 Lifestyle Factors

Every day, we are exposed to a wide range of factors: social clues, types of consumption and activities that influence our behaviours and practices; these are built on social habits, individual values and reasoned actions. The reproductive and developmental toxicities associated with lifestyle factors will be reviewed.

1.4.2.1 Alcohol Consumption

Although moderate wine drinking has protective effects on sperm motility and viability, mainly due to the antioxidants present in red wine, excessive consumption in men prior to conception may have an impact on the incidence of fetal alcohol syndromes as reviewed in Marinelly et al., 2004. Chronic paternal drinking can reduce the activity of DNA methyltransferases in sperm, decreasing the methylation status of normally hypermethylated genes; one example of such an imprinted gene is H19, involved in early embryonic development (Ouko et al., 2009). Chronic alcohol consumption prior to conception in male rats decreased the levels of cytosine methyltransferase mRNA in sperm, altering DNA methylation of critical genes regulating the development of early embryos and resulting in detrimental effects on fetal growth and offspring behavior and cognition (Bielawski et al., 2002).

1.4.2.2 Food Consumption

The incidence of hypercaloric diets and human obesity has increased over the past few years, partially due to the ready access to poor quality food and lack of physical activities. Male mice chronically fed a diet composed of lard exhibited reduced sperm motility and decreased physical activities having a direct impact on fertility and successful pregnancies (Ghanayem et al., 2010).

Folate is required for DNA synthesis and the regeneration of S-adenosylmethionine, the universal methyl donor for DNA methylation. Folate is an important epigenetic regulator of gene expression (Forges et al., 2008). Folate nutritional deficiency has been shown to decrease spermatogenesis, leading to male subfertility, in both newly reported human data and ongoing studies in rodents (Wong et al., 2000; Dunlap et al., 2011).

1.4.2.3 Cigarette Smoking

Paternal smoking has limited effects on sperm parameters as reviewed in Marinelli et al., 2004, but in some studies paternal transmission of sperm DNA adducts from a smoker to the embryo has been observed (Horak et al., 2003).

The effect of smoking on male fertility was assessed in a cohort study of 25 men (10 smokers, 20 cigarettes/day, and 15 non-smokers) from the Teplice district in Czech Republic, the Northern Bohemia brown coal basin, one of the worst environmentally polluted regions in Europe (Rubes et al., 1998). Smokers had an elevated frequency of sperm aneuploidy for chromosomes X, Y, and 8 ($p \leq 0.01$) and Y disomy ($p \leq 0.001$) assessed by fluorescent in situ hybridization compared to non-smokers.

Findings from three studies by the Oxford Survey of Childhood Cancers and one from the Inter Regional Epidemiological Survey of Childhood Cancers concluded that there was an association between paternal smoking before conception and childhood cancer. The childhood cancer risk increased in relation to daily cigarette consumption as reviewed in Sorahan, 2007.

Subfertility associated with paternal tobacco smoking can be due to the effect of reduced mitochondrial respiration on sperm motility (Chohan and Badawy, 2010), on changes in sperm chromatin structure and integrity (Potts et al., 1999), on the levels of sperm DNA guanosine oxidation (Fraga et al., 1996), or on the generation of sperm mitochondrial reactive oxygen species (Koppers et al, 2008). All of these possible mechanisms of damage are dose dependent and can be reversed if the insult is short-lived.

1.4.2.4 Recreational Use of Illicit Drugs

According to the National Survey of Drug Use and Health, the use of illicit drugs amongst men in the United States seeking infertility treatment is increasing. Amongst the most commonly used illicit drugs are marijuana, opioid narcotics, methamphetamines, cocaine, and anabolic-androgenic steroids; all have adverse effects on male fertility as reviewed in Fronczak et al., 2011. As a general mechanism of action, the use of illicit drugs suppresses the hypothalamic-pituitary axis, inhibiting the release of gonadotropin releasing hormone, suppressing the release of luteinizing hormone and subsequently the level of testosterone. The

impact of the recreational use of illicit drugs on male fertility impairs spermatogenesis resulting in lower sperm counts.

1.4.3 Therapeutic and Chemotherapeutic Exposures

Current chemotherapeutic regimens consist of a combination of radiation, alkylating agents, antibiotics, and alkaloids. The impact of cancer treatments on male fertility in cancer survivors varies depending on the type of cancer, the timing of cancer occurrence, and social factors (O'Flaherty et al., 2008; 2010). Young adult men treated with radiation and chemotherapeutics agents are faced with an initial drop in sperm production, causing infertility which can last many months to even years (Howell and Shalet 2005). Some patients will recover spermatogenesis with increased sperm count; despite this recovery, these men may be faced with the possibility of transmitting heritable genetic diseases to their offspring.

In the childhood cancer survivor study in North America between 1970 and 1986, there were no significant increases in genetic disease in survivors of childhood and adolescent cancers given modern therapies compared to the incidence in control siblings as reviewed in Mulvihil and Garlow, 2007. This finding is reassuring but the same analysis has to be done with cancer survivors given new drugs, combinations, and therapies once they mature into adulthood as reviewed in Green et al., 2010.

From population-based cohort studies from five Nordic cancer registries on cancer risk among parents, siblings and offspring of childhood cancer patients compared to the cancer incidence in the general population, there is less than 5% of childhood cancer which can be explained by hereditary factors as reviewed in Winther, 2007 (Olsen et al., 1995; Sankila et al., 1998; Winther et al., 2001). Nevertheless, children of fathers exposed to radionuclides had a greater risk of leukemia and congenital malformations through occupational or diagnostic radiation exposure (Shu et al., 1988; Gardner et al., 1990; Parker et al., 1999) than from the high dose of atomic radiation received by A-bomb survivors in

Hiroshima and Nagasaki (Yoshimoto and Mabuchi, 1991; Yoshimoto et al., 1991).

Paternal exposure to radiation and chemicals in mice induced transmissible genetic risk in offspring as reviewed in Nomura, 2007. Post-meiotic germ cell exposure to X-rays led to chromosomal aberrations and DNA damage, causing embryo loss, congenital malformations or increased transmissible genetic risk to the next generation. Spermatogonial exposure to X-rays led to dominant lethal chromosomal aberrations eliminated during meiosis or by apoptosis before the maturation of spermatozoa. In this mouse model, an increased sensitivity in offspring fathered by chemically exposed males to tumors following postnatal exposure to radiation or chemotherapy was noted.

Furthermore, acute exposure to 0.1 Gy induced sperm DNA damage when spermatogonia were exposed, predisposing the F2 and F3 generations to increased DNA instability and heritable germ cell effects as reviewed in Li and Baulch, 2007. DNA damage induced by acute spermatogonial exposure increased the sensitivity of sperm to subsequent breakage during spermatogenesis from unrepaired damage. The incidence of transgenerational cancer, such as leukaemia, lymphoma, skin cancers, and elevated mutation rates or instability in somatic and germ cells was increased in the non-exposed F1 and F2 offspring of male mice exposed to carcinogens and irradiation as reviewed in Dubrova, 2007. These authors concluded that the transgenerational risks associated with chemotherapeutic treatment may be due to epigenetic dysregulation, to cellular stress, or inflammatory responses in offspring of irradiated male germ cells mice. These results could explain the increased risk of childhood cancers in offspring fathered by cancer survivors in the human population. Delayed genetic risks of ionising radiation on transgenerational genomic instability could increase the mutation load in the human population, affecting mortality and cancer predisposition, and be more prevalent than previously thought as suggested in Dubrova, 2007.

Discrepancies between the effects of toxicants on male reproduction in animal and human models may be due to: dosage differences, spermatogenesis stage specific effects, species specific tumour predispositions, postnatal exposures, or a consequence of the absence of data on human adult diseases as reviewed in Nomura, 2007.

1.5 Cyclophosphamide

Cyclophosphamide (CPA) is an inactive prodrug, commonly used as an anticancer and immunosuppressive agent, targeting rapidly dividing cells and leading to cell death.

1.5.1 Pharmacokinetics

CPA is activated in the liver by cytochrome P450 enzymes, forming 4-hydroxycyclophosphamide and aldophosphamide (Figure 1.3). 4-Hydroxycyclophosphamide is decomposed by β-elimination into phosphoramide mustard and acrolein as reviewed in de Jonge et al., 2005. Phosphoramide mustard acts as a bi-functional alkylating agent, mediating the alkylation of DNA at the N7 position of guanine and leading to the formation of DNA-DNA and DNA-protein cross-links (Hengstler et al., 1997). Acrolein, on the other hand, is a highly reactive aldehyde and depletes the cell store of the antioxidant glutathione (Slott and Hales, 1987). Moreover, acrolein may enhance CPA cytotoxicity by covalently binding to DNA and causing DNA-protein cross-linking, as well as inhibiting DNA replication and transcription (Li et al., 2008).

Detoxification of CPA by side chain oxidation mediated by CYP3A4 leads to the formation of 2-dechloroethylcyclophosphamide and chloroacetaldehyde which represent less than 5% of the total elimination of CPA as reviewed in de Jonge et al., 2005 (Figure 1.3). Chloroacetaldehyde, similar to acrolein, may enhance phosphoramide mustard cytotoxicity by depleting glutathione in cells. A second level of CPA detoxification exists when 4-hydroxycyclophosphamide and aldophosphamide are irreversibly inactivated by alcohol dehydrogenases into 4-ketocyclophosphamide, a non-cytotoxic product, and by aldehyde dehydrogenase

enzymes into carboxyphosphamide, respectively (Mitchell and Petersen, 1989). The aldehyde dehydrogenase enzymes actively compete against the β-elimination decomposition of aldophosphamide into phosphoramide mustard, representing the most important detoxifying step during CPA metabolism.

Figure 1.3. Cyclophosphamide activation and detoxification pathways. The liver activates most of the administered cyclophosphamide dose while the remaining is deactivated by the side chain detoxification enzymes. Cyclophosphamide is an inactive prodrug converted by cytochrome P450 to 4-hydroxycyclophosphamide, which exists in equilibrium with aldophosphamide and decomposes by β-elimination into the active metabolites phosphoramide mustard and acrolein. Phosphoramide mustard and acrolein are responsible for the majority of cyclophosphamide toxicity: DNA strand breaks and DNA protein cross-links. Cyclophosphamide is inactivated by CYP3A4 to 2-dechlorocyclophosphamide and chloroacetaldehyde, 4-hydroxycyclophosphamide is inactivated by alcohol dehydrogenase into 4-ketocyclophosphamide while aldophosphamide is inactivated by aldehyde dehydrogenase into carboxyphosphamide. Adapted from de Jonge et al., (2005). Clin Pharmacokinet. 44, 1135-1164.

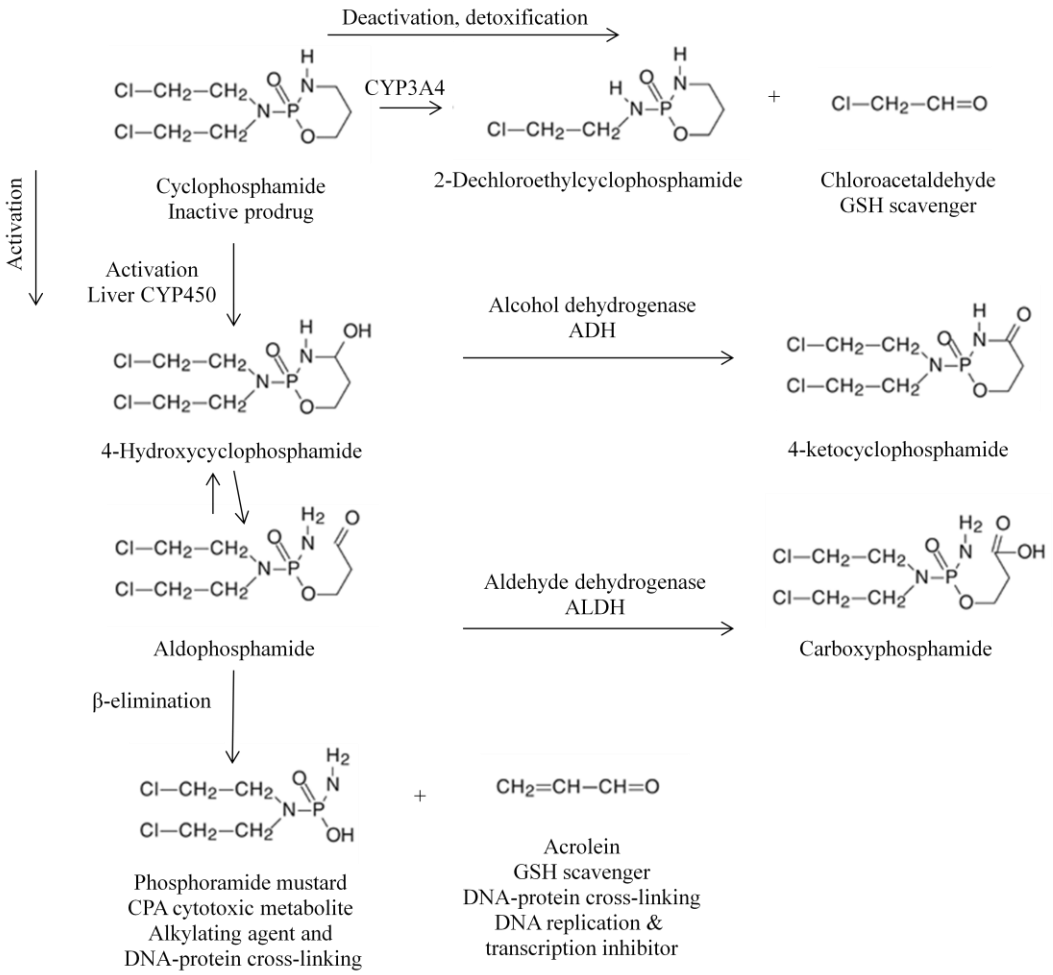
Deactivation, detoxification
CYP3A4
Cyclophosphamide
Inactive prodrug
2-Dechloroethylcyclophosphamide
Chloroacetaldehyde
GSH scavenger
Activation
Activation
Liver CYP450
Alcohol dehydrogenase
ADH
4-Hydroxycyclophosphamide
4-ketocyclophosphamide
Aldehyde dehydrogenase
ALDH
Aldophosphamide
Carboxyphosphamide
β-elimination
Phosphoramide mustard
CPA cytotoxic metabolite
Alkylating agent and
DNA-protein cross-linking
Acrolein
GSH scavenger
DNA-protein cross-linking
DNA replication &
transcription inhibitor

There are three well known disadvantages associated with CPA chronic treatment: the first one is the autoinduction of cytochrome P450 enzymes, increasing its own metabolism, accompanied by an increase in total body clearance of CPA. The second disadvantage is the drug interaction when CPA is used in combination with other agents that modulate cytochrome P450 or aldehyde dehydrogenase enzyme levels and activity (Huitema et al., 2001). The phenomena of autoinduction and drug-interaction may influence the therapeutic benefits and cytotoxicity associated with the use of this drug in chemotherapeutic treatments. Lastly, side effects associated with the non-specific drug targets of CPA, causing toxicity to numerous rapidly dividing tissues, may include carcinogenesis and teratogenicity as reviewed in Ahmed and Hombal, 1984, McCarroll et al., 2008 and Ozolins, 2010.

1.5.2 Human Relevance

Men chronically treated with CPA (1-2mg/kg) during 4 months had abnormal and lower sperm counts (Fairley et al., 1972; Qureshi et al., 1972; Fukutani et al., 1981) with an increase in follicle-stimulating hormone levels. One study reported a longer time to pregnancy (Buchanan et al., 1975) without any adverse effect on pregnancy outcome.

1.5.3 Spermatozoal Toxicities

Exposure to CPA during spermatogenesis induces a variety of types of DNA damage depending on the stage of male germ cells first exposed (Figure 1.4) (Trasler et al., 1986; 1987): treatment for 1-2 weeks targets spermatozoal maturation and epididymal transit, 3-4 weeks of treatment targets cytoplasmic reorganisation and chromatin remodelling during spermiogenesis, 5-6 weeks targets meiotic spermatid cells and 7-9 weeks targets active mitotic spermatogonia (Clermont, 1972). The extent of DNA damage depends on the ability of each type of male germ cell to respond to the insult by repair or cell death.

Chronic exposure of post-meiotic male germ cells to CPA depleted the products of genes involved in DNA repair, post-translational modification and

antioxidant activities (Aguilar-Mahecha et al., 2002). The gene products of poly(ADP)ribose polymerase and proliferating cell nuclear antigen, important enzymes involved in base excision repair and nucleotide excision repair pathways respectively, were decreased. Consequently, chronic paternal exposure to CPA deprives male germ cells of these defence mechanisms (Aguilar-Mahecha et al., 2002). In addition, while chronic low doses of CPA did not activate cell cycle checkpoints during meiotic progression, they did enhance the detection of DNA double strand breaks (DSBs) with γH2AX in spermatocytes (Figure 1.4) (Aguilar-Mahecha et al., 2005). Results from these last two studies confirmed that there was DNA damage accumulation in post-meiotic male germ cells as a consequence of a diminished DNA damage response and the lack of surveillance mechanisms following paternal exposure to CPA. Thus, repair in the conceptus, may rely on DNA damage response (DDR) mechanisms in the early embryo.

Chronic paternal exposure to CPA led to the alteration of spermatozoal chromatin compaction and increased DNA damage. Exposure to CPA during spermiogenesis led to DNA single strand breaks (SSBs) and decreased sulfhydryl cross-links in protamines of spermatozoa, altering chromatin packaging during spermatozoal maturation (Qiu et al., 1995a; 1995b). Moreover, indirect measurement of the protamine content with the fluorochrome chromomycin A3 showed an increased chromomycin A3 binding, suggesting underprotamination of spermatozoal chromatin packaging. Chronic low dose exposure to CPA resulted in DNA damage accumulation, based on DNA strand breaks measured by comet assay, when elongating spermatids were initially exposed; less damage was found in mature spermatozoa (Figure 1.4) (Codrington et al., 2004). Relaxation of the spermatozoon chromatin compaction caused by CPA exposure altered chromatin decondensation *in vitro* (Qiu et al., 1995b); this may contribute to a disruption of normal progression in the early embryo.

Figure 1.4. Cyclophosphamide as a model for male-mediated developmental toxicity studies. Cyclophosphamide has dose dependent and time specific effects on male germ cells which consequently affect progeny outcome. Post-implantation losses were induced by exposing elongating spermatids undergoing chromatin remodeling, inducing the maximal DNA damage after four weeks of treatment. Pre-implantation losses and abnormal progeny outcome were maximally induced after six and nine weeks of treatment, first exposing spermatocytes and spermatogonia, respectively. Adapted from Robaire and Hales, (1998). Germ cell development, division, disruption and death. (Zirkin, B.R., ed.), Springer-Verlag, New York, NY, 190-201.

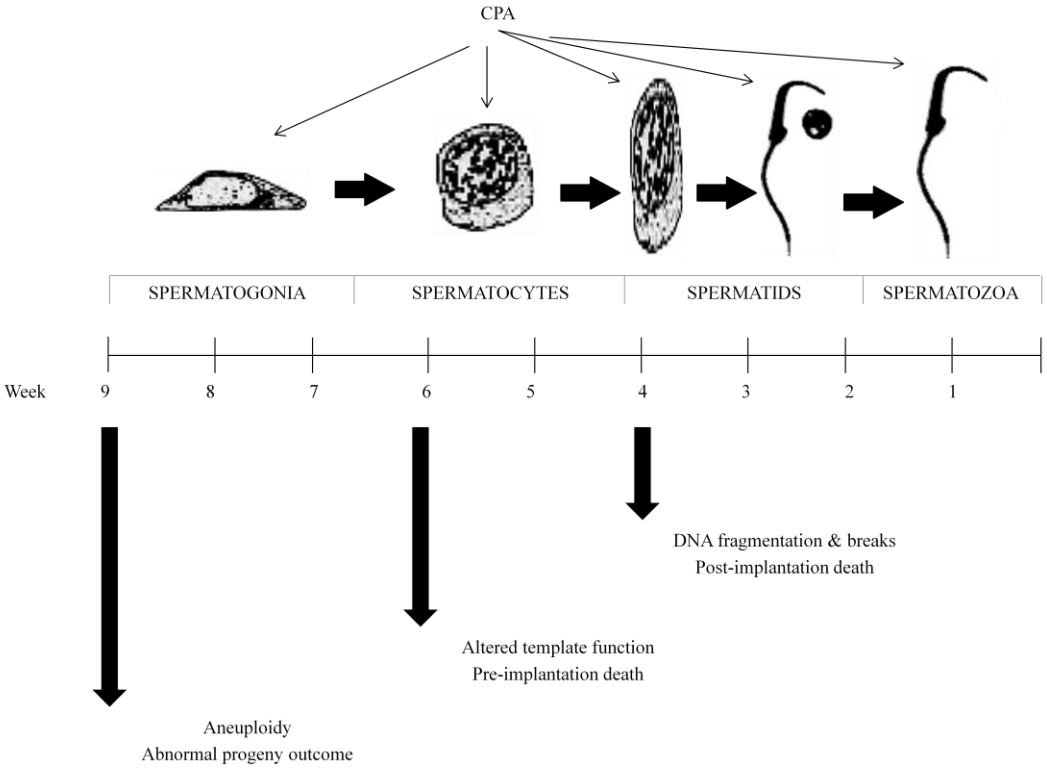
CPA
SPERMATOGONIA
SPERMATOCYTES
SPERMATIDS
SPERMATOZOA
Week
9
8
7
6
5
4
3
2
1
DNA fragmentation & breaks
Post-implantation death
Altered template function
Pre-implantation death
Aneuploidy
Abnormal progeny outcome

Furthermore, paternal exposure to CPA markedly affected spermatozoal DNA template function as determined using an *in vitro* DNA synthesis assay (Figure 1.4) (Qiu et al., 1995a). Exposure to CPA during spermiogenesis modified the nuclear matrix protein composition at the matrix attachment regions (Codrington et al., 2007a) essential for paternal PN DNA replication and transcriptional regulation during preimplantation development (Ward, 2010).

When compared to other types of germ cells, post-meiotic male germ cells are particularly sensitive to the cytotoxicity and alkylation effects of CPA. This differential susceptibility may be due to the absence of DNA repair mechanisms and consequent DNA damage accumulation (Cai et al., 1997), the open chromatin structure during the extensive remodelling of the sperm nucleus, and the vulnerability of the protein composition at the nuclear matrix attachment regions to alkylating agents.

1.5.4 Male-Mediated Developmental Toxicities of CPA

Male-mediated effects of chronic CPA exposure resulted in adverse progeny outcome in a dose and time-dependent manner (Figure 1.4): CPA treatment for 2 weeks led to postimplantation loss, while 5-6 weeks increased preimplantation loss, and 7-9 weeks of treatment resulted in malformations and growth retardation (Trasler et al., 1986; 1987).

Chronic low dose treatments of CPA led to the dysregulation of epigenetic programming of the development of early embryos. Paternal exposure to CPA altered DNA methylation and histone H4 acetylation at lysine 5 in the male and female genome in pronuclear stage zygotes, suggestive of pronuclear cross-talk (Barton et al., 2005). The epigenetic disruption in early embryos may explain the transmission of abnormal pregnancy outcomes to the F2 generation (Hales et al., 1992).

The relaxed chromatin packaging and DNA damage accumulation in spermatozoa may lead to an acceleration in the progression of pronuclear zygotes (Barton et al., 2005) while the epigenetic dysregulation following fertilization

may be involved in the developmental delay during the subsequent cleavage stage divisions (Kelly et al., 1994). In eight cell embryos, we found a decrease in the cell number and cell-cell interaction at the mRNA and protein levels could be a consequence of unsuccessful embryonic developmental progression and transcriptional regulation (Harrouk et al., 2000c).

Paternal exposure to CPA led to the early activation of DDR in embryos. Histone γH2A.X remodelling and reprogramming were altered in pronuclear zygotes sired by CPA treated males; increased γH2A.X foci numbers and size were detected in the paternal genome, indicative of DNA DSBs and DNA damage recognition (Barton et al., 2007). As a second biomarker of DNA damage recognition, PARP-1 was significantly increased in both parental pronuclear genomes (Barton et al., 2007). The major wave of zygotic transcriptional activation was dysregulated: the total RNA synthesis measured by BrUTP incorporation between the two- and four-cell stages was completely abolished in early embryos sired by CPA treated males (Harrouk et al., 2000b). Expression profiles of a subset of DNA repair genes involved in nucleotide excision repair, base excision repair, and mismatch repair were differentially altered in embryos as early as the zygote and eight-cell embryo (Harrouk et al., 2000a).

1.6 DNA Damage Responses, DDR

The DDR is influenced by cell cycle stage (meiosis, mitosis), cell type (somatic, germ cell), cell state (cancer cells, stem cells, ageing cells, embryos), species (mouse versus human cells), and of course, the nature of the DNA damage as reviewed in Ball and Yokomori, 2011. Careful interpretation of the meaning and impact of the DDR is crucial for the prediction of cellular fate.

Mammalian cells have developed specific mechanisms to protect and maintain the integrity of their genome by detecting the damage, repairing the damage, regulating cell cycle progression and deciding between cellular survival and death (Figure 1.5). In the presence of a damaged genome the cell has three options. The first option is to repair the damaged genome. The second option is to

partially repair the damage, predisposing the cell to tumor and cancer. The third option is to promote cell death, preventing the propagation of DNA damage as reviewed in Jaroudi and SenGupta, 2007 (Figure 1.5).

1.6.1 DNA Damage

There are many forms of DNA damage; these include DNA strand breaks, DNA-protein cross-links, and chemical modifications such as the generation of 8-hydroxydeoxyguanosine residues. DNA damage can result from normal cellular processes, including chromatin decondensation and remodelling, DNA replication, cellular senescence, and exposure to reactive oxygen species (Bonner et al., 2008). DNA damage can also result from exposure to DNA damaging agents, such as radiation and genotoxic chemotherapeutic therapies. The activation of DNA damage response (DDR) is influenced by the type of insult and the cell capacity to mount a response.

1.6.1.1 Micronuclei

Micronuclei (MNs) are formed as a consequence of DNA damage, either from broken pieces of a chromosome, a clastogenic effect, or a whole chromosome, an aneugenic effect, that is unable to attach to microtubules and segregate properly during mitosis. MNs are formed following toxicant exposure or due to the inappropriate functioning of the mitotic apparatus. As a consequence of MNs formation, cells may become aneuploid, with an unequal number of chromosomes between daughter cells. Although the formation of MNs following exposure to genotoxic agents is a well established sign of chromosome instability from inappropriate DNA repair or cell cycle arrest, their chromosomal content and impact on cellular fate remain controversial.

1.6.1.1.1 Mechanisms of Formation

The mechanisms of MNs formation depend on the type of insult as reviewed in Terradas et al., 2010 and Fenech et al., 2011. Exposure to aneugenic compounds impairs the attachment of kinetochore proteins to the microtubule

network, resulting in a lagging, mis-segregated whole chromosome. The attachment defects are most likely due to the hypomethylation of centromeres and pericentromeric DNA repeat sequences or to a dysfunctional spindle or anaphase checkpoint. Exposure to clastogenic compounds leads to the formation of small pieces of chromosomes or chromatin fragments from an excessive load of DNA damage and an inability of these fragments to adhere to the spindle fibres during mitosis. DNA synthesis inhibitors, such as hydroxyurea, induce the formation of a third type of MNs, double minutes or nuclear buds, small fragments lacking telomeres and active centromeres (Shimizu, 2009). Lastly, nucleoplasmic bridges are formed when a dicentric chromosome is pulled apart at anaphase; the two centromeres form a chromosomal bridge resulting in new chromosomal breaks or unprotected ends, providing the basis for the next breakage-fusion-bridge. These nucleoplasmic bridges are good indicators of tumor formation and cancer progression. Pancentromeric DNA probes, telomeric probes and cytokinesis block are molecular techniques useful to identify and differentiate all four mechanisms of MNs formation.

1.6.1.1.2 Impact on Cellular Fate

The impact of MNs on the cell survival will depend largely on the micronuclear genetic material, activity, and cell type as reviewed in Terradas et al., 2010. Micronuclear DNA replication can either be simultaneous to its nuclear counterpart or be defective and asynchronous due to the accumulation of micronuclear DNA damage (Crasta et al., 2012). The transcriptional activity of MNs depends on three factors: the presence of whole chromosomes for genomic RNA transcription, the presence of nucleolus like bodies for ribosomal RNA transcription, and the formation of a complete nuclear envelope for the controlled exchange between the MN and the cytoplasm.

Figure 1.5. **DNA damage responses.** The first event following DNA damage is the relaxation of the chromatin to open up the structure and to allow the recognition of DNA damage by phosphatidylinositol-3 kinase family members, PI3K: ataxia telangiectasia mutated ATM, ataxia telangiectasia mutated and Rad3-related ATR and DNA-dependent protein kinases DNA-PKs. Depending on the type of insult, phosphatidylinositol-3 kinases will either amplify the damage, recruit other DNA repair proteins or remodel the chromatin to enhance DNA repair activity. There are four different types of DNA repair mechanisms: base excision repair BER, double strand break DSB, mismatch repair MMR and nucleotide excision repair NER. Cell cycle checkpoints and spindle assembly represent some DNA damage responses to improve DNA repair. Successful DNA damage repair will increase cell survival while extensive DNA damage may lead to cell death. If the damage is inefficiently repaired, the cell may survive to propagate the damage in the next cell cycle divisions, making it vulnerable to cancer formation and cell death. Adapted from Redon et al., (2010). Clinical Cancer Research 16, 4532-4542.

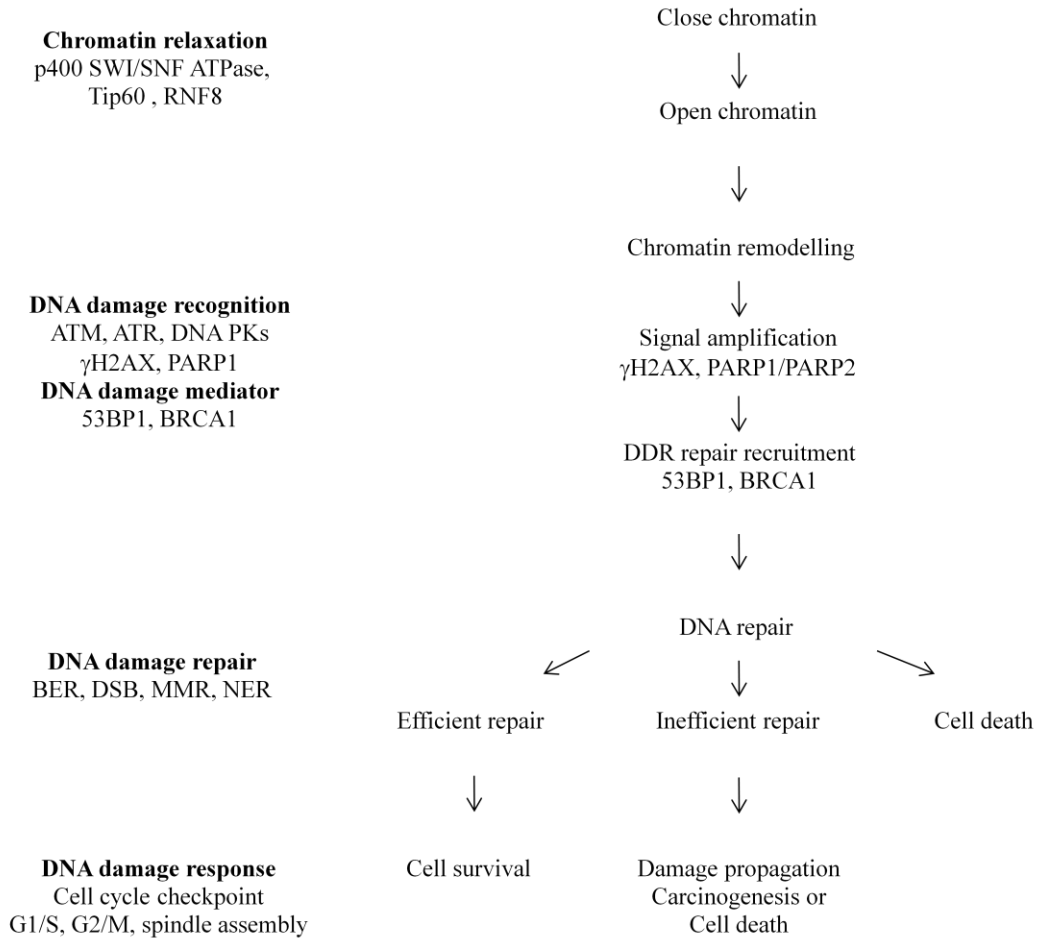
Close chromatin
Chromatin relaxation
p400 SWI/SNF ATPase,
Tip60 , RNF8
Open chromatin
Chromatin remodelling
DNA damage recognition
ATM, ATR, DNA PKs
γH2AX, PARP1
DNA damage mediator
53BP1, BRCA1
Signal amplification
γH2AX, PARP1/PARP2
DDR repair recruitment
53BP1, BRCA1
DNA repair
DNA damage repair
BER, DSB, MMR, NER
Efficient repair
Inefficient repair
Cell death
DNA damage response
Cell cycle checkpoint
G1/S, G2/M, spindle assembly
Cell survival
Damage propagation
Carcinogenesis or
Cell death

DDR mechanisms in MNs are functional but usually differ from the main nucleus as they accumulate in MNs. Micronuclear DDR accumulation was observed with TP53 following γ-irradiation (Lu and Lane 1993) and with γH2AX following replication stress induced by hydroxyurea, aphidicolin and thymidine (Xu et al., 2011). MNs formation was also observed in early embryos after parental exposure to γ-irradiation; these MNs increased the incidence of chromosomal mosaicism between blastomeres and caused a delay in embryonic development, predisposing the embryo to peri-implantation loss (Tian and Yamauchi, 2003; Marchetti et al., 2009; Mozdarani and Nazari, 2009).

Small micronuclear fragments can be either expulsed or degraded by the cell, losing chromatin information or eliminating extra chromosomal DNA as a protection mechanism (Marchetti et al., 2009). Alternatively, MNs may persist during many generations, becoming randomly distributed between daughter cells and eventually reincorporated into the cell genome (Crasta et al., 2012).

1.6.2 Chromatin Relaxation

The first and foremost step in the DNA damage recognition pathway is the relaxation of the chromatin at the site of damage. Along with histone post-translational modifications, motor ATPases are responsible for the alteration of chromatin dynamics by sliding along the DNA and removing nucleosomes from the chromatin (Figure 1.5) (Clapier and Cairns, 2009; Xu and Price, 2011). The dynamic chromatin remodelling occurring at sites of DNA strand breaks plays a crucial role in mounting the appropriate repair process. The action of p400 SWI/SNF ATPase (Chan et al., 2005; Gevry et al., 2007) and histone H2A and H4 acetylation by the Tip60 acetyltransferase (Downs et al., 2004; Kusch et al., 2004; Murr et al., 2006; Jha et al., 2008) decondenses the chromatin structure. Chromatin relaxation increases the accessibility of the linker DNA to nuclease digestion (Carrier et al., 1999; Rubbi & Milner 2003; Ziv et al., 2006; Xu and Price, 2011), amplifies DNA damaged repair signalling (Murga et al., 2007), and decreases nucleosomes stability in γH2AX enriched chromatin regions (Xu et al., 2010). Nucleosome destabilization subsequently promotes the methylation of

histone H4K20 (Sanders et al., 2004), facilitating the ubiquitination of histone H2A by the RNF8 ubiquitin ligase (Huen et al., 2007; Mailand et al., 2007) and the loading of DNA repair proteins, BRCA1 and 53BP1 (Huyen et al., 2004; Galanty et al., 2009; Morris et al., 2009; Xu et al., 2010).

1.6.3 DNA Repair Pathways

There are four main DNA repair pathways: the base excision repair (BER), the DNA double strand break repair (DSB), mismatch repair (MMR), and nucleotide excision repair (NER) as reviewed in Jaroudi and SenGupta, 2007. The base excision repair pathway consists in the activation of DNA glycosylases that recognise and excise aberrant DNA bases, endonucleases that cleave the aberrant bases, DNA synthesis machinery that resynthesizes the missing piece of DNA which is then ligated to the rest of the DNA. The recognition of DNA DSBs by DNA repair proteins amplifies the response and leads to the recruitment of other repair proteins to the site of damage which ligate the two broken pieces of DNA. The mismatch repair pathway is activated following the dysregulation of DNA replication or DNA damage and results in the removal and replacement of DNA base mismatches. The nucleotide excision repair pathway requires first the recognition of the DNA lesion, then the removal and replacement of damaged oligonucleotide by DNA synthesis and finally the ligation of the open ends.

1.6.3.1 Phosphorylation of H2AX, γH2AX

The relaxation of chromatin allows the detection of DNA DSBs by hundreds of H2AX molecules phosphorylated on serine 139 by members of the phosphatidylinositol-3 kinase family: ataxia telangiectasia mutated, ataxia telangiectasia mutated and Rad3-related, and DNA dependent protein kinase (Figure 1.6) (Rogakou et al., 1998; Bonner et al., 2008).

Figure 1.6. The detection of DNA double strand breaks by γH2AX. Upon the formation of DNA double strand breaks, phosphatidylinositol-3 kinase family members PI3Ks (ataxia telangiectasia mutated ATM, ataxia telangiectasia mutated and Rad3-related ATR and DNA-dependent protein kinases DNA-PKs) phosphorylate histone H2AX on serine 139 residue to form γH2AX. The activated γH2AX can either amplify the signal by recruiting more γH2AX or other DNA repair proteins, chromatin remodeling or cell cycle proteins to the site of DNA damage. The size of γH2AX foci is indicative of their function; small γH2AX foci are involved in chromatin remodeling events, DNA replication and cell cycle regulation while large γH2AX foci are involved in DNA damage responses and the recruitment of repair proteins. Adapted from Redon et al., (2010). Clinical Cancer Research 16, 4532-4542.

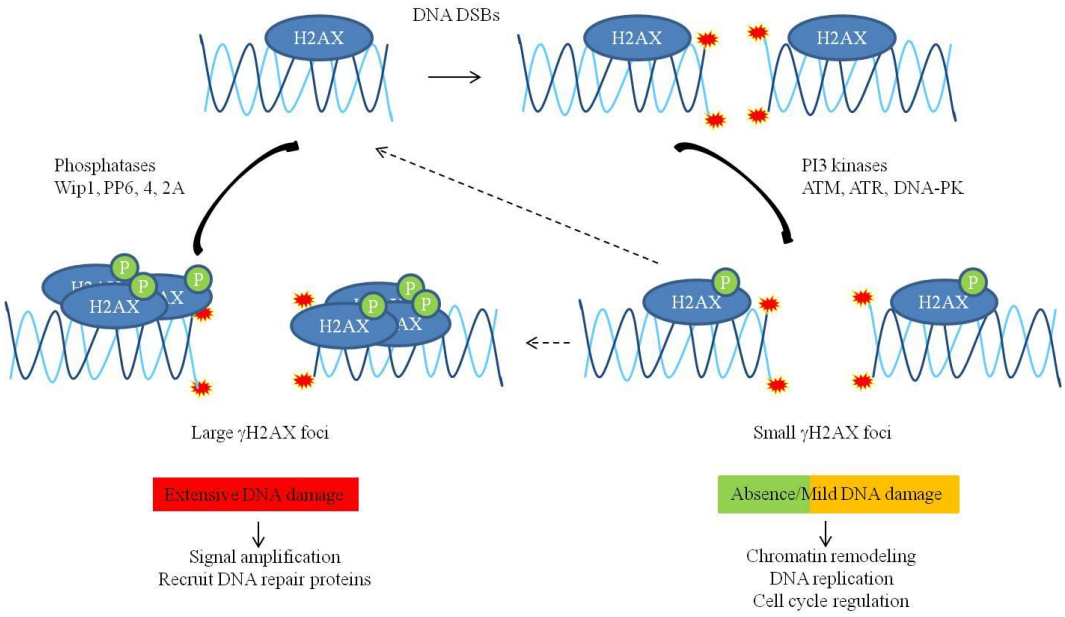
DNA DSBs
H2AX
H2AX
H2AX
Phosphatases
Wip1, PP6, 4, 2A
PI3 kinases
ATM, ATR, DNA-PK
P
H2AX
Large γH2AX foci
Small γH2AX foci
Extensive DNA damage
Absence/Mild DNA damage
Signal amplification
Recruit DNA repair proteins
Chromatin remodeling
DNA replication
Cell cycle regulation

The primary role of γH2AX is to further relax the chromatin at the site of damage and to allow the recruitment of repair proteins involved in the homologous recombination (error free), non-homologous end joining (error prone), or slow DNA dependent protein kinase-independent non-homologous end joining pathways (Audebert et al., 2004; IIiakis 2009). γH2AX is not necessary for the recruitment of the MRN complex (Mre11, Rad50 and Nbs1) and MDC1, 53BP1, BRCA1, ATM, and RNF8 DNA repair proteins (Celeste et al., 2002; Downs et al., 2004; van Attikum and Gasser, 2005; Rossetto et al., 2010) but γH2AX is required for their stabilization at the site of damage. The formation of γH2AX foci can also act as a signal amplification, cohesion recruitment and chromatin remodelling promoter. Upon the completion of DNA repair, phosphatases, such as p53-inducible phosphatase Wip 1 (Cha et al., 2010; Moon et al., 2010) and protein phosphatases 6, 4, and 2A (Chowdhury et al., 2005; Nakada et al., 2008; Douglas et al., 2010) dephosphorylate γH2AX and complete this cycle. The rapid detection and recruitment of γH2AX to DNA DSBs makes it a potential biodosimeter to measure genotoxic effects of drugs and radiation in cancer patients undergoing treatment (Rogakou et al., 1998; Bonner et al., 2008).

The detection of DNA DSBs by γH2AX can occur during physiological events, such as chromatin remodelling by topoisomerase II during spermiogenesis and early post-fertilization events, as well as during DNA replication by helicases (Figure 1.6). Even under physiological conditions, γH2AX is responsible for the DNA repair of DNA strand breaks and the regulation of cell cycle progression.

1.6.3.2 Poly(ADP-ribose) Polymerase 1, PARP1

Another cellular mechanism of defence against DNA damage is the recruitment and activity of PARP enzymes: PARP1, PARP2 (PARP1/2) and tankyrase 1 (Figure 1.7). PARP1 is the most abundant form and is activated in transcriptionally active cells or in response to DNA cleavage by topoiomerase II beta (Ju et al., 2006; Lis and Kraus, 2006). PARP1 is involved in the early detection and repair of DNA SSBs in the alternative non-homologous end joining

pathway of DSB repair (Audebert et al., 2004; IIiakis 2009), during spermatogenesis (Ahmed et al., 2010), and early embryonic development (Barton et al., 2007) and in the recruitment of DNA repair proteins involved in SSB/base excision repair pathways (Masson et al., 1998; Caldecott 2003; El-Khamisy et al., 2003).

Upon its activation and recruitment to DNA through its N-terminal zinc-binding domain, PARP forms poly (ADP-ribose) (PAR) polymers by transferring ADP-ribose moieties from NADH to a lysine or glutamate residue on acceptor proteins, such as chromatin binding proteins, DNA repair and checkpoint proteins (Figure 1.7). The principal acceptor protein for PAR is PARP1 (D'Amours et al., 1999); the auto-PARylation of PARP1 causes the release of PARP1 from DNA and inhibits PARP1 function. The long chains of PAR polymers signal the severity of the insult and promote a cellular fate decision between DNA repair and cell death (Altmeyer et al., 2009). Upon the completion of DNA repair, poly (ADP-ribose) glycosylase cleaves the glycosidic bonds between ADP-ribose units of PAR (Kim et al., 2005) and restores the normal DNA binding state of PARP1 for the next DDR event.

Extensive DNA damage can activate PARP-1 mediated caspase-independent cell death through the release of flavoprotein apoptosis inducible factor from mitochondria to the nucleus (Figure 1.7). Nuclear apoptosis inducible factor and endonuclease G induce large-scale DNA fragmentation, further activating PARP synthesis of PAR polymers (Schreiber et al., 2006). Excessive PAR hydrolysis may lead to energy depletion by increasing the adenosine monophosphate (AMP) to adenosine triphosphate (ATP) ratio, predisposing the cell to an autophagic state and cell death (Schreiber et al., 2006; Rouleau et al., 2010). The cellular decision between life and death is thought to be mediated by an unknown PAR threshold level.

Figure 1.7. PARP activity is a measure of DNA damage, repair and energy status. PARP1 is recruited to site of DNA SSBs and transfers ADP(ribose) from NADH to acceptor proteins to allow chromatin decondensation and the access of single strand repair SSR and base excision repair BER proteins to the site of DNA damage. PARG removes PAR polymers upon the completion of DNA repair and restores the DNA binding state of PARP1 for the next DDR event. Depending on the extent of DNA damage, the level of PAR polymer formation will influence the cell fate. In the absence of DNA damage, PAR regulates transcription and cell cycle progression. Mild DNA damage induces DNA repair and cell survival while extensive DNA damage depletes the cell of adenosine triphosphate (ATP) energy stores and promotes cell death. Adapted from Heeres and Hergenrother, (2007). Current Opinion in Chemical Biology 11, 644-653.

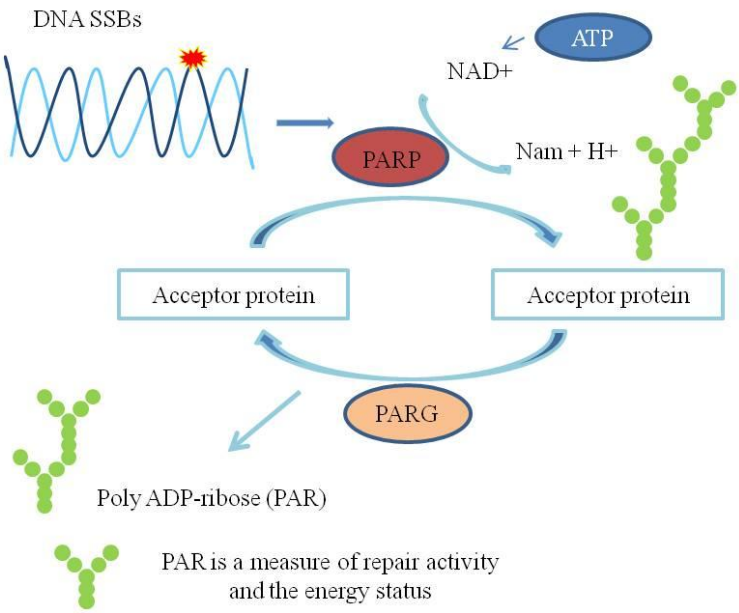

Absence of DNA damage

↓

Chromatin relaxation
Histones PARylation

↓

Regulation of transcription
Cell cycle division
Spindle checkpoint

Mild DNA damage

↓

Chromatin relaxation
Histones PARylation

↓

Recruitment of SSR and
BER repair proteins

↓

DNA repair
& cell survival

Extensive DNA damage

↓

PARP hyperactivation
NAD+, ATP energy depletion

↓

Caspase independent
cell death

Under physiological conditions, PARP participates in the regulation of transcription by the PARylation of histones and transcription factors, promoting chromatin relaxation (Figure 1.7). PARP also functions in the control of cell cycle division by the PARylation of kinetochore proteins, preventing chromosome mis-segregation during mitosis and promoting pericentric heterochromatin integrity. Moreover, the PARylation of centrosomes and spindle pole protein nuclear mitotic apparatus plays a role in the mitotic fidelity as a spindle checkpoint (Schreiber et al., 2006).

1.6.3.3 P53 Binding Protein 1, 53BP1

53BP1 is recruited to sites of DNA DSBs, marked by γH2AX, and acts as a mediator of DNA damage (Figure 1.8) (Anderson et al., 2001; Ward et al., 2006). 53BP1 mediates DNA damage repair by bringing the two broken DNA strands in close proximity. Depending on the extent of DNA damage, 53BP1 can induce cell cycle arrest (Figure 1.8) (Fernandez-Capetillo et al., 2002; Dimitrova et al., 2008). Independently of γH2AX, 53BP1 is recruited to sites of DNA DSBs by histone H4 (Sanders et al., 2004, Xie et al., 2007), H4K29me2 and H4K20me1 (Botuyan et al., 2006) to initiate alternative DNA repair pathways. 53BP1 was originally identified as a p53 binding protein promoting p53 transcription by its nuclear translocation and DNA binding functions (Iwabuchi et al., 1994; 1998).

In the absence of DNA damage, 53BP1 and γH2AX are expressed throughout preimplantation development and rarely co-localize suggesting an important role for 53BP1 in the early embryo (Figure 1.8) (Ziegler-Birling et al., 2009).

1.6.4 Spermatozoon DNA Damage Responses, DDR

The fate of the embryo fertilized by a spermatozoon with a damaged genome depends on three factors of increasing importance: the DNA damage response in the pre-meiotic male germ cell, the accumulation of DNA repair products in the oocyte and embryo, and the appropriate timing and gene expression profile of DDR during preimplantation development as reviewed in Jaroudi and SenGupta, 2007. There is an important disconnect between gene

expression profiles and protein levels in male and female gametes as well as in the early embryo. This disconnect is due to the uncoupling of transcription and translation to protein post-translational regulation and to protein degradation. Expression of genes involved in DNA damage responses is critical for the normal development of embryos, preventing infertility, birth defects, embryonic loss and cancer predisposition (Ronen and Glickman, 2001; Vinson and Hales, 2002; Friedberg and Meira, 2004).

Premeiotic male germ cells have an extensive proof reading and repair potential following DNA damage, with one of the lowest spontaneous mutation rates in the body (Baarends and Grootegoed, 2003; Hill et al., 2004). In addition, premeiotic male germ cells with extensive DNA damage are targeted for cell death during postmeiotic development; a minority of damaged spermatozoa are found in the epididymis (Roest et al., 1996). As opposed to premeiotic cells, post-meiotic male germ cells are more sensitive to genotoxic and epigenetic damage because they have lost their capacity to repair DNA and undergo apoptosis. Exposed postmeiotic male germ cells pass through chromatin silencing, when spermatids are remodelled into condensed spermatozoa, and escape both repair fidelity and cell death mechanisms; thus, these post-meiotic cells may transmit a damaged male genome to the early embryo. DNA damaged spermatozoa are a genetic source of point mutations, expanded simple tandem repeats and structural chromosome mutations (Chandley, 1991; Crow, 2000).

Once in the lumen of the testes, spermatozoa are no longer protected by the Sertoli cells and they must spend almost two weeks travelling through the epididymis, completing their post-testicular maturation. Moreover, spermatozoa can spend up to six days in the female reproductive tract waiting to fertilize an egg. The long post-testicular journey of spermatozoa renders them extremely vulnerable to DNA damaging agents, consequently decreasing their fertility potential as reviewed in Aitken et al., 2007.

Figure 1.8. p53 binding protein 1 as a mediator of DNA DSB damage. Independently of γH2AX or following γH2AX detection of DNA DSBs, 53BP1 mediates the repair of DNA DSBs by bringing the two broken strands in close proximity to promote ligation. In the absence of DNA damage, 53BP1 is an important regulator of preimplantation development while in the presence of mild to extensive DNA damage, 53BP1 mediates non-homologous end joining NHEJ repair or induces cell cycle arrest, respectively. Adapted from FitzGerald et al., (2009). Biochem Soc Trans. 37, 897-904.

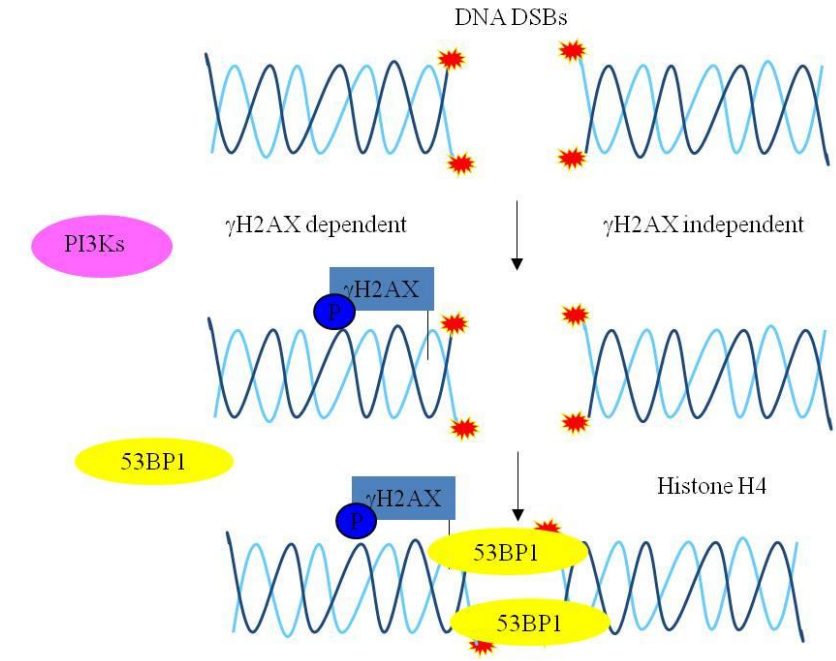

Absence of DNA damage	Mild DNA damage	Extensive DNA damage
↓	↓	↓
Embryonic development Regulation of mitosis	NHEJ DNA damage repair	Embryonic developmental delay Chromosome abnormality PCD

During the post-testicular journey of spermatozoa, DNA damage may occur during three important maturation processes as reviewed in Aitken et al., 2007. The first potential cause of DNA damage in spermatozoa is the progressive loss of the ability to undergo apoptosis. Advanced male germ cells have the potential to activate nucleases causing DNA fragmentation but are not able to complete the apoptotic pathway, leaving damaged germ cells to develop into spermatozoa. Second, the inefficient DNA repair system of DNA nicks during chromatin remodeling of spermatids is the second source of DNA damage, resulting in underprotamination and histone rich spermatozoa. The third source of DNA damage in spermatozoa is a reduction in the inter- and intra-molecular disulfide bonds in protamine during epididymal transit. Decreased protamine cross-linking affects spermatozoal chromatin compaction and enhances their sensitivity to oxidative stress. In specific cases, the load of DNA damage in spermatozoa is attenuated in infertile men taking anti-oxidant treatment.

Spermatozoa can be exposed to two sources of oxidative stress (Aitken et al., 2007). The first and most important producers of reactive oxygen species are the neutrophils present in the seminal fluid. Washing the sperm suspensions, as is done in infertility clinics, removes not only the neutrophils but also the antioxidant properties present in the seminal plasma. Deprived of the protection of antioxidant from seminal plasma, washed sperm are injected into the female reproductive tract and exposed to leukocytes, the female source of oxidative stress. To a much lesser extent, the residual cytoplasmic enzymatic content in non-functional spermatozoa is the second source of oxidative stress.

To overcome the potential sources of DNA damage, mammalian male germ cells have evolved mechanisms of DNA repair. During spermatogenesis, base excision repair seems to be the principal repair mechanism. Base excision repair proteins were detected in human and rat pre- and post-meiotic germ cells but their repair efficiency is enhanced in rat primary spermatocytes and round spermatids (Olsen et al., 2001). Human and rat germ cells contain high glycosylase enzymatic activity, important in the removal of uracil residues and the

repair of DNA alkylation bases as reviewed in Brunborg et al., 2007. Double strand break repair is active during spermiogenesis and participates in topoisomerase II induced DNA DSB repair by the recruitment of γH2AX during chromatin remodelling. Nucleotide excision repair activity varies among spermatogenic cell types and depends on the age of post-meiotic germ cells (Xu et al., 2005). Rat and human male germ cells are deprived of efficient nucleotide excision DNA repair against bulky DNA adducts induced by UV-light, benzo(a)pyrene and cisplatin. Low amounts of nucleotide excision repair associated proteins, as opposed to high amounts of mRNA transcripts of most nucleotide excision repair-related enzymes, are stored as ribonucleoprotein particles in a translational repressed state as reviewed in Brunborg et al., 2007. Mismatch repair is important during the mitotic phase of spermatogenesis, preventing the appearance of mutations and maintaining the germline integrity. In addition, mismatch repair is important for chromomosome recombination and pairing during gametogenesis (Baarends et al., 2001).

Post-meiotic round spermatids are expected to repair DSBs and chromosome aberrations by the non-homologous end-joining (NHEJ) pathway without initiating apoptosis following radiation exposures. The role of DNA repair during spermiogenesis was evaluated using the genetically modified male mouse SCID model for the classical NHEJ pathway and the Parp1-inhibited mice for the alternative Parp1/XRCC1 dependent NHEJ pathway. The additive effect of both active NHEJ repair pathways, DNA-PKcs and Parp1, during spermiogenesis was suggested by the loss of γH2AX foci after irradiation, indicating their role in modulating the amount of damage transmitted to the early zygote (Ahmed et al., 2010).

DNA damaged spermatozoa can only be repaired once they are in the oocyte by the accumulated and stored maternal repair products and by the early embryo after the first cell division. If the DNA damage is not repaired before the first zygotic division, it is propagated in all of the cells and potentially may be transmitted to the next generation (Marchetti et al., 2009).

1.6.5 Oocyte DNA Damage Responses, DDR

The best studied analysis of DDR during oogenesis was done in rhesus monkeys in which the expression of genes involved in DNA damage recognition, DNA repair and cell cycle arrest was investigated (Zheng et al., 2005). These investigators showed that there were variable expression levels of genes involved in DNA damage recognition, *ATM* and *ATR*, and genes involved in cell cycle progression, *CHECK1* and *CHECK2*. The DDR genomic expression profile was specific to the rhesus monkey oocyte since the human oocyte had a completely different profile (Wells et al., 2005; Zheng et al., 2005). A weak relative expression level of genes from all four repair pathways was observed throughout oogenesis, with some DDR and DNA repair genes peaking in mature MII oocytes compared to immature oocytes (Zheng et al., 2005). The overexpression of DNA repair genes in mature arrested oocytes has biological importance in the maintenance of the oocyte genomic integrity. The enhanced presence of DNA repair genes in mature oocytes is a mechanism of defence against insults during the long meiosis I arrest and time before ovulation (Zheng et al., 2005).

The oocyte specific stage and species specific expression level of genes involved in the repair of damage could severely impact the response of mature MII oocytes to certain types of DNA damaging insults. Therefore, the DDR efficiency of the fertilized oocyte to a damaged spermatozoon could ultimately affect the fate of the embryo. If a damaged oocyte is not repaired during oogenesis, the embryo relies on the maternal store of DNA repair for the first two cell cycle divisions and the newly synthesized zygotic DNA repair products for the next cell cycle cleavage stages.

1.6.6 Embryo DNA Damage Responses, DDR

1.6.6.1 DNA Repair

DNA repair genes are expressed throughout embryonic development but their level of expression varies depending on the embryonic developmental stage and genomic programming (Zheng et al., 2005). The oocyte and the zygote have

similar DNA repair gene expression profiles compared to the two-cell embryo because of the maternal to zygotic genomic transcription switch (Latham et al., 1991; Nothias et al., 1995). The genomic expression profile of DNA repair genes in four- to eight-cell embryos is completely different from the eight-cell embryo and the blastocyst due to the transcriptional transition during compaction (van Blerkom et al., 1975).

The genomic integrity of early embryos is under stress due to rapid DNA replication and proliferation; the absence of DNA repair genes and enzymes leads to death around the time of implantation (Vinson and Hales, 2002). Even with the presence of all four functional DNA repair pathways and the expression of many DNA repair genes at the cleavage stage, there may still be a limited capacity to repair DNA damage, leading to a high incidence of chromosomal abnormalities (Pfeiffer et al., 2000; Jackson, 2002; Bielanska et al., 2005).

Many zygotic features explain the genomic sensitivity to damage and the poor embryonic DDR. The first zygotic feature explaining the genomic sensitivity to DNA damage is the physical separation and epigenetic asymmetry between the male and female PNs (Adenot et al., 1997; Arney et al., 2002; van der Heijden et al., 2005).The second zygotic feature responsible for the DNA damage sensitivity is the transient DNA DSBs mediated by topoisomerase II during paternal chromatin remodelling in pre-pronuclear zygotes (Adenot et al., 1991; Bizzaro et al., 2000; Derijck et al., 2006). The third zygotic feature is the lack of transcription coupled translation. During the first two cell cycle divisions, the early embryo relies only on the maternal mRNAs and proteins stored in the oocyte (Schultz, 2002; Vinson and Hales, 2002; Hamatani et al., 2004). The last feature is the absence of G1/S checkpoint following fertilization (Shimura et al., 2002; Baart et al., 2004) and minimal functional cell cycle checkpoints in cleavage stage embryos (Delhanty and Handyside, 1995; Harrison et al., 2000). The cell cycle progression gene, *Check1*, is overexpressed in the mouse two-cell embryo compared to the zygote (Zeng et al., 2004). The regulation of mitotic progression in the cleavage stage embryo by the spindle assembly checkpoint is already active

at the first zygotic division in the mouse embryo, preventing premature metaphase-anaphase transition (Wei et al., 2011). Improper regulation or functioning of the spindle assembly checkpoint leads to misaligned chromosomes, increased incidence of micronuclei, aneuploidy, implantation failure, spontaneous abortion and embryonic loss (Wei et al., 2011).

1.6.6.2 Mitochondrial Activity

The progenitor pool of mitochondria following fertilization is entirely maternally inherited from the fully-grown oocyte. Mitochondria in oocytes and early embryos are the primary source of adenosine triphosphate (ATP) production (van Blerkom et al., 1995; Dumollard et al., 2007). In addition to the mitochondrial bioenergetic activities, mitochondria are important regulators of calcium homeostasis, cytoplasmic redox state and signal transduction. Defects in mitochondrial functions have detrimental consequences on fertilization and early embryonic development as reviewed in van Blerkom, 2011.

The contribution of mitochondria during early embryonic development is influenced by their numbers in mature oocytes, by the energy production required to support preimplantation development and by the equal distribution of mitochondria between blastomeres at every cell cycle division (van Blerkom, 2011). As the early embryo divides, the pool of mitochondria is evenly distributed between blastomeres; mitochondria begin their replication only after implantation (Larsson et al., 1998). The number of mitochondria per blastomere drops every cell division while the energetic requirements to support preimplantation development dramatically increase. In cleavage stage embryos mitochondria adopt a functional compartmentalization and structural transformation in a stage and space specific manner to provide higher bioenergetic levels in blastomere regions more efficiently when needed as reviewed in van Blerkom, 2011. The localization of high potential mitochondria is involved in the acquisition of fertilization competence (van Blerkom, 2011) by allowing sperm penetration (van Blerkom and Davis, 2007) and in cytokinesis, blastomere rotation and gap junction formation by increasing oolemmal fluidity (van Blerkom, 2008). It has

been proposed that the advantage of this stage and space specific regulation of energy supply and demand for the oocyte and early embryo is to limit the generation of reactive oxygen species from the activation of mitochondria to non-damaging levels. In the presence of DNA damage, the activation and maintenance of DDR and DNA repair enzymes require the energy produced by mitochondria.

1.7 Rationale for Thesis Studies

The incidence of cancer, such as testicular cancer, in men of reproductive age has been rising over the past decades in developed countries. High risk populations include men from Denmark, Switzerland and New Zealand; African-Americans have lower risk, while Chinese and Japanese men have a rare incidence of these tumors as reviewed in Joffe, 2001. Current chemotherapeutic regimens consist of a combination of radiation, alkylating agents, antibiotics, and alkaloids, all potent cytotoxic compounds. The early detection of cancer and aggressive chemotherapeutic treatments have increased the survival rate of these men and raised concerns about the long term effects of these treatments on their progeny outcome. Men treated with radiation and chemotherapeutics are faced with an initial drop in sperm production, causing infertility. This drop in spermatogenesis can last many months to several years (Howell and Shalet, 2005). Some of them will recover spermatogenesis with increased sperm count, while others show poor or no recovery. For those men who show a recovery, they face the possibility of transmitting heritable genetic diseases to their offspring.

Although the reproductive success rate in male cancer survivor couples wanting to conceive a child has been disappointing with longer time to pregnancy, spontaneous abortion, increase demand for assisted reproduction techniques (ARTs), increase childhood cancer and adult diseases, there is no clear cause-effect relationship to poorer semen quality (O'Flaherty et al., 2008; 2010). Normal pregnancy and development to term in human is a rather inefficient process (Edwards, 1986). It was suggested that over half of normally fertilized oocytes will not progress to term and this statistic increases with maternal age (Boue et al., 1975; Burgoyne et al., 1991; van Blerkom, 1994) due to

chromosomal mis-segregation and lethal aneuploidy. As opposed to the very limited epidemiological human data, we showed on numerous occasions in rodents a clear link between male germ cell quality and impact on pregnancy outcome and development and this over many generations.

1.8 Formulation of the Project

The purposes of these studies were first to evaluate the impact of paternal exposure to CPA on the progression of early embryonic developmental events and second to assess DNA damage responses activated in cleavage stage embryos. We hypothesized that paternal exposure to CPA will disrupt the early embryonic developmental events, epigenetic regulation and the activation of DNA damage responses, pre-determining the fate of cleavage stage embryos.

Research Objectives

(1) To elucidate the impact of paternal exposure to cyclophosphamide on epigenetic regulation of chromatin decondensation, remodelling and DNA damage recognition in pre-pronuclear zygotes.
(2) To characterise the micronuclei of cyclophosphamide-sired embryos during the first zygotic division and their impact on embryo survival.
(3) To assess the effect of paternal exposure to cyclophosphamide on the activation of DNA damage detection and repair responses in cleavage stage embryos.

The Sprague-Dawley rat is the model of choice for developmental toxicity studies for numerous reasons: stages of spermatogenesis and embryogenesis are very well characterized, mating studies are easily performed and female rats have short gestation period with consistent and large litter sizes. Cyclophosphamide is our drug model for the male-mediated developmental toxicity project. Male rats are treated with 6 mg/ kg/ day of CPA for a period of 4 weeks and mated to naturally cycling virgin females. This chemotherapeutic regimen is the human equivalent to chronic low doses given during immunosuppressive therapies. The embryos are collected at specific times following fertilization as determined by *in*

vivo or *in vitro* embryonic maturation experiments to assess the progression of early embryos during development. Immunofluorescence protocols are performed to elucidate the effect of paternal exposure on the early embryo development and activation of DNA damage responses.

Our results suggest that paternal exposure to CPA causes the dysregulation of early post-fertilization events as a consequence of epigenetic and genetic DNA damage. The activation of DDR is initiated by the early detection of DNA DSBs by γH2AX in pre-PN zygotes and cleavage stage embryos sired by cyclophosphamide exposed males. The DNA repair response measured by the formation of PAR polymers is decreased in cyclophosphamide sired eight-cell embryos. Paternal exposure to CPA induced the formation of functional MN enriched with γH2AX foci, 53BP1 immunoreactivity and PAR polymers compared to their nuclear counterparts. An increase in the incidence of MN was associated with a delay in the progression of embryos suggested a role in determining their fate.

Thus, this research evaluated the impact of paternal exposure to a DNA damaging agent on the capacity of the early embryo to mount an appropriate response. Secondly, it determined the potential value of measures of the DDR as markers of embryonic quality associated with developmental competence. The use of γH2AX and PAR as pharmacodynamic biomarkers to monitor DDR and guide clinical trials is already implemented in phase 0 in the field of cancer treatment to accelerate the validation of candidate drugs and identify suitable individuals to specific treatment (Redon et al., 2010). In light of our results, the detection of DNA damage by γH2AX and repair responses by PAR polymers in cleavage stage embryos have great potential for selective purposes in infertility clinics as biomarkers of embryonic developmental competence and survival capacity.

REFERENCES

Abdalla H, Yoshizawa Y, Hochi S. (2009). Active demethylation of paternal genome in mammalian zygotes. J Reprod Dev. 55, 356-360.

Adams RL, Burdon RH, Fulton J. (1983). Methylation of satellite DNA. Biochem Biophys Res Commun 113, 695-702.

Adenot PG, Mercier Y, Renard J-P, Thompson EM. (1997). Differential H4 acetylation of paternal and maternal chromatin precedes DNA replication and differential transcriptional activity in pronuclei of 1-cell mouse embryos. Development 124, 4615-4625.

Adenot PG, Szollosi MS, Geze M, Renard JP, Debey P. (1991). Dynamics of paternal chromatin changes in live one-cell mouse embryo after natural fertilization. Mol Reprod Dev. 2, 23-34.

Aguilar-Mahecha A, Hales BF, Robaire B. (2002). Chronic cyclophosphamide treatment alters the expression of stress response genes in rat male germ cells. Biology of Reproduction 66, 1024-1032.

Aguilar-Mahecha A, Hales BF, Robaire B. (2005). Effects of acute and chronic cyclophosphamide treatment on meiotic progression and the induction of DNA double-strand breaks in rat spermatocytes. Biology of Reproduction 72, 1297-1304.

Ahmed AR, Hombal SM. (1984). Cyclophosphamide (Cytoxan). A review on relevant pharmacology and clinical uses. J Am Acad Dermatol. 11, 1115-1126.

Ahmed EA, de Boer P, Philippens ME, Kal HB, de Rooij DG. (2010). Parp1-XRCC1 and the repair of DNA double strand breaks in mouse round spermatids. Mutat Res. 683, 84-90.

Aitken RJ, Roman SD, Baker MA, de Iuliis G. Redox regulation of DNA damage in the male germ line. In: Anderson D, Brinkworth MH (eds), Male-Mediated Developmental Toxicity, vol 1, 1st ed. Cambridge: RSC Publishing; 2007: 197-209.

Akabane H, Fan J, Xuehai Z, Zhu GZ. (2007). Protein kinase C activity in mouse eggs regulates gamete membrane interaction. Mol Reprod Dev. 74, 1465-1472.

Akiyama T, Kim JM, Nagata M, Aoki F. (2004). Regulation of histone acetylation during meiotic maturation in mouse oocytes. Mol Reprod Dev. 69, 222-227.

Akiyama T, Suzuki O, Matsuda J, Aoki F. Dynamic replacement of histone H3 variants reprograms epigenetic marks in early mouse embryos. PLoS Genetics published 7 October 2011; PMID 21998593.

Albertini DF. (1992). Regulation of meiotic maturation in the mammalian oocyte: interplay between exogenous cues and the microtubule cytoskeleton. BioEssays 14, 97-103.

Allard P, Yang Q, Marzluff WF, Clarke HJ. (2005). The stem-loop binding protein regulates translation of histone mRNA during mammalian oogenesis. Dev. Biol. 286, 195-206.

Altmeyer M, Messner S, Hassa PO, Fey M, Hottiger MO. (2009). Molecular mechanism of poly(ADP-ribosyl)ation by PARP1 and identification of lysine residues as ADP-ribose acceptor sites. Nucleic Acids Res. 37, 3723-3738.

Anderson D, Cemeli E, Schmid TE, Baumgartner A, Brinkworth MH, Wood JM. Oestrogenic compounds and oxidative stress. In: Anderson D, Brinkworth MH (eds), Male-mediated Developmental Toxicity, vol 1, 1st ed. Cambridge: RSC Publishing; 2007: 259-272.

Anderson L, Henderson C, Adachi Y. (2001). Phosphorylation and rapid relocalization of 53BP1 to nuclear foci upon DNA damage. Mol Cell Biol. 21, 1719-1729.

Anway MD, Cupp AS, Uzumcu M, Skinner MK. (2005). Epigenetic transgenerational actions of endocrine disruptors and male fertility. Science 308, 1466-1469.

Aoki F, Worrad DM, Schultz RM (1997). Regulation of transcriptional activity during the first and second cell cycles in the preimplantation mouse embryo. Dev Biol. 181, 296-307.

Arnold DR, Francon P, Zhang J, Martin K, Clarke HJ. (2008). Stem-loop binding protein expressed in growing oocytes is required for accumulation of mRNAs encoding histones H3 and H4 and for early embryonic development in the mouse. Dev Biol. 313, 347-358.

Arpanachi A, Brinkworth M, Iles D, Krawetz SA, Paradowska A, Platts AE, Saida M, Steger K, Tedder P, Miller D. (2009). Endonuclease-sensitive regions of human spermatozoa chromatin are highly enriched in promoter and CTCF binding sequences. Genome Res. 19, 1338-1349.

Arney KL, Bao S, Bannister AJ, Kouzarides T, Surani MA. (2002). Histone methylation defines epigenetic asymmetry in the mouse zygote. Int J Dev Biol. 46, 317-320.

Assey RJ, Hytell P, Greve T, Purwantara B. (1994). Oocyte morphology in dominant and subordinate follicles. Mol Reprod Dev. 37, 335-344.

Audebert M, Salles B, Calsou P. (2004). Involvement of poly(ADP-ribose) polymerase-1 and XRCC1/DNA ligase III in an alternative route for DNA double-strand breaks rejoining. J Biol Chem. 279, 55117-55126.

Baarends WM, Grootegoed JA. (2003). Chromatin dynamics in the male meiotic prophase. Cytogenet Genome Res. 103, 225-234.

Baart EB, van der Heijden GW, van der Hoeven FA, Bakker R, Cooper TG, de Boer P. (2004). Reduced oocyte activation and first cleavage rate after ICSI with spermatozoa from a sterile mouse chromosome mutant. Hum Reprod. 19, 1140-1147.

Balhorn R. (1982). A model for the structure of chromatin in mammalian sperm. J Cell Biol. 93, 298-305.

Balhorn R, Gledhill BL, Wyrobek AJ. (1977). Mouse sperm chromatin proteins: quantitative isolation and partial characterization. Biochemistry 16, 4074-4080.

Ball AR, Yokomori K. (2011). Damage site chromatin: open or closed? Current Opinion in Cell Biology 23, 277-283.

Barski A, Cuddapah S, Cui K, Roh TY, Schones DE, Wang Z, Wei G, Chepelev I, Zhao K. (2007). High-resolution profiling of histone methylations in the human genome. Cell 129, 823-837.

Barton TS, Robaire B, Hales BF. (2005). Epigenetic programming in the preimplantation rat embryo is disrupted by chronic paternal cyclophosphamide exposure. Proc Natl Acad Sci U S A 102, 7865-7870.

Barton TS, Robaire B, Hales BF. (2007). DNA damage recognition in the rat zygote following chronic paternal cyclophosphamide exposure. Toxicological Sciences 100, 495-503.

Bielanska M, Jin S, Bernier M, Tan SL, Ao A. (2005). Diploid-aneuploid mosaicism in human embryos cultured to the blastocyst stage. Fertil Steril. 84, 336-342.

Bonner WM, Redon CE, Dickey JS, Nakamura AJ, Sedelnikova OA, Solier S, Pommier Y. (2008). gammaH2AX and cancer. Nat Rev Cancer 8, 957-967.

Borum K. (1967). Oogenesis in the mouse. A study of the origin of the mature ova. Exp Cell Res. 45, 39-47.

Botuyan MV, Lee J, Ward IM, Kim JE, Thompson JR, Chen J, Mer G. (2006). Structural basis for the methylation state-specific recognition of histone H4-K20 by 53BP1 and Crb2 in DNA repair. Cell 127, 1361-1373.

Boue J, Boue A, Lazar P. (1975). Retrospective and prospective epidemiological studies of 1500 karyotyped spontaneous human abortions. Teratology 12, 11-26.

Bird AP. (1986). CpG-rich islands and the function of DNA methylation. Nature 321, 209-213.

Bizzaro D, Manicardi G, Bianchi PG, Sakkas D. (2000). Sperm decondensation during fertilisation in the mouse: presence of DNase I hypersensitive sites in situ and a putative role for topoisomerase II. Zygote 8, 197-202.

Bouniol C, Nguyen E, Debey P. (1995). Endogenous transcription occurs at the 1-cell stage in the mouse embryo. Exp Cell Res. 218, 57-62.

Brunborg G, Duale N, Tesdal Haaland J, Bjørge C, Søderlung E, Dybing E, Wiger R, Olsen AK. DNA repair capacities in testicular cells of rodents and man. In: Anderson D, Brinkworth MH (eds), Male-mediated Developmental Toxicity, vol 1, 1st ed. Cambridge: RSC Publishing; 2007: 273-285.

Buchanan JD, Fairley KF, Barrie JU. (1975). Return of spermatogenesis after stopping cyclophosphamide therapy. Lancet 2, 156-157.

Burgoyne P, Holland K, Stephens R. (1991). Incidence of numerical chromosome abnormalities in human pregnancy: estimation from induced and spontaneous abortion data. Hum Reprod. 6, 555-564.

Burkart AD, Xiong B, Baibakov B, Jiménez-Movilla M, Dean J. (2012). Ovastacin, a cortical granule protease, cleaves ZP2 in the zona pellucida to prevent polyspermy. J Cell Biol. 197, 37-44.

Cai L, Hales BF, Robaire B. (1997). Induction of apoptosis in the germ cells of adult male rats after exposure to cyclophosphamide. Biol Reprod. 56, 1490-1497.

Caldecott KW. (2003). XRCC1 and DNA strand break repair. DNA repair (AMSt) 2, 955-969.

Carrier F, Georgel PT, Pourquier P, Blake M, Kontny HU, Antinore MJ, Gariboldi M, Myers TG, Weinstein JN, Pommier Y, Fornace AJ Jr. (1999). Gadd45, a p53-responsive stress protein, modifies DNA accessibility on damaged chromatin. Mol Cell Biol. 19, 1673-1685.

Celeste A, Fernandez-Capetillo O, Kruhlak MJ, Pilch DR, Staudt DW, Lee A, Bonner RF, Bonner WM, Nussenzweig A. (2003). Histone H2AX phosphorylation is dispensable for the initial recognition of DNA breaks. Nat Cell Biol. 5, 675-679.

Celeste A, Petersen S, Romanienko PJ, Fernandez-Capetillo O, Chen HT, Sedelnikova OA, Reina-San-Martin B, Coppola V, Meffre E, Difilippantonio MJ, Redon C, Pilch DR, Olaru A, Eckhaus M, Camerini-Otero RD, Tessarollo L, Livak F, Manova K, Bonner WM, Nussenzweig MC, Nussenzweig A. (2002). Genomic instability in mice lacking histone H2AX. Science 296, 922-927.

Cha H, Lowe JM, Li H, Lee JS, Belova GI, Bulavin DV, Fornace AJ Jr. (2010). Wip1 directly dephosphorylates γ-H2AX and attenuates the DNA damage response. Cancer Res. 70, 4112-4122.

Chan HM, Narita M, Lowe SW, Livingston DM. (2005). The p400 E1A-associated protein is a novel component of the p53→p21 senescence pathway. Genes Dev. 19, 196-201.

Chandley AC. (1991). On the parental origin of de novo mutation in man. J Med Genet. 28, 217-223.

Chang CC, Ma Y, Jacobs S, Tian XC, Yang X, Rasmussen TP. (2005). A maternal store of macroH2A is removed from pronuclei prior to onset of somatic macroH2A expression in preimplantation embryos. Dev Biol. 278, 367-380.

Chen L, Wang D, Wu Z, Ma L, Daley G Q. (2010). Molecular basis of the first cell fate determination in mouse embryogenesis. Cell Res. 20, 982-993.

Chohan K, Badaway S. (2010). Cigarette smoking impairs sperm bioenergetics. Int Braz J Urol. 36, 60-65.

Chouinard LA. (1975). A light- and electron-microscope study of the oocyte nucleus during development of the antral follicle in the prepubertal mouse. J Cell Sci. 17, 589-615.

Chowdhury D, Keogh MC, Ishii H, Peterson CL, Buratowski S, Lieberman J. (2005). γ-H2AX dephosphorylation by protein phosphatise 2A facilitates DNA double-strand break repair. Mol Cell 20, 801-809.

Christian E, Rao VH, Renard JP. (1994). Sequential acquisition of transcriptional control during early embryonic development in the rabbit. Dev Biol. 164, 160-172.

Christova R, Oelgeschlager T. (2002). Association of human TFIID-promoter complexes with silenced mitotic chromatin in vivo. Nature Cell Biol. 4, 79-82.

Churikov D, Siino J, Svetlova M, Zhang K, Gineitis A, Morton Bradbury E, Zalensky A. (2004b). Novel human testis-specific histone H2B encoded by the interrupted gene on the X chromosome. Genomics 84, 745-756.

Churikov D, Zalenskaya IA, Zalensky AO. (2004a). Male-germline-specific histones in mouse and man. Cytogenetic and Genome Research 105, 203-214.

Cioffi JA, VanBlerkom J, Antczak M, et al. (1997). The expression of leptin and its receptors in pre-ovulatory human follicles. Mol Hum Reprod. 3, 467-472.

Clapier CR, Cairns BR. (2009). The biology of chromatin remodeling complexes. Annu Rev Biochem. 78, 273-304.

Clermont Y. (1972). Kinetics of spermatogenesis in mammals: seminiferous epithelium cycle and spermatogonial renewal. Physiol Rev. 52, 198-236.

Codrington AM, Hales BF, Robaire B. (2004). Spermiogenic germ cell phase-specific DNA damage following cyclophosphamide exposure. J Androl. 25, 354-362.

Crow JF. (2000). The origins, patterns and implications of human spontaneous mutation. Nat Rev Genet. 1, 40-47.

Curley JP, Mashoodh R, Champagne FA. (2011). Epigenetics and the origins of paternal effects. Horm Behav. 59, 306-314.

D'Amours D, Desnoyers S, D'Silva I, Poirier GG. (1999). Poly(ADP-ribosyl) ation reactions in the regulation of nuclear functions. Biochem J. 342, 249-268.

D'Occhio MJ, Hengstberger KJ, Johnston SD. (2007). Biology of sperm chromatin structure and relationship to male fertility and embryonic survival. Anim Reprod Sci. 101, 1-17.

de Jonge ME, Huitema ADR, Rodenhuis S, Beijnen JH. (2005). Clinical pharmacokinetics of cyclophosphamide. Clin Pharmacokinet. 44, 1135-1164.

de La Fuente R. (2006). Chromatin modifications in the germinal vesicle (GV) of mammalian oocytes. Dev Biol. 292, 1-12.

de Lamirande E, O'Flaherty C. (2008). Sperm activation: role of reactive oxygen species and kinases. Biochem Biophys Acta. 1784, 106-115.

de Vantery C, Stutz A, Vassalli JD, Schorderet-Slatkine S. (1997). Acquisition of meiotic competence in growing mouse oocytes is controlled at both translational and post-translational levels. Dev Biol. 174, 335-344.

Delhanty JD, Handyside AH. (1995). The origin of genetic defects in the human and their detection in the preimplantation embryo. Hum Reprod Update 1, 201-215.

Delouis C, Bonnerot C, Vernet M, Nicolas JF. (1992). Expression of microinjected DNA and RNA in early rabbit embryos : changes in permissiveness for expression and transcriptional selectivity. Exp Cell Res. 201, 284-291.

Derijck A, van der Heijden G, Giele M, Philippens M, de Boer P. (2008). DNA double-strand break repair in paternal chromatin of mouse zygotes, the first cell cycle as an origin of de novo mutation. Human Molecular Genetics 17, 1922-1937.

Derijck AA, van der Heijden GW, Giele M, Philippens ME, van Bavel CC, de Boer P. (2006). gammaH2AX signaling during sperm chromatin remodelling in the mouse zygote. DNA Repair (Amst.) 5, 959-971.

Dimitrova N, Chen YC, Spector DL, de Lange T. (2008). 53BP1 promotes non-homologous end joining of telomeres by increasing chromatin mobility. Nature 456, 524-528.

Dobrzyńska MM, Czajka U, Tyrkiel EJ. Male-mediated F1 effects in mice exposed to Di(2-ethylhexyl)phthalates (DEHP). In: Anderson D, Brinkworth MH (eds), Male-mediated Developmental Toxicity, vol 1, 1st ed. Cambridge: RSC Publishing; 2007: 97-113.

Douglas P, Zhong J, Ye R, Moorhead GB, Xu X, Lees-Miller SP. (2010). Protein phosphatase 6 intereacts with the DNA-dependent protein kinase catalytic subunit and dephosphorylates γ-H2AX. Mol Cell Biol. 30, 1368-1381.

Downs JA, Allard S, Jobin-Robitaille O, Javaheri A, Auger A, Bouchard N, Kron SJ, Jackson SP, Côté J. (2004). Binding of chromatin-modifying activities to phosphorylated histone H2A at DNA damage sites. Mol Cell 16, 979-990.

Dubrova YE. Radiation-induced transgenerational instability in mice. In: Anderson D, Brinkworth MH (eds), Male-mediated Developmental Toxicity, vol 1, 1st ed. Cambridge: RSC Publishing; 2007: 224-234.

Dumollard R, Duchen M, Carroll J. (2007). The role of mitochondrial function in the oocyte and embryo. Curr Top Dev Biol. 77, 21-49.

Eberharter A, Becker PB. (2002). Histone acetylation: a switch between repressive and permissive chromatin. Second in review series on chromatin dynamics. EMBO Rep. 3, 224-229.

Edwards R. (1986). Causes of early pregnancy loss. Hum Reprod. 1, 185-198.

El-Khamisy SF, Masutani M, Suzuki H, Caldecott KW. (2003). A requirement for PARP-1 for the assembly or stability of XRCC1 nuclear foci at sites of oxidative DNA damage. Nucleic Acids Res. 31, 5526-5533.

Eskenazi B, Kidd SA, Marks AR, Sloter E, Block G, Wyrobek AJ. (2005). Antioxidant intake is associated with semen quality in healthy men. Hum Reprod. 20, 1006-1012.

Fairley KF, Barrie JU, Johnson W. (1972). Sterility and testicular atrophy related to cyclophosphamide therapy. Lancet 1, 568-569.

Farthing CR, Ficz G, Ng RK, Chan CF, Andrews S, Dean W, Hemberger M, Reik W. Global mapping of DNA methylation in mouse promoters reveals epigenetic reprogramming of pluripotency genes. PLoS Genet published 27 June 2008; PMID 18584034.

Fawcett DW. (1975). The mammalian spermatozoon. Dev Biol. 44, 394-436.

Feinberg AP, Tycko B. (2004). The history of cancer epigenetics. Nat Rev Cancer 4, 143-153.

Felsenfeld G. (1992). Chromatin as an essential part of the transcriptional mechanism. Nature 355, 219-224.

Fenech M, Kirsch-Volders M, Natarajan AT, Surralles J, Crott JW, Parry J, Norppa H, Eastmond DA, Tucker JD, Thomas P. (2011). Molecular mechanisms of micronucleus, nucleoplasmic bridge and nuclear bud formation in mammalian and human cells. Mutagenesis 26, 125-132.

Fernandez-Capetillo O, Chen HT, Celeste A, Ward I, Romanienko PJ, Morales JC, Naka K, Xia Z, Camerini-Otero RD, Motoyama N, Carpenter PB, Bonner WM, Chen J, Nussenzweig A. (2002). DNA damage-induced G2-M checkpoint activation by histone H2AX and 53BP1. Nat Cell Biol. 4, 993-997.

FitzGerald JE, Grenon M, Lowndes NF. (2009). 53BP1: function and mechanisms of focal recruitment. Biochem Sci Trans. 37, 897-904.

Fraga C, Motchnik P, Wyrobek A, Rempel D, Ames B. (1996). Smoking and low antioxidant levels increase oxidative damage to sperm DNA. Mutat Res. 351, 199-203.

Friedberg EC, Meira LB. (2004). Database of mouse strains carrying targeted mutations in genes affecting biological responses to DNA damage. (Version 6). DNA repair (Amst.) 3, 1617-1638.

Fronczak CM, Kim ED, Barqawi AB. (2011). The insults of illicit drug use on male fertility. Journal of Andrology Epub PMID: 21799144.

Fukutani K, Ishida H, Shinohara M, Minowada S, Niijima T, Hijikata K, Izawa Y. (1981). Suppression of spermatogenesis in patients with Behcet's disease treated with cyclophosphamide and colchicines. Fertil Steril. 36, 76-80.

Fulka Jr J, First NL, Moor RM. (1998). Nuclear and cytoplasmic determinants involved in the regulation of mammalian oocyte maturation. Molecular Human Reproduction 4, 41-49.

Gahlay G, Gauthier L, Baibakov B, Epifano O, Dean J. (2010). Gamete recognition in mice depends on the cleavage status of an egg's zona pellucid protein. Science 329, 216-219.

Galanty Y, Belotserkovskaya R, Coates J, Polo S, Miller KM, Jackson SP. (2009). Mammalian SUMO E3-ligases PIAS1 and PIAS4 promote responses to DNA double-strand breaks. Nature 462, 935-939.

Gao S, Chung YG, Parseghian MH, King GJ, Adashi EY, Latham KE. (2004). Rapid H1 linker histone transitions following fertilization or somatic cell nuclear

transfer: evidence for a uniform developmental program in mice. Dev Biol. 266, 62-75.

Gardner MJ, Snee MP, Hall AJ, Powell CA, Downes, Terrell JD. (1990). Results of case-control study of leukaemia and lymphoma among young people near Sellafield nuclear plant in west Cumbria. Br Med J. 300, 423-429.

Gatewood JM, Cook GR, Balhorn R, Bradbury EM, Schmid CW. (1987). Sequence-specific packaging of DNA in human sperm chromatin. Science 236, 962-964.

Gatewood JM, Cook GR, Balhorn R, Schmid CW, Bradbury EM. (1990). Isolation of four core histones from human sperm chromatin representing a minor subset of somatic histones. J Biol Chem. 265, 20662-20666.

Gevry N, Chan HM, Laflamme L, Livingston DM, Gaudreau L. (2007). P21 transcription is regulated by differential localization of histone H2A.Z. Genes Dev. 21, 1869-1881.

Gineitis AA, Zalenskaya IA, Yau PM, Bradbury EM, Zalensky AO. (2000). Human sperm telomere-binding complex involves histone H2B and secures telomere membrane attachment. J Cell Biol. 151, 1591-1598.

Govin J, Escoffier E, Rousseaux S, Kuhn L, Ferro M, Thevenon J, Catena R, Davidson I, Garin J, Khochbin S, Caron C. (2007). Pericentric heterochromatin reprogramming by new histone variants during mouse spermiogenesis. J of Cell Biology 176, 283-294.

Green DM, Kawashima T, Stovall M, Leisenring W, Sklar CA, Mertens AC, Donaldson SS, Byrne J, Robinson LL. (2010). Fertility of male survivors of childhood cancer: a report from the childhood cancer survivor study. J Clin Oncol. 28, 332-339.

Grenier L, Robaire B, Hales BF. (2010). Paternal exposure to cyclophosphamide affects the progression of sperm chromatin decondensation and activates a DNA damage response in the prepronuclear rat zygote. Biol Reprod. 83, 195-204.

Grenier L, Robaire B, Hales BF. Paternal cyclophosphamide exposure induces the formation of functional micronuclei during the first zygotic division. PLoS One published 16 November 2011; PMID 22110683.

Guenther MG, Levine SS, Boyer LA, Jaenisch R, Young RA. (2007). A chromatin landmark and transcription initiation at most promoters in human cells. Cell 130, 77-88.

Gupta SK, Bansal P, Ganguly A, Bhandari B, Chakrabarti K. (2009). Human zona pellucida glycoproteins: functional relevance during fertilization. J Reprod Immunol. 83**,** 50–55.

Gupta SK, Bhandari B. (2011). Acrosome reaction: relevance of zona pellucida glycoproteins. Asian Journal of Andrology 13, 97–105.

Haaf T. (2006). Methylation dynamics in the early mammalian embryo: implications of genome reprogramming defects for development. Curr Top Microbiol Immunol. 310, 13-22.

Hajkova P. (2010). Epigenetic reprogramming-taking a lesson from the embryo. Curr Opin Cell Biol 22, 342-350.

Hales BF, Crosman K, Robaire B. (1992). Increased postimplantation loss and malformations among the F2 progeny of male rats chronically treated with cyclophosphamide. Teratology 45, 671-678.

Hales BF, Grenier L, Lalancette C, Robaire B. (2011). Epigenetic programming : from gametes to blastocyst. Birth Defects Research A Clin Mol Teratol. 91, 652-665.

Hamatani T, Carter MG, Sharov AA, Ko MS. (2004). Dynamics of global gene expression changes during mouse preimplantation development. Dev Cell 6, 117-131.

Hammoud SS, Nix DA, Zhang H, Purwar J, Carrell DT, Cairns BR. (2009). Distinctive chromatin in human sperm packages genes for embryo development. Nature 460, 473-478.

Handel MA, Cobb J, Eaker S. (1999). What are the spermatocyte's requirements for successful meiotic division? J Exp Zool. 285, 243-250.

Harrison RH, Kuo HC, Scriven PN, Handy side AH, Ogilvie CM. (2000). Lack of cell cycle checkpoints in human cleavage stage embryos revealed by a clonal pattern of chromosomal mosaicism analysed by sequential multicolour FISH. Zygote 8, 217-224.

Harrouk W, Codrington A, Vinson B, Robaire B, Hales BF. (2000a). Paternal exposure to cyclophosphamide induces DNA damage and alters the expression of DNA repair genes in the rat preimplantation embryo. Mutation Research 461, 229-241.

Harrouk W, Khatabaksh S, Robaire B, Hales BF. (2000b). Paternal exposure to cyclophosphamide dysregulates the gene activation program in rat preimplantation embryos. Mol Reprod Devel. 57, 214-223.

Harrouk W, Robaire B, Hales BF. (2000c). Paternal exposure to cyclophosphamide alters cell-cell contacts and activation of embryonic transcription in the preimplantation rat embryo. Biol Reprod. 63, 74-81.

Heeres JT & Hergenrother PJ. (2007). Poly(ADP-ribose) makes a date with death. Current Opinion in Chemical Biology 11, 644-653.

Hengstler JG, Hengst A, Fuchs J, Tanner B, Pohl J, Oesch F. (1997). Induction of DNA crosslinks and DNA strand lesions by cyclophosphamide after activation by cytochrome P450 2B1. Mutat Res. 373, 215-223.

Hill KA, Buettner VL, Halangoda A, Kunishige M, Moore SR, Longmate J, Scaringe WA, Sommer SS. (2004). Spontaneous mutation in Big Blue mice from fetus to old age: tissue-specific time courses of mutation frequency but similar mutation types. Environ Mol Mutagen 43, 110-120.

Horak S, Polanska J, Widlak P. (2003). Bulky DNA adducts in human sperm: relationship with fertility, semen quality, smoking, and environmental factors. Mutat Res. 537, 53-65.

Howell SJ, Shalet SM. (2005). Spermatogenesis after cancer treatment: damage and recovery. J Natl Cancer Inst Monogr. 34,12-17.

Huang S, Ratliff K, Matouschek A. (2002). Protein unfolding by the mitochondrial membrane potential. Nat Struc Biol. 9, 301-307.

Huber A, Bai P, de Murcia JM, de Murcia G. (2004). PARP-1, PARP-2 and ATM in the DNA damage response: functional synergy in mouse development. DNA Repair 3, 1103-1108.

Huckins C. (1971). Cell cycle properties of differentiating spermatogonia in adult Sprague-Dawley rats. Cell Tissue Kinet. 4,139-154.

Hud NV, Downing KH, Balhorn R. (1995). A constant radius of curvature model for the organization of DNA in toroidal condensates. Proc Natl Acad Sci USA 92, 3581-3585.

Huen MS, Grant R, Manke I, Minn K, Yu X, Yaffe MB, Chen J. (2007). RNF8 transduces the DNA-damage signal via histone ubiquitylation and checkpoint protein assembly. Cell 131, 901-914.

Huitema AD, Mathôt RA, Tibben MM, Rodenhuis S, Beijnen JH. (2001). A mechanism-based pharmacokinetic model for the cytochrome P450 drug-drug interaction between cyclophosphamide and thioTEPA and the autoinduction of cyclophosphamide. J Pharmacokinet Pharmacodyn. 28, 211-230.

Huyen Y, Zgheib O, Ditullio RAJr, Gorgoulis VG, Zacharatos P, Petty TJ, Sheston EA, Mellert HS, Stavridi ES, Halazonetis TD. (2004). Methylated lysine 79 of histone H3 targets 53BP1 to DNA double-strand breaks. Nature 432, 406-411.

IIiakis G. (2009). Backup pathways of NHEJ in cells of higher eukaryotes: cell cycle dependence. Radiother Oncol. 92, 310-315.

Iwabuchi K, Bartel PL, Li B, Marraccino R, Fields S. (1994). Two cellular proteins that bind to wild-type but not mutant p53. Proc Natl Acad Sci USA 91, 6098-6102.

Iwabuchi K, Li B, Massa HF, Trask BJ, Date T, Fields S. (1998). Stimulation of p53-mediated transcriptional activation by the p53-binding proteins, 53BP1 and 53BP2. J Biol Chem. 273, 26061-26068.

Iwamatsu T, Chang MC. (1970). Further investigation of capacitation of sperm and fertilization of mouse eggs in vitro. J Exp Zool. 175, 271-281.

Jackson SP. (2002). Sensing and repairing DNA double-strand breaks. Carcinogenesis 23, 687-696.

Jaroudi S, SenGupta S. (2007). DNA repair in mammalian embryos. Mutation Research 635, 53-77.

Jha S, Shibata E, Dutta A. (2008). Human Rvb1/Tip49 is required for the histone acetylatransferase activity of Tip60/NuA4 and for the downregulation of phosphorylation on H2AX after DNA damage. Mol Cell Biol. 28, 2690-2700.

Joffe M. What harms the developing male reproductive system? In: Anderson D, Brinkworth MH (eds), Male-Mediated Developmental Toxicity, vol 1, 1st ed. Cambridge: RSC Publishing; 2007: 28-50.

Joffe M. (2001). Are problems with male reproductive health caused by endocrine disruption? Occup Environ Med. 58, 281-288.

Ju BG, Lunyak VV, Perissi V, Garcia-Bassets I, Rose DW, Glass CK, Rosenfeld MG. (2006). A topoisomerase IIbeta-mediated dsDNA break required for regulated transcription. Science 312, 1798-1802.

Karmakar P, Seki M, Kanamori M, Hashiguchi K, Ohtsuki M, Murata E, Inoue E, Tada S, Lan L, Yasui A, Enomoto T. (2006). BLM is an early responder to DNA double-strand breaks. Biochem Biophys Res Commun. 348, 62-69.

Kavlock R, Boeckelheide K, Chapin R, Cunningham M, Faustman E, Foster P, Golub M, Henderson R, Hinberg I, Little R, Seed J, Shea K, Tabacova S, Tyl R, Williams P, Zacharowski T. (2002). NTP center for the evaluation of risks to human reproduction: phthalates expert panel report on the reproductive and developmental toxicity of di(2-ethylhexyl)phthalate. Reprod Tox. 16, 529-653.

Kelly SM, Robaire B, Hales BF. (1994). Paternal cyclophosphamide exposure causes decreased cell proliferation in cleavage-stage embryos. Biol Reprod. 50, 55-64.

Kim MY, Zhang T, Kraus WL. (2005). Poly(ADP-ribosyl)ation by PARP-1: ‘PAR-laying’ NAD+ into a nuclear signal. Genes Dev. 19, 1951-1967.

Koppers A, De Luliis G, Finnie J, McLaughlin E, Aitken R. (2008). Significant mitochondrial reactive oxygen species in the generation of oxidative stress in spermatozoa. J Clin Endocrinol Metab. 93, 3199-3207.

Kourmouli N, Jeppesen P, Mahadevhaiah S, Burgoyne P, Wu R, Gilbert DM, Bongiorni S, Prantera G, Fanti L, Pimpinelli S, Shi W, Fundele R, Singh PB. (2004). Heterochromatin and tri-methylated lysine 20 of histone H4 in animals. J Cell Sci. 117, 2491-2501.

Krishnakumar R, Kraus WL. (2010). The PARP side of the nucleus: molecular actions, physiological outcomes, and clinical targets. Mol Cell 39, 8-24.

Kusch T, Florens L, Macdonald WH, Swanson SK, Glaser RL, Yates JR, 3rd, Abmayr SM, Washburn MP, Workman JL. (2004). Acetylation by Tip60 is required for selective histone variant exchange at DNA lesions. Science 306, 2084-2087.

Kuretake S, Kimura Y, Hoshi K, Yanagimachi R. (1996). Fertilization and development of mouse oocytes injected with isolated sperm heads. Biol Reprod. 55, 789-795.

Lan J, Hua S, Yuan Y, Zhan L, He X, Zhang Y. (2010). Methylation patterns in 5' terminal regions of pluripotency-related genes in mature bovine gametes. Zygote 7, 1-5.

Lan L, Nakajima S, Komatsu K, Nussenzweig A, Shimamoto A, Oshima J, Yasui A. (2005). Accumulation of Werner protein at DNA double-strand breaks in human cells. J Cell Sci. 118, 4153-4162.

Larsson N, Wang J, Wilhemsson H, Oldfors A, Rustin P, Lewandoski M, Barsh G, Clayton D. (1998). Mitochondria transcription factor A is necessary for mtDNA maintenance and embryogenesis in mice. Nat Genet. 18, 231-236.

Lantham KE, Garrels JI, Chang C, Solter D. (1991). Quantitative analysis of protein synthesis in mouse embryos. I. Extensive reprogramming at the one- and two-cell stages. Development 112, 921-932.

Latham KE, Solter D, Schultz RM. (1991). Activation of a two-cell stage-specific gene following transfer of heterologous nuclei into enucleated mouse embryos. Mol Reprod Dev. 30, 182-186.

Lemasters J, Ramshesh V. (2007). Imaging of mitochondrial polarization and depolarization with cationic fluorophores. Meth Cell Biol. 80, 283-295.

Leno GH, Mills AD, Philpott A, Laskey RA. Hyperphosphorylation of nucleoplasmin facilitates Xenopus sperm decondensation at fertilization. J Biol Chem. 1996; 271:7253-7256.

Lepikhov K, Walter J. (2004). Differential dynamics of histone H3 methylation at positions K4 and K9 in the mouse zygote. BMC Dev Biol. 4, 12.

Li L, Jiang L, Geng C, Cao J, Zhong L. (2008). The role of oxidative stress in acrolein-induced DNA damage in HepG2 cells. Free Radic Res. 42, 354-361,

Li MW, Baulch JE. Heritable effects of DNA damage following paternal F0 germline irradiation. In: Anderson D, Brinkworth MH (eds), Male-Mediated Developmental Toxicity, vol 1, 1st ed. Cambridge: RSC Publishing; 2007: 149-164.

Li Z, Yang J, Huang H. (2006). Oxidative stress induces H2AX phosphorylation in human spermatozoa. FEBS Letters 580, 6161-6168.

Lis JT, Kraus WL. (2006). Promoter cleavage: a topoIIbeta and PARP-1 collaboration. Cell 125, 1225-1227.

Loppin B, Bonnefoy E, Anselme C, Laurençon A, Karr TL, Couble P. (2005). The histone H3.3 chaperone HIRA is essential for chromatin assembly in the male pronucleus. Nature 437, 1386-1390.

Lu X, Lane DP. (1993). Differential induction of transcriptionally active p53 following UV or ionizing radiation; defects in chromosome instability syndromes? Cell 75, 765-778.

Mailand N, Bekker-Jensen S, Faustrup H, Melander F, Bartek J, Lukas C, Lukas J. (2007). RNF8 ubiquitylates histones at DNA double-strand breaks and promotes assembly of repair proteins. Cell 131, 887-900.

Marinelli D, Gaspari L, Pedotti P, Taioli E. (2004). Mini-review of studies on the effect of smoking and drinking habits on semen parameters. Int J Environ Health 207, 185-192.

Martins RP, Krawetz SA. (2005). RNA in human sperm. Asian J Androl. 7, 115-120.

Martins RP, Ostermeier GC, Krawetz SA. (2004). Nuclear matrix interactions at the human protamine domain : a working model of potentiation. J Biol Chem. 279, 51862-51868.

Mattick JS, Amaral PP, Dinger ME, Mercer TR, Mehler MF. (2009). RNA regulation of epigenetic processes. Bioessays 31, 51-59.

Masson M, Niedergang C, Schreiber V, Muller S, Menissier-de Murcia J, de Murcia G. (1998). XRCC1 is specifically associated with poly(ADP-ribose) polymerase and negatively regulates its activity following DNA damage. Mol Cell Biol. 18, 3563-3571.

Matsumoto K, Anzai M, Nakagata N, Takahashi A, Takahashi Y, Miyata K. (1994). Onset of paternal gene activation in early mouse embryos fertilized with transgenic mouse sperm. Mol Reprod Dev. 39, 136-140.

McCarroll N, Keshava N, Cimino M, Chu M, Dearfield K, Keshava C, Kligerman A, Owen R, Protzel A, Putzrath R, Schoeny R. (2008). An evaluation of the mode of action framework for mutagenic carcinogens case study: Cyclophosphamide. Envrion Mol Mutagen. 49, 117-131.

Miller D, Brinkworth M, Iles D. Information content of ejaculate spermatozoa and its potential utility in toxicology and infertility based research programmes. In: Anderson D, Brinkworth MH (eds), Male-Mediated Developmental Toxicity, vol 1, 1st ed. Cambridge: RSC Publishing; 2007: 176-187.

Mitchell DY, Petersen DR. (1989). Metabolism of the glutathione-acrolein adduct, S-(2-aldehydo-ehtyl)glutathione, by rat liver alcohol and aldehyde dehydrogenase. J Pharmacol Exp Ther. 251, 193-198.

Moon SH, Nguyen TA, Darlington Y, Lu X, Donehower LA. (2010). Dephosphorylation of γH2AX by WIP1: An important homeostatic regulatory event in DNA repair and cell cycle control. Cell Cycle 9, 2092-2096.

Morgan HD, Santos F, Green K, Dean W, Reik W. (2005). Epigenetic reprogramming in mammals. Hum Mol Genet. 15, 47-58.

Morris JR, Boutell C, Keppler M, Densham R, Weekes D, Alamshah A, Butler L, Galanty Y, Pangon L, Kiuchi T, Ng T, Solomon E. (2009). The SUMO modification pathway is involved in the BRCA1 response to genotoxic stress. Nature 42, 886-890.

Mozdarani H, Nazari E. 2009. Cytogenetic damage in preimplantation mouse embryos generated after paternal and parental γ-irradiation and the influence of vitamin C. Reproduction 137:35-43.

Mruk DD, Cheng CY. (2011). Environmental contaminants: Is male reproductive health at risk? Spermatogenesis 1, 283-290.

Mulvihill JJ, Garlow TJ. Reproductive outcomes among men treated for cancer. In: Anderson D, Brinkworth MH (eds), Male-Mediated Developmental Toxicity, vol 1, 1st ed. Cambridge: RSC Publishing; 2007: 7-14.

Murga M, Jaco I, Fan Y, Soria R, Martinez-Pastor B, Cuadrado M, Yang SM, Blasco MA, Skoultchi AI, Fernandez-Capetillo O. (2007). Global chromatin compaction limits the strength of the DNA damage response. J Cell Biol. 178, 1101-1108.

Murr R, Loizou JI, Yang YG, Cuenin C, Li H, Wang ZQ, Herceg Z. (2006). Histone acetylation by Trrap-Tip60 modulates loading of repair proteins and repair of DNA double-strand breaks. Nat Cell Biol. 8, 91-99.

Nadel B, de Lara J, Finkernagel SW, Ward WS. (1995). Cell-specific organization of the 5S ribosomal RNA gene cluster DNA loop domains in spermatozoa and somatic cells. Biol Reprod. 53, 1222-1228.

Nakada S, Chen GI, Gingras AC, Durocher D. (2008). PP4 is a γ H2AX phosphatase required for recovery from the DNA damage checkpoint. EMBO Rep. 9, 1019-1026.

Nakamura T, Arai Y, Umehara H, Masuhara M, Kimura T, Taniguchi H, Sekimoto T, Ikawa M, Yoneda Y, Okabe M, Tanaka S, Shiota K, Nakano T. (2007). PGC7/Stella protects against DNA demethylation in early embryogenesis. Nat Cell Biol. 9, 64-71.

Nichols J, Zevnik B, Anastassiadis K, Niwa H, Klewe-Nebenius D, Chambers I, Schöler H, Smith A. (1998). Formation of pluripotent stem cells in the mammalian embryo depends on the POU transcription factor Oct4. Cell 95, 379-391.

Nomura T. Transmissible genetic risk causing tumours in mice and humans. In: Anderson D, Brinkworth MH (eds), Male-Mediated Developmental Toxicity, vol 1, 1st ed. Cambridge: RSC Publishing; 2007: 134-148.

Nothias JY, Majumder S, Kaneko KJ, DePamphilis ML. (1995). Regulation of gene expression at the beginning of mammalian development. J Biol Chem. 270, 22077-22080.

Nothias JY, Miranda M, DePamphilis ML. (1996). Uncoupling of transcription and translation during zygotic gene activation in the mouse. EMBO J. 15, 5715-5725.

O'Flaherty C, Hales BF, Chan P, Robaire B. (2010). Impact of chemotherapeutics and advanced testicular cancer or Hodgkin lymphoma on sperm deoxyribonucleic acid integrity. Fertil Steril. 94, 1374-1379.

O'Flaherty C, Vaisheva F, Hales BF, Chan P, Robaire B. (2008). Characterization of sperm chromatin quality in testicular cancer and Hodgkin's lymphoma patients prior to chemotherapy. Hum Reprod. 23, 1044-1052.

Ogura A, Matsuda J, Yanagimachi R. (1994). Birth of normal young after electrofusion of mouse oocytes with round spermatids. Proc Natl Acad Sci USA 91, 7460-7462.

Olsen AK, Bjortuft H, Wiger R, Holme J, Seeberg E, Bjoras M, Brunborg G. (2001). Highly efficient base excision repair (BER) in human and rat germ cells. Nucleic Acids Res. 29, 1781-1790.

Olsen JH, Boice Jr. JD, Seersholm N, Bautz A, Fraumeni JF Jr. (1995). Cancer in the parents of children with cancer. N Engl J Med. 333, 1594-1599.

Osada T, Ogino H, Hino T, Ichinose S, Nakamura K, Omori A, Noce T, Masutani M. PolyADP-ribosylation is required for pronuclear fusion during postfertilization in mice. Plos One published September 2 2010; PMID 20824066.

Ostermeier GC, Goodrich RJ, Diamond MP, Dix DJ, Krawetz SA. (2005). Toward using stable spermatozoa RNAs for prognostic assessment of male factor fertility. Fertil Steril. 83, 1687-1694.

Ouko LA, Shantikumar K, Knezovich J, Haycock P, Schnugh DJ, Ramsay M. (2009). Effect of alcohol consumption on CpG methylation in the differentially methylated regions of H19 and IG-DMR in male gametes: implications for fetal alcohol spectrum disorders. Alcohol Clin Exp Res. 33, 1615-1627.

Ozolins TR. (2010). Cyclophosphamide and the Teratology Society: an awkward marriage. Birth Defects Red B Dev Reprod Toxicol. 89, 289-299.

Parker L, Pearce MS, Dickinson HO, Aitkin M, Craft AW. (1999). Stillbirths among offspring of male radiation workers at sellafield nuclear reprocessing plant. Lancet 354, 1407-1414.

Peng JC, Karpen GH. (2008). Epigenetic regulation of heterochromatic DNA stability. Curr Opin Genet Dev. 18, 204-211.

Perreault SD, Barbee RR, Slott VL. (1988). Importance of glutathione in the acquisition and maintenance of sperm nuclear decondensing activity in maturing hamster oocyte. Dev Biol. 125, 181-186.

Perreault SD, Zirkin BR. (1982). Sperm nuclear decondensation in mammals: role of sperm-associated proteinase in vivo. J Exp Zool. 224, 253-257.

Pfanner N, Truscott K. (2005). Powering mitochondria protein import. Nat Struct Biol. 9, 234-236.

Pfeiffer P, Goedecke W, Obe G. (2000). Mechanisms of DNA double-strand break repair and their potential to induce chromosomal aberrations. Mutagenesis 15, 289-302.

Piña-Guzmán B, Sánchez-Gutiérrez M, Marchetti F, Hernández-Ochoa I, Solís-Heredia MJ, Quintanilla-Vega B. (2009). Methyl-parathion decreases sperm function and fertilization capacity after targeting spermatocytes and maturing spermatozoa. Toxicol Appl Pharmacol. 238, 141-149.

Pittoggi C, Renzi L, Zaccagnini G, Cimini D, Degrassi F, Giordano R, Magnano AR, Lorenzini R, Lavia P, Spadafora C. (1999). A fraction of mouse sperm chromatin is organized in nucleosomal hypersensitive domains enriched in retroposon DNA. J of Cell Science 112, 3537-3548.

Pokholok DK, Harbison CT, Levine S, Cole M, Hannett NM, Lee TI, et al. (2005). Genome-wide map of nucleosome acetylation and methylation in yeast. Cell 122, 517-527.

Potts R, Newbury C, Smith G, Notarianni L, Jefferies T. (1999). Sperm chromatin damage associated with male smoking. Mutat Res. 423, 103-111.

Puschendorf, M., Terranova, R., Boutsma, E., Mao, X., Isono, K., Brykczynska, U., Kolb C, Otte AP, Koseki H, Orkin SH, van Lohuizen M, Peters AH. (2008). PRC1 and Suv39h specify paternal asymmetry at constitutive heterochromatin in early mouse embryos. Nat Genet. 40, 411-420.

Qiu J, Hales BF, Robaire B. (1995a). Damage to rat spermatozoal DNA after chronic cyclophosphamide exposure. Biol Reprod. 53, 1465-1473.

Qiu J, Hales BF, Robaire B. (1995b). Effects of chronic low-dose cyclophosphamide exposure on the nuclei of rat spermatozoa. Biol Reprod. 52, 33-40.

Qureshi MSA, Pennington JH, Goldsmith HJ, Cox PE. (1972). Cyclophosphamide therapy and sterility. Lancet 2, 1290-1291.

Ram PT, Schultz RM. (1993). Reporter gene expression in G2 of the 1-cell mouse embryo. Dev Biol. 156, 552-556.

Rangasamy D, Berven L, Ridgway P, Tremethick DJ. (2003). Pericentric heterochromatin becomes enriched with H2A.Z during early mammalian development. EMBO J. 22, 1599-1607.

Redon CE, Nakamura AJ, Zhang YW, Ji JJ, Bonner WM, Kinders RJ, Parchment RE, Doroshow JH, Pommier Y. (2010). Histone γH2AX and poly(ADP-ribose) as clinical pharmacodynamic biomarkers. Clinical Cancer Research 16, 4532-4542.

Rivera RM. (2010). Epigenetic aspects of fertilization and preimplantation development in mammals: lessons from the mouse. Syst Biol Reprod Med. 56, 388-404.

Robaire B, Hales BF. Targets of chemotherapeutic drug action in testis and epididymis. In: Zirkin, BR (ed.), Germ cell development, division, disruption and death, Springer-Verlag, New York, NY, 190-201.

Robbins WA, Young KE, Wei F and the Boron Epidemiology research group. Feasibility study of metal effects on the X:Y ratio in human sperm. In: Anderson D, Brinkworth MH (eds), Male-Mediated Developmental Toxicity, vol 1, 1st ed. Cambridge: RSC Publishing; 2007: 61-76.

Roest HP, van Klaveren J, de Wit J, van Gurp CG, Koken MH, Vermey M, van Roijen JH, Hoogerbrugge JW, Vreeburg JT, Baarends WM, Bootsma D, Grootegoed JW, Hoeijmakers JH. (1996). Inactivation of the HR6B ubiquitin-

conjugating DNA repair enzyme in mice causes male sterility associated with chromatin modification. Cell 86, 799-810.

Rogakou EP, Pilch DR, Orr AH, Ivanova VS, Bonner WM. (1998). DNA double-stranded breaks induce histone H2AX phosphorylation on serine 139. J Biol Chem. 273, 5858-5868.

Ronen A, Glickman BW. (2001). Human DNA repair genes. Environ Mol Mutagen. 37, 241-283.

Rossetto D, Truman AW, Kron SJ, Côté J. (2010). Epigenetic modification in double-strand break DNA damage signaling and repair. Clin Cancer Res. 16, 4543-4552.

Rouleau M, Patel A, Hendzel MJ, Kaufmann SH, Poirier GG. (2010). PARP inhibition: PARP1 and beyond. Nat Rev Cancer 10, 293-301.

Rubbi CP, Milner J. (2003). P53 is a chromatin accessibility factor for nucleotide excision repair of DNA damage. EMBO J. 22, 975-986.

Rubes J, Lowe X, Moore D 2nd, Perreault S, Slott V, Evenson D, Selevan SG, Wyrobek AJ. (1998). Smoking cigarettes is associated with increased sperm disomy in teenage men. Fertil Steril. 70, 715-723.

Rubes J, Selevan SG, Evenson DP, Zudova D, Vozdova M, Zudova Z, Robbins WA, Perreault SD. (2005). Episodic air pollution is associated with increased DNA fragmentation in human sperm without other changes in semen quality. Hum Reprod. 20, 2776-2783.

Rubes J, Vozdova M, Robbins WA, Rezacova O, Perreault SD, Wyrobek AJ. (2002). Stable variants of sperm aneuploidy among healthy men show associations between germinal and somatic aneuploidy. Am J Hum Genet. 70, 1507-1519.

Salazar-Arredondo E, de Jesús Solís-Heredia M, Rojas-García E, Hernández-Ochoa I, Quintanilla-Vega B. (2008). Sperm chromatin alteration and DNA damage by methyl-parathion, chlorpyrifos and diazinon and their oxon metabolites in human spermatozoa. Reprod Toxicol. 25, 455-460.

Sanders SL, Portoso M, Mata J, Bahler J, Allshire RC, Kouzarides T. (2004). Methylation of histone H4 lysine 20 controls recruitment of Crb2 to sites of DNA damage. Cell 119, 603-614.

Sankila R, Olsen JH, Anderson H, Garwicz S, Glattre E, Hertz h, Langmark F, Lanning M, Møller T, Tulinius H. (1998). Risk of cancer among offspring of childhood-cancer survivors. Association of the Nordic cancer registries and the Nordic society of paediatric haematology and oncology. N Engl J Med. 338, 1339-1344.

Santenard A, Ziegler-Birling C, Koch M, Tora L, Bannister AJ, Torres-Padilla M-E. (2010). Heterochromatin formation in the mouse embryo requires critical residues of the histone variant H3.3. Nat Cell Biol. 12, 853-862.

Santenard A, Torres-Padilla ME. (2009). Epigenetic reprogramming in mammalian reproduction: contribution from histone variants. Epigenetics 4, 80-84.

Santos F, Hendrich B, Reik W, Dean W. (2002). Dynamic reprogramming of DNA methylation in the early mouse embryo. Dev Biol. 241, 172-182.

Santos F, Peters AH, Otte AP, Reik W, Dean W. (2005). Dynamic chromatin modifications characterize the first cell cycle in mouse embryos. Developmental Biology 280, 225-236.

Sarmento OF, Digilio LC, Wang Y, Perlin J, Herr JC, Allis CD, Coonrod SA. (2004). Dynamic alterations of specific histone modifications during early murine development. J Cell Sci. 117, 4449-4459.

Schatten G, Simerly C and Schatten H. (1985). Microtubule configurations during fertilization, mitosis, and early development in the mouse and the requirement for egg microtubule-mediated motility during mammalian fertilization. Proc Natl Acad Sci USA 82, 4152-4156.

Schatten G, Simerly C and Schatten H. (1986). Microtubules in mouse oocytes, zygotes, and embryos during fertilization and early development – unsual configurations and arrest of mammalian fertilization with microtubule inhibitors. Annals of the New York Academy of Sciences 466, 945-948.

Schreiber V, Dantzer F, Ame JC, de Murcia G. (2006). Poly(ADP-ribose): novel functions for an old molecule. Nat Rev Mol Cell Biol. 7, 517-528.

Schultz RM. (2002). The molecular foundations of the maternal to zygotic transition in the preimplantation embryo. Human Reproduction Update 8, 323-331.

Schultz RM. (1993). Regulation of zygotic gene activation in the mouse. BioEssays 15, 531-538.

Shaman JA, Yamauchi Y, Ward WS. (2007). The sperm nuclear matrix is required for paternal DNA replication. J Cell Biochem. 102, 680-688.

Shimizu N. (2009). Extrachromosomal double minutes and chromosomal homogeneously staining regions as probes for chromosome research. Cytogenet Genome Res. 124, 312-326.

Shimura T, Inoue M, Taga M, Shiraishi K, Uematsu N, Takei N, Yuan Z-M, Shinohara T, Niwa O. (2002). P53-Dependent S-phase damage checkpoint and

pronuclear cross talk in mouse zygotes with X-irradiated sperm. Mol Cell Biol. 22, 2220-2228.

Shinohara A, Ogawa T. (1999). Rad51/RecA protein families and the associated proteins in eukaryotes. Mutat Res. 435, 13-21.

Shu XO, Gao YT, Brinton LA, Linet MS, Tu JT, Zheng W, Fraumeni JF Jr. (1988). A population-based case-control study of childhood leukemia in shanghai. Cancer 62, 635-644.

Skinner MK. Epigenetic transgenerational actions of endocrine disruptors through the male germ-line. In: Anderson D, Brinkworth MH (eds), Male-Mediated Developmental Toxicity, vol 1, 1st ed. Cambridge: RSC Publishing; 2007: 1-6.

Slott VL, Hales BF. (1987). Enhancement of the embryotoxicity of acrolein, but not phosphoramide mustard, by glutathione depletion in rat embryos in vitro. Biochem Pharmacol. 36, 2019-2025.

Smith GC, d'Adda di Fagagna F, Lakin ND, Jackson SP. (1999). Cleavage and inactivation of ATM during apoptosis. Mol Cell Biol. 19, 6076-6084.

Somers CM, Yauk CL, White PA, Parfett CL, Quinn JS. (2002). Air pollution induces heritable DNA mutations. Proc Natl Acad Sci USA 99, 15904-15907.

Sorahan T. Links between paternal smoking and childhood cancer. In: Anderson D, Brinkworth MH (eds), Male-Mediated Developmental Toxicity, vol 1, 1st ed. Cambridge: RSC Publishing; 2007: 51-60.

Spirin AS. (1994). Storage of messenger RNA in eukaryotes: envelopment with protein, translational barrier at 5' side, or conformational masking by 3' side? Mol Reprod Dev. 38, 107-117.

Sram RJ, Rubes J. Sperm abnormalities in exposed humans. In: Anderson D, Brinkworth MH (eds), Male-Mediated Developmental Toxicity, vol 1, 1st ed. Cambridge: RSC Publishing; 2007: 247-258.

Stein P, Worrad DM, Belyaev ND, Turner BM, Schultz RM. (1997). Stage-dependent redistributions of acetylated histones in nuclei of the early preimplantation mouse embryo. Mol Reprod Dev. 47, 421-429.

Sun QY. (2003). Cellular and molecular mechanisms leading to cortical reaction and polyspermy block in mammalian eggs. Microscopy Research and Technique 61, 342–348.

Sun QY, Breitbart H, Schatten H. (1999). Role of the MAPK cascade in mammalian germ cells. Reprod Fertil Dev. 11, 443-450.

Swan SH, Brazil C, Drobnis EZ, Liu F, Kruse RL, Hatch M, Redmon JB, Wang C, Overstreet JW. (2003). Geographic differences in semen quality of fertile U.S. males. Environ Health Perspect. 111, 414-420.

Tanaka Y, Kato S, Tanaka M, Kuji N, Yoshimura Y. (2003). Structure and expression of the human oocyte-specific histone H1 gene elucidated by direct RT-nested PCR of a single oocyte. Biochem Biophys Res Commun. 304, 351-357.

Terradas M, Martín M, Tusell L, Genescà A. (2010). Genetic activities in micronuclei: Is the DNA entrapped in micronuclei lost for the cell? Mutation Research 705, 60-67.

Tian Y, Yamauchi T. (2003). Micronucleus formation in 3-day mouse embryos associated with maternal exposure to chlorpyrifos during the early preimplantation period. Reprod Tox. 17, 401-405.

Tokoro M, Shin SW, Nishikawa S, Lee HH, Hatanaka Y, Amano T, Mitani T, Kato H, Anzai M, Kishigami S, Saeki K, Hosoi Y, Iritani A, Matsumoto K. (2010). Deposition of acetylated histones by RNAPII promoter clearance may occur at onset of zygotic gene activation in preimplantation mouse embryos. J Reprod Dev. 56, 607-615.

Torres-Padilla ME, Bannister AJ, Hurd PJ, Kouzarides T, Zernicka-Goetz M. (2006). Dynamic distribution of the replacement histone variant H3.3 in the mouse oocyte and preimplantation embryos. Int J Dev Biol. 50, 455-461.

Torres-Padilla ME, Parfitt DE, Kouzarides T, Zernicka-Goetz M. (2007). Histone arginine methylation regulates pluripotency in the early mouse embryo. Nature 445, 214-218.

Trasler JM, Hales B, Robaire B. (1986). Chronic low dose cyclophosphamide treatment of adult male rats: Effects on fertility, pregnancy outcome and progeny. Biol Reprod. 34, 275-283.

Trasler JM, Hales, BF, Robaire B. (1987). A time-course study of chronic paternal cyclophosphamide treatment in rats: Effects on pregnancy outcome and the male reproductive and hematologic systems. Biol Reprod. 37, 317-326.

Vakoc CR, Sachdeva MM, Wang H, Blobel GA. (2006). Profile of histone lysine methylation across transcribed mammalian chromatin. Mol Cell Biol. 26, 185-195.

van Attikum H, Gasser SM. (2005). ATP-dependent chromatin remodeling and DNA double-strand break repair. Cell Cycle 4, 1011-1014.

van Blerkom J. (2011). Mitochondrial function in the human oocyte and embryo and their role in developmental competence. Mitochondrion 11, 797-813.

van Blerkom J. (2008). Mitochondria as regulatory forces in oocytes, preimplantation embryos and stem cells. Reprod Biomed. 16, 553-569.

van Blerkom J, Brockway GO. (1975). Qualitative patterns of protein synthesis in the preimplantation mouse embryo. I. Normal pregnancy Dev Biol. 44, 148-157.

van Blerkom J, Davis P. (2007). Mitochondrial signaling and fertilization. Mol Hum Reprod. 13, 759-770.

van blerkom J, Davis P, Merriam J. (1994). A retrospective analysis of unfertilized and presumed parthenogenetically activated human oocytes demonstrated a high frequency of sperm penetration. Hum Reprod. 9, 2381-2388.

van Blerkom J, Davis P, Lee J. (1995). ATP content of human oocytes and developmental potential and outcome after in-vitro fertilization and embryo transfer. Hum Reprod. 10, 415-424.

van Blerkom J, Davis P, Mawhig V, Alexander S. (2003). Domains of high and low polarized mitochondria in mouse and human oocytes and early embryos. Hum Reprod. 17, 393-406.

van der Heijden GW, Derijck AAHA, Ramos L, Giele M, van der Vlag J, de Boer P. (2006). Transmission of modified nucleosomes from the mouse male germline to the zygote and subsequent remodeling of paternal chromatin. Dev Biol. 298, 458-469.

van der Heijden GW, Dieker JW, Derijck AAHA, Muller S, Berden JHM, Braat DDM, van der Vlag J, de Boer P. (2005). Asymmetry in histone H3 variants and lysine methylation between paternal and maternal chromatin of the early mouse zygote. Mech Dev. 122, 1008-1022.

van der Heijden GW, Ramos L, Baart EB, van der Berg IM, Derijck AA, van der Vlag J, Martini E, de Boer P. (2008). Sperm-derived histones contribute to zygotic chromatin in humans. BMC Developmental Biology 8, 34.

Vinson RK, Hales BF. (2002). DNA repair during organogenesis. Mutat Res. 509, 79-91.

Ward I, Kim JE, Minn K, Chini CC, Mer G, Chen J. (2006). The tandem BRCT domain of 53BP1 is not required for its repair function. J Biol Chem. 281, 38472-38477.

Ward WS. (2010). Function of sperm chromatin structural elements in fertilization and development. Mol Hum Reprod. 16, 30-36.

Wei Y, Multi S, Yang CR, Ma J, Zhang QH, Wang ZB, Li M, Wei L, Ge ZJ, Zhang CH, Ouyang YC, Hou Y, Schatten H, Sun QY. Spindle assembly checkpoint regulates mitotic cell cycle progression during preimplantation embryo development. PLoS One published 24 June 2011; PMID 21720555.

Wells D, Bermudez MG, Steuerwald N, Malter HE, Thornhill AR, Cohen J. (2005). Association of abnormal morphology and altered gene expression in human preimplantation embryos. Fertil Steril. 84, 343-355.

Wells D, Bermudez MG, Steuerwald N, Thornhill AR, Walker DL, Malter H, Delhanty JD, Cohen J. (2005). Expression of genes regulating chromosome segregation, the cell cycle and apoptosis during human preimplantation development. Hum Reprod. 20, 1339-1348.

Wiekowski M, Miranda M, DePamphilis ML. (1993). Requirements for promoter activity in mouse oocytes and embryos distinguish paternal pronuclei from maternal and zygotic nuclei. Dev Biol. 156, 366-378.

Wilcox A, Weinberger C, O'Connor J, Baird D, Schlatterer J, Canfield R, Armstrong G, Nisula B. (1988). Incidence of early pregnancy loss. N Engl J Med. 319, 189-194.

Winther JF. Cancer in siblings of children with cancer in the Nordic countries: A Population-based cohort study paediatric cancer: An indicator of familial cancer risk? In: Anderson D, Brinkworth MH (eds), Male-Mediated Developmental Toxicity, vol 1, 1st ed. Cambridge: RSC Publishing; 2007: 15-27.

Winther JF, Sankila R, Boice Jr. JD, Tulinius H, Bautz A, Barlow L, Glattre E, Langmark F, Møller T, Mulvihill JJ, Olafsdottir GH, Ritvanen A, Olsen JH. (2001). Cancer in siblings of children with cancer in the Nordic countries: a population-based cohort study. Lancet 358, 711-717.

Wolffe AP. (1991). Implications of DNA replication for eukaryotic gene expression. J Cell Sci. 99, 201-206.

Wolffe AP, Hayes JJ. (1999). Chromatin disruption and modification. Nucleic Acids Res. 27, 711-720.

Worrad DM, Ram PT, Schultz RM. (1994). Regulation of gene expression in the mouse oocyte and early preimplantation embryo: developmental changes in Sp1 and TATA box-binding protein, TBP. Development 120, 2347-2357.

Worrad DM, Turner BM, Schultz RM. (1995). Temporally restricted spatial localization of acetylated isoforms of histone H4 and RNA polymerase II in the 2-cell mouse embryo. Development 121, 2949-2959.

Wossidlo M, Arand J, Sebastiano V, Lepikhov K, Boiani M, Reinhardt R, Schöler H, Walter J. (2010). Dynamic link of DNA demethylation, DNA strand breaks and repair in mouse zygotes. EMBO J. 29, 1877-1888.

Xie A, Hartlerode A, Stucki M, Odate S, Puget N, Kwok A, Nagaraju G, Yan C, Alt FW, Chen J, Jackson SP, Scully R. (2007). Distinct roles of chromatin-

associated proteins MDC1 and 53BP1 in mammalian double-strand break repair. Mol Cell 28, 1045-1057.

Xu B, Zhaoliang S, Liu Z, Guo H, Liu Q, Jiang H, Zou Y, Gong Y, Tischfield JA, Shao C. Replication stress induces micronuclei comprising of aggregated DNA double-strand breaks. PLoS One published 15 April 2011; PMID 21525980.

Xu G, Spivak G, Mitchell DL, Mori T, McCarrey JR, McMahan CA, Walter RB, Hanawalt PC, Walter CA. (2005). Nucleotide excision repair activity varies among murine spermatogenic cell types. Biol Reprod. 73, 123-130.

Xu Y, Price BD. (2011). Chromatin dynamics and the repair of DNA double strand breaks. Cell Cycle 10, 261-267.

Xu Y, Sun Y, Jiang X, Ayrapetov MK, Moskwa P, Yang S, Weinstock DM, Price BD. (2010). The p400 ATPase regulates nucleosome stability and chromatin ubiquitination during DNA repair. J Cell Biol. 191, 31-43.

Yamauchi Y, Shaman JA, Boaz SM, Ward WS. (2007a). Paternal pronuclear DNA degradation is functionally linked to DNA replication in mouse oocytes. Biol Reprod. 77, 407-415.

Yamauchi Y, Shaman JA, Ward WS. (2007b). Topoisomerase II mediated breaks in spermatozoa cause the specific degradation of paternal DNA in fertilized oocytes. Biol Reprod. 76, 666-672.

Yanagimachi R. (2011). Mammalian sperm acrosome reaction: Where does it begin before fertilization? Biol Reprod. 85, 4-5.

Yoshimoto Y, Kato H, Schull WJ. (1991). A review of forty-five years study of Hiroshima and Nagasaki atomic bomb survivors. Cancer risk among in utero-exposed survivors. J Radiat Res. 32, 231-238.

Yoshimoto Y, Mabuchi K. (1991). Mortality and cancer risk among the offspring (F1) of atomic bomb survivors. J Radiat Res. 32, 294-300.

Yu Y, Halet G, Lai FA, Swann K. (2008). Regulation of diacylglycerol production and protein kinase C stimulation during sperm- and PLCζ-mediated mouse egg activation. Biol Cell 100, 633-643.

Yu J, Hecht NB, Schultz RM. (2001). Expression of MSY2 in mouse oocytes and preimplantation embryos. Biol Reprod. 65, 1260-1270.

Yuan J, Chen J. (2010). MRE11-RAD50-NBS1 complex dictates DNA repair independent of H2AX. J Biol Chem. 285, 1097-1104.

Zeitlin SG, Baker NM, Chapados BR, Soutoglou E, Wand JY, Berns MW, Cleveland DW. (2009). Double-strand DNA breaks recruit the centromeric histone CENP-A. Proc Natl Acad Sci USA 106, 15762-15767.

Zeng F, Baldwin DA, Schultz RM. (2004). Transcript profiling during preimplantation mouse development. Dev Biol. 272, 483-496.

Zheng P, Schramm RD, Latham KE. (2005). Developmental regulation and in vitro culture effects on expression of DNA repair and cell cycle checkpoint control genes in rhesus monkey oocytes and embryos. Biol Reprod. 72, 1359-1369.

Ziegler-Birling C, Helmrich A, Tora L, Torres-Padilla ME. (2009). Distribution of p53 binding protein 1 (53BP1) and phosphorylated H2A.X during mouse preimplantation development in the absence of DNA damage. Int J Dev Biol. 53, 1003-1011.

Ziv Y, Bielopolski D, Galanty Y, Lukas C, Taya Y, Schultz DC, Lukas J, Bekker-Jensen S, Bartek J, Shiloh Y. (2006). Chromatin relaxation in response to DNA double-strand breaks is modulated by a novel ATM- and KAP-1 dependent pathway. Nat Cell Biol. 8, 870-876.

Zollner U, Zollner KP, Steck T, Dietl J. (2003). Pronuclear scoring. Time for international standardization. J Reprod Med. 48, 365-369.

CHAPTER II

Paternal Exposure to Cyclophosphamide Affects the Progression of Sperm Chromatin Decondensation and Activates a DNA Damage Response in the Prepronuclear Rat Zygote

Lisanne Grenier, Bernard Robaire, Barbara F. Hales

Biology of Reproduction (2010) 83(2): 195-204.

ABSTRACT

Spermatozoon decondensation in the zygote leads to the initiation of chromatin remodeling during which protamines are removed and replaced with maternal histones. We hypothesize that damage to male germ cells induced by paternal exposure to cyclophosphamide may alter the timing of spermatozoal decondensation and the pattern of chromatin remodeling in the prepronuclear rat zygote. A specific order of sperm decondensation was observed, starting at the posterior end, proceeding to the ventral sides, followed by the tip, and finally the midbody region of the sperm head nucleus; subgroups of partially decondensed type *a* sperm nuclei were defined as types *a*1, *a*2, *a*3, and *a*4. Based on their frequencies relative to controls, paternal exposure to cyclophosphamide accelerated the timing of spermatozoal decondensation. Two distinct patterns of chromatin remodeling were observed for totally decondensed (type *b*) and recondensing (type *c*) sperm nuclei: H4K12ac showed a homogenous staining, whereas H3S10ph displayed a ring-like staining around the sperm nucleus; the distribution of these posttranslationally modified histones was not affected by cyclophosphamide exposure. In contrast, paternal cyclophosphamide treatment increased the number of gammaH2AX foci found in decondensing sperm nuclei. Small foci were significantly increased in type *a*2 and *a*3 nuclei, whereas a significant increase in the numbers of large foci was found in type *b* and *c* nuclei. This increase in gammaH2AX foci in the decondensing male genome suggests that damage recognition and repair pathways are initiated in prepronuclear rat zygotes. Thus, exposure of male rats to chronic low doses of cyclophosphamide accelerates spermatozoal decondensation and leads to the activation of gammaH2AX recognition of DNA damage in the male genome of the prepronuclear zygote.

INTRODUCTION

The entry of the spermatozoon triggers the mature oocyte arrested at metaphase II to complete its second meiotic division. Once activated, stored oocyte proteins will block polyspermy and initiate major chromatin reorganization and reprogramming events in both the maternal and paternal genomes during an early window of embryonic development, defined as the zygotic prepronuclear (pre-PN) formation [1].

Chromatin decondensation of spermatozoa is a multistep process, starting with the induction of calcium influx by gamete membrane fusion and the resumption of meiosis by maternally activated protein kinase C [2–3] and the reduction of interprotamine sulfhydryl bonds by glutathione (GSH) [4]. In pre-PN zygotes, there are four stages of mouse sperm chromatin decondensation: condensed, partially decondensed (type *a*), totally decondensed (type *b*), and recondensing (type *c*); nuclei always decondense in the same order, from the posterior end, to the ventral sides, and then the tip of the sperm nucleus [5]. Chromatin remodeling is initiated when the spermatozoon chromatin begins to decondense; the male germ cell chromatin is packaged into a somatic cell chromatin by replacing sperm-specific protamines with somatic histones. Maternally provided cysteine protease degrades sperm-specific protamines, leaving the maternal somatic histones unaffected, while histone cell cycle regulation defective homolog A and nucleoplasmin chaperone proteins assemble nucleosomes, remodeling the paternal chromatin [6, 7]. Once this reprogramming is complete, the paternal chromatin recondenses and subsequently expands into the male pronucleus.

During sperm chromatin remodeling, the two parental sets of chromosomes exhibit striking epigenetic differences. The paternal chromosomal histones are mostly acetylated and devoid of methylation marks, while the maternal chromosomal histones are mostly methylated and lack acetylation marks [5, 8, 9]. Changes in histone modifications, induced by environmental and

developmental cues, may play a role in regulating gene expression during early embryo development. The presence and localization of histones H4K12ac and H3S10ph were visualized in pre-PN zygotes and evaluated as indicators of the progression of chromatin remodeling in sperm from control and cyclophosphamide (CPA)-exposed rats. H4K12ac is one of the first maternally modified histones to be incorporated on the decondensing paternal chromatin [1], marking an open and active chromatin structure to support early embryonic events following fertilization [10]. H3S10ph marks (peri)centromeric heterochromatin important for homologous chromosome segregation during mouse oocyte maturation [11], the remodeling of paternal chromatin [1], and mitosis [12] in postfertilized oocytes. H3S10ph can be a marker of relaxed chromatin during transcription [13], or a marker of condensed chromatin during mitosis [14] and meiosis [11]. Thus, during pre-PN events, the epigenetic marks of the remodeling paternal chromatin are highly dynamic, potentially influencing the zygote as it progresses through the different sperm decondensation stages.

Histone modifications may also serve to mark DNA damage and recruit maternally stored DNA repair proteins following fertilization [15–17]. A histone H2A variant protein, H2AX (official symbol, H2AFX), is phosphorylated at serine 139 by phosphoinositide 3-kinase-related kinases to form γH2AX, which accumulates in foci to mark DNA double-strand breaks [18–20]. There are two types of γH2AX foci: a large population of small foci is important for the assembly of embryonic chromatin and mitotic cell cycle regulation, while a small population of large foci is indicative of the recruitment of DNA repair proteins [21–23]. In a previous study [24], we observed a striking increase in γH2AX focal numbers and volume in remodeled pronuclear-stage embryos in response to paternal CPA exposure, in support of a role for this modified histone in the processing of the DNA lesions by recruiting and maintaining repair factors in the vicinity of the damage during the first cell division in the zygote.

CPA (Cytoxan) is a chemotherapeutic [25, 26] and immunosuppressive agent used mainly in the treatment of breast cancer and non-Hodgkin disease.

CPA is an alkylating agent, inducing DNA-DNA and DNA-protein cross-links, and single-strand breaks in rapidly dividing cells [26, 27]. Paternal exposure to CPA targets spermatogenesis in a dose- and time-specific manner [28]. The step of spermatogenesis most sensitive to CPA exposure is during spermiogenesis, at a time when most of the somatic histones are being replaced with sperm nuclear basic proteins, protamines, and histone variants [29–31].

The objectives of this study were to determine if paternal exposure to CPA impacts events during the development of early pre-PN zygotes. Since sperm DNA integrity and chromatin packaging are essential for the accurate and successful transmission of genetic information to progeny, we hypothesize that CPA-related alterations in sperm chromatin structure may affect the progression of sperm chromatin decondensation and remodeling after fertilization. If so, this could result in dysregulation of paternal and maternal gene expression, and, thereby, potentially account for the previously observed impaired pregnancy outcomes [28].

MATERIALS AND METHODS

Drug Treatment and Collection of Rat Pre-PN Zygotes Generated In Vivo

Adult male (body weight, 350–400 g) and virgin female (body weight, 225–250 g) Sprague-Dawley rats were purchased from Charles River Canada (St. Constant, QC, Canada) and housed at the Animal Resources Centre, McIntyre Medical Building, McGill University (Montreal, QC, Canada). Animals received food and water ad libitum, and were maintained on a 0700–1900 h light/dark cycle. The drug treatment and zygote protocols previously described [32] were followed with minor modifications. After 1 wk of acclimatization, male rats were randomly assigned to one of two treatment groups (n = 11 per group) and gavaged with saline (vehicle) or CPA (CAS 6055-19-2; Sigma Chemical Co., St. Louis, MO), 6 mg/kg per day, six times per week for 4 wk [33, 34].

On the fifth week of treatment, control virgin females in proestrus were selected by a vaginal wash in the midafternoon, and were caged overnight in groups of two, with either a control or CPA-treated male. Pregnancies were confirmed with sperm-positive vaginal smears the following morning, designated as Gestation Day 0. Sperm-positive females were euthanized at 0900 h on Day 0 to collect pre-PN-stage zygotes. Since fertilization occurred after in vivo mating, the exact timing was not known. Thus, the progression of spermatozoal decondensation was assessed by analyzing the distribution of the stages of spermatozoa decondensation observed in the population of early pre-PN zygotes captured at one time point. Oviducts and proximal uteri were isolated and cleaned in prewarmed (37°) M2 culture medium (Sigma Chemical Co.). Zygotes were released from the ampullae into a drop of prewarmed (37°C) 1% hyaluronidase (Sigma Chemical Co.) in M2 medium to digest the cumulus cells. All animal protocols were carried out according to the guidelines of the Canadian Council on Animal Care, and were approved by the institutional animal care committee.

Immunofluorescence

The indirect immunofluorescence protocols used were described previously [18]. Zygotes fertilized by saline and CPA-exposed males were stained in parallel at room temperature unless otherwise stated. Briefly, zygotes were washed in 1× PBS (pH 7.4; Mg^{2+} and Ca^{2+} free), containing 1 mg/ml polyvinylpyrrolidone. Zona pellucidae were removed in prewarmed (37°C) acid Tyrode solution (pH 2.5) by pipetting up and down for 5 sec, and then washed in 1× PBS (pH 7.4; Mg^{2+} and Ca^{2+} free), containing 1 mg/ml polyvinylpyrrolidone. Zygotes were then fixed in 4% paraformaldehyde in Ca^{2+}-/Mg^{2+}-free PBS for 15 min, washed in 0.05% Tween 20 in PBS for 5 min, permeabilized in 0.2% Triton X-100 in PBS for 30 min, rewashed in 0.05% Tween 20 in PBS for 5 min, and blocked for 4–5 h in 10% goat serum, 3% BSA, and 0.1% Tween 20 in PBS.

To visualize chromatin remodeling of the paternal genome, we incubated the zygotes in rabbit polyclonal IgG anti-acetyl-histone H4 (Lys12) [1, 10] (1:200

dilution; catalog no. 06761; Upstate Cell Signaling Solutions, Billerica, MA) and rabbit polyclonal IgG anti-phosphorylated-histone H3 (S10ph) [1, 35] (1:200 dilution; catalog no. 06–570; Upstate Cell Signaling Solutions) overnight at 4°C in a humidified chamber. To visualize sites of DNA damage recognition and repair, we incubated the zygotes with mouse monoclonal IgG anti-γH2AX phospho-Serine-139 [20] (1:500 dilution; catalog no. 05–636, clone JBW103; Upstate Biotechnology, Charlottesville, VA) overnight at 4°C in a humidified chamber. Both primary and secondary antibodies were diluted in goat blocking solution (10% goat serum, 3% BSA, and 0.1% Tween 20 in PBS). Zygotes were then washed three times for 20 min in goat blocking solution, incubated for 1 h in goat fluorescein anti-rabbit IgG (H + L) (1:200 dilution; catalog no. F1–1000; Vector Laboratories, Burlington, ON, Canada) for H4K12ac and H3S10ph, and for 1 h in sheep fluorescein anti-mouse IgG (H + L) (1:200 dilution; catalog no. N1031V; Amersham Pharmacia Biosciences, Baie d'Urfe, QC, Canada) for γH2AX, and rewashed three times for 20 min in goat blocking solution. DNA was stained with propidium iodide (catalog no. P4864; Sigma Chemical Co.) at 10 μg/ml in goat blocking solution for 20 min, washed in 0.05% Tween 20 in PBS for 10 min, mounted in 3 μl of VectaShield mounting medium (Vector Laboratories) on a premarked pap pen slide, and covered with a cover slip. Slides were then stored at 4°C and visualized by confocal microcopy during the next 2 days. A total of 11 experimental replicates were done for each histone H4K12ac and H3S10ph marker, while 6 experimental replicates were done for the γH2AX study.

Confocal Microscopy

A Zeiss LSM 510 Axiovert 100M confocal microscope with a Plan-Apochromat ×63/1.4 oil differential interference contrast objective was used to visualize the fluorescence of early postfertilized zygotes. The best settings for laser scanning fluorescence imaging were determined experimentally for both primary H4K12ac and H3S10ph antibodies. All zygotes stained for H4K12ac and H3S10ph were scanned at a speed of 5, with an optical slice of 0.6 μm, zoom

factor equal to 1, and a pinhole setting of 96 μm. Two scans of each optical section were compiled and averaged by the Zeiss LSM 510 computer software to give a final image that was 1024 × 1024 pixels in size. Due to significant variation in the H4K12ac signal intensity over the different paternal chromatin compaction levels, images of early pre-PN zygotes at the condensed and type *a* sperm nuclear decondensation stages were taken with a detector gain setting of 979, whereas the setting was 949 for type *b* and *c* sperm nuclei. Images of all zygotes stained with anti-H3S10ph were taken with a detector gain setting of 740. Images from Z-stacks were further analyzed and quantified using the Profile Program on the confocal microscope.

All zygotes stained for γH2AX were scanned at a speed of 6, with optical slice of <0.7μm, keeping the other settings unchanged. For qualitative purposes only, all γH2AX zygote images were taken at the optimized detector gain set for both the maternal nucleus and polar body. Images from Z-stacks were further reconstituted in three-dimensional images, and focal numbers and sizes were quantified using the overlay option on the confocal microscope.

Quantitative Analysis

H4K12ac and H3S10ph. Polyspermic zygotes (18 from the saline group, 14 from the CPA treatment group) were excluded from this analysis, leaving a total of 298 saline-sired zygotes and 300 CPA-sired zygotes. Quantitative analysis for all nonpolyspermic zygotes was done by drawing a single line, starting at the posterior end and proceeding to the anterior end of the sperm nucleus, across the longitudinal section of the sperm. The average fluorescence intensity was calculated from the middle two to three optical images across the longitudinal sperm section for each 10% of the sperm length. The number of zygotes analyzed for each sperm decondensation stage varied from 10 to 75 for each treatment group. The classification of pre-PN-stage zygotes as condensed, partially decondensed (type *a*), totally decondensed (type *b*), or recondensing (type *c*) sperm nuclei was described previously [5].

Representative staining patterns of the sperm chromatin remodeling in control and CPA-treated groups are shown above the graphs for each sperm decondensation stage. Each graph represents the average staining intensity of modified histones over 10% segments of the longitudinal section of the sperm nucleus, starting at the posterior end and proceeding to the tip region. The signal intensity was compared between adjacent sperm segments within the same treatment group and within the same sperm segment between treatment groups. The signal intensity was also qualitatively compared between sperm decondensation stages measured with the same detection settings.

γH2AX. Qualitative analysis of γH2AX foci number and size was done using a three-dimensional reconstitution of each zygote from the Z-stack sections of all individual zygotes. We then used the overlay option to measure the diameter of all foci and count the total number of foci in each size category: 0.01–0.79 or 0.80–2.5 μm in diameter. Unfertilized oocytes (54 saline, 44 CPA), polyspermic zygotes (1 saline, 9 CPA), and pronuclear zygotes (3 saline, 5 CPA) were excluded from this analysis, leaving a total of 79 zygotes sired by saline-treated males and 64 zygotes sired by CPA-treated males. The number of zygotes analyzed for each sperm decondensation stage varied from 2 to 30 for each treatment group.

Statistical Analyses

Chi-square analysis (Systat Version 10.2) and the Fisher exact test, with Bonferroni correction, were used to compare the progression of early zygotic development for all sperm decondensation stages observed in both treatment groups. Unbalanced two-way ANOVA with repeated measures and a logarithmic transformation of the data were done to detect any distance effect along the length of the sperm nucleus, any CPA drug effect, and any interaction between distance and treatment on chromatin remodeling with H4K12ac and H3S10ph for all sperm decondensation stages. Logarithmic transformation of the intensity was done because of the large variation in SEM. A post hoc contrast test for pair-wise

comparison was done to confirm and complement the two-way ANOVA analysis by specifically identifying where along the sperm length segment chromatin remodeling with H4K12ac and H3S10ph differed between treatment groups and among specific adjacent sperm length segments within the same treatment group. These analyses were done with the SAS statistical analysis program (version 9.1). Comparison of the averaged intensity of DNA with the intensity values of H4K12ac is qualitative, since different dyes, propidium iodide, and FITC were used.

The Mann-Whitney *U*-test was used to compare the numbers of γH2AX foci between the control and CPA-treated groups for each individual sperm decondensation stage. This statistical analysis was done for both small (0.01–0.79 μm in diameter) and large (0.79–2.5 μm in diameter) foci. Both condensed and type *a*4 sperm nuclei were excluded from the analysis, since condensed sperm nuclei never had foci, and we did not obtain sufficient type *a*4 sperm nuclei for analysis due to the rapid rate of sperm decondensation at this stage. We did not compare stages for the same treatment group, since the data were dependent and zygotes were not obtained at all stages from at least three different males.

RESULTS

Subclassification of Type *a* Sperm Nuclei in the Rat Zygote

Following fertilization, sperm chromatin decondensation was divided into four stages based on the extent of chromatin compaction, as distinguished by the propidium iodide staining intensity. These sperm decondensation stages are: condensed sperm nuclei, type *a* partially decondensed sperm nuclei, type *b* totally decondensed sperm nuclei, and type *c* recondensing sperm nuclei. These stages are then followed by pronuclear formation (Fig. 2.1, top panel) [5]. Since we observed previously uncharacterized partially decondensed sperm nuclear patterns, type *a* sperm nuclei were further subdivided into four subgroups: 1) type *a*1, the sperm nucleus was starting to decondense at the posterior end; 2) type *a*2, half of the sperm nucleus was decondensed at the posterior end, and

decondensation had progressed to a small extent on both ventral sides; 3) type *a*3, the posterior, ventral sides, and the tip of the sperm nucleus were decondensed; and 4) type *a*4, almost all of the sperm nucleus was decondensed, with the exception of a small condensed region in the midbody area (Fig. 2.1, bottom panel). This subclassification of type *a* sperm nuclei in the rat model facilitated our analysis of the sperm chromatin remodeling patterns described later, and highlights the unique sequential order of sperm decondensation in this species.

Paternal Exposure to CPA Alters the Progression of Sperm Chromatin Decondensation in Early Zygotes

Treatment of male rats with CPA did not affect the fertilizing capacity of their spermatozoa, since the proportion of unfertilized to fertilized oocytes among females mated to saline- or CPA-treated males did not differ (saline, 92/316; CPA, 100/314). Since in vitro fertilization is not a commonly accessible technique in the rat, we collected zygotes at one time point and reported our data as the total number at each sperm nuclear stage at this time. The distribution of zygotes at the time of collection formed a bell-shaped curve, where most zygotes were found in the type *b* sperm nuclei decondensation stage (Fig. 2.2). Paternal exposure to CPA disturbed the distribution of these early zygotes by significantly increasing the number of type *c* sperm nuclei in the CPA group compared with controls (see type *c* sperm nuclei in Fig. 2.2) ($P < 0.001$).

H4K12ac Sperm Chromatin Remodeling Pattern in Pre-PN Zygotes

The signal intensity of histone H4K12ac on the decondensing and remodeling sperm chromatin was quantified for both saline- and CPA-treated groups in all sperm decondensation stages (Fig. 2.3). In zygotes sired by saline-treated males, no visible staining with H4K12ac was seen across the whole sperm length in condensed sperm nuclei (Fig. 2.3a). A faint but visible H4K12ac mark initially appeared in type *a*1 sperm nuclei on the posterior end of the decondensing sperm chromatin, and gradually decreased from the midbody region to the tip of the sperm nucleus (Fig. 2.3b). In type *a*2 sperm nuclei, half of the

sperm length had bright staining, with H4K12ac at the posterior end, and increased intensity to a small extent at the midbody and the tip of the sperm nucleus (Fig. 2.3c). In type *a*3 sperm nuclei, the posterior end, both ventral sides and tip showed positive H4K12ac staining, excluding the midbody region of the sperm head nucleus (Fig. 2.3d). The pattern of histone H4K12ac staining in type *a*4 sperm nuclei was very similar to type *a*3, except that the midbody of the sperm nucleus had started to decondense and stained with H4K12ac (Fig. 2.3e).

The initial appearance and progression of H4K12ac deposition followed the order of sperm chromatin decondensation. The signal intensity of H4K12ac between stages increased significantly as the paternal chromatin progressed through the earliest stages of sperm chromatin remodeling, where the greatest increase was observed at the posterior end, then at the tip, and then at the midbody region of the sperm head nucleus. In type *b* and *c* sperm nuclei, the entire sperm nucleus showed a bright and homogenous staining pattern with H4K12ac (Fig. 2.3, f and g). The specific pattern of staining observed in these three regions in type *a* subgroups was no longer distinguishable in type *b* and *c* sperm nuclei. The location along the longitudinal section of the sperm chromatin dictated the pattern of sperm chromatin remodeling with H4K12ac in nearly all sperm decondensation stages in both treatment groups (Fig. 2.3, Table 2.1; two-way ANOVA with post hoc contrast tests).

The relationship between the pattern of chromatin remodeling with H4K12ac and the DNA content was assessed in type *a*3 sperm nuclei (Fig. 2.3d), because they were partially decondensed and clearly showed the three characteristic chromatin regions of the sperm head. Type *c* sperm nuclei (Fig. 2.3g) were selected because the remodeling of the sperm chromatin was completed by this stage [5]. In type *a*3 sperm nuclei, the level of DNA compaction was inversely related to the signal intensity with H4K12ac for all three regions of the sperm head (Fig. 2.3d). In type *c* sperm nuclei, the level of DNA compaction paralleled the staining intensity of H4K12ac (Fig. 2.3g).

The pattern of H4K12ac staining was also analyzed for the maternal nucleus and polar body of all sperm decondensation stages. The maternal chromosomes of unfertilized oocytes had a spot-like pattern of staining with H4K12ac. Following fertilization, in zygotes with either condensed or type *a*1 sperm nuclei, the maternal nuclear and polar body H4K12ac staining pattern and signal intensity were not distinguishable; both had many bright foci, mostly located in condensed or heterochromatin regions, while euchromatin regions had a low homogenous staining pattern (Supplemental Fig. S2.1a available online at www.biolreprod.org). The pattern of H4K12ac staining began to differ in zygotes with type *a*2 sperm nuclei. Here, the maternal nucleus appeared to have an increased number of foci, and the polar body had a reduced number, with four to five foci. In zygotes with type *a*3 and *a*4 sperm nuclei, there was a more marked difference in the number of foci between the maternal nucleus and the polar body (two to three foci) (Supplemental Fig. S2.1b available online at www.biolreprod.org). The pattern of H4K12ac staining became clearly distinguishable in zygotes with type *b* and *c* sperm nuclei, where the maternal nuclei had numerous, homogenously distributed foci, while the number of foci in the polar body was reduced to zero to one (Supplemental Fig. S2.1c available online at www.biolreprod.org).

Paternal exposure to CPA did not affect sperm chromatin remodeling, as depicted by the unchanged pattern of histone H4K12ac deposition for any of the sperm decondensation stages observed following fertilization (Fig. 2.3, a′–g′) and confirmed by the two-way ANOVA analysis (Table 2.1). In addition, paternal exposure to CPA did not affect the pattern of histone H4K12ac deposition in the maternal nucleus and polar body (data not shown).

H3S10ph Sperm Chromatin Remodeling Pattern in Pre-PN Zygotes

The pattern of histone H3S10ph deposition on the decondensing paternal chromatin was recorded for both saline- and CPA-treated groups in all sperm decondensation stages (Fig. 2.4). In zygotes sired by saline-treated males, no

visible staining with histone H3S10ph was seen in condensed sperm nuclei, with a small peak in the midbody region of the sperm head nucleus (Fig. 2.4a). In type *a*1 sperm nuclei, a very faint staining at the posterior and ventral sides of the sperm head nucleus was observed (Fig. 2.4b). In type *a*2 sperm nuclei, H3S10ph signal intensity increased mostly at the posterior end, and stayed constant at the ventral sides of the sperm head nucleus (Fig. 2.4c). In type *a*3 sperm nuclei, a dramatic increase in H3S10ph signal intensity was observed at the posterior end, ventral sides, and the tip of the sperm head nucleus stained with H3S10ph (Fig. 2.4d). In type *a*4 sperm nuclei, H3S10ph pattern, and signal intensity resembled *a*3 sperm nuclei, except that H3S10ph localized to a greater extent in the midbody and tip regions of the sperm head nucleus (Fig. 2.4e). When comparing the staining intensity of histone H3S10ph in condensed, type *a*1, *a*2, *a*3, and *a*4 sperm nuclei, the greatest change was observed at the posterior end, then at the tip, and lastly at the midbody region of the sperm head nucleus. A ring-like pattern started to form in type *a*4 sperm nuclei at both extremities of the sperm head nucleus; this ring closed completely in type *b* and *c* sperm nuclei (Fig. 2.4, e–g). In type *b* and *c* sperm nuclei, the signal intensity with histone H3S10ph was the highest at both posterior and tip ends, and decreased to a small extent at the midbody region of the sperm head nucleus in type *c* sperm nuclei (Fig. 2.4, f and g). The pattern of sperm chromatin remodeling with H3S10ph was dependent on the location along the longitudinal section of the sperm chromatin in nearly all sperm decondensation stages in both treatment groups (Fig. 2.4 and Table 2.1; two-way ANOVA with post hoc contrast tests).

The relationship between the level of DNA compaction and histone H3S10ph intensity was examined in both type *a*3 and type *c* sperm nuclei. In type *a*3 sperm nuclei, the level of DNA compaction was inversely related to histone H3S10ph staining intensity in all three sperm regions. When the sperm chromatin was decondensed, the signal for H3S10ph was high, and vice versa (Fig. 2.4d). In type *c* sperm nuclei, the level of DNA compaction was still inversely related to the staining intensity of histone H3S10ph; the signal intensity was high at the circumference of sperm nucleus, and low in the middle, while the DNA was

decondensed around the circumference and condensed in the core of the sperm nucleus (Fig. 2.4g).

In zygotes from all the sperm decondensation stages analyzed, the maternal nucleus and polar body were not distinguishable (Supplemental Fig. S2.2 available online at www.biolreprod.org). They both had numerous fine, bright foci forming a ring pattern with histone H3S10ph at the circumference of the nucleus, with very low to no staining in the center. Occasionally, both the maternal and polar body had a single larger focus of the same intensity as the ring pattern. The ring observed in both maternal nuclei and polar bodies was very similar to the perinuclear ring observed on the sperm chromatin of type *b* and *c* sperm nuclei (Fig. 2.4, f and g).

The initial appearance, localization, and pattern of histone H3S10ph deposition on the remodeling sperm chromatin were not affected by paternal exposure to CPA (Fig. 2.4, a′–g′). The two-way ANOVA showed no effect of CPA treatment on the pattern of sperm chromatin remodeling with H3S10ph and no interaction between treatment and distance effect for any of the sperm decondensation stages analyzed (Table 2.1). In addition, paternal exposure to CPA did not affect histone H3S10ph pattern of deposition in either the maternal nucleus or the polar body (data not shown).

Characterization of the Distribution of γH2AX Foci in Pre-PN Zygotes

The appearance and pattern of distribution of γH2AX foci were analyzed in pre-PN zygotes at all stages of sperm decondensation (Fig. 2.5, a–g). In control zygotes, no γH2AX foci were observed in condensed and type *a*1 sperm nuclei (Fig. 2.5, a and b). A gradual increase in the population of small γH2AX foci was found in the later stages of sperm decondensation (Fig. 2.5, f and g), with a constant low occurrence of large γH2AX foci (Fig. 2.5, a–g).

In zygotes sired by sperm from CPA-exposed rats, there were a few small γH2AX foci in the posterior open sperm chromatin region in early decondensing

sperm nuclei, such as the type *a*1 sperm nuclei (Fig. 2.5b′). γH2AX foci appeared on the decondensing posterior end of type *a*2, *a*3, and *a*4 sperm nuclei (Fig. 2.5, c′–e′). In type *b* and *c* sperm nuclei, an enhanced population of large γH2AX foci was detected (Fig. 2.5, f′ and g′).

In the type *a* sperm nuclear subgroups of zygotes sired by CPA-exposed rats, the average number of small diameter (0.01–0.79 μm) foci significantly increased (Fig. 2.6, top panel). In addition, we observed a significant appearance of larger 0.80–2.5 μm diameter foci in type *a*3 and *a*4 sperm nuclei; this increase was enhanced in later stage *b* and *c* sperm nuclei (Fig. 2.6, bottom panel). Type *a*4 sperm nuclei were excluded from the analysis due to the very small number of zygotes within that stage.

In both the maternal nucleus and polar body of control zygotes, we observed a perinuclear ring-like pattern with γH2AX staining formed by numerous small foci; occasionally, a large reaction was found on the ring in zygotes from all of the sperm decondensation stages analyzed (Supplemental Fig. S2.3 available online at www.biolreprod.org). Paternal exposure to CPA did not affect the pattern of γH2AX staining in the maternal nucleus or the polar body at any of the sperm decondensation stages (Supplemental Fig. S2.3 available online at www.biolreprod.org).

Using sperm 3D reconstruction, in type *a* subgroups γH2AX foci were always found in regions of open and loose sperm chromatin structure (Fig. 2.5 and Supplemental Movie S1 available online at www.biolreprod.org); in totally decondensed and recondensing type *b* and *c* sperm nuclei, foci were evenly distributed (Fig. 2.5 and Supplemental Movie S2 available online at www.biolreprod.org). Small γH2AX foci appeared precociously in the earliest sperm decondensation stages (Fig. 2.5 and Supplemental Movie S3 available online at www.biolreprod.org); a dramatic increase in the number of the larger γH2AX foci was observed in the later stages of sperm chromatin remodeling (Fig. 2.5 and Supplemental Movie S4 available online at www.biolreprod.org). This

was not accompanied by a parallel impact on the maternal genome (data not shown).

DISCUSSION

Chromatin remodeling of the paternal genome in early zygotes is not a random event: the pattern of deposition of maternally modified histones, H4K12ac and H3S10ph, on the remodeling of paternal chromatin is extremely precise and orderly. In almost all sperm decondensation stages, with the exception of condensed sperm nuclei, modified histone deposition varied significantly along the sperm and between sperm decondensation stages. These results suggest that sperm chromatin remodeling in the zygote is a highly dynamic process regulated by the order and level of DNA chromatin compaction.

Four phases of chromatin decondensation were observed in sperm nuclei during pre-PN zygotic development: condensed, type *a* partially decondensed, type *b* totally decondensed, and type *c* recondensing sperm nuclei [5]. In type *a* sperm nuclei, three sperm segments were clearly visible; the posterior, the anterior, and the midbody region of the sperm head. Decondensation always proceeded in the same order, from the posterior, to the ventral sides, to the tip and the midbody of the sperm head nucleus. Due to the novel segmental pattern of sperm chromatin decondensation in the rat, type *a* sperm nuclei were further subdivided into four subgroups: type *a*1, type *a*2, type *a*3, and type *a*4 sperm nuclei. Differences in the segmental pattern of sperm nuclear decondensation in rats from that previously described in mice [1] may be attributed to a species difference in sperm chromatin packaging, with two protamines in mice, but only one in rat sperm, or to the region-specific retention of nucleosomes during spermiogenesis [36–38].

Since the midbody region of the sperm head nucleus was the last segment of the sperm chromatin to decondense, we speculate that this may be the region of the sperm nucleus most protected against insult. The midbody, also referred to as the chromocenter, is a spermatozoal region enriched in modified nucleosomes and

poor in protamine [1]. The presence of modified nucleosomes in the midbody may protect it against active paternal genome demethylation, and act as a barrier for sperm chromatin decondensation [1, 8, 38]. Alternatively, the midbody of the sperm nucleus may decondense last, due to its central location.

The initial appearance and distribution of H4K12ac and H3S10ph on the remodeling sperm chromatin in type *a* subgroups followed the exact order of paternal chromatin decondensation: from the posterior, ventral sides, tip, and finally the midbody region of the sperm head nucleus. In type *a*1, *a*2, *a*3, and *a*4 sperm nuclei, the order and level of sperm DNA decondensation dictated the initial appearance and deposition pattern of modified histones H4K12ac and H3S10ph. The rare and distinct epigenetic marks retained in spermatozoa may also regulate the sequential order of sperm chromatin decondensation and the pattern of sperm chromatin remodeling in pre-PN zygotes, since spermatozoal nucleosomes have been found on genes guiding embryonic development [1, 39].

Posttranslational modifications on histone tails, such as H4K12ac and H3S10ph, are responsible for faithful chromatin compaction and cellular processes [40] in early postfertilized oocytes. We report two distinct patterns of chromatin remodeling in early postfertilized oocytes: one for H4K12ac, and a second for H3S10ph. We postulate that the high, homogenous pattern of staining with histone H4K12ac in type *b* and *c* sperm nuclei marks the open and active chromatin structure necessary for subsequent gene transcription and mitosis; this pattern was not affected by the level of DNA compaction. Furthermore, we speculate that the ring pattern of staining with histone H3S10ph in type *b* and *c* sperm nuclei marks the condensed chromatin structure characteristic of the early phase of mitosis [12], which is necessary for the recondensation of the paternal chromatin and the formation of the male pronucleus [41].

Previous work on the effects of paternal exposure to CPA on the formation and maturation of spermatozoa showed altered sperm chromatin packaging, decreased protamine, and thiol contents [42], changes in sperm nuclear matrix

proteins [43], and altered in vitro nuclear decondensation patterns [27]. It has been suggested that these effects of CPA lead to a looser packaging of the sperm chromatin during spermiogenesis, perhaps linking these effects of drug exposure to an altered rate of nuclear decondensation during pre-PN zygotic development [44]. This suggestion is supported by our observation of an increase in the number of zygotes with type *c* sperm nuclei in the CPA group compared with controls. The absence of any effect of CPA on the pattern of sperm chromatin remodeling may be due to compensation mechanisms in the oocyte.

Our results suggest a cross-talk between the male and the female nucleus, since the zygote was able to sense and synchronize its development with the accelerated rate of the sperm chromatin decondensation. Previous work from our laboratory showed that paternal exposure to CPA accelerated the progression of later pronuclear-stage zygotes, and induced aberrant epigenetic reprogramming with histone H4K5ac and DNA methylation [32] and a biphasic DNA damage recognition response in the male genome [24, 32]. The time window of zygotic development, and the events taking place during this window, are distinct in the present study. In early pre-PN zygotes, the oocyte is completing its second cycle of meiosis, and the sperm chromatin is undergoing a complete protamine-to-histone remodeling. Here, we report that early events, such as the progression of sperm chromatin decondensation after fertilization, are disturbed without impacting sperm chromatin remodeling, as depicted by the patterns of two posttranslationally modified histones, H4K12ac and H3S10ph.

We then asked how early the zygote was able to recognize and respond to DNA damage induced by paternal CPA exposure. Small γH2AX foci were already visible in type *a*1 sperm nuclei. The increase in the number of small foci was significant in type *a*2 and *a*3 sperm nuclei, representing stages of rapid chromatin remodeling, when protamines are removed and replaced with histones [5]. In later stages of sperm decondensation, type *c* sperm nuclei, the average number of small foci in the CPA-treated group was comparable to control level. We observed an increase in the numbers of large γH2AX foci beginning in type

*a*3 sperm nuclei and persisting through to type *b* and *c* sperm nuclei after paternal CPA exposure. The early induction of small γH2AX foci suggests a role for γH2AX during chromatin remodeling in the detection of CPA-damaged sperm chromatin during the removal and exchange of protamine for histones [23]. The subsequent disappearance of small γH2AX foci in remodeled sperm chromatin coincides with the increase in large foci, suggesting that these large foci may represent the accumulation of γH2AX marks at already existing sites of damage [23]. A progressive elevation in γH2AX focal volumes was observed in the male pronuclei of zygotes fertilized by CPA-exposed sperm, through S phase (PN3 and −4) into G2 (PN5) [24]. Previous studies showed that early pre-PN zygotes responded in a dose-dependent manner to DNA-damaging agents by activating the γH2AX signaling pathway following gamete fusion, and showed differences in parental DNA repair efficiency [22]. The pattern of γH2AX staining in the maternal nucleus and polar body was not affected by paternal CPA exposure, but may be sensitive to other DNA-damaging agents [21]. A dynamic interaction between small and large γH2AX foci in pre-PN zygotes fertilized by CPA-exposed sperm may indicate the presence of intricate control of damage recognition and repair mechanisms in the oocyte.

In summary, our data demonstrate that paternal exposure to CPA affects the progression of sperm chromatin decondensation, and activates a DNA damage response in the pre-PN rat zygote. The effects on sperm decondensation that are observed in pre-PN zygotes may represent the first manifestation of the detrimental effects previously observed among the progeny of CPA-treated males [28, 32, 34]. Both an undamaged sperm genome and an intact sperm nuclear matrix are necessary for the paternal genome to support embryonic development [45].

ACKNOWLEDGEMENTS

We thank Dr. H. J. Clarke (McGill University, Montreal, QC) for the gift of H4K12ac antibody and useful discussion, Ms. J. Laliberté (McGill University) for her assistance with confocal microscopy, and Jose Correa (McGill University) for his help with the statistical analysis of the H4K12ac and H3S10ph quantification data.

REFERENCES

1. Van der Heijden GW, Derijck AAHA, Ramos L, Giele M, van der Vlag J, de Boer P. Transmission of modified nucleosomes from the mouse male germline to the zygote and subsequent remodeling of paternal chromatin. Dev Biol 2006; 298:458-469.

2. Akabane H, Fan J, Xuehai Z, Zhu GZ. Protein kinase C activity in mouse eggs regulates gamete membrane interaction. Mol Reprod and Devel 2007; 74:1465-1472.

3. Yu Y, Halet G, Lai FA, Swann K. Regulation of diacylglycerol production and protein kinase C stimulation during sperm- and PLCζ-mediated mouse egg activation. Biol Cell 2008; 100:633-643.

4. Perreault SD, Barbee RR, Slott VL. Importance of glutathione in the acquisition and maintenance of sperm nuclear decondensing activity in maturing hamster oocyte. Dev Biol. 1988; 125:181-186.

5. Van der Heijden GW, Dieker JW, Derijck AAHA, Muller S, Berden JHM, Braat DDM, van der Vlag J, de Boer P. Asymmetry in histone H3 variants and lysine methylation between paternal and maternal chromatin of the early mouse zygote. Mech Dev 2005; 122:1008-1022.

6. Leno GH, Mills AD, Philpott A, Laskey RA. Hyperphosphorylation of nucleoplasmin facilitates Xenopus sperm decondensation at fertilization. J Biol Chem 1996; 271:7253-7256.

7. Loppin B, Bonnefoy E, Anselme C, Laurençon A, Karr TL, Couble P. The histone H3.3 chaperone HIRA is essential for chromatin assembly in the male pronucleus. Nature 2005; 437:1386-1390.

8. Santos F, Peters AH, Otte AP, Reik W, Dean W. Dynamic chromatin modifications characterise the first cell cycle in mouse embryos. Dev Biol 2005; 280:225-236.

9. Yoshida N, Brahmajosyula M, Shoji S, Amanai M, Perry ACF. Epigenetic discrimination by mouse metaphase II oocytes mediates asymmetric chromatin remodeling independently of meiotic exit. Dev Biol 2007; 301:464-477.

10. Adenot PG, Mercier Y, Renard J-P, Thompson EM. Differential H4 acetylation of paternal and maternal chromatin precedes DNA replication and differential transcriptional activity in pronuclei of 1-cell mouse embryos. Devel 1997; 124:4615-4625.

11. Wang Q, Wang C-M, Ai J-S, Xiong B, Yin S, Hou Y, Chen D-Y, Schatten H, Sun Q-Y. Histone phosphorylation and pericentromeric histone modifications in oocyte meiosis. Cell Cycle 2006; 5:1974-1982.

12. Song L, Li D, Liu R, Zhou H, Chen J, Huang X. Ser-10 phosphorylated histone H3 is involved in cytokinesis as a chromosomal passenger. Cell Biol Int 2007; 31:1184-1190.

13. DeManno DA, Cottom JE, Kline MP, Peters CA, Maizels ET, Hunzicker-Dunn M. Follicle-stimulating hormone promotes histone H3 phosphorylation on serine-10. Mol Endocrinol 1999; 13:91-105.

14. De la Barre AE, Gerson V, Gout S, Creaven M, Allis CD, Dimitrov S. Core histone N-termini play an essential role in mitotic chromosome condensation. EMBO J 2000; 19:379-391.

15. Jaroudi S, SenGupta S. DNA repair in mammalian embryos. Matat Res 2007; 635:53-77.

16. Perry AC. Hijacking oocyte DNA repair machinery in transgenesis? Mol Reprod Dev 2000; 56:319-324.

17. Generoso WM, Cain KT, Krishna M, Huff SW. Genetic lesions induced by chemicals in spermatozoa and spermatids of mice are repaired in the egg. Proc Natl Acad Sci 1979; 76:435-437.

18. Stiff T, O'Driscoll M, Rief N, Iwabuchi K, Lobrich M, Jeggo PA. ATM and DNA-PK function redundantly to phosphorylate H2AX after exposure to ionizing radiation. Cancer Res 2004; 64:2390-2396.

19. Rogakou EP, Boon C, Redon C, Bonner WM. Megabase chromatin domains involved in DNA double-strand breaks in vivo. J Cell Biol 1999; 146:905-916.

20. Rogakou EP, Pilch DR, Orr VS, Ivanova VS, Bonner WM. DNA double-stranded breaks induce histone H2AX phosphorylation on serine 139. J Biol Chem 1998; 273:5858-5868.

21. Ziegler-Birling C, Helmrich A, Tora L, Torres-Padilla M-E. Distribution of p53 binding protein 1 (53BP1) and phosphorylated H2A.X during mouse preimplantation development in the absence of DNA damage. Int J Dev Biol 2009; 53:1003-1011.

22. Derijck AAHA, van der Heijden GW, Giele M, Philippens MEP, van Bavel CCAW, de Boer P. γH2AX signilling during sperm chromatin remodeling in the mouse zygote. DNA repair 2006; 5:959-971.

23. McManus KJ, Hendzel MJ. ATM-dependent DNA damage-independent mitotic phosphorylation of H2AX in normally growing mammalian cells. Mol Biol Cell 2005; 16:5013-5025.

24. Barton TS, Robaire B, Hales BF. DNA damage recognition in the rat zygote following chronic paternal cyclophosphamide exposure. Tox Sci 2007; 100:495-503.

25. Thomson AB. Late reproductive sequelae following treatment of childhood cancer and options for fertility preservation. Best Pract Res Clin Endocrinol Metab 2002; 16:311-334.

26. Colvin OM. An overview of cyclophosphamide development and clinical applications. Curr Pharm Des 1999; 5:555-560.

27. Qiu J, Hales BF, Robaire B. Effects of chronic low-dose cyclophosphamide exposure on the nuclei of rat spermatozoa. Biol Reprod 1995; 52:33-40.

28. Trasler JM, Hales BF, Robaire B. A time-course study of chronic paternal cyclophosphamide treatment in rats: effects on pregnancy outcome and the male reproductive and hematologic systems. Biol Reprod 1987; 37:317-326.

29. Lewis JD, Song Y, de Jong ME, Bagha SM, Ausió J. A walk though vertebrate and invertebrate protamines. Chromosoma 2003; 111:473-482.

30. Hazzouri M, Pivot-Pajot C, Faure A-K, Usson Y, Pelletier R, Sèle B, Khochbin S, Rousseaux S. Regulated hyperacetylation of core histones during mouse spermatogenesis : involvement of histone deacetylases. Eur J Cell Biol 2000; 79:950-960.

31. Codrington AM, Hales BF, Robaire B. Spermiogenic germ cell phase-specific DNA damage following cyclophosphamide exposure. J Androl 2004; 25**:**354-362.

32. Barton TS, Robaire B, Hales BF. Epigenetic programming in the preimplantation rat embryo is disrupted by chronic paternal cyclophosphamide exposure. PNAS 2005; 102:7865-7870.

33. Trasler JM, Hales BF, Robaire B. Paternal cyclophosphamide treatment of rats causes fetal loss and malformations without affecting male fertility. Nature 1985; 316**:**144–146.

34. Harrouk W, Khatabaksh S, Robaire B, Hales BF. Paternal exposure to cyclophosphamide dysregualtes the gene activation program in rat preimplantation embryos. Mol Reprod Dev 2000; 57:214-223.

35. De la Barre AE, Angelov D, Molla A, Dimitrov S. The N-terminus of histone H2B, but not that of histone H3 or its phosphorylation, is essential for chromosome condensation. EMBO J 2001; 20:6383-6393.

36. Calvin HI. Comparative analysis of the nuclear basic proteins in rat, human, guinea pig, mouse and rabbit spermatozoa. Biochem Biophys Acta 1976; 434:377-389.

37. Kistler WS, Keim PS, Heinriksom RL. Partial structural analysis of the basic chromosomal protein of rat spermatozoa. Biochem Biophys Acta 1976; 427:752-757.

38. Balhorn R, Gledhill BL, Wyrobek AJ. Mouse sperm chromatin proteins: quantitative isolation and partial characterization. Biochemistry 1977; 16:4074-4080.

39. Hammoud SS, Nix DA, Zhang H, Purwar J, Carrell DT, Cairns BR. Distinctive chromatin in human sperm packages genes for embryo development. Nature published 14 June 2009; PMID: 19525931.

40. Eberlin A, Grauffel C, Oulad-Abdelghani M, Robert F, Torres-Padilla ME, Lambrot R, Spehmer D, Ponce-Perez L, Würtz JM, Stote RH, Kimmins S, Schultz P, et al. Histone H3 tails containing dimethylated lysine and adjacent phosphorylated serine modifications adopt a specific conformation during mitosis and meiosis. Mol Cell Biol 2008; 28:1739-1754.

41. Prigent C, Dimitrov S. Phosphorylation of serine 10 in histone H3, what for? J Cell Sci. 2003; 116:3677-3685.

42. Codrington AM, Hales BF, Robaire B. Exposure of male rats to cyclophosphamide alters the chromatin structure and basic proteome in spermatozoa. Hum Reprod 2007; 22:1431-1442.

43. Codrington AM, Hales BF, Robaire B. Chronic cyclophosphamide exposure alters the profile of rat sperm nuclear matrix proteins. Biol of Reprod 2007; 77:303-311.

44. Perreault SD, Naish SJ, Zirkin BR. The timing of hamster sperm nuclear decondensation and male pronucleus formation is related to sperm nuclear disulfide bond content. Biol Reprod 1987; 36:239-244.

45. Ward WS, Kimura Y, Yanagimachi R. An intact sperm nuclear matrix may be necessary for the mouse paternal genome to participate in embryonic development. Biol Reprod 1999; 60:702-706.

FIGURES

Figure 2.1. Types of paternal nuclei observed in early postfertilization zygotes. The DNA was stained with propidium iodide (red). **Top panel**) Condensed, type *a*, type *b*, type *c* and pronuclear sperm (PN) nuclei. **Bottom panel**) Subclassification of type *a* sperm nuclei: type *a*1, type *a*2, type *a*3, and type *a*4. Pictures were taken by confocal microscopy. Bar = 10 μm.

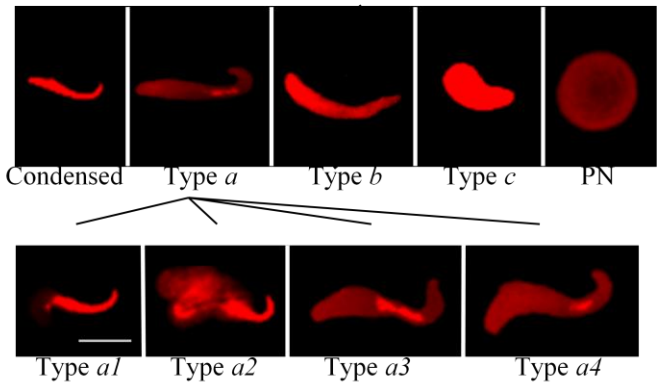
Condensed
Type a
Type b
Type c
PN
Type a1
Type a2
Type a3
Type a4

Figure 2.2. The distribution of types of paternal nuclei in early pre-PN zygotes. The progression of early zygotes is accelerated following chronic paternal CPA treatment to type *c* sperm nuclei (n = 20 males for saline; n = 20 males for CPA). The gray bars represent the zygotes sired by sperm from saline-treated males, and the black bars represent zygotes sired by CPA-exposed sperm. Number of zygotes within each type of paternal nuclei: saline, 34, 83, 109, 27, 45; and CPA, 30, 63, 109, 59, 39 for condensed, type *a*, type *b*, type *c*, and PNs, respectively. Statistical analysis performed: χ^2 analyses, Fisher exact test, with Bonferroni correction; $^{**}P < 0.001$.

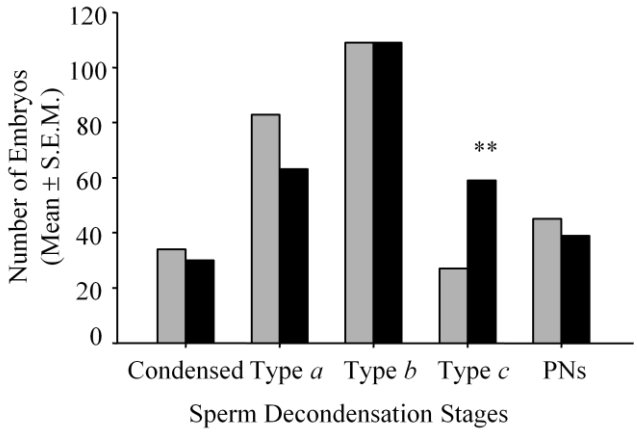
120
100
80
60
40
20
0
Number of Embryos
(Mean ± S.E.M.)
**
Condensed
Type a
Type b
Type c
PNs
Sperm Decondensation Stages

Figure 2.3. Quantitative analysis of the initial appearance, progression, and pattern of H4K12ac staining intensity on the paternal chromatin for all sperm decondensation stages of pre-PN zygotes. The sperm decondensation stage is on the top of each graph; below each stage, there is the best representative picture of saline-exposed sperm on the left (**a**) and CPA-exposed sperm on the right (**a′**) for each stage. DNA was stained with propidium iodide (red) and H4K12ac with FITC (green). The y axes represent H4K12ac intensity (mean ± SEM), and the x axes represent sperm length in 10% segments; error bars are the SEM. Light gray line, saline group; black line, CPA group; dashed dark gray line, DNA content. For each individual type of paternal nuclei, the staining intensity of histone H4K12ac differed significantly across the longitudinal section of the sperm length for almost all sperm decondensation stages with the exception of condensed sperm nuclei. CPA did not affect histone H4K12ac staining intensity and patterning in any of the sperm decondensation stages. Number of pre-PN zygotes analyzed in each sperm decondensation stage: saline, (**a**) n = 6, 11 zygotes, (**b**) n = 6, 12 zygotes, (**c**) n = 6, 8 zygotes, (**d**) n = 9, 18 zygotes, (**e**) n = 7, 10 zygotes, (**f**) n = 8, 39 zygotes, (**g**) n = 6, 10 zygotes; and CPA, (**a′**) n = 6, 15 zygotes, (**b′**) n = 5, 7 zygotes, (**c′**) n = 4, 7 zygotes, (**d′**) n = 8, 13 zygotes, (**e′**) n = 2, 2 zygotes, (**f′**) n = 9, 34 zygotes, (**g′**) n = 8, 26 zygotes for sperm decondensation stages: condensed, type *a*1, type *a*2, type *a*3, type *a*4, type *b*, and type *c* sperm nuclei, respectively. Statistical analyses were done using an unbalanced two-way ANOVA with repeated measures and a logarithmic transformation of the intensity followed by post hoc contrast tests with the SAS program. The asterisks are from the post hoc contrast test results; the color of the asterisks indicates treatment group, and the horizontal bars indicate between which sperm length segments there was a significant difference in the H4K12ac intensity; $*P < 0.05$, $**P < 0.001$, $***P < 0.0001$. Bar in **a** = 10 μm for **a**–**g′**.

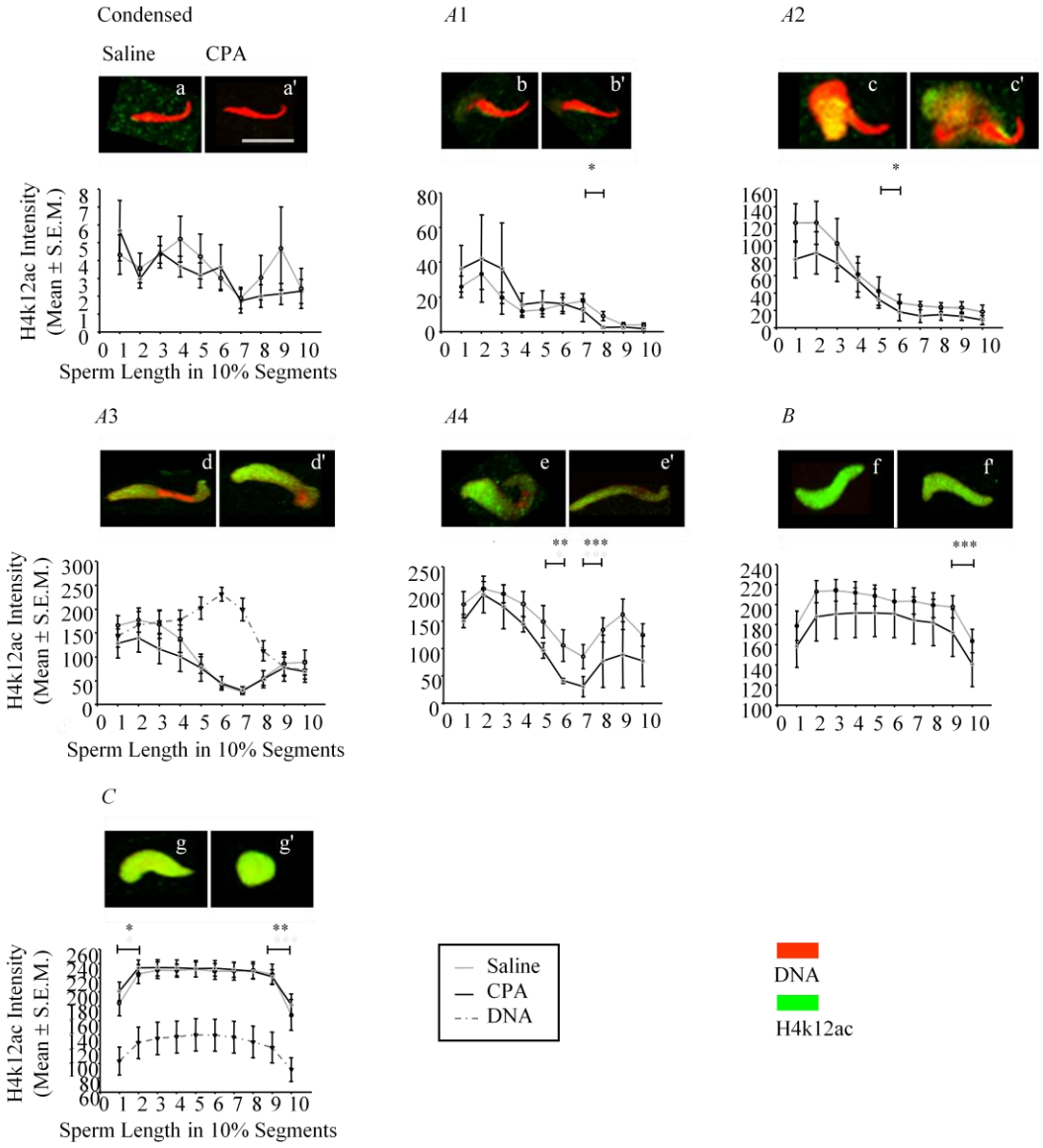
Condensed
A1
A2
Saline
CPA
a
a'
b
b'
c
c'
H4k12ac Intensity
(Mean ± S.E.M.)
Sperm Length in 10% Segments
A3
A4
B
d
d'
e
e'
f
f'
C
g
g'
Saline
CPA
DNA
DNA
H4k12ac

<u>Figure 2.4.</u> Quantitative analysis of the initial appearance, progression, and pattern of histone H3 phosphorylated at serine 10, H3S10ph, on the decondensing paternal nuclei in pre-PN zygotes. The sperm decondensation stage is on the top of each graph; below each stage, there is the best representative picture of saline-exposed sperm on the left (**a**) and CPA-exposed sperm on the right (**a′**) for each stage. DNA was stained with propidium iodide (red) and H3S10ph with FITC (green). The y axes represent H3S10ph intensity (mean ± SEM), and the x axes represent sperm length in 10% segments. Error bars are the SEM. Light gray line, saline group; black line, CPA group; dashed dark gray line, DNA content. For each individual type of paternal nuclei, the localization and staining intensity of histone H3S10ph differed significantly along the different segments of the sperm length in all sperm decondensation stages. CPA exposure did not affect histone H3S10ph staining intensity or patterning for any of the sperm decondensation stages. Number of pre-PN zygotes analyzed at each sperm decondensation stage: saline, (**a**) n = 10, 33 zygotes, (**b**) n = 6, 7 zygotes, (**c**) n = 8, 15 zygotes, (**d**) n = 10, 17 zygotes, (**e**) n = 5, 6 zygotes, (**f**) n = 9, 70 zygotes, (**g**) n = 9, 17 zygotes; and CPA, (**a′**) n = 7, 17 zygotes, (**b′**) n = 4, 4 zygotes, (**c′**) n = 9, 15 zygotes, (**d′**) n = 8, 18 zygotes, (**e′**) n = 3, 3 zygotes, (**f′**) n = 9, 75 zygotes, (**g′**) n = 9, 33 zygotes for sperm decondensation stages: condensed, type *a*1, type *a*2, type *a*3, type *a*4, type *b*, and type *c* sperm nuclei, respectively. Statistical analyses, unbalanced two-way ANOVA with repeated measures, and a logarithmic transformation of the intensity followed by post hoc contrast tests were performed with the SAS program; the asterisks are from the post hoc contrast tests results, and the color refers to the appropriate treatment group. The horizontal bars indicate between which two adjacent sperm length segments there is a significant difference in H3S10ph intensity; $*P < 0.05$, $**P < 0.001$, $***P < 0.0001$. Bar in **a** = 10 μm for **a**–**g′**.

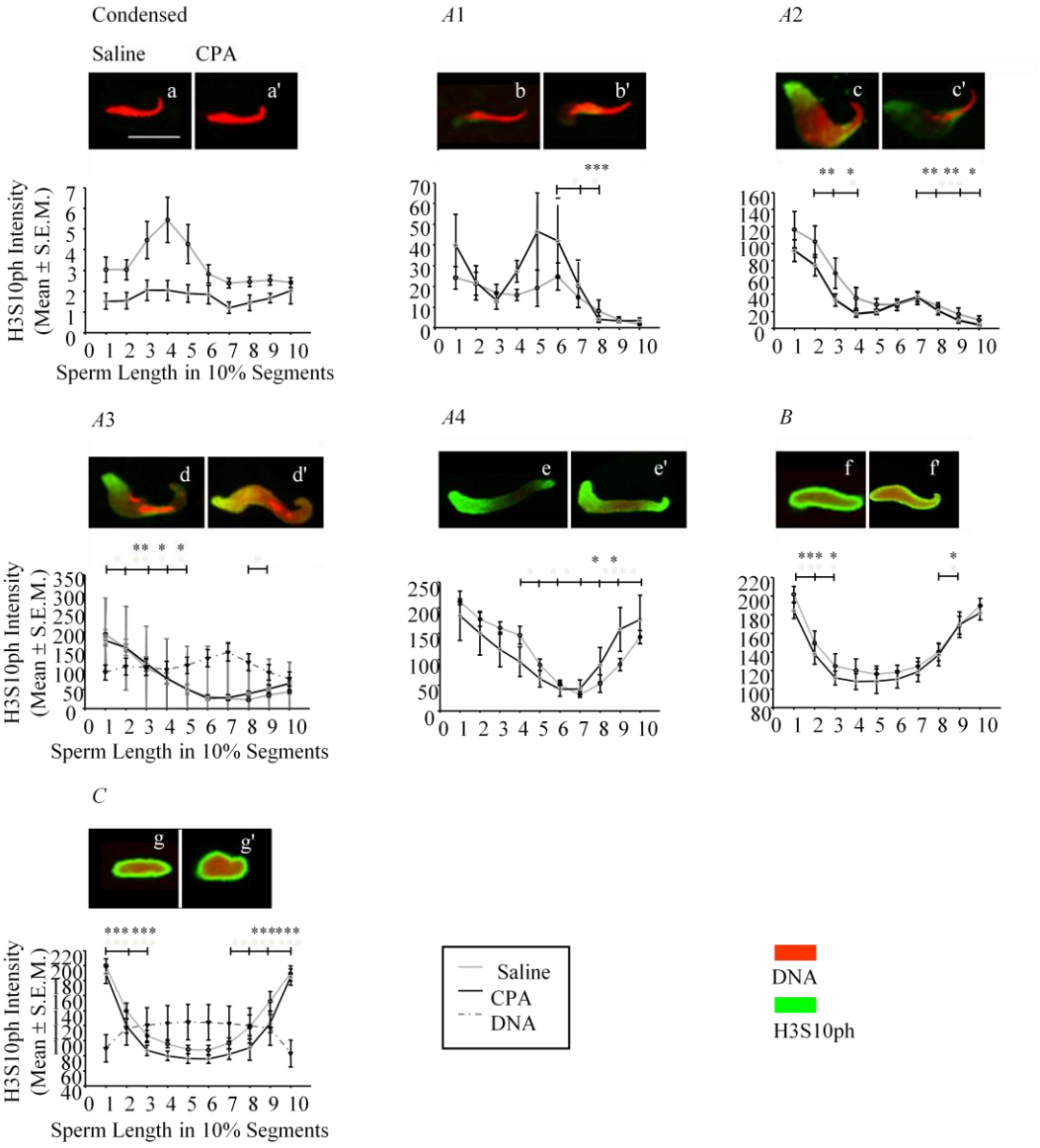
Condensed
A1
A2
Saline
CPA
a
a'
b
b'
c
c'
H3S10ph Intensity
(Mean ± S.E.M.)
Sperm Length in 10% Segments
A3
A4
B
d
d'
e
e'
f
f'
C
g
g'
Saline
CPA
DNA
DNA
H3S10ph

Figure 2.5. The appearance and distribution of γH2AX foci on the decondensing sperm chromatin is altered in decondensing sperm nuclei after CPA exposure. The top panels are immunofluorescence projection images of saline-exposed sperm (**a**–**g**), and the bottom panels represent CPA-exposed sperm (**a′**–**g′**) at every sperm decondensation stage in pre-PN zygotes. The top row are projections of γH2AX with FITC (green) only, the middle row are projections of DNA stained with propidium iodide (red) only, and the last row represents the merged images of both γH2AX and DNA. Control group (**a**) condensed, (**b**) type *a*1, (**c**) type *a*2, (**d**) type *a*3 (still image from Supplemental Movie S1), (**e**) type *a*4, (**f**) type *b*, and (**g**) type *c* (still image from Supplemental Movie S2) sperm nuclei. CPA-treated group (**a′**) condensed, (**b′**) type *a*1, (**c′**) type *a*2, (**d′**) type *a*3 (still image from Supplemental Movie S3), (**e′**) type *a*4, (**f′**) type *b*, and (**g′**) type *c* (still image from Supplemental Movie S4) sperm nuclei. Foci were only distributed in regions of decondensed sperm chromatin. We observed an earlier appearance and an increase in the number and size of γH2AX foci, starting from type *a*2 sperm nuclei in our CPA treatment group. Bar = 10 μm.

Sperm decondensation stages

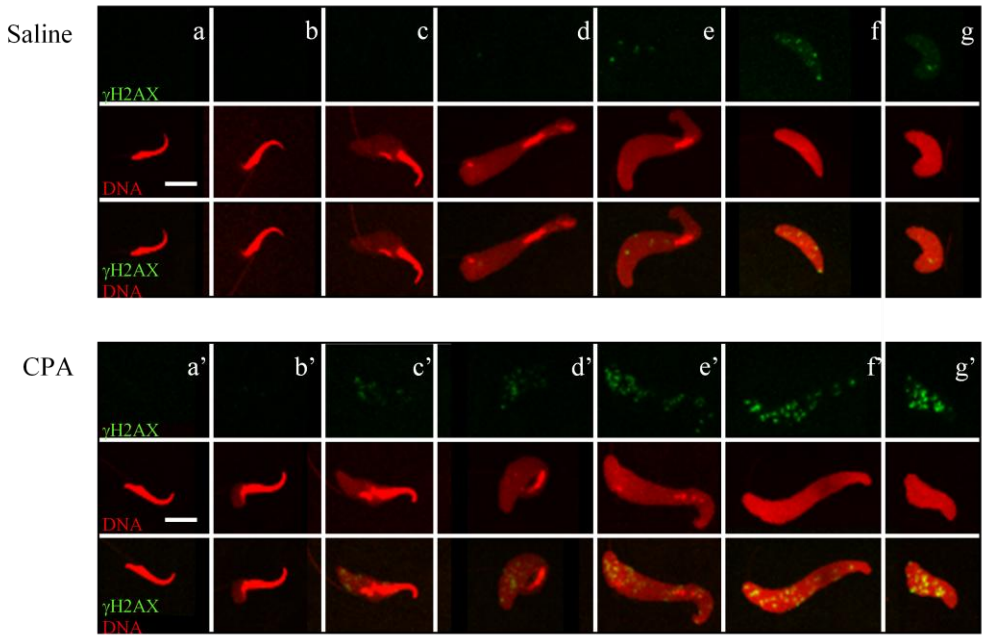

<u>Figure 2.6.</u> Quantitative analysis of the average number of small (Top panel) and large (Bottom panel) γH2AX foci per sperm per male for all sperm decondensation stages. Bar = 10 μm. The y axis is the average number of foci per sperm per male ± SEM, and the x axis represents the sperm decondensation stages. Number of pre-PN zygotes analyzed at each sperm decondensation stage: saline, (**a**) n = 4, 16 zygotes, (**b**) n = 3, 5 zygotes, (**c**) n = 3, 4 zygotes, (**d**) n = 5, 9 zygotes, (**e**) n = 3, 4 zygotes, (**f**) n = 6, 30 zygotes, (**g**) n = 3, 11 zygotes; and CPA, (**a′**) n = 5, 17 zygotes, (**b′**) n = 3, 3 zygotes, (**c′**) n = 4, 8 zygotes, (**d′**) n = 4, 8 zygotes, (**e′**) n = 1, 2 zygotes, (**f′**) n = 6, 20 zygotes, (**g′**) n = 3, 6 zygotes for sperm decondensation stages: condensed, type *a*1, type *a*2, type *a*3, type *a*4, type *b*, and type *c* sperm nuclei, respectively. Mann-Whitney *U*-test was done to compare the average number of foci between CPA-treated and control group at all stages of sperm decondensation, independently and for both populations of γH2AX foci. $*P < 0.05$.

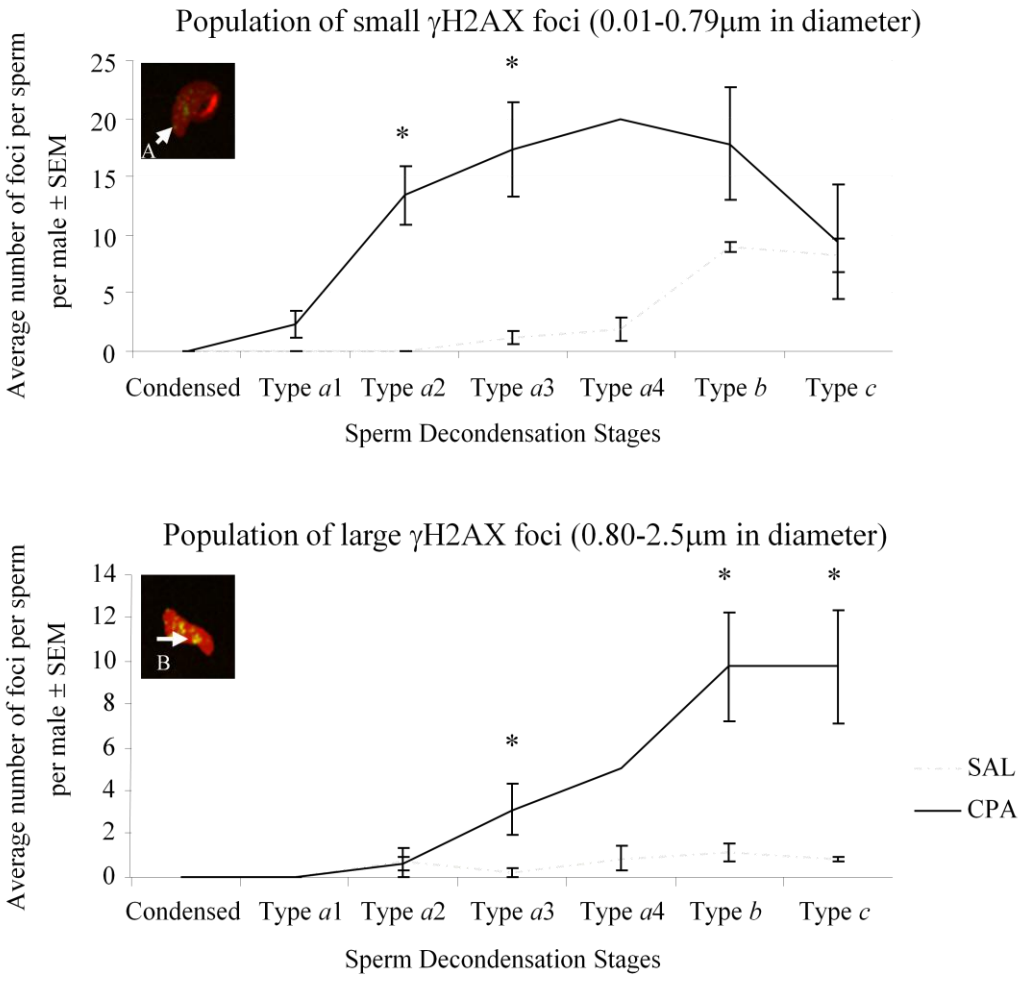
Population of small γH2AX foci (0.01-0.79μm in diameter)
Average number of foci per sperm per male ± SEM
25
20
15
10
5
0
A
*
*
Condensed
Type a1
Type a2
Type a3
Type a4
Type b
Type c
Sperm Decondensation Stages
Population of large γH2AX foci (0.80-2.5μm in diameter)
Average number of foci per sperm per male ± SEM
14
12
10
8
6
4
2
0
B
*
*
*
Condensed
Type a1
Type a2
Type a3
Type a4
Type b
Type c
Sperm Decondensation Stages
SAL
CPA

TABLES

<u>Table 2.1.</u> Quantification of the pattern of deposition of modified histones H4K12ac and H3S10ph in all sperm decondensation stages. Statistical analyses for H4k12ac and H3S10ph immunofluorescence by unbalanced Two-Way ANOVA with repeated measures and a logarithmic transformation of the intensity using SAS program. The CPA drug effect, the sperm length distance and the interaction of both factors were analyzed in all sperm decondensation stages for both modified histones. These results demonstrate that there were no treatment effects or interactions between the drug and distance effect for both H4k12ac and H3S10ph signal intensity but that there was a significant distance effect on the intensity of both modified histones for most sperm decondensation stages with the exception of H4k12ac in condensed sperm nuclei group. H4k12ac, the same embryos from figure 3 were analyzed in table 1. H3S10ph, the same embryos from figure 4 were analyzed in table 1. P values are adjusted; * $P< 0.05$, ** $P< 0.001$, *** $P< 0.0001$.

Type of paternal nuclei	H4k12ac			H3S10ph		
	Drug P value	Distance P value	Interaction P value	Drug P value	Distance P value	Interaction P value
Condensed	0.8201	0.1521	0.4277	0.0605	0.0017*	0.3891
Type *a*1	0.4847	<0.0001***	0.285	0.3947	<0.0001***	0.1
Type *a*2	0.4352	<0.0001***	0.6543	0.2277	<0.0001***	0.5185
Type *a*3	0.4647	<0.0004**	0.7738	0.3744	<0.0001***	0.421
Type *a*4	0.201	<0.0001***	0.2361	0.7626	<0.0001***	0.3307
Type *b*	0.3269	<0.0001***	0.4832	0.5038	<0.0001***	0.9855
Type *c*	0.7429	<0.0001***	0.7771	0.1181	<0.0001***	0.0297

SUPPLEMENTAL FIGURES

Supplemental figure 2.1. **The pattern of H4k12ac staining on the maternal nucleus and polar body of pre-pronuclear zygotes.** The sperm decondensation stage is on the top of each stage best representative picture. The top picture is the confocal phase contrast picture (gray scale) where you can see the whole one cell zygote with the sperm tail (red arrow head). The bottom picture is the immunofluorescence picture, DNA was stained with propidium iodide (red) and H4k12ac with FITC (green), arrows point to P (paternal nucleus), M (maternal nucleus) and PB (polar body). Following fertilization, the pattern of H4k12ac staining is the same for both the maternal nucleus and the polar body with 5 to 6 foci. As the sperm chromatin decondenses, the maternal nucleus gradually increases its foci number while the polar body decreases its foci number to be completely different in type *b* and *c* sperm nuclei, where the maternal nucleus has clearly more foci compared to only one foci on the polar body. This progression in the pattern of staining was not affected by our CPA drug treatment. (Scale bar = 10μm).

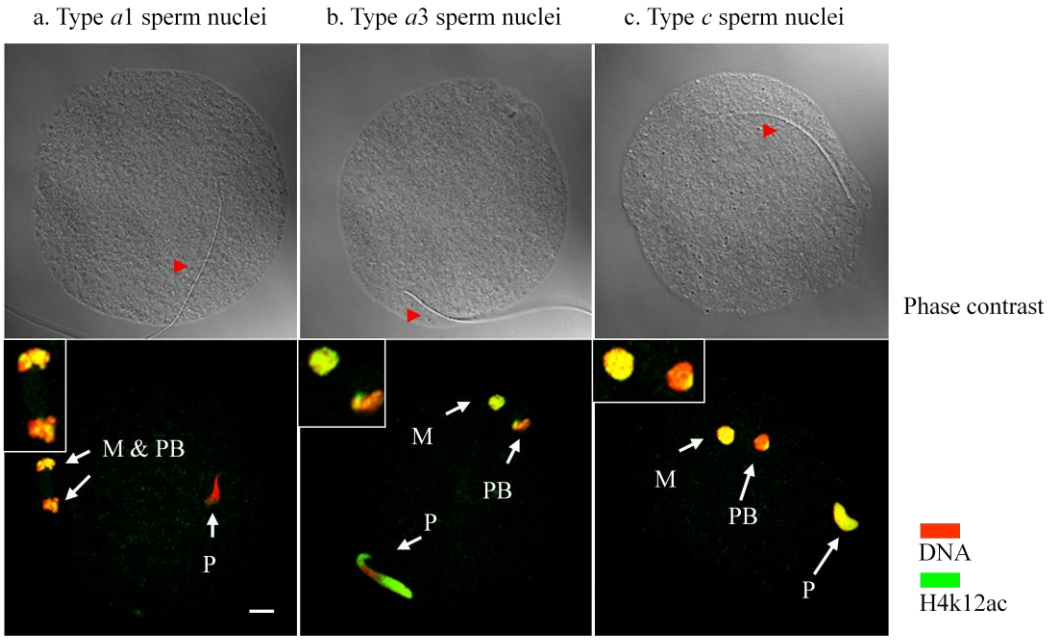
a. Type a1 sperm nuclei
b. Type a3 sperm nuclei
c. Type c sperm nuclei
Phase contrast
M & PB
P
M
PB
P
M
PB
P
DNA
H4k12ac

Supplemental figure 2.2. **The pattern of H3S10ph staining on the maternal nucleus and polar body of pre-pronuclear zygotes.** The sperm decondensation stage is on the top of each stage best representative picture. The top picture is the confocal phase contrast picture (gray scale) where you can see the whole one cell zygote with the sperm tail (red arrow head). The bottom picture is the immunofluorescence picture, DNA was stained with propidium iodide (red) and H3S10ph with FITC (green), arrows point to P (paternal nucleus), M (maternal nucleus) and PB (polar body). At all stages of sperm chromatin decondensation, we observed on both the maternal nucleus and polar body a peri-nuclear ring pattern of staining with H3S10ph. This ring pattern was not affected by our CPA drug treatment. (Scale bar = 10μm).

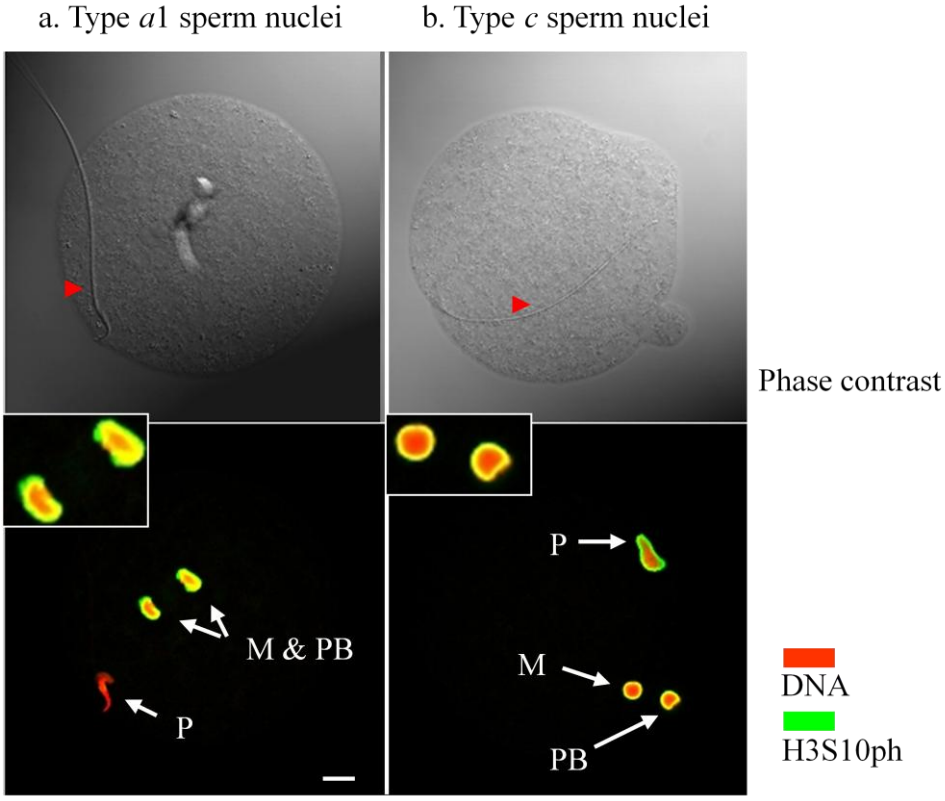
a. Type a1 sperm nuclei
b. Type c sperm nuclei
Phase contrast
M & PB
P
P
M
PB
DNA
H3S10ph

Supplemental figure 2.3. **The pattern of γH2AX staining on the maternal nucleus and polar body of pre-pronuclear zygotes.** The sperm decondensation stage is on the top of each column. The top picture is the confocal phase contrast picture (gray scale) where you can see the whole one cell zygote with the sperm tail (red arrow head). In the lower image, DNA was stained with propidium iodide (red) and γH2AX with FITC (green); arrows point to P (paternal nucleus), M (maternal nucleus) and PB (polar body). At all stages of sperm chromatin decondensation we observed, on both the maternal nucleus and polar body, numerous small foci forming a peri-nuclear ring with γH2AX staining. In most cases, we also observed a single big focus in the peri-nuclear ring pattern on both maternal nucleus and polar body from type *a*4 to type *c* sperm nuclei stages. This ring pattern was not affected by CPA drug treatment (scale bar = 10μm).

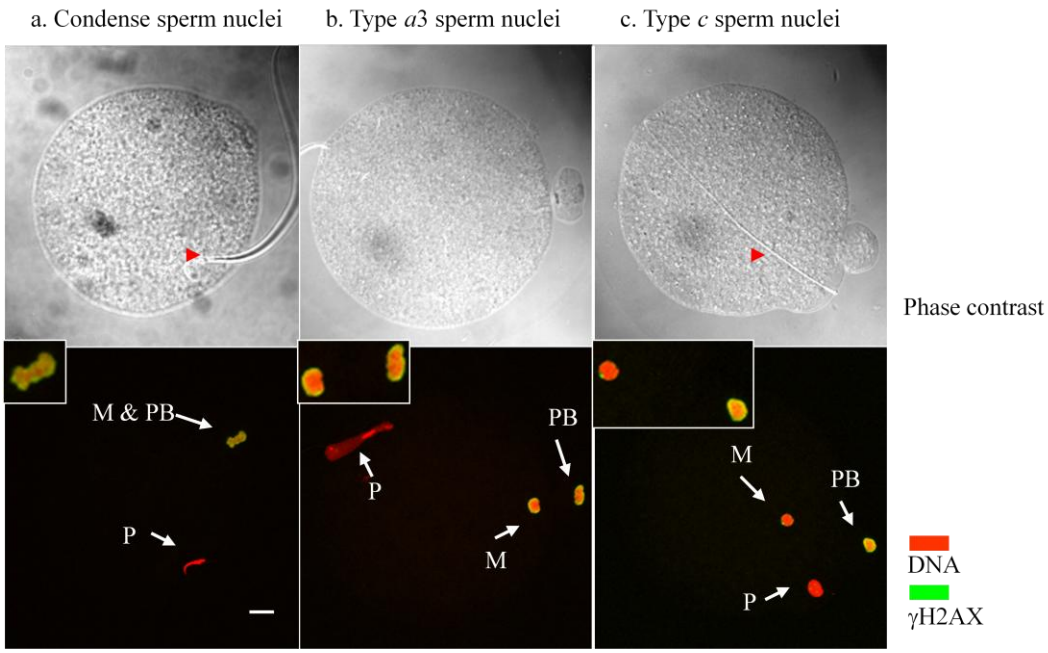
a. Condense sperm nuclei
b. Type a3 sperm nuclei
c. Type c sperm nuclei
Phase contrast
M & PB
P
P
PB
M
M
PB
P
DNA
γH2AX

CONNECTING TEXT

In chapter II we found that chronic paternal exposure to cyclophosphamide led to the acceleration of sperm chromatin decondensation and the activation of DNA damage recognition in pre-pronuclear zygotes. Previous work from our lab suggested that the progression of pronuclear zygotes was also accelerated and eventually delayed in cleavage stage embryos. In chapter III, we performed *in vivo* and *in vitro* embryonic developmental experiments using immunofluorescence and confocal microscopy to determine the exact timing and possible mechanism responsible for this switch in the rate of embryonic development.

CHAPTER III

Paternal Cyclophosphamide Exposure Induces the Formation of Functional Micronuclei during the First Zygotic Division

Lisanne Grenier, Bernard Robaire & Barbara F. Hales

PLoS One published 16 November 2011; doi:10.1371/journal.pone.0027600:
PMID 22110683

ABSTRACT

Paternal exposures to cancer chemotherapeutics or environmental chemicals may have adverse effects on progeny outcome that are manifested in the preimplantation embryo. The objectives of this study were to determine the impact of paternal exposure to cyclophosphamide, an anticancer alkylating agent, on the formation, chromatin origin and function of micronuclei in cleavage stage rat embryos. Male Sprague-Dawley rats were gavaged with saline or cyclophosphamide (6 mg/kg/day) for 4 weeks and mated to naturally cycling females to collect pronuclear zygotes and 2 to 8 cell embryos. Micronuclear chromatin structure was characterized using confocal microscopy to detect immunoreactivities for H3K9me3, a marker for maternal chromatin, and lamin B, a nuclear membrane marker. DNA synthesis was monitored using EdU (5-ethynyl-2′-deoxyuridine) incorporation. Fertilization by cyclophosphamide-exposed spermatozoa led to a dramatic elevation in micronuclei in cleavage stage embryos (control embryos: 1% to 5%; embryos sired by treated males: 70%). The formation of micronuclei occurred during the first zygotic division and was associated with a subsequent developmental delay. The absence of H3K9me3 indicated that these micronuclei were of paternal origin. The micronuclei had incomplete peri-nuclear and peri-nucleolar lamin B1 membrane formation but incorporated EdU into DNA to the same extent as the main nucleus. The formation of micronuclei in response to the presence of a damaged paternal genome may play a role in increasing the rate of embryo loss that is associated with the use of assisted reproductive technologies, parenthood among cancer survivors, and paternal aging.

INTRODUCTION

The incidence of cancer in man of reproductive age has been on the rise over the past few decades; consequently, treatment with chemotherapeutics and radiotherapy is now common amongst the younger male population [1]. Many of these young men survive and experience compromised fertility; their decrease in the likelihood of fathering a child is dependent on the treatment regimen [2]–[4]. Cyclophosphamide (CPA) is a commonly used chemotherapeutic agent that is an alkylating agent and induces DNA double strand breaks [5]. Previous studies, from our laboratories and others, have shown that the treatment of male rats with CPA has dose dependent and time specific effects on spermatogenesis with adverse effects on embryo development [6]–[9]. The greatest amount of DNA damage in male germ cells exposed to CPA was observed when elongating spermatids were targeted; when CPA-exposed male rats were mated to untreated, healthy females, a marked delay in the formation of blastocysts was observed, followed by an increase in peri-implantation embryonic loss [6], [10]. Indeed, a DNA damage response was activated in the early post-fertilization zygote [11].

Exposure of various cell types to radiation or to a wide range of chemicals damages DNA or disrupts microtubules and spindle assembly, resulting in chromosomal aberrations and the formation of micronuclei [12], [13]. Micronuclei are small, extranuclear, DNA containing structures. In toxicology, the formation of micronuclei is used as an in vitro assay to detect putative chemical mutagens or carcinogens [14]. However, recent studies have revealed that non-genotoxic chemicals, such as retinoic acid, may also induce the formation of micronuclei in pluripotent stem cells, suggesting an association between the formation of micronuclei and neural differentiation [15]. Thus, the formation and fate of micronuclei may have important implications for both the genomic stability and plasticity of cells.

Studies with cancer patients and using animal models have revealed that exposure to cancer chemotherapeutics during germ cell formation in the testis or maturation in the epididymis may adversely affect the quality of spermatozoa, as

assessed by a variety of sperm quality tests [16], [17]. Spermatozoa with damaged chromatin are capable of fertilizing oocytes, thus transferring this lesion to the zygote [18]. Indeed, paternal exposure to acrylamide, a chemical found in tobacco smoke and produced during the cooking of starchy foods, increased the formation of micronuclei in two cell embryos, during the first mitotic division, resulting in chromosomal mosaicism [19]. Intracytoplasmic sperm injection was associated with abnormal chromosome segregation and micronuclear formation in two-cell stage mouse embryos [20]. Despite the extensive use of assisted reproductive techniques, the numbers of live offspring produced after intracytoplasmic sperm injection are low [20], [21]. Thus, it is important to investigate the possible consequences of micronuclear formation on events in early embryos. The goal of this study was to determine the impact of paternal exposure to cyclophosphamide on early cleavage stage embryo development and on the formation, chromatin origin and function of micronuclei.

MATERIALS AND METHODS

Drug treatment and embryo collection *in vivo*

Ethics Statement.

This study was done in accordance with the guidelines of the Canadian Council on Animal Care for the ethical use and care of animals in science. The protocol (Protocol Number: 2144) was approved by the Animal Care Committee of McGill University.

Adult male (350–400 g) and virgin female (225–250 g) Sprague-Dawley rats were purchased from Charles River Canada (St. Constant, Quebec, Canada) and housed at the Animal Resources Centre, McIntyre Medical Building, McGill University (Montreal, Canada). Animals received food and water ad libitum and were maintained on a 0700–1900hr light/dark cycle. The drug treatment and zygote protocols previously described [6] were followed with minor modifications. After one week of acclimatization, male rats were randomly assigned to one of two treatment groups and gavaged with saline (vehicle) or CPA

(CAS 6055-19-2; Sigma Chemical Co., St Louis, Missouri), 6 mg/kg per day, six times per week for four weeks.

On the fifth week of treatment, proestrus control virgin females were selected by a vaginal wash in the mid-afternoon and were caged overnight, in groups of two, with either a control or CPA treated male. Pregnancies were confirmed with sperm positive vaginal smears the following morning, designated as gestation day 0. Sperm positive females were euthanized on day 0 at 1300hr, on day 1 at 1000hr, on day 2 at 1400hr and day 3 at 1000hr to collect pronuclear zygotes, 2 cell, 4 cell and 8 cell embryos, respectively. Oviducts and whole uteri were isolated and cleaned in pre-warmed (37°C) M2 culture medium (Sigma Chemical Co.), pronuclear zygotes were collected from the ampullae in warm M2 medium, and early cell cleavage embryos were flushed with a 30 round gauge needle from the infundibulum of the oviduct with 0.2 ml of warm M2 medium.

Immunofluorescence

The immunofluorescence protocols used were described previously [22]. To characterize micronuclei from embryos sired by CPA exposed males, embryos were incubated with rabbit polyclonal anti-lamin B1 (1:500 dilution; catalogue number ab16048, Abcam, Cambridge, MA) or rabbit polyclonal anti-trimethyl-histone H3 (Lys9) (1:200 dilution; catalogue number 07-442, Millipore, Billerica, MA) overnight at 4°C in a humidified chamber. Both primary and secondary antibodies were diluted in goat blocking solution (10% goat serum, 3% BSA and 0.1% Tween 20 in PBS). Zygotes were then washed 3×15 min in goat blocking solution, incubated for 1 hr at room temperature with the secondary antibody, goat fluorescein anti-rabbit IgG (H+L) (1:200 dilution; catalogue number F1-1000, Vector Laboratories, Burlington, Ontario, Canada), and rewashed 3×15 min in goat blocking solution. DNA was stained with propidium iodide (catalogue number P4864, Sigma Chemical Co.) at 10 µg/mL in goat blocking solution for 20 min, washed in 0.05% Tween 20 in PBS for 10 min, mounted in 3 µl of VectaShield mounting medium (Vector Laboratories) on a premarked pap pen

slide and covered with a cover slip. Slides were then stored at 4°C and visualized with confocal microscopy within two days.

In vitro zygotic development and detection of DNA synthesis

In vitro zygotic development was followed using the mR1ECM milieu [23]. To detect DNA synthesis, the Click-It kit (catalogue number C10337, Invitrogen, Burlington, Ontario, Canada) was used. A final concentration of 100 μM EdU (5-ethynyl-2′-deoxyuridine) was supplemented to mR1ECM+BSA (pH equilibrated to 7.4 with 10N HCl). This zygotic development milieu was covered with light mineral oil to prevent evaporation and pre-equilibrated for 3 h before its use in an incubator at 37°C and 5% CO2. All solutions were prepared fresh the day of the experiment.

Embryo collection for *in vitro* incubation

Sperm positive females were euthanized at 1100hr on day 0 to collect pre-pronuclear stage zygotes in prewarmed (37°) M2 culture medium (Sigma Chemical Co.). Zygotes were released from the ampullae or flushed into a drop of prewarmed (37°C) 1% hyaluronidase (Sigma Chemical Co.) in M2 medium to digest the cumulus cells, washed three times in prewarmed (37°C) mR1ECM+BSA, and incubated in pre-equilibrated (37°C and 5%CO2) mR1ECM+BSA+100 uM EdU. The embryos were incubated overnight and analyzed under the light microscope every 15 min between 0900 and 1030hr on day 1 to assess the proportion of zygotes that divided to the 2 cell stage and thus completed the first zygotic division. To assess DNA synthesis in embryos collected on day 3 at 1000hr embryos were incubated in vitro for three hours. All of these steps. from the time of embryo collection to the in vitro incubation, were done within 7 min to preserve embryonic quality. Following collection of the embryos, EdU incorporation was detected as described below.

Click-iT EdU Immunodetection

For a more complete Click-iT protocol please refer to the instruction manual from Invitrogen (catalogue number C10337). Embryos were washed in 3% BSA in 1× PBS (pH 7.4; Mg2+ and Ca2+ free). Zona pellucidae were removed in prewarmed (37°C) acid Tyrode solution (pH 2.5) by pipetting up and down for 5 sec, and then washed in 3% BSA in 1× PBS (pH 7.4; Mg2+ and Ca2+ free). During the permeabilization step, the Click-iT reaction cocktail was prepared in the following sequence: 1×Click-iT reaction buffer, 430 µl; CuSO4, 20 µl; Alexa Fluor azide, 1.2 µl; reaction buffer additive, 50 µl, and used within 15 min of preparation. Following the permeabilization step, the embryos were washed in 3% BSA in 1× PBS (pH 7.4; Mg2+ and Ca2+ free) and incubated for 30 min at room temperature with the Click-iT reaction cocktail. DNA was stained with propidium iodide (catalogue no. P4864, Sigma Chemical Co.) at 10 µg/ml in 3% BSA in 1× PBS (pH 7.4; Mg2+ and Ca2+ free) for 20 min and washed 1× PBS (pH 7.4; Mg2+ and Ca2+ free) twice, mounted in 3 µl of VectaShield mounting medium (Vector Laboratories) on a premarked pap pen slide, and covered with a cover slip. Slides were stored at 4°C and visualized by confocal microscopy during the next two days.

Confocal microscopy

A Zeiss LSM 510 Axiovert 100 M confocal microscope with a Plan-Apochromat ×63/1.4 oil DIC objective was used to visualize the fluorescence of early post-fertilization zygotes. The best settings for laser scanning fluorescence imaging were determined experimentally for all primary antibodies and maintained for all cell cleavage stage embryos. All zygotes were scanned at a speed of 5–7 with an optical slice of 0.6 µm, zoom factor equal to one and a pinhole setting of 96 µm. Two scans of each optical section were compiled and averaged by the Zeiss LSM 510 computer software to give a final image that was 1024×1024 pixels in size. The embryonic cell cleavage stage was determined by counting the number of nuclei stained with propidium iodide and confirmed with phase contrast images. Qualitative analysis of embryo images was done for histone H3 trimethylated at K9 (H3K9me3) immunoreactivity to determine the

parental origin of the chromatin (staining positive for maternal/female chromatin and negative for paternal/male chromatin) [24]. Analysis of the embryo images for lamin B1 reactivity, to characterize the nuclear and micronuclear membranes [25], [26], was also qualitative. The EdU embryo images from Z-stacks were further analyzed and quantified using the Imaris image analysis program version 7.2.3.

Quantitative analysis

Polyspermic pronuclear zygotes were excluded from this analysis. To assess in vitro development, we counted the number of 2 cell embryos and divided this by the total number of fertilized oocytes, determined by propidium iodide nuclear staining, per replicate every 15 min between 0900 and 1030hr on day 1 (in vitro progression of the first zygotic division, SAL N = 5 to 8 males with total of 76 to 97 embryos assessed; CPA N = 2 to 5 males, with total of 31–75 embryos). To assess in vivo progression through early cell cleavage stages, based on propidium iodide nuclear staining, embryos were subdivided into four groups: 2, 3–4, 5–8 and 9–16 cells (on day 1 we collected SAL N = 8, 115 embryos, CPA N = 5, 56 embryos, day 2 SAL N = 4, 40 embryos, CPA N = 3, 26 embryos, day 3 SAL N = 8, 135 embryos, CPA N = 8, 120 embryos). The same embryos were analyzed for the incidence and average number of micronuclei per embryo and per cell. Micronuclei were differentiated from the main nucleus based on their smaller volume, with a similar nuclear morphology. Quantitative analysis of the nuclear and micronuclear volumes was done on day 0.5, with SAL N = 6, 109 embryos, CPA N = 5, 84 embryos; day 1, with SAL N = 8, 115 embryos, CPA N = 5, 64 embryos; and day 3, with SAL N = 8, 129 embryos, CPA N = 8, 120. Qualitative characterization of micronuclei with H3K9me3 and lamin B1 staining was done with SAL and CPA N = 2–3 with 15–30 embryos per group per embryonic cell cleavage stage. Quantification of in vitro overnight incubation with EdU for immunodetection on day 0–1 was done with SAL N = 6, 93 2 cell embryos CPA N = 5, 29 2 cell embryos; on day 3, the analysis of EdU after a 3 h in vitro

incubation with EdU in 8 cell embryos was done with SAL N = 5, 55 embryos CPA N = 6, 73 embryos.

The Imaris image analysis program (Bitplane Inc., South Windsor, CT) was used to quantify the data on EdU immunodetection and the nuclear and micronuclear volumes. Basically, a nuclear and micronuclear surface was created from propidium iodide staining for each embryo to measure the average volume and average DNA content and a second nuclear and micronuclear surface was created from EdU staining to measure the average EdU incorporation per embryo. The data were graphed as the intensity mean per embryo per replicate.

Statistical analyses

Chi squared analysis and the Fisher exact test, with Bonferroni correction when needed, were done to compare the proportion of embryos progressing either in vitro or in vivo between and within treatment groups, for the incidence of micronuclei and the proportion of cells that were EdU positive or contained EdU positive micronuclei during specific cell cleavage stages. Kruskal-Wallis analysis, with Bonferroni correction when needed, was done to determine the numbers of micronuclei per embryo and per embryonic cell, the transient volume changes and the micronuclear to nuclear volume ratios; these methods were also used to analyze EdU nuclear intensity means, DNA intensity means and their micronuclear to nuclear intensity ratios in early cell cleavage stage embryos between and within treatment groups. All statistical analyses were done using Systat (program version 10.2). Values are reported either as an average proportion or number per embryo per replicate ± standard error of the mean.

RESULTS

Paternal exposure to cyclophosphamide affects the in vitro timing of the first zygotic division

The overnight in vitro incubation of pre-pronuclear zygotes allowed us to follow the timing of the first zygotic division. Paternal exposure to CPA

significantly delayed the appearance of 2 cell embryos between 0900 and 1000hr on day 1 without affecting the capacity of all embryos to divide to the 2 cell stage by 1015hr (Fig. 3.1A). On day 1 at 0900hr, 100% of control versus 65% of CPA sired embryos had divided to the 2 cell stage; the remaining CPA sired embryos (35%) were actively undergoing mitosis, gradually reaching the 2 cell stage (Fig. 3.1A). Lagging, fragmented pieces of condensed chromatin were clearly visible at metaphase and telophase during the first zygotic division of in vitro incubated CPA sired embryos; in contrast, pronuclear zygotes did not show any sign of fragmented pieces of DNA (Fig. 3.1B). It is highly likely that micronuclei are formed from this fragmented chromatin (Fig. 3.1B, 2 cell embryo). The morphology of the micronuclei in interphase stage 2 cell embryos was very similar to that of the nuclei; micronuclei were round with a nucleolus, had a smaller volume and a lower DNA staining intensity, compared to the main nucleus (Fig. 3.1B).

Effects of paternal exposure to cyclophosphamide on the in vivo progression of early cell cleavage stage embryos

The developmental progression of cell cleavage embryos was significantly delayed in embryos fertilized by CPA exposed males (Fig. 3.2). Embryos collected on day 1 were all at the 2 cell stage (Fig. 3.2A). In contrast, on collection day 2, 23% of control embryos, compared to 55% of CPA sired embryos, were still at the 2 cell stage (Fig. 3.2B, $P \leq 0.05$)). On day 3 of collection, the delay in the progression of early cell cleavage embryos was even more significant ($P \leq 0.001$); none of the control embryos were at the 3–4 cell stage as opposed to 14% of the CPA sired embryos; 71% of both control and CPA sired embryos were at the 5–8 cell stage, while 29% of control compared to only 15% of the CPA sired embryos had progressed to form 9–16 cell stage embryos (Fig. 3.2C).

The incidence of micronuclei in control and CPA sired cell cleavage embryos

A small increase in the proportion of control embryos with micronuclei (from 1% to 5%, P≤0.05) was observed between collection days 1 and 3, suggesting the formation of new micronuclei by day 3 (Fig. 3.3A). In contrast to this low percentage of control embryos containing micronuclei, the incidence of micronuclei in early cell cleavage embryos fertilized by CPA- exposed males was dramatically increased to 70% (P≤0.001, compared to control embryos). CPA treatment did not affect the average number of micronuclei found in micronuclei positive embryos collected on day 1 or 3; when micronuclei were present, there were 2–3 micronuclei per CPA sired embryo as compared to 1–2 micronuclei per control embryo (Fig. 3.3B). Furthermore, micronuclei were distributed randomly into the two daughter cells following the first zygotic division (Fig. 3.3C, P≤0.05). Interestingly, in the CPA sired embryos with micronuclei, both the incidence of micronuclei/embryo and the average number of micronuclei/embryonic cell were significantly increased (P≤0.05) in the embryos with a delay in progression (3–4 cells: 79%, 0.9) compared to the normally progressing (5–8 cells: 79%, 0.4) and rapidly dividing (9–16 cells: 46%, 0.2) embryos (Fig. 3.3D & E). Thus, micronuclear formation during the first zygotic division was associated with a developmental delay in early cell cleavage embryos.

Chromatin compaction in the nuclei and micronuclei of early cleavage stage embryos sired by CPA exposed males

The volumes of the female and male pronuclei (day 0.5) did not differ (Fig. 3.4A); however, the nuclear volumes were doubled in the progression from pronuclear zygote (1440 μm3) to 2 cell embryo (2750 μm3) (P≤0.05). A decrease in nuclear volume was observed as embryos progressed from 2 cell to 8 cell (1070 μm3) (P≤0.05), returning to the volume in pronuclear zygotes. Paternal exposure to CPA did not affect these transient nuclear volume changes (Fig. 3.4A). The volume ratios as well as the chromatin compaction of the nuclei and micronuclei were assessed only in embryos sired by CPA exposed males since the incidence of micronuclei in control embryos was very low. The volume of micronuclei in CPA sired embryos, as a ratio of the nuclear volume, did not change from day 1 to day

3 (0.05 to 0.07, respectively) (Fig. 3.4B). In addition, the compaction state of the chromatin in micronuclei was similar to that of the main nucleus within each cell, i.e. condensed during mitosis and decondensed during interphase (Fig. 3.4C), suggesting that the micronuclei were responding to signals from the main nucleus or the cytoplasm.

Micronuclear characterization in early cell cleavage embryos fertilized by CPA exposed males

H3K9me3 is a female specific epigenetic mark. In both control and CPA sired embryos, only the female pronucleus in the zygote and the chromatin of female origin (half of the nucleus) in 2 cell embryos contained this epigenetic mark; the male pronucleus and the remaining half of the nucleus in 2 cell embryos were negative for H3K9me3 (Fig. 3.5). The micronuclear chromatin of day 1 embryos fertilized by CPA exposed spermatozoa was always negative for H3K9me3, suggesting that the micronuclei are of paternal origin (Fig. 3.5, bottom panel).

Since lamin proteins are thought to be involved in nuclear stability, chromatin structure and gene expression, we visualized lamin B1 immunoreactivity in control and CPA sired pronuclear, 2 cell and 8 cell embryos. In control pronuclear and 2 cell embryos, a clear peri-nuclear ring was observed (Fig. 3.6). By the 8 cell stage, lamim B1 immunoreactivity was redistributed, forming an intense peri-nucleolar ring with a much fainter peri-nuclear ring. While the lamin B1 reactivity of the main nucleus in CPA sired embryos was similar to that in the control embryos, the CPA induced micronuclei had much fainter or even absent lamin B1 membrane staining (Fig. 3.6, bottom panel), suggesting incomplete formation of the micronuclear and their associated micronucleolar membranes.

DNA replication in the micronuclei of CPA sired embryos

In vitro incubation of early cell cleavage stage embryos with the EdU click-it kit allowed the visualization of DNA synthesis as a marker of function.

EdU was incorporated into all embryonic cells independently of the treatment group, thus the capacity of CPA sired embryos to synthesize DNA as they progressed from the pre-pronuclear zygote to the 2 cell stage did not differ from control (Fig. 3.7A, top panel). Again, at the 8 cell stage, DNA synthesis in control and CPA sired embryos did not differ significantly, although in control embryos 81% of the embryonic cells incorporated EdU, whereas in CPA sired embryos 65% of the cells incorporated EdU (Fig. 3.7A, bottom panel). The observation that all cells did not incorporate EdU within the 3 hr incubation time is not surprising since mitosis is asynchronous between cells.

EdU incorporation in the micronuclei of CPA sired 2 cell embryos (collected on day 1) was the same as that of the main nucleus since the ratio of micronuclear to nuclear EdU reactivity (0.77) was the same as that for the DNA content (0.79) (Fig. 3.7B, left graph). The ratio of EdU reactivity (0.74) to DNA content (0.68) in micronuclei versus the main nucleus in CPA sired 8 cell embryos was also similar (Fig. 3.7B, right graph). However, the proportion of micronuclei in EdU positive cells that were capable of synthesizing DNA decreased significantly, from 100% to 78%, between the 2 and 8 cell stages (Fig. 3.7C, $P \leq 0.001$).

DISCUSSION

Lagging, fragmented pieces of DNA at metaphase and telophase during the first zygotic division are a visible mark of DNA damage as a consequence of paternal exposure to CPA; these fragments form micronuclei in 2 cell embryos. Thus, damaged DNA is released from the main nucleus to form micronuclei at the time of the first zygotic division, during chromatin decondensation and removal of the pronuclear membrane. Using an epigenetic mark, we confirmed that these micronuclei represent paternal chromatin. Within an embryo that had micronuclei, it was not unusual to observe some blastomeres with micronuclei and others without; even those blastomeres that did not have micronuclei may have DNA damage.

The presence of micronuclei was associated with a delay in progression through the early cell cleavage stages of development. This delay in progression of the CPA sired embryos was seen as early as the first zygotic division but did not affect the ability of the zygote to reach the 2 cell stage. This initial delay may become greater in later cleavage divisions since a greater proportion of delayed embryos was observed among the CPA treated group on collection day 3 compared to the controls. Interestingly, we have reported that paternal exposure to CPA led to an enhanced rate of sperm DNA decondensation and chromatin remodelling in the pre-pronuclear zygote [22] and an acceleration in progression through the stages of pronuclear zygote development [9]. Thus, damage to the male genome may initially speed up unpackaging of the paternal chromatin after fertilization but subsequently the damage, if it is extensive and is not repaired by embryonic DNA repair processes, has adverse effects on early cell divisions. Previous studies have reported a decrease in cell numbers in preimplantation embryos sired by CPA treated males [8], [27].

A similar relationship between the formation of micronuclei and a delay in embryonic progression was reported following parental exposure to irradiation, other alkylating chemicals and pesticides [28]–[30]. The proportion of embryos with micronuclei is the same from the 2 to 8 cell stage, so all micronuclei are formed during the first zygotic division. Since no new micronuclei are generated in the next two cleavage divisions, the average number of micronuclei per cell decreases as the cell number increases. This suggests that replicated micronuclei segregate randomly into the daughter cells during mitosis, as plasmids do in bacteria. Thus, genetic material is lost to the embryo. This probably contributes to embryo death. Indeed, previous studies established that the CPA treatment regimen used here induced approximately an 80% incidence of peri-implantation loss [6]. The 2 cell embryos that are free of micronuclei may have a reasonable chance to survive while the CPA sired embryos with micronuclei display progressive delays in cell division.

Our data indicate that the extent of DNA damage caused by paternal exposure to CPA, as assessed by the number of micronuclei per embryo, has a direct impact on fate of the embryo. It is likely that CPA sired early cleavage stage embryos have the capacity to undergo a certain number of cell cycles but die around the time of implantation from damage accumulation. It has been suggested that embryonic cell death pathways may be triggered by the activation of DNA damage-sensing checkpoint kinases [31], spindle associated checkpoints [32], an inadequate DNA damage repair response [33], or energy depletion [34] and that at least some of these pathways are p53-dependent [35].

Micronuclear formation and function may differ depending on the type of chemical exposure and the cell type [13]. The micronuclei that are induced in CPA sired embryos during the first zygotic division were very similar to the main nuclei: during interphase, the micronuclear chromatin was decondensed and round with a single nucleolus, while during mitosis the micronuclear chromatin was condensed. In cleavage stage embryos, the micronuclei followed the same transient nuclear volume change exerted on the main nucleus, suggesting that micronuclei are in communication with the main nucleus and cytoplasm within the cell.

The characterization of CPA induced micronuclear chromatin structure was initially done using H3K9me3, a female specific epigenetic mark, in early pronuclear and 2 cell embryos. As anticipated based on previous studies with mouse embryos [36], a clear delineation between the female chromatin and male chromatin was observed in both control and CPA sired 2 cell embryos. H3K9me3, was absent from all of the micronuclei observed in CPA-sired embryos. Thus, the genetic material in the micronuclei is of paternal origin.

Lamin B1 immunoreactivity was localized to the peri-nuclear (pronuclear and 2 cell) and both the peri-nuclear and peri-nucleolar membranes (4 and 8 cell stages) in control and CPA sired embryos. While there was no effect of paternal CPA treatment on the localization of lamin B1, the micronuclei that were induced had incomplete peri-micronuclear and peri-micronucleolar lamin B1 membrane

formation. Since lamins play a central role in formation of the nuclear pore complex in cells [37], these data may indicate a disturbance in the communication or exchange processes between the nucleus, micronucleus and cytoplasm within the embryos. Despite this indication of altered structure, the function of micronuclei, as indicated by their ability to incorporate EdU into newly synthesized DNA, was maintained. In addition, we did not observe any correlation between EdU incorporation and development delay in CPA sired embryos.

Micronuclear formation may result from a number of different causes. These include: DNA damage that is either not repaired or misrepaired, hypomethylation of repeat sequences in centromeric and pericentromeric DNA, defects in kinetochore proteins or assembly, or dysfunctional spindle and defective anaphase checkpoint genes [38]. In this context, it is interesting to note that the extensive DNA methylation reprogramming that is crucial for embryogenesis is disrupted in zygotes sired by cyclophosphamide-treated males [9]; the male pronuclei in zygotes fertilized by drug-exposed spermatozoa were dramatically hypomethylated in pronuclear stage 3 embryos. Protein modifications may also play a role since the H3K9me3 methylation mark may be necessary for the connection of microtubules to the kinetochores during mitosis [38]. However, since microtubule and spindle assembly components are of maternal origin, it is most likely that DNA damage, genetic or epigenetic, is responsible for driving the process by which micronuclei are formed in these experiments.

It has been reported that in human embryos generated by assisted reproductive technologies, nearly 60% exhibit chromosomal mosaicism and aneuploidy by the 4 cell stage and over 90% by the blastocyst stage [39], [40]. It is clear that spermatozoa from men who are sub-fertile have an increased likelihood of containing DNA damage [41] as do those from cancer survivors who have received treatment with radiation or DNA damaging chemotherapeutics [3], [42]. Advances in our understanding of the molecular mechanisms involved in the

formation of micronuclei and the consequences in terms of changes in the genome, epigenome, transcriptome, and proteome of the early embryo will help to elucidate biomarkers that may indicate the health of the paternal genome.

ACKNOWLEDGEMENTS

We thank Jacynthe Laliberté (McGill University, Montreal) for her assistance with confocal microscopy and Alekander Spurmanis and Claire Brown (McGill University, Montreal) and Cory Glowinski (Bitplane Inc., South Windsor, CT) for their assistance with Imaris image analysis.

REFERENCES

1. Huyghe E, Plante P, Thonneau PF (2007) Testicular cancer variations in time and space in Europe. Eur Urol 51: 621–628.

2. Thomson AB, Campbell AJ, Irvine DC, Anderson RA, Kelnar CJ, et al. (2002) Semen quality and spermatozoa DNA integrity in survivors of childhood cancer: a case-control study. Lancet 360: 361–367.

3. Green DM, Kawashima T, Stovall M, Leisenring W, Sklar CA, et al. (2010) Fertility of male survivors of childhood cancer: a report from the Childhood Cancer Survivor Study. J Clin Oncol 28: 332–339.

4. Stahl O, Boyd HA, Giwercman A, Lindholm M, Jensen A, et al. (2011) Risk of birth abnormalities in the offspring of men with a history of cancer: a cohort study using Danish and Swedish national registries. J Natl Cancer Inst 103: 398–406.

5. Colvin OM (1999) An overview of cyclophosphamide development and clinical applications. Curr Pharm Des 5: 555–560.

6. Trasler JM, Hales BF, Robaire B (1986) Chronic low dose cyclophosphamide treatment of adult male rats: effect on fertility, pregnancy outcome and progeny. Biol Reprod 34: 275–283.

7. Kelly SM, Robaire B, Hales BF (1992) Paternal cyclophosphamide treatment causes postimplantation loss via inner cell mass-specific cell death. Teratology 45: 313–318.

8. Harrouk W, Robaire B, Hales BF (2000) Paternal exposure to cyclophosphamide alters cell-cell contacts and activation of embryonic transcription in the preimplantation rat embryo. Biol Reprod 63: 74–81.

9. Barton TS, Robaire B, Hales BF (2005) Epigenetic programming in the preimplantation rat embryo is disrupted by chronic paternal cyclophosphamide exposure. Proc Natl Acad Sci U S A 102: 7865–7870.

10. Codrington AM, Hales BF, Robaire B (2004) Spermiogenic germ cell phase-specific DNA damage following cyclophosphamide exposure. J Androl 25: 354–362.

11. Harrouk W, Codrington A, Vinson R, Robaire B, Hales BF (2000) Paternal exposure to cyclophosphamide induces DNA damage and alters the expression of DNA repair genes in the rat preimplantation embryo. Mutat Res 461: 229–241.

12. Au WW, Giri AK, Ruchirawat M (2010) Challenge assay: A functional biomarker for exposure-induced DNA repair deficiency and for risk of cancer. Int J Hyg Environ Health 213: 32–39.

13. Terradas M, Martín M, Tusell L, Genescà A (2010) Genetic activities in micronuclei: is the DNA entrapped in micronuclei lost for the cell? Mutat Res 705: 60–67.

14. Kirsch-Volders M, Plas G, Elhajouji A, Lukamowicz M, Gonzalez L, et al. (2011) The in vitro MN assay in 2011: origin and fate, biological significance, protocols, high throughput methodologies and toxicological relevance. Arch Toxicol 85: 873–899.

15. Sartore RC, Campos PB, Trujillo CA, Ramalho BL, Negraes PD, et al. (2011) Retinoic acid-treated pluripotent stem cells undergoing neurogenesis present increased aneuploidy and micronuclei formation. PLoS One. In press.

16. Delbes G, Hales BF, Robaire B (2007) Effects of the chemotherapy cocktail used to treat testicular cancer on sperm chromatin integrity. J Androl 28: 241–249.

17. O'Flaherty C, Vaisheva F, Hales BF, Chan P, Robaire B (2008) Characterization of sperm chromatin quality in testicular cancer and Hodgkin's lymphoma patients prior to chemotherapy. Hum Reprod 23: 1044–1052.

18. Trasler JM, Hales BF, Robaire B (1985) Paternal cyclophosphamide treatment of rats causes fetal loss and malformations without affecting male fertility. Nature 316: 144–146.

19. Marchetti F, Bishop J, Lowe X, Wyrobek AJ (2009) Chromosomal mosaicism in mouse two-cell embryos after paternal exposure to acrylamide. Toxicol Sci 107: 194–205.

20. Yamagata K, Suetsugu R, Wakayama T (2009) Assessment of chromosomal integrity using a novel live-cell imaging technique in mouse

embryos produced by intracytoplasmic sperm injection. Hum Reprod 24: 2490–2499.

21. Nygren KG, Sullivan E, Zegers-Hochschild F, Mansour R, Ishihara O, et al. (2011) International Committee for Monitoring Assisted Reproductive Technology (ICMART) world report: assisted reproductive technology 2003. Fertil Steril 95: 2209–2222.

22. Grenier L, Robaire B, Hales BF (2010) Paternal exposure to cyclophosphamide affects the progression of sperm chromatin decondensation and activates a DNA damage response in the prepronuclear rat zygote. Biol Reprod 83: 195–204.

23. Oh SH, Miyoshi K, Funahashi H (1998) Rat oocytes fertilized in modified rat 1-cell embryo culture medium containing a high sodium chloride concentration and bovine serum albumin maintain developmental ability to the blastocyst stage. Biol Reprod 59: 884–889.

24. van der Heijden GW, Dieker JW, Derijck AAHA, Muller S, Berden JHM, et al. (2005) Asymmetry in Histone H3 variants and lysine methylation between paternal and maternal chromatin of the early mouse zygote. Mech Dev 122: 1008–1022.

25. Hutchison CJ (2002) Lamins: building blocks or regulators of gene expression? Nat Rev Mol Cell Biol 3: 848–858.

26. Broers JL, Machiels BM, Kuijpers HJ, Smedts F, van den Kieboom R, et al. (1997) A- and B-type lamins are differentially expressed in normal human tissues. Histochem Cell Biol 107: 505–517.

27. Austin SM, Robaire B, Hales BF, Kelly SM (1994) Paternal cyclophosphamide exposure causes decreased cell proliferation in cleavage-stage embryos. Biol Reprod 50: 55–64.

28. Mozdarani H, Nazari E (2009) Cytogenetic damage in preimplantation mouse embryos generated after paternal and parental gamma-irradiation and the influence of vitamin C. Reproduction 137: 35–43.

29. Tian Y, Yamauchi T (2003) Micronucleus formation in 3-day mouse embryos associated with maternal exposure to chlorpyrifos during the early preimplantation period. Reprod Toxicol 17: 401–405.

30. Titenko-Holland N, Ahlborn T, Lowe X, Shang N, Smith MT, et al. (1998) Micronuclei and developmental abnormalities in 4-day mouse embryos after paternal treatment with acrylamide. Environ Mol Mutagen 31: 206–217.

31. Mu XF, Jin XL, Farnham M, Li Y, O'Neill C (2011) DNA Damage-Sensing Kinases Mediate the Mouse Two-Cell Embryo's Response to Genotoxic Stress. Biol Reprod 85: 524–535.

32. Wei Y, Multi S, Yang CR, Ma J, Zhang QH, et al. (2011) Spindle Assembly Checkpoint Regulates Mitotic Cell Cycle Progression during Preimplantation Embryo Development. PLoS ONE 6(6): e21557.

33. Yukawa M, Oda S, Mitani H, Nagata M, Aoki F (2007) Deficiency in the response to DNA double-strand breaks in mouse early preimplantation embryos. Biochem Biophys Res Commun 358: 578–584.

34. Wakefield SL, Lane M, Mitchell M (2011) Impaired mitochondrial function in the preimplantation embryo perturbs fetal and placental development in the mouse. Biol Reprod 84: 572–580.

35. Toyoshima M (2009) Analysis of p53 dependent damage response in sperm-irradiated mouse embryos. J Radiat Res (Tokyo) 50: 11–17.

36. Santenard A, Ziegler-Birling C, Koch M, Tora L, Bannister AJ, et al. (2010) Heterochromatin formation in the mouse embryo requires critical residues of the histone variant H3.3. Nat Cell Biol 12: 853–862.

37. Fiserova J, Goldberg MW (2010) Relationships at the nuclear envelope: lamins and nuclear pore complexes in animals and plants. Biochem Soc Trans 38: 829–831.

38. Fenech M, Kirsch-Volders M, Natarajan AT, Surralles J, Crott JW, et al. (2011) Molecular mechanisms of micronucleus, nucleoplasmic bridge and nuclear bud formation in mammalian and human cells. Mutagenesis 26: 125–132.

39. Sandalinas M, Sadowy S, Alikani M, Calderon G, Cohen J, et al. (2001) Developmental ability of chromosomally abnormal human embryos to develop to the blastocyst stage. Hum Reprod 16: 1954–1958.

40. Bielanska M, Tan SL, Ao A (2002) Chromosomal mosaicism throughout human preimplantation development in vitro: incidence, type, and relevance to embryo outcome. Hum Reprod 17: 413–419.

41. Zini A (2011) Are sperm chromatin and DNA defects relevant in the clinic? Syst Biol Reprod Med 57: 78–85.

42. O'Flaherty C, Hales BF, Chan P, Robaire B (2010) Impact of chemotherapeutics and advanced testicular cancer or Hodgkin lymphoma on sperm deoxyribonucleic acid integrity. Fertil Steril 94: 1374–1379.

FIGURES

Figure 3.1. In vitro timing of the first zygotic division. (A) The proportion of fertilized oocytes that reached the 2 cell stage as assessed by light microscopy at 15 min intervals between 0900 and 1030hr on day 1. Paternal exposure to CPA delayed the timing of the first zygotic division without affecting their capacity to divide. Bar graphs represent the means per replicate ± standard errors of the mean; controls are in hatched bars and CPA-sired embryos in black bars. (B) Immunofluorescence images of CPA-sired embryos cultured in vitro and stained with propidium iodide, in red. Lagging pieces of chromatin are visible during the first metaphase and telophase of the zygotic cell cycle and micronuclei (MN) are clearly visible in 2 cell embryos. MN are formed during the first zygotic division in zygotes fertilized by CPA-exposed spermatozoa. Lagging chromatin and MN are circled in white. We collected SAL N = 5–8 males, 76 to 97 embryos and CPA N = 2–5 males, 31–75 embryos. Data were statistically analyzed by Chi-square, Fisher Exact test with Bonferroni's correction ** $P \leq 0.01$, *** $P \leq 0.001$.

A

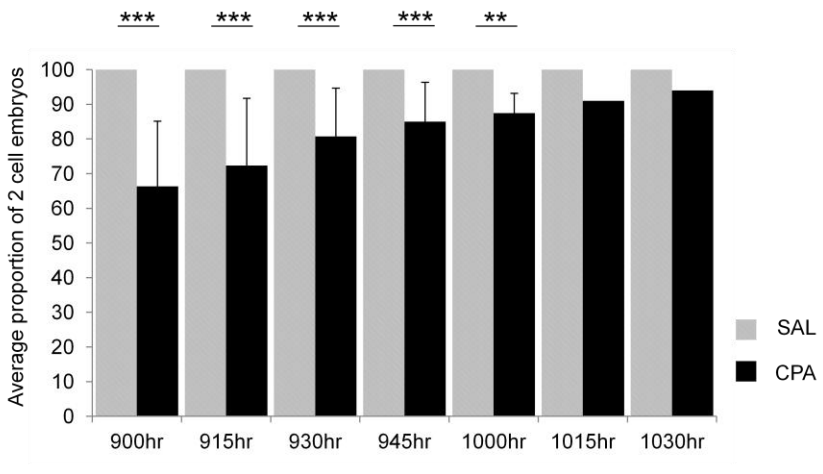
***
***
***
***
**
Average proportion of 2 cell embryos
100
90
80
70
60
50
40
30
20
10
0
900hr
915hr
930hr
945hr
1000hr
1015hr
1030hr
SAL
CPA

B

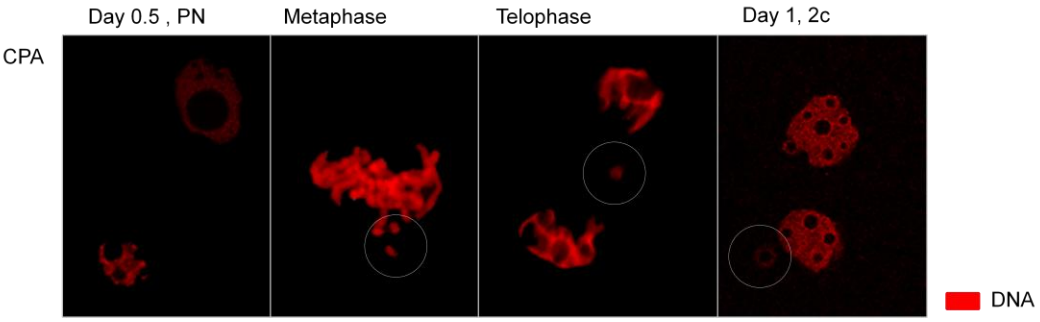
Day 0.5 , PN
Metaphase
Telophase
Day 1, 2c
CPA
DNA

Figure 3.2. In vivo progression of early cell cleavage stage embryos. Early cell cleavage embryos were collected following in vivo fertilization on (A) day 1 at 1000hr; (B) day 2 at 1400hr; (C) day 3 at 1000hr. Embryonic stages were determined by counting the number of nuclei and cells using confocal microscopy, grouped within developmental stages (refer to the figure legend) and are reported as an average percent per replicate; error bars represent the standard errors of the mean. Paternal exposure to CPA delayed the progression of early cleavage stage embryos on day 2 and day 3 of collection. We collected: (A) day 1, SAL N = 8 males, 115 2-cell embryos, CPA N = 5 males, 56 2-cell embryos; (B) day 2, SAL N = 4 males, 43 embryos, CPA N = 3 males, 36 embryos; (C) day 3, SAL N = 8 males, 135 embryos, CPA N = 8 males, 120 embryos. Data were statistically analyzed with Chi-square, Fisher exact test for statistical analysis * $P \leq 0.05$, *** $P \leq 0.001$.

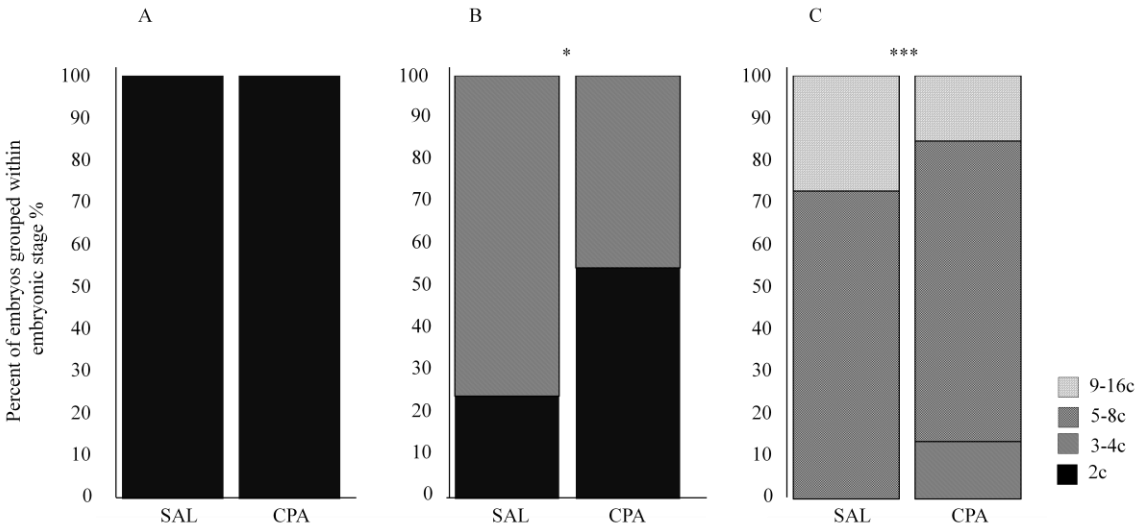
A
B
C
*
***
Percent of embryos grouped within embryonic stage %
100
90
80
70
60
50
40
30
20
10
0
SAL
CPA
9-16c
5-8c
3-4c
2c

Figure 3.3. The incidence of micronuclei in cell cleavage embryos. (A) The incidence of micronuclei (MN) in cell cleavage embryos. (B) The average number of MN per embryo with MN. Paternal exposure to CPA significantly increased the incidence of MN in early cell cleavage embryos with an average of 2–3 MN per embryo compared to control. C) MN distribution following the first zygotic division in 2 cell embryos containing at least 2 MN. MN induced by paternal exposure to CPA were distributed randomly into the two cells during the first zygotic division. (D) The incidence of MN and (E) the average number of MN per embryonic cell in day 3 embryos sired by CPA treated males. The incidence of MN and number of MN per cell were significantly greater in delayed 3–4c embryos compared to normally dividing 5–8c and rapidly dividing 9–16c embryos. Line graphs are the average per replicate and error bars are standard errors of the means; the gray line represents SAL and black line CPA-sired embryos. We collected: day 1 SAL N = 8 males, 115 2 cell embryos, CPA N = 5 males, 56 2 cell embryos; day 3 SAL N = 8 males, 135 embryos, CPA N = 8 males, 120 embryos. The incidence of MN and average number of MN were analyzed by Chi-square Fisher Exact test and Kruskal Wallis, respectively. * $P \leq 0.05$, *** $P \leq 0.001$.

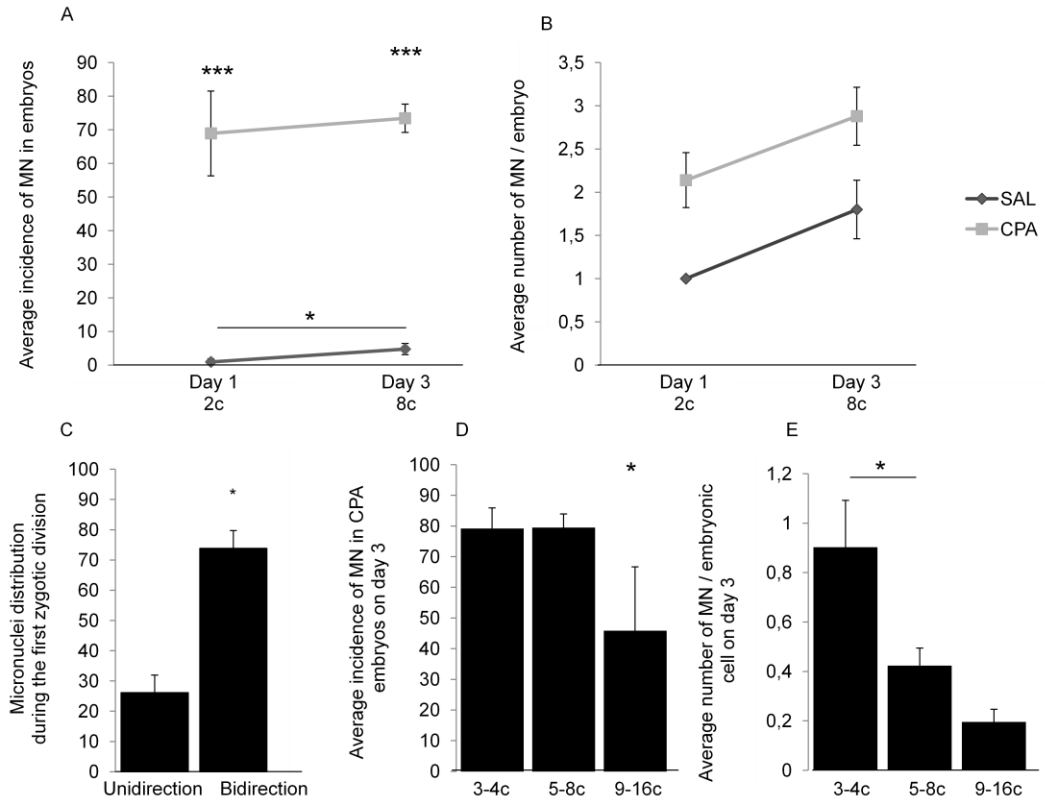
A
Average incidence of MN in embryos
90
80
70
60
50
40
30
20
10
0
***
***
*
Day 1
2c
Day 3
8c
B
Average number of MN / embryo
3,5
3
2,5
2
1,5
1
0,5
0
Day 1
2c
Day 3
8c
SAL
CPA
C
Micronuclei distribution
during the first zygotic division
100
90
80
70
60
50
40
30
20
10
0
*
Unidirection
Bidirection
D
Average incidence of MN in CPA
embryos on day 3
100
90
80
70
60
50
40
30
20
10
0
*
3-4c
5-8c
9-16c
E
Average number of MN / embryonic
cell on day 3
1,2
1
0,8
0,6
0,4
0,2
0
*
3-4c
5-8c
9-16c

Figure 3.4. Nuclear and micronuclear (MN) chromatin compaction in early cleavage stage embryos. (A) The nuclear volumes in early cleavage stage control and CPA-sired embryos and the (B) relative ratio of MN to nuclear volumes on collection days 1 and 3 in CPA-sired embryos. Paternal exposure to CPA did not affect the transient nuclear volume changes in early cell cleavage stage embryos and the volume of CPA-induced MN remained comparable to the main nucleus on days 1 and 3 of collection. Line graphs represent the average per replicate and error bars the standard errors of the means; the gray line with diamond symbols designates control and the black line with squares the CPA-sired embryos. (C) Immunofluorescence images of CPA embryos with MN stained with propidium iodide in red to compare the chromatin compaction of MN and nuclei within the same embryonic cell at different mitotic phases. Within the same cell, the MN and nuclear chromatin was condensed during mitosis and decondensed during interphase, suggesting communication. Arrows point towards decondensed MN chromatin while condensed MN chromatin is circled in white. We collected: day 0.5 SAL N = 6 males, 109 embryos, CPA N = 5 males, 84 embryos; day 1 SAL N = 8 males, 115 embryos, CPA N = 5 males, 64 embryos; day 3 SAL N = 8males, 129 embryos, CPA N = 8 males, 120. The Kruskal Wallis test with Bonferroni's correction was performed for statistical analysis * $P \leq 0.05$, ** $P \leq 0.01$.

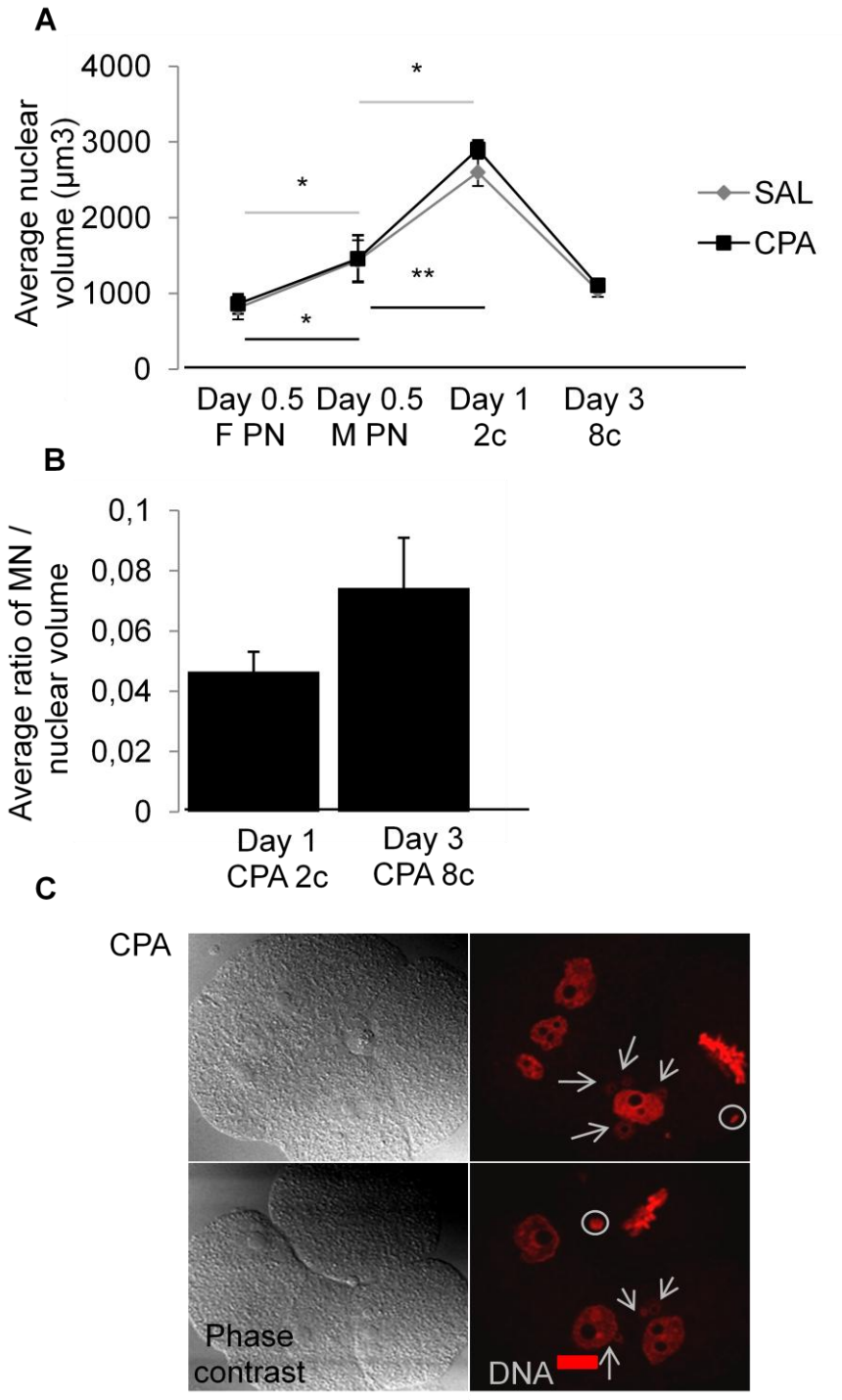
A
4000
3000
2000
1000
0
Average nuclear volume (µm3)
*
*
*
**
SAL
CPA
Day 0.5 F PN
Day 0.5 M PN
Day 1 2c
Day 3 8c
B
0,1
0,08
0,06
0,04
0,02
0
Average ratio of MN / nuclear volume
Day 1 CPA 2c
Day 3 CPA 8c
C
CPA
Phase contrast
DNA

Figure 3.5. Parental origin of micronuclear chromatin in early cell cleavage embryos fertilized by CPA exposed males. Pronuclear zygotes and 2 cell embryos were stained for the maternal epigenetic chromatin specific mark H3K9me3 (in green), DNA (counterstained with propidium iodide in red) with the merged image in yellow. The top panels are control and the bottom panels are CPA-sired embryos. Only the female pronucleus and polar body stained with H3K9me3 in zygotes; in 2 cell embryos half of each nucleus stained with H3K9me3, representing the chromatin of female origin. Paternal CPA treatment did not affect this parental chromatin mark. The absence of H3K9me3 in MN in CPA-sired embryos indicates that these MN are of paternal chromatin origin in 2 cell embryos. The immunofluorescence images were acquired with a confocal microscope. Arrows point to the Female (F) and Male (M) pronuclei, MN are circled in white, dashed white lines delineate the female (positive signal for H3K9me3) from the male (negative signal for H3K9me3) chromatin in 2 cell embryos; a magnified image of MN is presented on the right side of the CPA-sired 2 cell embryos. We collected SAL and CPA, N = 2–3 males with 15–30 embryos per group per embryonic cell cleavage stage for qualitative analysis.

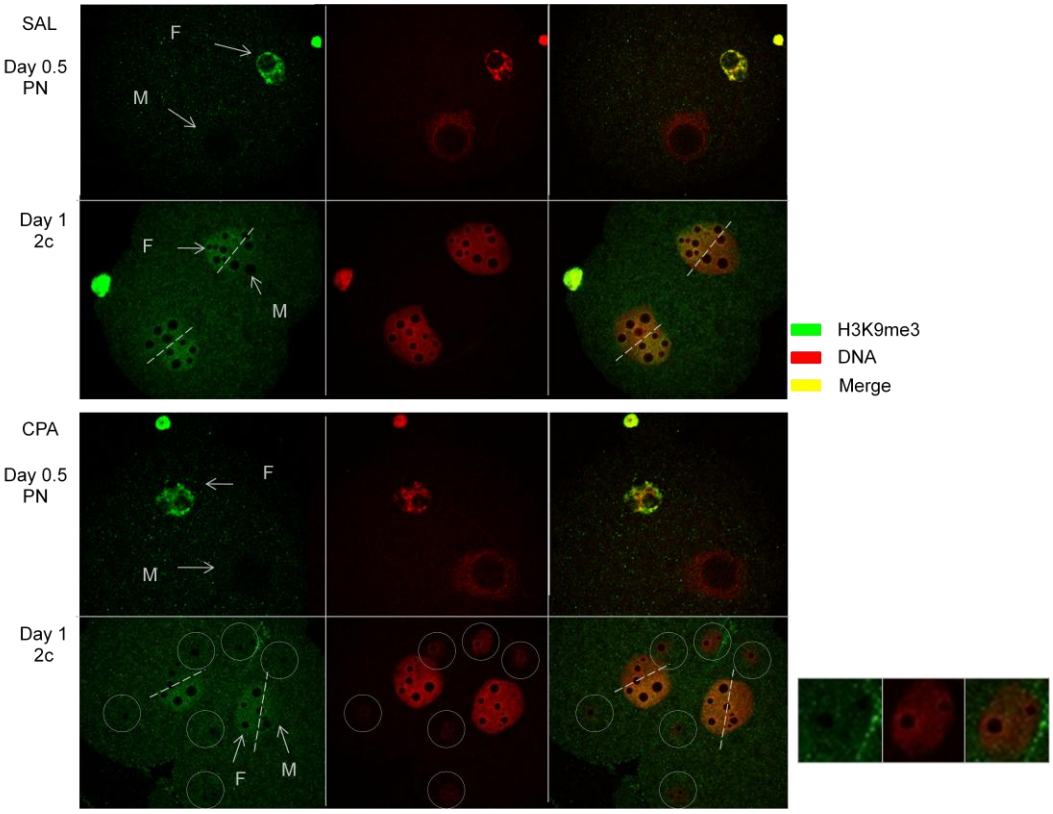
SAL
Day 0.5
PN
F
M
Day 1
2c
F
M
H3K9me3
DNA
Merge
CPA
Day 0.5
PN
F
M
Day 1
2c
F
M

Figure 3.6. Micronuclear membrane characterization in early cell cleavage embryos fertilized by CPA exposed spermatozoa. Pronuclear zygotes and 2 and 8 cell CPA-sired embryos were collected on days 0.5, 1 and 3 and stained for nuclear membrane lamin B1 (in green), DNA (propidium iodide, in red) with the merged image in yellow. We observed a clear nuclear to peri-nucleolar membrane redistribution of lamin B1 in early 2 and 8 cell embryos, respectively; this was not affected by paternal CPA treatment. MN in CPA-sired embryos showed the formation of incomplete nuclear and peri-nucleolar membranes at both embryonic collection time points. These images were acquired with a confocal microscope. Arrows point to Female (F) and Male (M) pronuclei, MN are circled in white, with a magnified image on the left of each respective embryonic stage. We collected N = 2–3 males, 15–30 embryos per group per embryonic cell cleavage stage for both SAL and CPA for qualitative analysis.

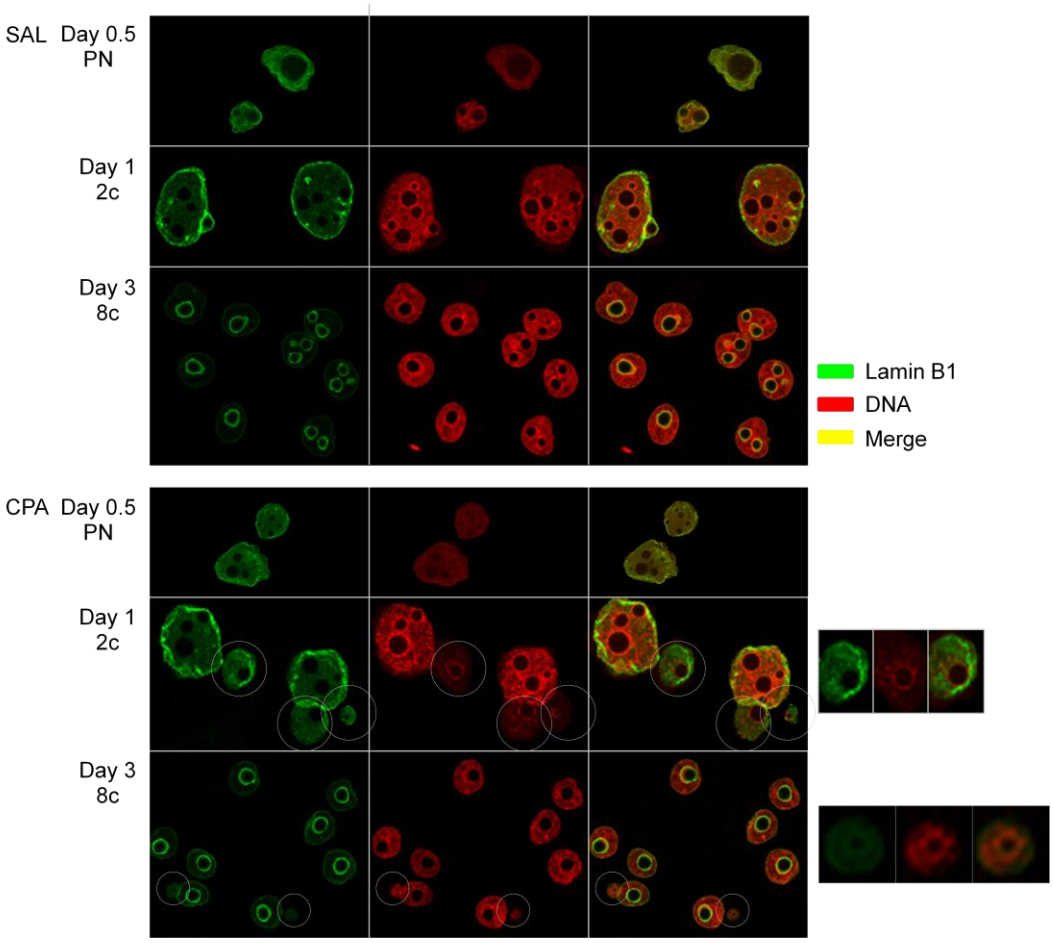
SAL Day 0.5 PN
Day 1 2c
Day 3 8c
Lamin B1
DNA
Merge
CPA Day 0.5 PN
Day 1 2c
Day 3 8c

Figure 3.7. DNA replication in the micronuclei of CPA sired embryos. Immunofluorescence images of embryos stained with EdU Click-it (in green) and DNA (propidium iodide in red) with the merged images in yellow. MN are circled in white, the arrows point to the polar body (PB) (internal negative control for EdU). (A) top panel: overnight in vitro incubation during the first zygotic division; bottom panel: 3 h in vitro incubation of day 3 embryos with EdU to assess DNA replication in early cell cleavage embryos. Paternal exposure to CPA did not affect on the proportion of cells incorporating EdU in early cell cleavage embryos. (B) Comparison of the MN to nuclear ratios of EdU incorporation relative to DNA content in day 1 and 3 embryos sired by CPA exposed males. We observed that MN synthesized DNA to the same extent as the nuclei in both 2 and 8 cell embryos. (C) Comparison of the proportion of EdU positive MN in EdU positive cells in day 1 and day 3 embryos sired by CPA exposed males. A decrease in the proportion of functional MN incorporating EdU was observed in 8 cell embryos compared to 2 cell embryos. Bar graphs are the average ratio or proportion per replicate; error bars represent the standard errors of the means. We collected on day 1 SAL N = 6 males, 93 embryos CPA N = 5 males, 29 embryos and on day 3 SAL N = 5 males, 55 embryos CPA N = 6 males, 73 embryos. The ratio comparisons were analyzed statistically by Kruskal-Wallis and the proportions of embryos were analyzed statistically by Chi-square, Fisher Exact test and: *** $P \leq 0.001$.

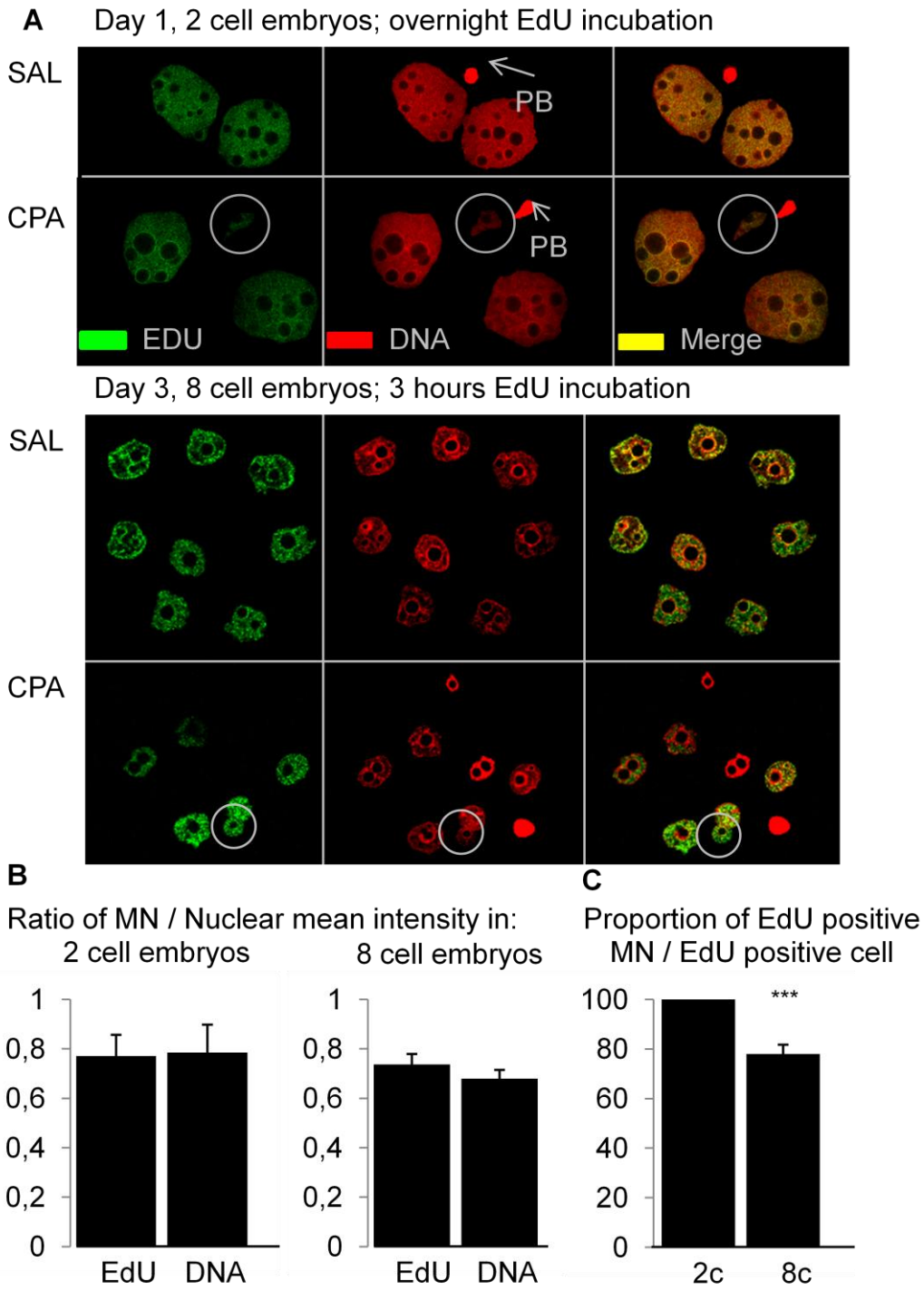
A
Day 1, 2 cell embryos; overnight EdU incubation
SAL
CPA
PB
PB
EDU
DNA
Merge
Day 3, 8 cell embryos; 3 hours EdU incubation
SAL
CPA
B
Ratio of MN / Nuclear mean intensity in:
2 cell embryos
8 cell embryos
1
0,8
0,6
0,4
0,2
0
EdU
DNA
C
Proportion of EdU positive MN / EdU positive cell
100
80
60
40
20
0
***
2c
8c

CONNECTING TEXT

In chapter III, we determined that the formation of micronuclei during the first zygotic division caused the embryonic developmental delay. In the next chapter IV, we wanted to determine the effect of chronic paternal exposure and the impact of micronuclei formation on the activation of DNA damage recognition and repair responses in the cleavage stage embryos. Experiments using immunofluorecence protocols and confocal microscopy were designed to elucidate active mechanisms of defence in cleavage stage embryos.

CHAPTER IV

The Activation of DNA Damage Detection and Repair Responses in Cleavage Stage Rat Embryos by a Damaged Paternal Genome

Lisanne Grenier, Bernard Robaire, Barbara F. Hales

Toxicological Science published 27 March 2012; doi:10.1093/toxsci/kfs120:
PMID 22454429

ABSTRACT

Male germ cell DNA damage, after exposure to radiation, exogenous chemicals, or chemotherapeutic agents, is a major cause of male infertility. The potential of DNA damaged spermatozoa to fertilize oocytes is of concern since there is limited information on the capacity of early embryos to repair a damaged male genome or on the fate of these embryos if repair is inadequate. We hypothesized that the early activation of DNA damage response in the early embryo is a critical determinant of its fate. The objective of this study was to assess mitochondrial function and the DNA damage response in cleavage stage embryos sired by males chronically exposed to an anticancer alkylating agent, cyclophosphamide. Male rats were treated with saline or cyclophosphamide (6 mg/kg/day) for four weeks and mated to naturally cycling females. Pronuclear, two- and eight-cell embryos were collected for immunofluorescence analysis of mitochondrial function and biomarkers of the DNA damage response: γH2AX foci, 53BP1 reactivity, and poly(ADP-ribose) polymer formation. Mitochondrial activities did not differ between embryos sired by control and cyclophosphamide-exposed males. At the two-cell stage there was no treatment-related increase in DNA double strand breaks; by the eight-cell stage, a significant increase was noted, as indicated by increased medium and large γH2AX foci. This was accompanied by a dampened DNA repair response, detected as a decrease in the nuclear intensity of poly(ADP-ribose) polymers. The micronuclei formed in cyclophosphamide-sired embryos contained large γH2AX foci and enhanced poly(ADP-ribose) polymer and 53BP1 reactivity compared to their nuclear counterparts. Thus, paternal cyclophosphamide exposure activated a DNA damage response in cleavage stage embryos. Furthermore, this damage response may be useful in assessing embryo quality and developmental competence.

INTRODUCTION

Millions of men of reproductive age now survive cancer as a consequence of improvements in cancer treatment regimens, consisting of chemotherapeutic agents and/or radiation (Green et al., 2010). However, fertility is of concern to many of these men since these treatment regimens usually lead to an initial drop in sperm production that may be sustained for months to years, causing infertility in a large proportion of subjects (Green et al., 2010). Even men who recover spermatogenesis may still be infertile and may be faced with the possibility of transmitting heritable genetic diseases to their offspring. Cyclophosphamide, a nitrogen mustard compound, is commonly used as a cancer therapeutic and immunosuppressant agent. This drug is a bi-functional alkylating agent, forming DNA adducts, DNA cross-links, and single and double strand DNA breaks in dividing cells. The exposure of male rats to cyclophosphamide induces DNA damage in spermatozoa that ranges from DNA double and single strand breaks to chromosomal aberrations (Barton et al., 2003; Codrington et al., 2004). Furthermore, this paternal cyclophosphamide treatment results in dose dependent and time specific effects on progeny outcome, including pre- and post-implantation loss, malformations, and deficits in learning behaviour; some of these outcomes are observed in subsequent generations (Auroux et al., 1990; Hales et al., 1992; Trasler et al., 1986). Our labs, and others, have used cyclophosphamide to elucidate the mechanisms underlying male-mediated developmental toxicity (Barton et al., 2007; Grenier et al., 2011).

The male genome is tightly packaged for delivery to the oocyte (Ward, 2010); paternal drug exposures may disturb the packaging of male germ cell chromatin. Indeed, paternal cyclophosphamide treatment alters the sperm basic proteome and, specifically, some components of the nuclear matrix that may be involved in events during spermiogenesis and fertilization (Codrington et al., 2007a, 2007b). The timing of spermatozoal decondensation and the deposition of modified histones is accelerated in zygotes fertilized by spermatozoa from cyclophosphamide-treated males (Grenier et al., 2010). In pronuclear stage embryos sired by drug-treated males, the epigenetic programming of both parental

genomes is disrupted, as manifested by changes in the regulation of histone H4 acetylation at lysine 5 and in DNA methylation (Barton et al., 2005). The incidence of micronuclei is dramatically elevated in two-cell embryos fertilized by spermatozoa from cyclophosphamide treated fathers; moreover, the presence of these micronuclei is associated with developmental delay (Grenier et al., 2011) and is reflected by the proportion of peri-implantation embryonic loss observed in previous studies (Trasler et al., 1986). Together, these findings demonstrate that paternal exposure to cyclophosphamide damages the male genome and disrupts post-fertilization events in the early embryo.

Functional mitochondria are crucial for fertilization and determine the developmental potential of early embryos. Stage-specific changes in the functional compartmentalization of mitochondria are required to meet the energy needs of embryos throughout preimplantation development (van Blerkom 2011). Furthermore, the activation and maintenance of DNA damage responses require the energy produced by mitochondria.

There are multiple DNA damage and repair pathways in cells. DNA damage, in the form of double strand breaks, is detected by the rapid phosphorylation of histone H2AX at serine 139 (Rogakou et al., 1998). Small γH2AX foci are associated with cell cycle regulation and mitosis, medium foci (0.30-9.99μm^3) act as repair platforms, recruiting DNA repair proteins to sites of damage, and large foci are indicative of DNA damage accumulation and DNA double strand break aggregates (McManus and Hendzel, 2005; Paull et al., 2000). γH2AX foci are induced in the male pronuclei of zygotes sired by cyclophosphamide-treated male rats (Barton et al., 2007; Grenier et al., 2010).

Large γH2AX foci co-localize with DNA double strand break repair proteins (McManus and Hendzel, 2005), including p53-binding protein 1 (53BP1) and poly(ADP-ribose) polymerase-1 (PARP-1) (Paull et al., 2000). 53BP1, a component of the non-homologous end joining repair pathway, is involved in DNA damage induced cell cycle arrest and participates in DNA repair (Wang et al., 2002; Ward et al., 2003). In somatic cells, 53BP1 displays both cytoplasmic and nuclear localisations (Iwabuchi et al., 1998*).* Inhibition of the nuclear

importation of 53BP1 decreases ionizing radiation-induced 53BP1 focus formation, delays DNA repair, and impairs cell survival (Moudry et al., 2011). In the early mouse zygote, 53BP1 is present only in the cytoplasm, whereas by the late pronuclear stage some staining is found in the pronuclei (Ziegler-Birling et al., 2009). In the two and eight cell stages, staining is enriched in the nuclei but no particular association is observed with any nuclear structure.

Poly(ADP-ribose) (PAR) polymerase-1 (PARP1) is activated by DNA single-strand breaks and at stalled replication forks to facilitate DNA repair. In response to DNA damage, PARP-1 catalyzes the formation of poly(ADP-ribose) (PAR) polymers, with NADH as an energy cofactor, covalently modifying acceptor structural chromatin proteins (Schreiber et al., 2006) and decondensing the chromatin to allow access of other repair factors to sites of DNA damage (Zhou et al., 2010). The removal of PAR polymers is primarily catalyzed by PAR glycohydrolase (PARG) (Brochu et al., 1994). The metabolism of PAR is important during chromatin dynamics, DNA replication, and repair (D'Amours et al., 1999; Kim et al., 2004). The proper regulation of PARP-1 is critical for the maintenance of genomic stability (Schreiber et al., 2006) since PARP1 functions as a DNA repair protein in response to single strand breaks, in the base excision repair pathway (Dantzer et al., 1999) and in the induction of cell death in response to genotoxic stress (Yu et al., 2002). Interestingly, in pronuclear stage zygotes sired by cyclophosphamide-treated males, PARP1 immunoreactivity is substantially elevated, not only in the damaged paternal genome but also in the maternal genome (Barton et al., 2007).

The genetic disruption of maternal DNA double strand break repair in mice significantly increased the frequency of zygotes with chromosomal structural aberrations after paternal exposure to ionizing radiation (Marchetti et al., 2007). Thus, DNA damage detection and repair responses play an important role in determining progeny outcome. The first goal of these studies was to elucidate the impact of a damaged male genome on mitochondrial bioenergetics and DNA damage detection and repair responses in the cleavage stage embryo. The second goal was to determine the impact of the formation of micronuclei and

of developmental delay in the cleavage stage embryos on their capacity to mount appropriate DNA damage responses.

MATERIALS AND METHODS

Animals, drug treatment and embryo collection

This study was done in accordance with the guidelines of the Canadian Council on Animal Care for the ethical use and care of animals in science. The animal treatment protocol (Protocol Number: 2144) was approved by the Animal Care Committee of McGill University.

Adult male (350–400 g) and virgin female (225–250 g) Sprague-Dawley rats were purchased from Charles River Canada (St. Constant, Quebec, Canada) and housed at the Animal Resources Centre, McIntyre Medical Building, McGill University (Montreal, Canada). Animals received food and water *ad libitum* and were maintained on a 0700-1900hr light/dark cycle. The drug treatment and zygote protocols previously described (Trasler et al., 1986; Grenier et al., 2011) were followed with minor modifications. After one week of acclimatization, male rats were randomly assigned to one of two treatment groups and gavaged with saline (vehicle) or cyclophosphamide (CAS 6055-19-2; Sigma Chemical Co., St Louis, Missouri), 6 mg/kg per day, six times per week for four weeks.

On the fifth week of treatment, control virgin females in proestrus (as assessed by a vaginal wash in mid-afternoon) were caged overnight in groups of two with either a control or cyclophosphamide-treated male. Pregnancies were confirmed with sperm positive vaginal smears the following morning, designated as gestation day 0. Sperm positive females were euthanized on day 0 at 1300hr, on day 1 at 1000hr, and day 3 at 1000hr to collect pronuclear zygotes, two-cell and eight- to sixteen-cell embryos, respectively. Oviducts and whole uteri were isolated and cleaned in pre-warmed (37°C) M2 culture medium (Sigma Chemical Co.); pronuclear zygotes were collected from the ampullae in warm M2 medium, and early cell cleavage embryos were flushed with a 30 round gauge needle from the infundibulum of the oviduct with 0.2 ml of warm M2 medium.

Detection of mitochondrial activity in cleavage stage embryos

Functional mitochondria were visualized in cleavage stage embryos using MitoTracker Green FM (catalog number M7514, Invitrogen, Burlington, Ontario, Canada) and MitoSox Red mitochondrial superoxide indicator (catalog number M36008, Invitrogen) probes. Embryos were incubated in vitro in modified rat 1-cell embryo culture medium (mR1ECM) milieu (Oh et al., 1998). Final concentrations of 100nM for MitoTracker Green FM and of 2μM for MitoSox Red were prepared in mR1ECM plus bovine serum albumin (BSA, 4.0 mg/ml; pH equilibrated to 7.4 with 12N HCl). This zygotic development milieu was covered with light mineral oil to prevent evaporation and pre-equilibrated for 3h before incubation at 37°C and 5% CO_2. All solutions and dilutions were prepared fresh the day of the experiment.

Sperm positive females were euthanized at 1000hr on days 1 and 3 to collect 2 and 8 cell embryos in prewarmed (37°) M2 culture medium (Sigma Chemical Co.). Embryos were flushed with prewarmed (37°C) M2 medium, washed three times in prewarmed (37°C) mR1ECM plus BSA, and incubated in pre-equilibrated (37°C and 5%CO2) mR1ECM plus BSA with either 100nM MitoTracker Green FM or 2μM MitoSox Red. The time from embryo collection to the in vitro incubation was completed in less than 7 min to preserve embryo quality. Live in vitro embryos were incubated with MitoTracker probes for 20 min to allow the accumulation of the probes in active respiring mitochondria. For the immunodetection of MitoTracker mitochondrion-selective probes, the same immunofluorescence protocols were used as previously described for the Invitrogen molecular probes under the experimental protocol requiring fixation and permeabilization after staining with minor changes. Fixed and permeabilized embryos were incubated for 1 h in goat blocking solution (10% goat serum, 3% BSA and 0.1% Tween 20 in PBS), DNA was then stained with DAPI, 10 μg/ml, diluted in goat blocking solution, for 20 min. Embryos were then washed in 0.05% Tween 20 in PBS for 10 min and mounted in 3μl of VectaShield mounting medium (Vector Laboratories) on a premarked pap pen slide and covered with a

cover slip. Slides were then stored at 4°C and visualized with confocal microscopy within two days.

Immunofluorescence detection of markers of DNA damage and repair

The immunofluorescence protocols used were described previously (Grenier et al., 2010). To characterize DNA damage responses, cleavage stage embryos were incubated with mouse monoclonal IgG anti-δH2AX phospho-serine 139 (clone JBW103, 1:100 dilution; catalog number 05-636, Upstate Biotechnology, Charlottesville, VA) for 1 hour at 37°C; rabbit polyclonal anti-53BP1 (1:100 dilution; catalog number NB100-304, Novus Biological, Oakville, ON); or rabbit polyclonal anti-Poly (ADP-Ribose) (PAR) (1:100 dilution; catalog number 51-8114KC, BD Bioscience Pharmingen, Mississauga, Ontario, Canada) overnight at 4°C in a humidified chamber. Both primary and secondary antibodies were diluted in goat blocking solution (10% goat serum, 3% BSA and 0.1% Tween 20 in PBS). Zygotes were then washed 3x15 min in goat blocking solution, incubated for 1 hr at room temperature with the secondary antibody, goat fluorescein anti-mouse IgG (FITC) (1:100 dilution; catalog number ab97022, Abcam, Cambridge, MA) and goat fluorescein anti-rabbit IgG (H+L) (1:200 dilution; catalog number F1-1000, Vector Laboratories, Burlington, Ontario, Canada), and rewashed 3x15 min in goat blocking solution. DNA was stained with propidium iodide (catalog number P4864, Sigma Chemical Co.) at 10μg/mL in goat blocking solution for 20 min, washed in 0.05% Tween 20 in PBS for 10 min, mounted in 3μl of VectaShield mounting medium (Vector Laboratories) on a premarked pap pen slide and covered with a cover slip. Slides were then stored at 4°C and visualized with confocal microscopy within two days.

Confocal microscopy

A Zeiss LSM 510 Axiovert 100M confocal microscope with a Plan-Apochromat ×63/1.4 oil DIC objective was used to visualize the fluorescence of early cleavage stage embryos. The best settings for laser scanning fluorescence imaging were determined experimentally for all primary antibodies and

maintained for all cell cleavage stage embryos. All embryos were scanned at a speed of 5-7 with an optical slice of 0.6 μm, zoom factor equal to one and a pinhole setting of 96 μm. Two scans of each optical section were compiled and averaged by the Zeiss LSM 510 computer software to give a final image that was 1024 × 1024 pixels in size. The embryonic cell cleavage stage was determined by counting the number of nuclei stained with propidium iodide or DAPI and confirmed with phase contrast images. The presence of micronuclei as nuclear entities detached from the main nucleus in an embryo was determined with the nuclear propidium iodide stain or DAPI. In addition, the nuclei of blastomeres containing micronuclei were identified using the phase contrast images. The γH2AX, 53BP1, PAR and MitoSox embryo immunofluorescence images from Z-stacks were further analyzed and quantified using the Imaris image analysis program version 7.2.3 (Bitplane, Inc., South Windsor, CT).

Quantitative analysis

The unit of measure (N) was the number of males; the number of embryos that is indicated below was the average number per male. Quantification of mitochondrial activity was done using the MitoSox probe since the quality of the images with this probe was superior to those obtained with MitoTracker Green; at the 2- and 8-cell stages, N=5 control males, with 28 and 41 embryos, and N=6 cyclophosphamide-treated males, with 32 and 39 embryos, respectively, were analyzed. We analyzed all mitochondria above a set minimun threshold intensity; the mitochondrial MitoSox intensity means and counts of all mitochondria were compared in control and cyclophosphamide-sired embryos from each cleavage stage.

Immunofluorescence z-stack images were used to quantify γH2AX foci per nucleus in 2 and 8 cell embryos sired by control and cyclophosphamide-treated males and in the micronuclei found in embryos sired by cyclophosphamide-treated males. For the control group, N=7 males with 64 embryos and N=10 males with 99 embryos were analyzed at the 2- and 8-cell stage, respectively, and in the cyclophosphamide-sired embryo group, N=5 males

with 56 embryos and N=7 males with 112 embryos were analyzed at the 2- and 8-cell stage, respectively. For the analysis of 53BP1 reactivity, at the pronuclear, 2- and 8-cell stages in the control group, the sample size was N=6 males, with 58 embryos, N=8 males with 57 embryos, N=7 males with 63 embryos, respectively; in the cyclophosphamide-treated group there were N=5 males with 39 embryos, N=4 males with 32 embryos and N=7 males with 68 embryos analyzed. PAR polymers were quantified in pronuclear zygotes, 2 and 8 cell embryos: in controls, sample sizes of N=6 males with 51 embryos, N=7 males with 58 embryos and N=8 males with 72 embryos, respectively, were studied; in the cyclophosphamide-treated group, a sample size of N=4 males with 45 embryos, N=5 males with 34 embryos and N=6 males with 52 embryos was analyzed at each cleavage stage, respectively. The chromatin structure in nuclei was compared at the 2- and 8-cell stages to that in micronuclei in cyclophosphamide-sired embryos, using N=5 and 7 males with 41 and 112 embryos for γH2AX analysis, N=4 and 6 males with 24 and 45 embryos for 53BP1, and N=5 and 6 males with 23 and 37 for PAR detection, respectively.

Measurements relevant to our hypothesis and specific for each DNA damage response marker were analyzed using Imaris (Bitplane Inc., South Windsor, CT). In our analysis of DNA damage with γH2AX as a marker, a nuclear surface was created from propidium iodide staining for each embryo to measure the average nuclear and micronuclear volume; within that surface, the total number of nuclear and micronuclear γH2AX foci were quantified based on their volume: small foci, 0-0.29μm^3; medium foci, 0.30-9.99μm^3; or large foci, 10μm^3 and above. The data were graphed as the average number of γH2AX foci per nucleus on each embryo collection day. To compare the DNA damage in nuclei to that in micronuclei, the nuclear value was set to 1 and the fold difference between the micronuclei and nuclei was examined; all values were corrected for nuclear and micronuclear volume.

The 53BP1 and PAR average nuclear and micronuclear intensity means were assessed relative to the DNA intensity assessed based on the nuclear surface created from propidium iodide staining for each embryo. A second surface was

created inversely from propidium iodide staining to capture all the cytoplasmic staining to measure the average intensity mean of 53BP1 and PAR immunofluorescence in the cytoplasm. To characterize the micronuclear chromatin content of these DNA repair indicators, data were graphed as the 53BP1 and PAR fold difference from nuclear average intensity, comparing the micronuclear to nuclear ratios; the 53BP1 and PAR intensity ratio are relative to the micronuclear to nuclear DNA intensity ratio, set at 1 to correct for the difference in DNA intensity.

Statistical analyses

All statistical analyses were done using Systat (program version 10.2, Chicago, IL). Kruskal-Wallis analysis was done to analyze for the drug effect between control and cyclophosphamide-sired embryos with respect to 53BP1 and PAR nuclear and cytoplasmic staining and nuclear to cytoplasmic intensity mean ratios at each cleavage stage. Kruskal-Wallis analysis, with Bonferroni correction when needed, was done to determine a time effect between cleavage stages within a treatment group on the 53BP1 and PAR nuclear, cytoplasmic and the nuclear to cytoplasmic intensity mean ratios.

Mann-Whitney U test was used to assess any differences in the number of γH2AX foci between treatment groups at a specific cleavage stage and between cleavage stages within a treatment group. We also used the Mann-Whitney U test to assess the difference in the micronuclear and nuclear chromatin structure for γH2AX, 53BP1 and PAR immunoreactivity, as well as the average numbers of small, medium and large γH2AX foci per micronucleus (corrected for volume) between cleavage stages. Values are reported either as an average number of foci or intensity mean per embryo per replicate ± standard error of the mean or fold difference from the nuclear number of foci or micronuclear to nuclear DNA intensity means, set to 1 ± standard error of the mean.

RESULTS

Mitochondrial function

Since mitochondrial activity is a useful measure of embryo quality, we monitored their localization, numbers and activity within each blastomere of live cleavage stage embryos using MitoTracker green and MitoSox red probes (Figure 4.1). These fluorescent mitochondrial probes are selective indicators of mitochondrial function and energy production. In addition, MitoSox red provides a measure of oxidative stress since it indicates the presence of superoxide generated as a byproduct of oxidative phosphorylation by a leaky mitochondrial electron transport chain during ATP production. We obtained similar mitochondrial staining patterns with both MitoTracker probes, but for stability, reproducibility and image quality reasons the data analysis was focused on the MitoSox red probe. As anticipated, the mitochondrial staining pattern was excluded from the nucleus in all cleavage stage embryos. In 2- to 4-cell embryos, we detected the presence of numerous bean shape mitochondria distributed throughout each individual blastomere (Figure 4.1a). Furthermore, at the 2-cell stage, following the first zygotic division, there was an even distribution of mitochondria between blastomeres. Due to the differences in staining patterns observed with the mitochondrial probes in embryos collected on day 3, we analyzed the 6 to 12-cell embryos separately from the 13 to 16-cell embryos. In 6- to 12-cell embryos, a clear compartmental distribution of mitochondria between the nucleus and the exterior membrane of the embryo in each blastomere was observed. In 16-cell embryos, there was a very limited number of mitochondria in the central blastomeres; many more mitochondria, with a specific compartmental distribution, were found in the external blastomeres. In addition, in 16-cell embryos the staining intensity of mitochondria in the central blastomeres was extremely low compared to the high staining intensity in mitochondria located in the external blastomeres. The pattern of distribution of mitochondria was influenced by cell cycle phase in all cleavage stage embryos; mitochondria in mitotic blastomeres lost their bean shape, were diffusely distributed in the whole

cell, and stained less intensely than those in interphasic blastomeres (Figure 4.1b). The specific localization of mitochondria in the blastomeres of cleavage stage embryos may dictate the plan of cellular division with a concentration of all the energy producing organelles where they are most needed, thus playing a role in the cell fate decision.

While quantification revealed a trend towards an increase in the mitochondrial mean intensity and a decrease in mitochondrial count per embryo from the 2- to the 8-cell stage, these parameters were not significantly different between cleavage stages and treatment groups (Suppl. Figure 4.1a), nor did the presence of micronuclei within a cell influence our results with MitoTracker probes at any of the cell cleavage stages (Suppl. Figure 4.1b).

The characterization of δH2AX foci in control and cyclophosphamide-sired cleavage stage embryos

To evaluate the level of DNA damage as a consequence of paternal exposure to cyclophosphamide in cleavage stage embryos we assessed the distribution pattern of γH2AX signals (Figure 4.2). In both control and cyclophosphamide-sired 2 cell embryos γH2AX foci were uniformly distributed, suggesting that these foci may be indicative of replication stress (Figure 4.2, top 2 rows). The staining pattern with γH2AX in embryos collected on day 3 did not differ in 8 and 16 cell embryos; therefore, we pooled these data and show only the 8 cell embryos. In the 8 cell embryos, γH2AX foci appeared to be increased in size and be more irregularly distributed in embryos sired by cyclophosphamide-treated males compared to controls (Figure 4.2, bottom 2 rows).

To further characterize the population of γH2AX foci, we subdivided them into three subgroups, based on their volumes, and calculated the average number of each type of foci per nucleus (Figure 4.3). Control and cyclophosphamide-sired 2 cell embryos had nearly four times as many foci as 8 cell stage embryos; paternal exposure to cyclophosphamide had no impact on the number of small foci at the 2 cell and 8-cell stages (Figure 4.3a, left panel). Although a similar decreasing trend, by just over 50%, in the number of medium-sized foci γH2AX

was observed between 2- and 8-cell embryos in the control group, embryos sired by cyclophosphamide treated males showed a steeper decline and the numbers were more elevated than for control at the 8-cell stage ($P \leq 0.05$) (Figure 4.3a, middle panel). In contrast to the decrease observed in small and medium sized foci between 2 and 8 cell stage embryos, a significant increase was observed in the numbers of large γH2AX foci in both treatment groups ($P \leq 0.05$) (Figure 4.3a, right panel). Few large γH2AX foci were observed in control and cyclophosphamide-sired 2 cell embryos. A dramatic increase in the number of large γH2AX foci was observed in 8 cell embryos sired by cyclophosphamide-treated males compared to same stage control embryos ($P \leq 0.01$).The decrease in small and medium γH2AX foci per nucleus between the 2 and 8 cell embryos may reflect important events in preimplantation embryo development, such as the major and minor waves of transcription and active DNA replication in 2 and 4 cell embryos; the significant increase in the number of large γH2AX foci in 8 cell embryos sired by males treated with cyclophosphamide compared to control 8 cell embryos is likely to reflect an increase in the formation of DNA double strand break aggregates.

Since the amount of DNA damage, represented by γH2AX foci, depends on the nuclear volume, to compare DNA damage in micronuclei to nuclei we divided the number of foci by the average nuclear volume for the nucleus and by the average micronuclear volume for the micronucleus and report the fold differences for the relative values in 2- and 8- cell embryos (Figure 4.3b). The majority of micronuclei were punctuated with numerous γH2AX foci. There were no differences between the nuclei and micronuclei in the numbers of small, medium and large γH2AX foci in 2 cell embryos (Figure 4.3b). However, in cyclophosphamide-sired 8 cell embryos, a 1.5 fold increase in the medium γH2AX foci ($P \leq 0.001$) and a 45 fold increase in the large γH2AX foci ($P \leq 0.001$) were observed in micronuclei compared to nuclei (Figure 4.3b). Thus, medium ($P \leq 0.05$) and large foci ($P \leq 0.01$) accumulate in the micronuclei of cyclophosphamide-sired 8 cell embryos (Figure 4.3c). This accumulation of damage marks may represent an increase in the formation of DNA double strand

breaks or in the sites of replication errors or a failure to recruit the appropriate DNA repair proteins.

Since micronuclei represent visible signs of DNA damage in cyclophosphamide-sired embryos, we hypothesized that the DNA damage response would be elevated in embryos with micronuclei compared to those without. To test this hypothesis, we compared the number of γH2AX foci in the nuclei of cyclophosphamide-sired 2- and 8-cell embryos with and without micronuclei (Suppl. Figure 4.2). Strikingly, the number of γH2AX foci within each subgroup, classified by their volume, was not dependent on the presence and/or abundance of micronuclei in the embryos; there was also no correlation between the nuclear DNA damage response in individual blastomeres and the presence or absence of micronuclei within the cell (Suppl. Figure 4.2a). Embryos fertilized by cyclophosphamide exposed spermatozoa and collected on day 3 were considered developmentally delayed if they were at the 3- and 4-cell stage; normally dividing embryos, sired by control or cyclophosphamide treated males, were at the 5- to 16-cell stage at this time (Grenier et al., 2011). Developmentally delayed cyclophosphamide-sired embryos, with the highest incidence of micronuclei, had the same DNA damage response profile, as assessed by the numbers of γH2AX foci, as normally dividing embryos (Suppl. Figure 4.2b). Thus, the presence of micronuclei did not affect the numbers of γH2AX foci in the nuclei of cells within cleavage stage embryos.

53BP1 in cleavage stage embryos

Our next objective was to determine whether fertilization with cyclophosphamide exposed spermatozoa would affect markers of DNA repair in cleavage stage embryos. The localization of 53BP1 immunoreactivity in pronuclear (PN), 2- and 8-cell embryos is depicted in figure 4.4. The 53BP1 signal was distributed throughout the nucleus and cytoplasm. To determine the relative amounts of 53BP1 reactivity in these two compartments, we quantified the average intensities in the nucleus and the cytoplasm as well as the nuclear to cytoplasmic ratio in the female and male pronuclei of the 2- and 8-cell embryos

(Figure 4.4b). Since intensities did not differ between the male and female pronuclei, the average nuclear staining intensity is given as a single value for the pronuclear stage embryos (Figure 4.4b, left graph day 0.5, PN). The staining pattern of 53BP1 in 8-16 cell embryos collected on day 3 was identical irrespective of the treatment group; therefore, we pooled these data and show only the 8 cell embryos. The nuclear staining tended to increase as the embryos progressed from the pronuclear stage to the 8 cell stage in both the control and cyclophosphamide-sired groups (Figure 4.4b, left graph); this was accompanied by a trend towards a decrease in the cytoplasmic 53BP1 signal (Figure 4.4b, middle graph). Together, these changes resulted in a significant increase in the nuclear to cytoplasmic ratio of the localization of the 53BP1 signal from the pronuclear stage to the 8 cell embryo in both the control (0.84 to 1.74, $P \leq 0.01$) and the cyclophosphamide-treated group (0.85 to 1.45, $P \leq 0.05$) (Figure 4.4b, right graph).

To characterize DNA repair capacity in the chromatin of micronuclei found in cyclophosphamide-sired embryos, we compared the intensity of 53BP1 reactivity in the micronuclei to that in the nuclei. The 53BP1 intensities in the micronuclei and nuclei were adjusted by the ratios of DNA intensity since micronuclei have less DNA per equivalent volume. In both the 2 and 8-cell cyclophosphamide-sired embryos, the micronuclear chromatin contained significantly more 53BP1 repair protein (1.4 fold in 2-cell, $P \leq 0.05$; 1.2 fold in 8-cell, $P \leq 0.01$) compared to the nuclear chromatin (Figure 4.4c). Thus, this repair protein is actively recruited to micronuclear chromatin.

Similar to the number of γH2AX foci, 53BP1 nuclear reactivity was not affected by the presence and/or abundance of micronuclei in the embryos; there was also no correlation between the nuclear DNA damage response in individual blastomeres and the presence or absence of micronuclei with the cell (Suppl. Figure 4.3a). In addition, developmentally delayed cyclophosphamide-sired embryos had the same DNA damage response profile, assessed by the nuclear reactivity with 53BP1, as normally dividing embryos (Suppl. Figure 4.3b).

Poly(ADP-ribose) polymers in cleavage stage embryos

The immunoreactive poly(ADP-ribose) polymers (PAR), representing the product of poly(ADP-ribose) polymerase activities, in pronuclear (PN), 2- and 8-cell embryos are shown in figure 4.5a. The PAR signal was consistently more intense in the nucleus compared to the cytoplasm. As for 53BP1, the PAR immunoreactivity did not differ between the male and female pronuclei of pronuclear stage embryos. The staining pattern also did not differ between 8- and 16-cell embryos irrespective of the treatment group. Neither developmental stage nor treatment significantly affected the intensity of the PAR signal in the cytoplasm or the nuclear to cytoplasmic ratio (Figure 4.5b, middle and right graph). In contrast, embryos sired by cyclophosphamide-treated males displayed a dramatic decrease in PAR nuclear mean intensity at the 8 cell cleavage stage ($P \leq 0.01$) (Figure 4.5b, left graph). In both the 2 and 8-cell cyclophosphamide-sired embryos, the micronuclear chromatin contained significantly more PAR polymers (1.5 fold in 2-cell, $P \leq 0.01$; 1.3 fold in 8-cell, $P \leq 0.01$) compared to the nuclear chromatin (Figure 4.5c).

Once again, the nuclear signal of PAR polymers was not affected by the presence and/or abundance of micronuclei in the 2- and 8-cell cyclophosphamide-sired embryos (Suppl. Figure 4.4a) or, in 8-cell cyclophosphamide-sired embryos, by a delay in the rate of development (Suppl. Figure 4.4b).

DISCUSSION

Paternal exposure to cyclophosphamide did not affect mitochondrial functional compartmentalization or bioenergetic activities in cleavage stage embryos. However, markers of the DNA damage detection and repair responses were affected: in the 8-cell embryo paternal cyclophosphamide exposure led to the selective formation of medium and large γH2AX foci and a decrease in nuclear PAR polymers, in the absence of an effect on 53BP1 reactivity. All three DNA damage response indicators were enriched in micronuclei.

The specialized localization of mitochondria during embryonic development is hypothesized to play a critical role in the regulation of energy

production and consumption, as well as roles in calcium homeostasis, cytoplasmic redox state and signal transduction (van Blerkom, 2011). As observed for human and mouse embryos (van Blerkom, 2011), the staining intensities and distribution patterns of MitoTracker green and MitoSox red in early embryos display embryonic developmental stage and compartmental specificity. In 8-cell embryos, the localization of mitochondria between the nucleus and the plasma membrane on a specific side of the embryo may determine the plane of the next cycle of division by concentrating the energy necessary to allow normal developmental progression. In 16-cell embryos, we observed a very faint diffuse type of staining for mitochondria in central blastomeres, as opposed to a stronger and compartmentalized type of staining in blastomeres surrounding the embryo. These stage and space specific mitochondrial distributions closely resemble the differences in mitochondrial structure and number between the two cell types in the future blastocyst; inner cell mass cells are hypopolarized, almost metabolically quiescent, as opposed to the trophectoderm cells, that are hyperpolarized at the basal aspect of the plasma membrane and produce almost 80% of the net ATP (Houghton, 2006; van Blerkom et al., 2002). Since the initial pool of mitochondria in the oocyte is not replenished until after blastocyst implantation and mitochondria are evenly divided between blastomeres, there was a tendency for the mitochondrial count per blastomere to decrease as the embryos progressed through cleavage stages (Larsson et al., 1998).

If fertilization with cyclophosphamide exposed spermatozoa had increased energy demand in the embryo due to the requirement for an enhanced DNA repair response, we might have anticipated a decrease in energy stores. However, fertilization with cyclophosphamide exposed spermatozoa did not have any impact on the distribution or staining intensity of the mitochondrial MitoTracker Green or MitoSox Red probes, indicating that the general energy stores and intracellular redox status of cleavage stage embryos were unaltered. Thus, the MitoSox and MitoTracker probes were valuable tools to show that embryos with damaged DNA may be otherwise normal, at least in terms of energy stores. It is clear that the mitochondrial energetic status observed in early cleavage stage

embryos is sufficient to allow the progression of embryos during preimplantation development even in the presence of heavy DNA damage. Moreover, these results indicate that mitochondrial function is not, by itself, sufficient to predict development competence, especially for male-mediated DNA damage such as that induced by cyclophosphamide.

In cleavage stage embryos, we observed the greatest level of H2AX phosphorylation at the 2-cell stage, coincident with major chromatin reorganization during DNA replication and zygotic genome activation; the level of staining was significantly reduced at the 8-cell stage. H2AX is phosphorylated in response to DNA double strand breaks (DSBs) that arise from exposure to exogenous chemicals, radiation or reactive oxygen species that induce replication stress (Ismail et al., 2007; Rogakou et al., 1998) as well as in response to physiological processes, such as DNA replication errors, chromatin remodelling during protamine to histone transition in pre-pronuclear zygotes, and meiosis (Grenier et al., 2010). The small γH2AX foci observed support a role for the phosphorylation of H2AX in the control of chromatin structural reorganization (Barton et al., 2007) and proper developmental progression of rapidly dividing stressed embryos (Ziegler-Birling et al., 2009*)* in the absence of induced DNA damage. The significant increase in medium γH2AX foci in cyclophosphamide-sired 8-cell embryos, compared to controls, suggests that these medium foci may be important in the recognition of DNA damage. The large γH2AX foci visualized in 8 cell embryos sired by cyclophosphamide-treated males are likely to represent the accumulation of γH2AX at hot spots of DNA damage, perhaps as a consequence of the failure to complete the repair process in early embryos (Barton et al., 2007; Grenier et al., 2010). Earlier studies have reported a similar phenomenon in a murine model; paternal exposure to radiation impaired blastocyst development due to inappropriate repair during the first cell cycle division and led to de novo mutations (Derijck et al., 2008*).* Interestingly, the presence of micronuclei in early embryos did not influence the quantity or nature of the γH2AX foci in the nuclei of these embryos.

DNA damage repair capacity in cleavage stage embryos was assessed in the pronuclear zygote, 2- and 8-cell embryo with two markers of DNA repair, 53BP1 and poly(ADP-ribose) polymers, that are known to be recruited to the sites of DNA double strand breaks detected by γH2AX. It is not likely that the 53BP1 immunoreactivity is strongly co-localized with γH2AX in these embryos since a faint diffuse and homogenous pattern of 53BP1 distribution was observed in both the nuclear and cytoplasmic compartments throughout the cell cleavage stages studied. In addition, 53BP1 protein expression was unaffected by the presence of a damaged male genome. Similar findings were reported previously in a damage free mouse embryonic model in which 53BP1 protein localisation changed upon blastocyst formation. The failure of 53BP1 and γH2AX to co-localise in the embryo (Ziegler-Birling et al., 2009) reinforces the notion that the high levels of H2AX phosphorylation may be linked to chromatin remodelling in the early embryo, rather than directly to a DNA damage response (Ziegler-Birling et al., 2009). The developmental significance of the nuclear retention of 53BP1 as a partial mediator of p53 activity in regulating cell cycle checkpoints, allowing the progression of cell cycle division of cleavage stage embryos, has been established previously (Fernandez-Capetillo et al., 2003).

A decrease in nuclear poly(ADP-ribose) polymers was observed in 8-cell embryos sired by cyclophosphamide exposed spermatozoa. The presence of micronuclei did not influence the amount of poly(ADP-ribose) polymers in the nucleus. In general, a decrease in poly(ADP-ribose) polymers is suggestive of a decrease in the poly(ADP-ribosyl)ation of histones and/or PARP-1 (Zhou et al., 2010). This may result in the recondensation of chromatin, reducing the accessibility of potential DNA damage repair proteins to DNA (Zhou et al., 2010); however, examination of the gross nuclear morphology of cyclophosphamide-sired 8 cell embryos did not reveal any apparent increase in condensed chromatin. Numerous scenarios could lead to a decrease in poly(ADP-ribosyl)ation in early embryos; these include NADH energy depletion, reducing PARP-1 activity, an increase in PARP-1 activity, leading to auto-poly(ADP-ribosyl)ation of PARP-1 and its inactivation, or an increase in PARG catalytic

activity, removing poly(ADP-ribose) polymers. Previously, we reported that paternal exposure to cyclophosphamide led to an increase in PARP-1 immunoreactivity in both male and female pronuclei (Barton et al., 2007). Our data show that there is no drug treatment effect on the level of poly(ADP-ribosyl)ation in pronuclear or 2 cell embryos, suggesting that the increase in PARP-1 immunoreactivity may be accompanied by an increase in PARG catalytic activity, dampening the repair capacity of cleavage stage embryos. The reduced PARP-1 activity observed in 8 cell embryos was not associated with a decrease in mitochondrial energy status, as assessed with the MitoTracker probes; therefore, the reduction in PAR polymers does not appear to be due to a decrease in energy stores in the embryo.

Energy depletion as a result of PARP induced NADH depletion may contribute to the delay in cell cycle progression seen at the 8 cell stage (Grenier et al., 2011). Developmental arrest was reported in pronuclear stage mouse embryos treated with a PARP inhibitor (Osada et al., 2010). It is clear that the proper functioning of the complex poly(ADP-ribosyl)ation system is necessary for the early stages of mouse embryogenesis (Osada et al., 2010).

Micronuclei are a readily identifiable mark of DNA damage in the paternal genome in embryos sired by cyclophosphamide-treated males. In 2- and 8-cell embryos, both 53BP1 and poly(ADP-ribose) polymers were enriched in chromatin in the micronuclei compared to the nuclei; this enrichment was observed in the absence of any increase in γH2AX foci, tagging DNA double strand breaks. These findings suggest that there may be a γH2AX independent mechanism of recruitment of 53BP1 and poly(ADP-ribose) polymers in micronuclei at the 2-cell stage. By the 8-cell stage, a marked accumulation of medium and large γH2AX foci was observed in micronuclei; this occurred in the absence of an increase in the intensity of the staining for 53BP1 or poly(ADP-ribose) polymers in comparison to the 2-cell embryos. The accumulation of γH2AX foci in the micronuclei of 8-cell embryos may indicate the failure of DNA repair processes to resolve DNA double strand breaks (Celeste et al., 2003). Micronuclei may gradually lose functionality as the embryo progresses from 2-

cells to 8-cells; indeed, we reported previously that the incorporation of EdU (5-ethynyl-2´-deoxyuridine) into DNA was decreased in micronuclei at the 8 cell stage (Grenier et al., 2011).

In summary, we have demonstrated that fertilization by sperm from cyclophosphamide-treated male rats produces a conceptus with a heavily damaged paternal genome. The damaged paternal genome triggers both a γH2AX dependent and a γH2AX independent DNA damage response with respect to micronuclear formation, within the same cells. The 2-cell embryo is capable of mounting a DNA damage response since there is a recruitment of 53BP1 and an increase in poly(ADP-ribose polymers in micronuclei. However, the DNA repair response is not adequate to prevent the accumulation of medium and large γH2AX foci in micronuclei by the 8 cell stage. The accumulation of DNA damage and the inability of the embryo to adequately repair the paternal genome are likely to contribute to the elevated pre- and post-implantation death observed as a consequence of paternal cyclophosphamide exposure.

ACKNOWLEDGMENTS

We thank Jacynthe Laliberté (McGill University, Montreal) for her assistance with confocal microscopy and Aleksandrs Spurmanis and Claire Brown (McGill University, Montreal) and Cory Glowinski (Bitplane Inc., South Windsor, CT) for their assistance with Imaris image analysis.

REFERENCES

Auroux, M., Dulioust, E., Selva, J., and Rince, P. (1990). Cyclophosphamide in the F0 male rate: physical and behavioral changes in three successive adult generations. *Mutat. Res*. **229,** 189-200.

Barton, T.S., Robaire, B., and Hales, B.F. (2005). Epigenetic programming in the preimplantation rat embryo is disrupted by chronic paternal cyclophosphamide exposure. *Proc. Natl. Acad. Sci. U. S. A.* **31,** 7865-7870.

Barton, T.S., Robaire, B., and Hales, B.F. (2007). DNA damage recognition in the rat zygote following chronic paternal cyclophosphamide exposure. *Toxicol. Sci.* **100,** 495-503.

Barton, T.S., Wyrobek, A.J., Hill, F.S., Robaire, B., and Hales, B.F. (2003). Numerical chromosomal abnormalities in rat epididymal spermatozoa following chronic cyclophosphamide exposure. *Biol. Reprod*. **69,** 1150-1157.

Brochu, G., Duchaine, C., Thibeault, L., Lagueux, J., Shah, G.M., and Poirier, G.G. (1994). Mode of action of poly(ADP-ribose) glycohydrolase. *Biochim. Biophys. Acta* **1219,** 342-350.

Celeste, A., Fernandez-Capetillo, O., Kruhlak, M.J., Pilch, D.R., Staudt, D.W., Lee, A., Bonner, R.F., Bonner, W.M., and Nussenzweig, A. (2003). Histone H2AX phosphorylation is dispensable for the initial recognition of DNA breaks. Nat. Cell Biol. **5**, 675-679.

Codrington, A.M., Hales, B.F., and Robaire, B. (2004). Spermiogenic germ cell phase-specific DNA damage following cyclophosphamide exposure. *J. Androl.* **25,** 354-362.

Codrington, A.M., Hales, B.F., and Robaire, B. (2007a). Chronic cyclophosphamide exposure alters the profile of rat sperm nuclear matrix proteins. *Biol. Reprod.* **77,** 303-311.

Codrington, A.M., Hales, B.F., and Robaire, B. (2007b). Exposure of male rats to cyclophosphamide alters the chromatin structure and basic proteome in spermatozoa. *Hum. Reprod*. **22,** 1431-1442.

Dantzer, F., Schreiber, V., Niedergang, C., Trucco, C., Flatter, E., De La Rubia, G., Oliver, J., Rolli, V., Meissier-de Murcia, J., and de Murcia, G. (1999). Involvement of poly(ADP-ribose) polymerase in base excision repair. Biochimie **81,** 69-75.

D'Amours, D., Desnoyers, S., D'Silva, I., and Poirier, G.G. (1999). Poly(ADP-ribosyl)ation reactions in the regulation of nuclear functions. *Biochem. J.* **342(**Part 2), 249-268.

Derijck, A., van der Heijden, G., Giele, M., Philippens, M., and de Boer, P. (2008). DNA double-strand break repair in parental chromatin of mouse zygotes, the first cell cycle as an origin of de novo mutation. *Hum. Mol. Genet.* **17,** 1992-1937.

Fernandez-Capetillo, O., Chen, H.T., Celeste, A., Ward, I., Romanienko, P.J., Morales, J.C., Naka, K., Xia, Z., Camerini-Otero, R.D., Motoyama, N., Carpenter, P.B., Bonner, W.M., Chen, J., and Nussenzweig, A. (2003). DNA damage-induced G2-M checkpoint activation by histone H2AX and 53BP1. *Nat. Cell Biol*. **4,** 993-997.

Green, D.M., Kawashima, T., Stovall, M., Leisenring, W., Sklar, C.A., Mertens, A.C., Donaldson, S.S., Byrne, J., and Robison, L.L. (2010). Fertility of male survivors of childhood cancer: A report from the childhood cancer survivor study. *J. Clin. Oncol*. **28**, 332-339.

Grenier, L., Robaire, B., and Hales, B.F. (2010). Paternal exposure to cyclophosphamide affects the progression of sperm chromatin decondensation and activates a DNA damage response in the prepronuclear rat zygote. *Biol. Reprod.* **83,** 195-204.

Grenier, L., Robaire, B., and Hales, B.F. 2011. Paternal cyclophosphamide exposure induces the formation of functional micronuclei during the first zygotic division. *PLoS One.* **6**:e27600. 10.1371/journal.pone.0027600.

Hales, B.F., Crosman, K., and Robaire B. (1992). Increased postimplantation loss and malformations among the F2 progeny of male rats chronically treated with cyclophosphamide. *Teratology* **45,** 671-678.

Houghton, F. (2006). Energy metabolism of the inner cell mass and trophectoderm of the mouse blastocyst. *Differentiation* **74,** 11-18.

Ismail, I.H., Wadhra, T.I., and Hammarsten, O. (2007). An optimized method for detecting gamma-H2AX in blood cells reveals a significant interindividual variation in the gamma-H2AX response among humans. *Nucleic Acids Res*. **35**:e36. 10.1093/nar/gk11169.

Iwabuchi, K., Li, B., Massa, H.F., Trask, B.J., Date, T., and Fields, S. (1998). Stimulation of p53-mediated transcriptional activation by the p53-binding proteins, 53BP1 and 53BP2. J. *Biol. Chem.* **273,** 26061-26068.

Kim, M.Y., Mauro, S., Gevry, N., Lis, J.T., and Kraus, W.L. (2004). NAD+-dependent modulation of chromatin structure and transcription by nucleosome binding properties of PARP-1. *Cell* **119,** 803-814.

Larsson, N., Wang, J., Wilhemsson, H., Oldfors, A., Rustin, P., Lewandoski, M., Barsh, G., and Clayton, D. (1998). Mitochondria transcription factor A is necessary for mtDNA maintenance and embryogenesis in mice. *Nat. Genet.* **18,** 231-236.

Marchetti, F., Essers, J., Kanaar, R., and Wyrobek, A.J. (2007). Disruption of maternal DNA repair increases sperm-derived chromosomal aberrations. *Proc. Natl. Acad. Sci. U. S. A.* **104,** 17725-17729.

McManus, K.J., Hendzel, M.J. (2005). ATM-dependent DNA damage-independent mitotic phosphorylation of H2AX in normally growing mammalian cells. *Mol. Biol. Cell* **16,** 5013-5025.

Moudry. P., Lukas, C., Macurek, L., Neumann, B., Heriche, J.K., Pepperkok, R., Ellenberg, J., Hodny, Z., Lukas, J., and Bartek, J. (2011). Nucleoporin NUP153 guards genome integrity by promoting nuclear import of 53BP1. *Cell Death Differ*. 10.1038/cdd.2011.150.

Oh, S.H., Miyoshi, K., and Funahashi, H. (1998). Rat oocytes fertilized in modified rat 1-cell embryo culture medium containing a high sodium chloride concentration and bovine serum albumin maintain developmental ability to the blastocyst stage. *Biol, Reprod.* **59,** 884-889.

Osada, T., Ogino, H., Hino, T., Ichinose, S., Nakamura, K., Omori, A., Noce, T., and Masutani, M. (2010). PolyADP-ribosylation is required for pronuclear fusion during postfertilization in mice. *Plos One* **5,** pii:e12526. 10.1371/journal.pone.0012526.

Paull, T.T., Rogakou, E.P., Yamazaki, V., Kirchgessner, C.U., Gellert, M., and Bonner, W.M. (2000). A critical role for histone H2AX in recruitment of repair factors to nuclear foci after DNA damage. *Curr. Biol.* **10,** 886-895.

Rogakou, E.P., Pilch, D.R., Orr, A.H., Ivanova, V.S., and Bonner, W.M. (1998). DNA double-stranded breaks induce histone H2AX phosphorylation on serine 139. *J. Biol. Chem*. **273,** 5858-5868.

Schreiber, V., Dantzer, F., Ame, J.C., and de Murcia, G. (2006). Poly(ADP-ribose): Novel functions for an old molecule. *Nat. Rev. Mol. Cell Biol.* **7,** 517-528.

Trasler, J.M., Hales, B.F., and Robaire, B. (1986). Chronic low dose cyclophosphamide treatment of adult male rats: effect on fertility, pregnancy outcome and progeny. *Biol. Reprod.* **34,** 275-283.

van Blerkom, J. (2011). Mitochondrial function in the human oocyte and embryo and their role in developmental competence. *Mitochondrion* **11,** 797-813.

van Blerkom, J., Davis, P., Mawhig, V., and Alexander, S. (2002). Domains of high and low polarized mitochondria in mouse and human oocytes and early embryos. *Hum. Reprod.* **17,** 393-406.

Wang, B., Matsuoka, S., Carpentier, P.B., and Elledge, S.J. (2002). 53BP1, a mediator of the DNA damage checkpoint. *Science* **298,** 1435-1438.

Ward, I.M., Minn, K., Van Deursen, J., and Chen, J. (2003). P53 binding protein 53BP1 is required for DNA damage responses and tumor suppression in mice. *Mol. Cell Biol.* **23,** 2556-2563.

Ward, W.S. (2010). Function of sperm chromatin structural elements in fertilization and development. *Mol. Hum. Reprod*. **16**:30-36.

Yu, S.W., Wang, H., Poitras, M.F., Coombs, C., Bowers, W.J., Federoff, H.J., Poirier, G.G, Dawson, T.M., and Dawson, V.L. (2002). Mediation of poly(ADP-ribose) polymerase-1-dependent cell death by apoptosis-inducing factor. *Science* **297,** 259-263.

Ziegler-Birling, C., Helmrich, A., Tora, L., and Torres-Padilla, M.E. (2009). Distribution of p53 binding protein 1 (53BP1) and phosphorylated H2A.X during mouse preimplantation development in the absence of DNA damage. *Int. J. Dev. Biol*. **53,** 1003-1011.

Zhou, Y., Feng, X., Koh, D.W. (2010). Enhanced DNA accessibility and increased DNA damage induced by the absence of poly(ADP-ribose) hydrolysis. *Biochemistry* **49,** 7360-7366.

FIGURES

Figure 4.1. Distribution of MitoTracker probes in cleavage stage embryos.

Immunodetection of active mitochondria by MitoSox red, indicated in red, and Mitotracker green, depicted in green, in 2-, 8- and 16-cell embryos. A. Even distribution of mitochondria in blastomeres of 2-cell embryos compared to the stage specific functional compartmentalization in 8-cell embryos. A faint low count of mitochondria was observed in central blastomeres compared to the specialized darker distribution of mitochondria in the external blastomeres of 16-cell embryos. B. Cell cycle dependent mitochondrial pattern of staining; mitotic blastomeres, circled in white, had a fainter diffuse pattern of staining, as opposed to the darker, specific distribution, in interphasic blastomeres.

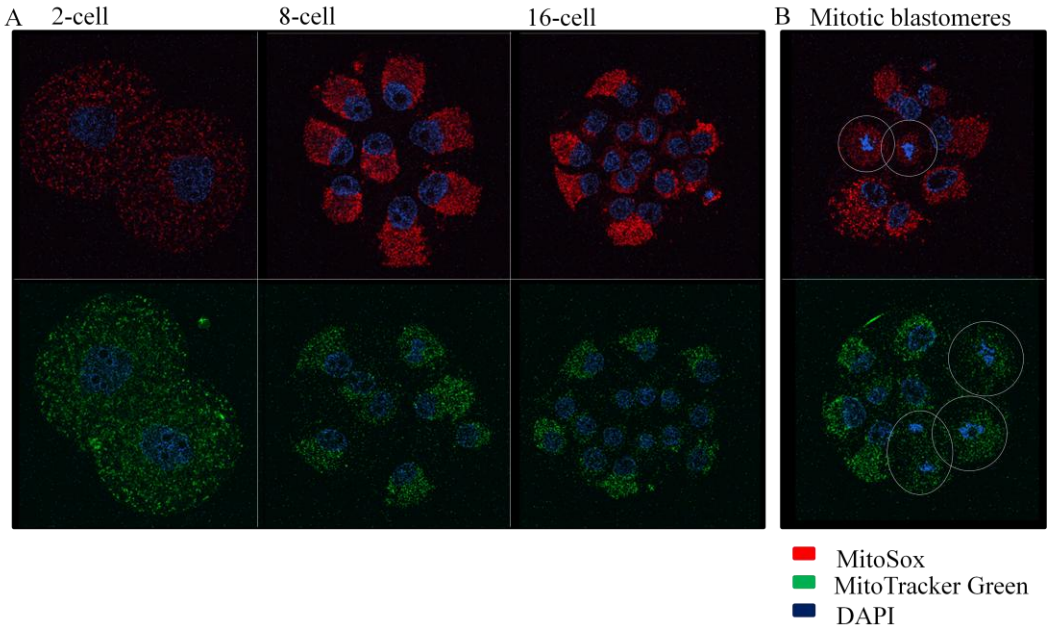
A
2-cell
8-cell
16-cell
B
Mitotic blastomeres
MitoSox
MitoTracker Green
DAPI

<u>Figure 4.2.</u> γH2AX detection of DNA double strand breaks in cleavage stage embryos.

The detection of DNA double strand breaks with γH2AX in control and cyclophosphamide-sired 2- and 8-cell embryos. Phase contrast images with immunodetection of γH2AX in green, nuclear propidium iodide dye in red, and merged images in yellow. The top two rows are control and cyclophosphamide-sired 2-cell embryos, showing an even distribution of small γH2AX foci. The bottom two rows are control and cyclophosphamide-sired 8-cell embryos, showing nuclear region specific large γH2AX foci in the cyclophosphamide-sired 8-cell embryos compared to control.

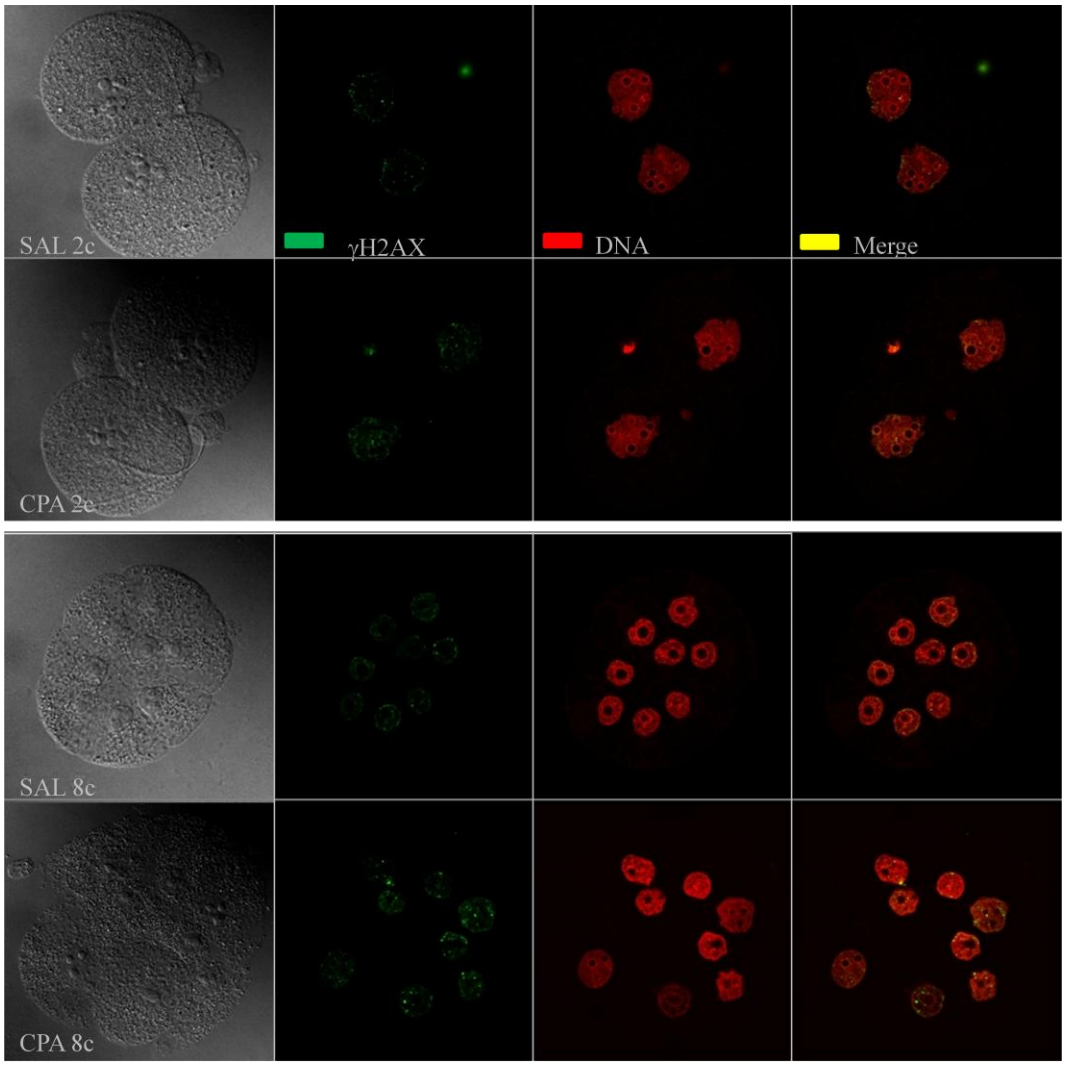
SAL 2c
γH2AX
DNA
Merge
CPA 2c
SAL 8c
CPA 8c

<u>Figure 4.3.</u> Large γH2AX foci as sites of DNA damage in cyclophosphamide-sired 8-cell embryos.

The focal populations of γH2AX foci were divided into three subgroups based on their volumes: Small foci, 0-0.29μm3; Medium foci, 0.30-9.99μm3; Large foci, 10μm3 and above. The numbers of foci were quantified from immunofluorescence images of 2- and 8-cell embryos. A. Average numbers of foci per nucleus ± SEM are graphed; dashed lines are control and full lines are cyclophosphamide-sired embryos. There were significantly more medium and large γH2AX foci in the cyclophosphamide-sired 8-cell embryos compared to control (medium foci: control or SAL, 14.77±1.97 vs cyclophosphamide-sired, CPA, 22.96±3.05; large foci: SAL, 0.03±0.02, vs CPA, 0.21±0.07). B. Comparison of the micronuclear (MN) to nuclear chromatin content of DNA double strand breaks in cyclophosphamide-sired cleavage stage embryos with MN. Average number of small, medium and large γH2AX foci per MN or nucleus corrected for their volume in 2- and 8-cell embryos. Bar graphs represent the MN fold difference from nuclei; MN values are relative to the nuclear value set to 1 ± SEM. Gray bars represent nuclei and black bars are the MN. MN in cyclophosphamide-sired 8-cell embryos have 1.52 and 45.65 fold increases in the numbers of medium and large γH2AX foci relative to their nuclear counterparts. C. Changes in the numbers of γH2AX foci in MN of cyclophosphamide-sired early cleavage stage embryos. Line graphs represent the average number of γH2AX foci, within their respective groups, per MN corrected for MN volume ± SEM. Illustrated in the figure legend, small, medium and large dashed lines represent the sizes of the γH2AX foci, respectively. MN significantly accumulated medium (0.009-0.024) and large (0.000-0.003) γH2AX foci in cyclophosphamide-sired 2- and 8-cell embryos. Mann-Whitney U test was performed with N=7, 10 males with 64, 99 embryos in control and N= 5, 7 males with 41, 112 embryos in cyclophosphamide-sired in 2- and 8-cell embryos, respectively. * $P \leq 0.05$, ** $P \leq 0.01$, *** $P \leq 0.001$.

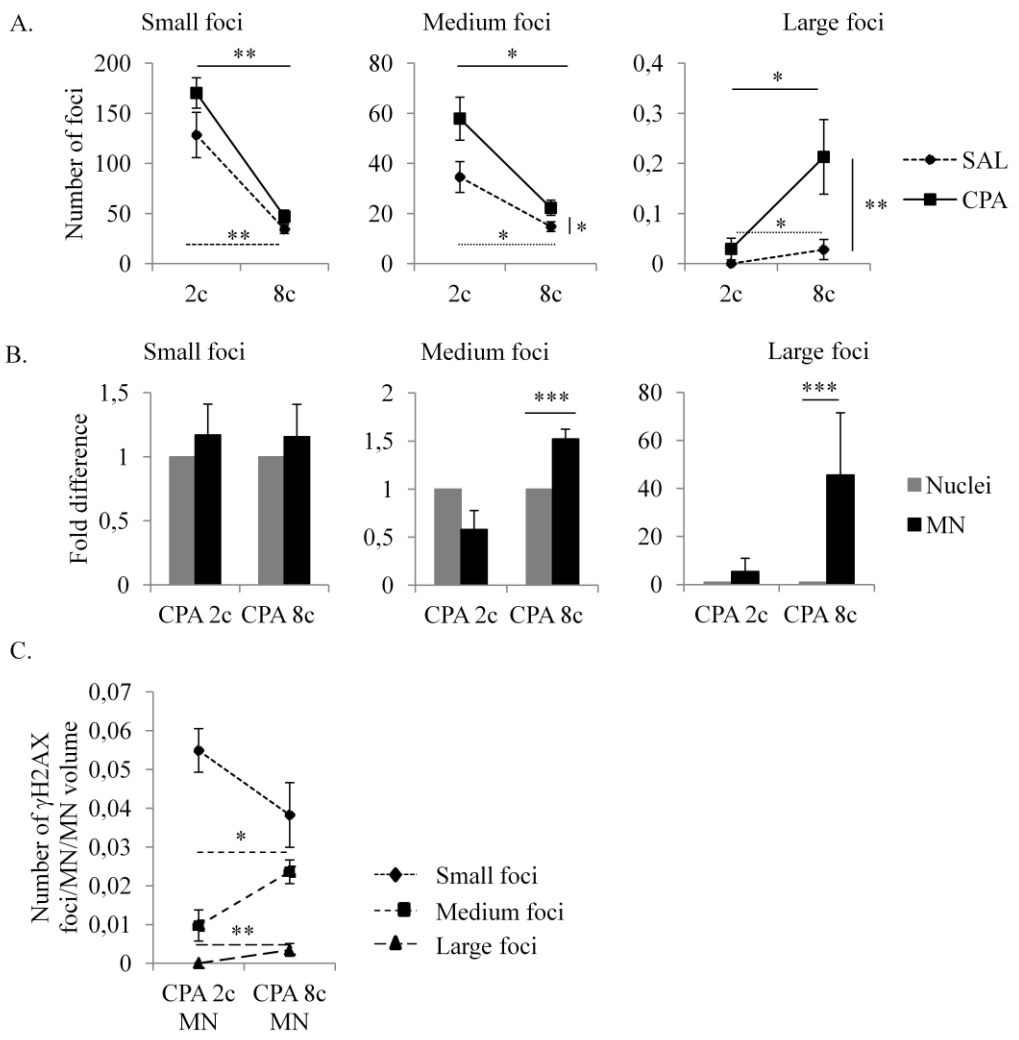
A.
Small foci
Medium foci
Large foci
Number of foci
200
150
100
50
0
80
60
40
20
0
0,4
0,3
0,2
0,1
0
2c
8c
SAL
CPA
**
*
B.
Small foci
Medium foci
Large foci
Fold difference
1,5
1
0,5
0
2
1,5
1
0,5
0
80
60
40
20
0
***
CPA 2c
CPA 8c
Nuclei
MN
C.
Number of γH2AX foci/MN/MN volume
0,07
0,06
0,05
0,04
0,03
0,02
0,01
0
CPA 2c MN
CPA 8c MN
Small foci
Medium foci
Large foci

Figure 4.4. 53BP1 reactivity in cleavage stage embryos.

A. 53BP1 reactivity in pronuclear (PN) zygotes, 2- and 8-cell embryos from control and cyclophosphamide-sired groups. 53BP1 is in green, nuclear propidium iodide dye in red, and merged images in yellow. The top row images are control embryos while bottom row images are cyclophosphamide-sired embryos at all embryonic cleavage stages. Arrows point towards the female (F) and male (M) pronuclei (PN) and the micronuclei (MN) as circled in white. B. Immunofluorescence images are quantified as the 53BP1 intensity in the nucleus, the cytoplasm and the ratio of the nucleus to cytoplasm as means ± SEM. Dashed lines represent control and full lines cyclophosphamide-sired embryos. Independent of treatment group, there was a cytoplasmic to nuclear shift in the localization of 53BP1 repair protein as the cleavage stage embryo divided (SAL PN 0.84 ± 0.06; SAL 8c 1.74 ± 0.12; CPA PN 0.85 ± 0.09; CPA 8c 1.45 ± 0.17). C. Comparision of the MN to nuclear chromatin content of 53BP1 repair protein in cyclophosphamide-sired cleavage stage embryos with MN. Bar graphs illustrate the 53BP1 reactivity fold difference between MN and their nuclear counterparts, comparing the relative MN to nuclear average 53BP1 intensity mean ratios with DNA intensity ratios, both set to 1 ± SEM. Gray bars are the DNA ratios and black bars are the 53BP1 intensity ratios. In 2- and 8-cell embryos, MN are enriched with 53BP1 repair proteins (1.43 and 1.20 fold increases in cyclophosphamide-sired 2 and 8 cell embryos), relative to the nuclei. Kruskal Wallis analysis plus Bonferoni correction, when needed, was performed with N=6-8 males with 57-63 embryos in the control group and N= 4-7 males with 32-68 embryos in the cyclophosphamide-sired group. Comparisons of the intensity means using the Mann-Whitney U test was performed with N= 4-6 males with 24-45 embryos for the micronuclei to nuclei comparison. * $P \leq 0.05$, ** $P \leq 0.01$, *** $P \leq 0.001$.

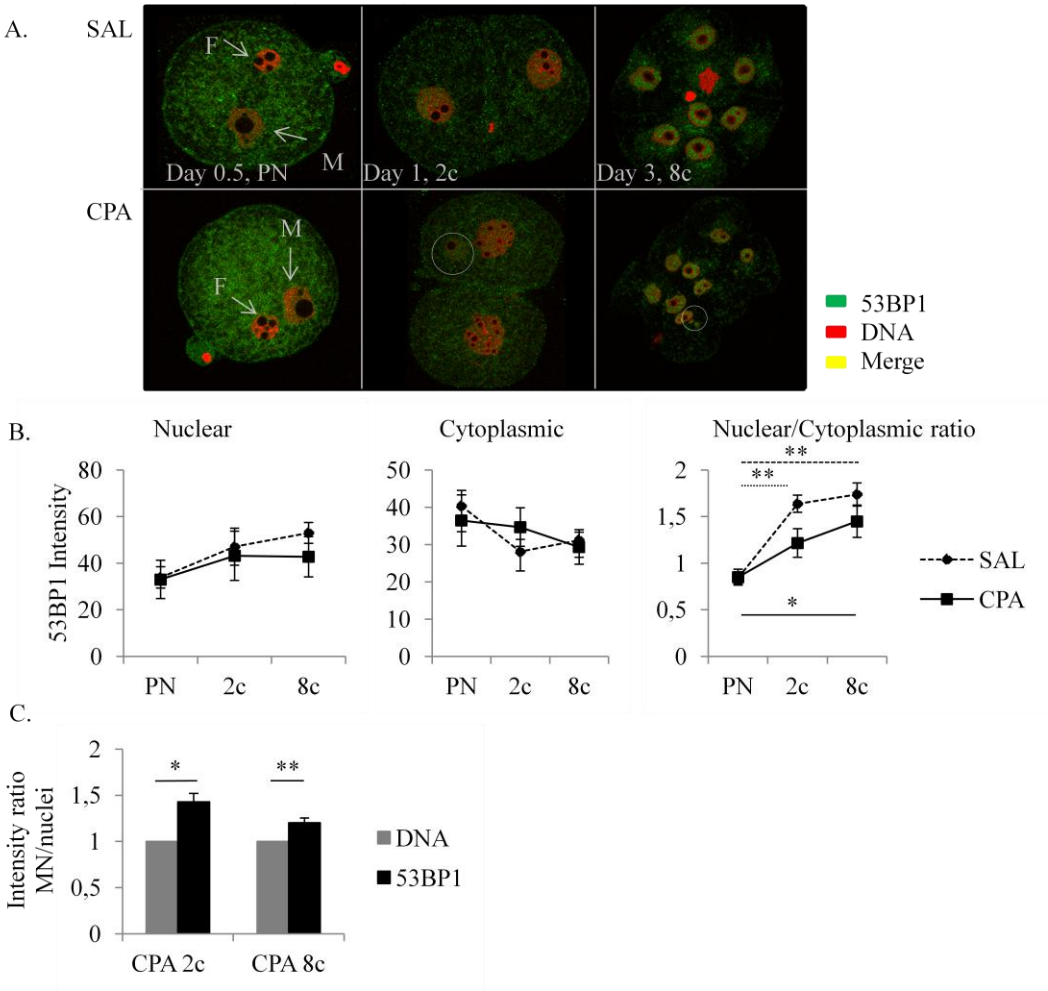
A.
SAL
CPA
F
M
Day 0.5, PN
Day 1, 2c
Day 3, 8c
53BP1
DNA
Merge
B.
Nuclear
Cytoplasmic
Nuclear/Cytoplasmic ratio
53BP1 Intensity
PN
2c
8c
SAL
CPA
C.
Intensity ratio MN/nuclei
CPA 2c
CPA 8c
DNA
53BP1

<u>Figure 4.5.</u> Poly(ADP-ribose) (PAR) polymer reactivity in cleavage stage embryos.

A. Poly(ADP-ribose) polymer (PAR) reactivity in pronuclear zygotes, 2- and 8-cell control and cyclophosphamide-sired embryos. PAR is in green, nuclear propidium iodide dye in red, and merged images in yellow. The top row of images are control embryos while the bottom row images are cyclophosphamide-sired embryos at all embryonic cleavage stages. Arrows point towards the female (F) and male (M) pronucleus and micronuclei (MN) are circled in white. B. Immunofluorescence images are quantified into nuclear, cytoplasmic and nuclear to cytoplasmic ratios of PAR intensity means ± SEM, dashed lines are control and full lines are cyclophosphamide-sired embryos. There is a significant decrease in the nuclear PAR reactivity in cyclophosphamide-sired embryos at the 8-cell stage compared to control embryos (SAL 8c is 116.68±7.67 vs cyclophosphamide 8c at 74.17±11.19). C. Comparision of the micronuclear to nuclear chromatin content of PAR polymer reactivity in cyclophosphamide-sired cleavage stage embryos with MN. Bar graphs illustrate the MN fold difference in PAR reactivity from their nuclear counterpart by comparing the relative MN to nuclear average PAR intensity mean ratios with the DNA intensity ratios, both set to 1 ± SEM. Gray bars are the DNA ratios and black bars are the PAR ratios. In 2- and 8-cell embryos, MN are enriched with PAR polymers (1.49 and 1.30 fold increase in cyclophosphamide-sired 2- and 8-cell embryos) relative to the nuclei. Kruskal Wallis analysis plus Bonferoni correction, when necessary, was performed, N=6-8 males with 51-72 embryos in control and N= 4-6 males with 34-52 embryos in the cyclophosphamide-sired group for the PAR localization and intensity means. The Mann-Whitney U test was performed with N= 5-6 males with 23-37 embryos for the MN to nuclear comparison. * $P \leq 0.05$, ** $P \leq 0.01$, *** $P \leq 0.001$.

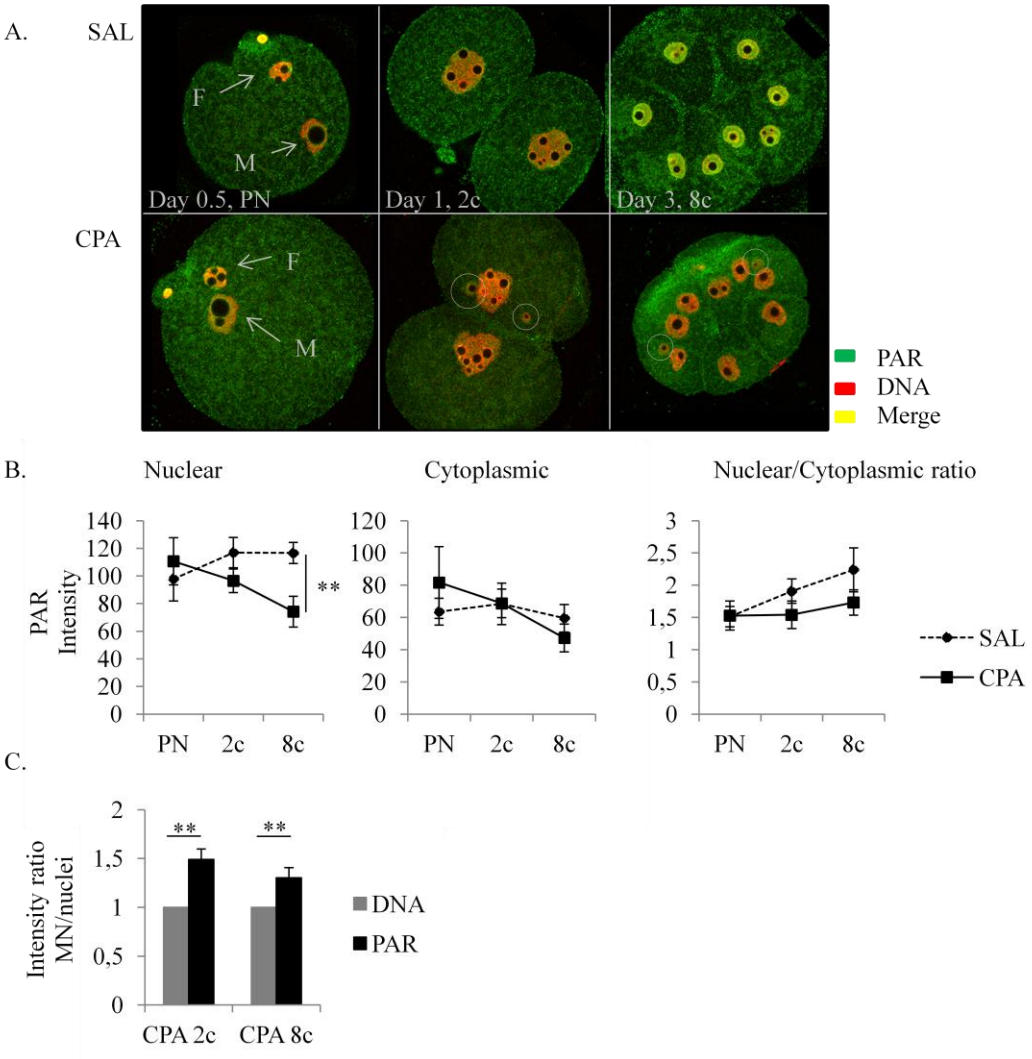
A.
SAL
CPA
F
M
Day 0.5, PN
Day 1, 2c
Day 3, 8c
PAR
DNA
Merge
B.
Nuclear
Cytoplasmic
Nuclear/Cytoplasmic ratio
PAR Intensity
**
PN
2c
8c
SAL
CPA
C.
Intensity ratio MN/nuclei
**
**
DNA
PAR
CPA 2c
CPA 8c

SUPPLEMENTARY FIGURES

<u>Suppl. Figure 4.1.</u> Quantification of mitochondrial selective MitoSox probes in cleavage stage embryos.

A. A comparison of the average MitoSox intensity and counts between control (gray lines) and cyclophosphamide (CPA, black lines) sired embryos at the 2- and 8-cell stages. Paternal exposure to CPA had no impact on the parameters measured with MitoSox probe during the early embryonic cleavage stages. B. A comparison of the average MitoSox intensity and counts between CPA sired embryos without micronuclei (MN, gray lines) and CPA sired embryos with MN (black lines) at the 2- and 8-cell stages. The presence of CPA induced MN had no impact on the parameters measured with MitoSox probe during the early embryonic cleavage stages. Mann-Whitney U test was performed on SAL N=5 males, 28-41 embryos and CPA N=6, 32-39 embryos. Data are represented as means ± SEM.

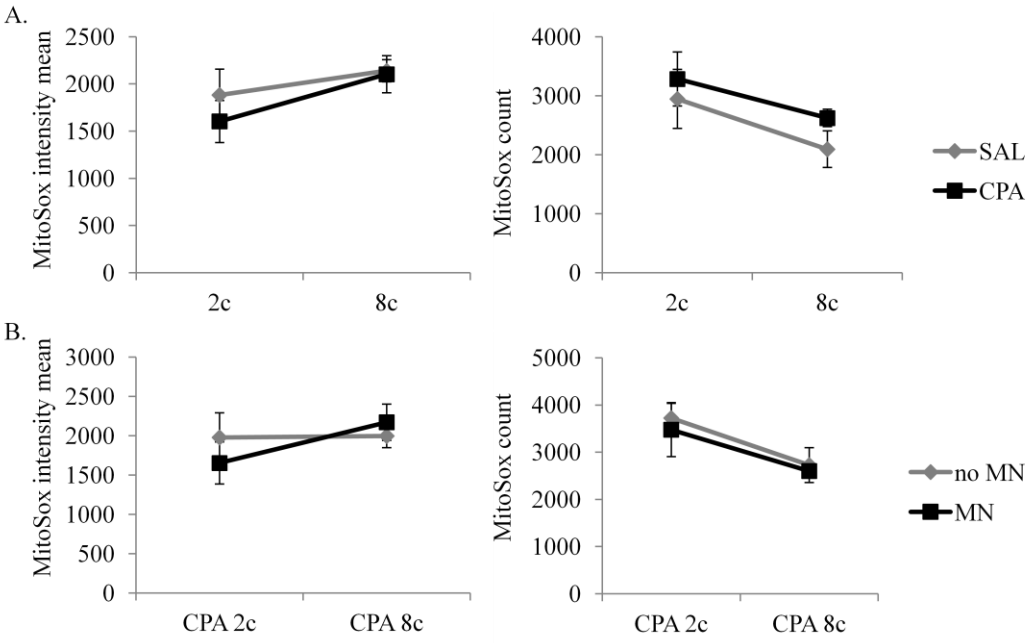
A.
MitoSox intensity mean
2500
2000
1500
1000
500
0
2c
8c
MitoSox count
4000
3000
2000
1000
0
2c
8c
SAL
CPA
B.
MitoSox intensity mean
3000
2500
2000
1500
1000
500
0
CPA 2c
CPA 8c
MitoSox count
5000
4000
3000
2000
1000
0
CPA 2c
CPA 8c
no MN
MN

<u>Suppl. Figure 4.2.</u> The presence of micronuclei (MN) and the rate of embryonic development had no impact on the detection of δH2AX foci, marking DNA double strand breaks.

A. Average number of small, medium and large γH2AX foci per nucleus in cyclophosphamide (CPA) sired embryos without micronuclei (MN, gray bars) and in CPA sired embryos with MN (black bars). The presence of MN induced by CPA exposure had no impact on the numbers of δH2AX foci in 2- and 8-cell embryos. B. A comparison of the average numbers of small, medium and large γH2AX foci per nucleus between normally dividing CPA-sired 8-cell embryos (gray bars) and developmentally delayed CPA sired embryos (black bars). The rate of embryonic progression assessed on day 3 of embryonic collection did not influence the numbers of small, medium and large foci δH2AX per nucleus. Mann-Whitney U test was performed on CPA sired embryos without MN (N=5-7 males, 15-27 embryos) and with MN (N=5-7, 41-85 embryos) and on normally dividing CPA sired embryos (N=7 males, 77 embryos) and delayed CPA sired embryos (N=6 males, 35 embryos). Data are represented as means ± SEM.

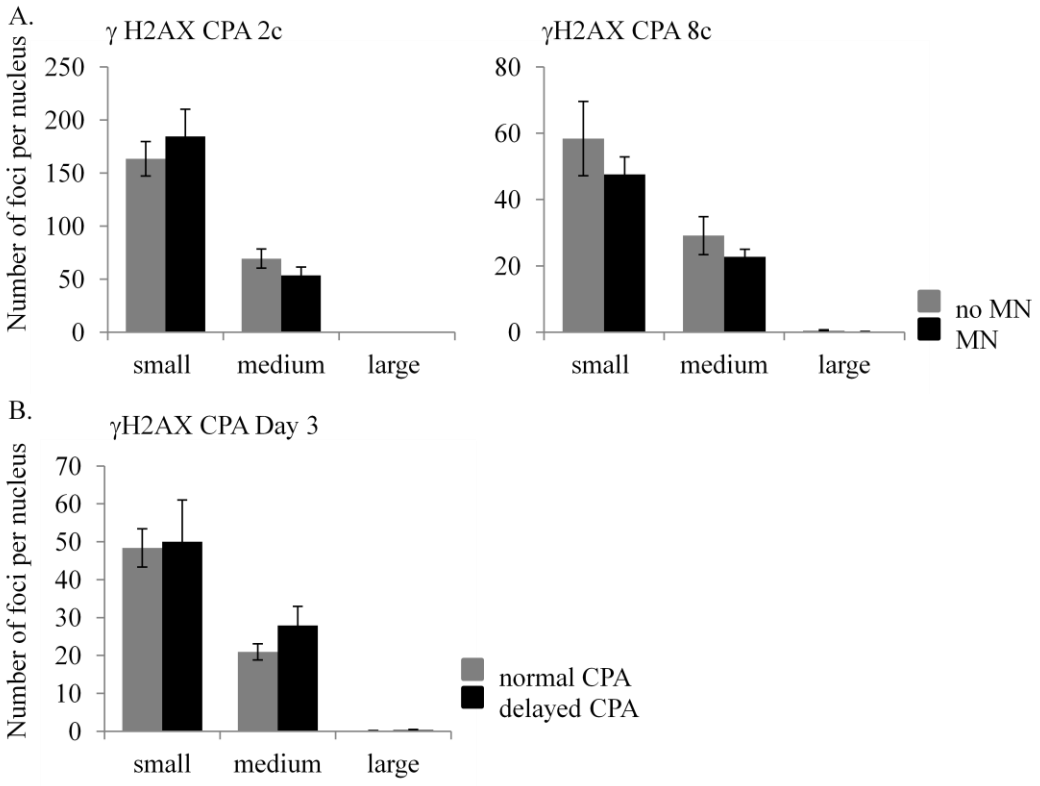
A.
γ H2AX CPA 2c
Number of foci per nucleus
250
200
150
100
50
0
small
medium
large
γH2AX CPA 8c
80
60
40
20
0
small
medium
large
no MN
MN
B.
γH2AX CPA Day 3
Number of foci per nucleus
70
60
50
40
30
20
10
0
small
medium
large
normal CPA
delayed CPA

<u>Suppl. Figure 4.3.</u> The presence of micronuclei (MN) and the rate of embryonic development had no impact on the nuclear localization of 53BP1.

A. A comparison of the nuclear 53BP1 average intensity between cyclophosphamide (CPA) sired embryos without MN (gray bars) and CPA sired embryos with MN (black bars) at the 2- and 8-cell stages. The nuclear immunodetection of 53BP1 was not affected by the presence of CPA induced MN. B. A comparison of nuclear 53BP1 average intensity between CPA sired normally dividing embryos (gray bars) and CPA sired delayed embryos (black bars) collected on day 3. The rate of embryo progression during the early cleavage stages did not have any impact on the nuclear localization of 53BP1. Mann-Whitney U test was performed on CPA sired embryos without MN (N=3-7 males, 4-18 embryos) and CPA sired embryos with MN (N=4-7, 28-50 embryos), and on normally dividing CPA sired embryos (N=7 males, 61 embryos) and developmentally delayed CPA sired embryos (N=5 males, 7 embryos). Data are represented as means ± SEM.

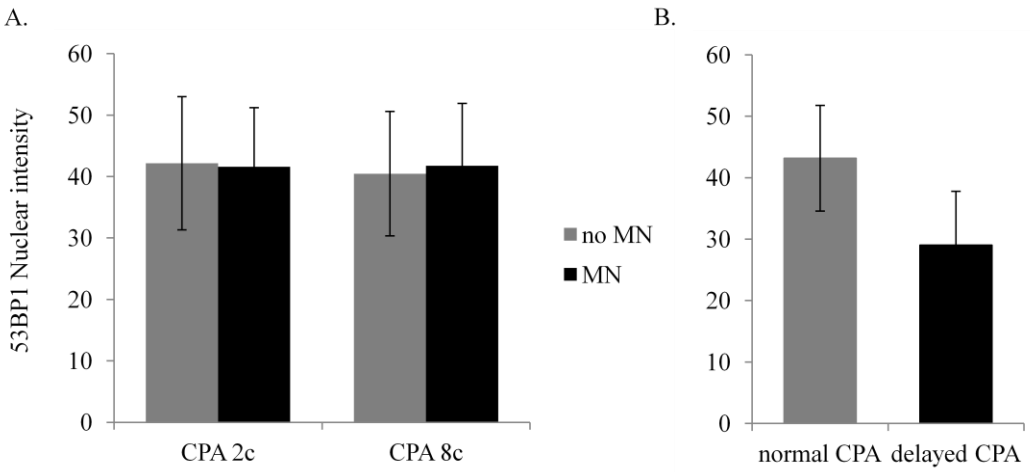
A.
B.
53BP1 Nuclear intensity
60
50
40
30
20
10
0
CPA 2c
CPA 8c
no MN
MN
normal CPA
delayed CPA

<u>Suppl. Figure 4.4.</u> The presence of micronuclei (MN) and the rate of embryonic development had no impact on the nuclear localization of Poly(ADP-ribose) polymers (PAR).

A. A comparison of the nuclear PAR average intensity between CPA sired embryos without MN, gray bars, and CPA sired embryos with MN, black bars, at the 2- and 8-cell stages. The nuclear immunodetection of PAR was not affected by the presence of MN in the CPA-sired group. B. A comparison of the nuclear PAR average intensity between CPA-sired normally dividing embryos, gray bars, and CPA-sired delayed embryos, black bars, collected on day 3. The rate of embryo progression during the early cleavage stages did not have any impact on the nuclear localization of PAR. Mann-Whitney U test was performed on CPA-sired embryos without MN, N=5-6 males, 15 embryos, and CPA-sired embryos with MN, N=5-6, 29-37 embryos, normally dividing CPA-sired embryos, N=6 males, 42 embryos, and delayed CPA-sired embryos N=5 males, 10 embryos. Data are represented as mean ± SEM.

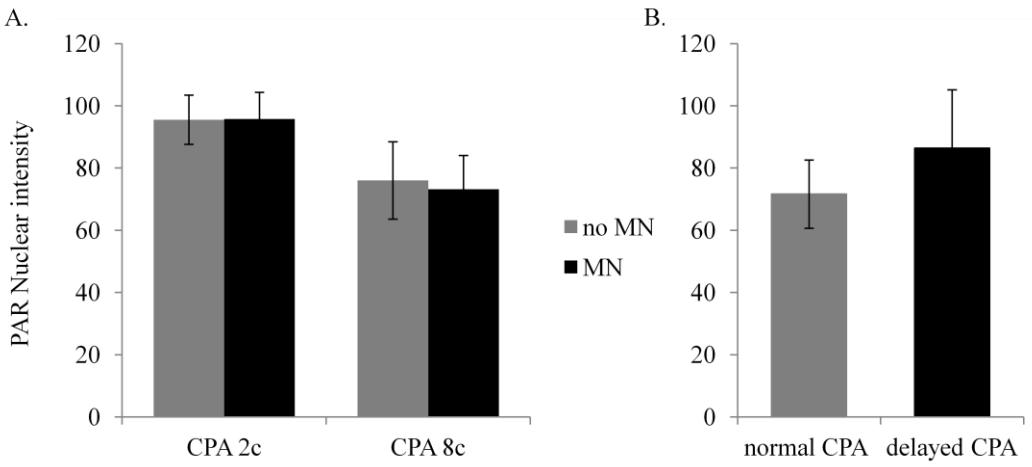
A.
PAR Nuclear intensity
120
100
80
60
40
20
0
CPA 2c
CPA 8c
no MN
MN
B.
120
100
80
60
40
20
0
normal CPA
delayed CPA

CHAPTER V

DISCUSSION

DISCUSSION

5.1 DNA Damaged Paternal Genome and its Contribution to the Zygote

Human exposures to environmental and chemotherapeutic toxicants during spermatogenesis are contributing factors to male subfertility (Jurewicz et al., 2009; Delbès et al., 2010; Pacey, 2010). Male subfertility may be attributed to: altered nuclear protein composition, altered chromatin structure, increased DNA damage, altered epigenetic and genetic programming affecting the maturation of spermatozoa. In most cases, paternal exposure to toxicants has no impact on the ability of damaged spermatozoa to fertilize an oocyte; there may be no discernible effect on sperm morphology, motility, sperm-egg binding or egg penetration (Tamburrino et al., 2012; Yamauchi et al., 2012). The fertilization with damaged spermatozoa contributes to the developmental reprogramming of the embryo, consequently altering embryonic developmental progression and activation of DNA damage responses (DDR) influencing the fate of the embryo. Previous work from our lab using the male-mediated developmental toxicity model of CPA exposure showed that damaged male germ cells are able to fertilize mature oocytes and lead to deleterious consequences on the development of pre- and postimplantation embryos (Trasler et al., 1986). The purpose of these studies was to determine the effects of paternal exposure to CPA on the acquisition and activation of diverse DDR impacting the progression and regulation of developmental events of cleavage stage embryos.

5.2 The Acquisition and Activation of DNA Damage Responses during the Development of Cleavage Stage Embryos

Following fertilization with a damaged spermatozoon, the early embryo depends on the maternal stored products and zygotic gene activation (ZGA) to identify DNA damage and activate DDR. The proper functioning and appropriate timing of these events are crucial to maintain embryonic genomic integrity. An impressive number of key repair genes involved in DNA damage response are expressed during preimplantation development in a stage specific manner; the

unregulated expression or absence of any of the key repair genes is embryonic lethal around the time of implantation as reviewed in Jaroudi and SenGupta, 2007. In contrast to the mRNA expression of DNA repair genes, limited data exist on the protein expression of these genes and on the early embryonic capacity to respond to DNA damage. Their limited capacity to mount an appropriate defence against fertilization by spermatozoon exposed to a DNA damaging agent may explain the vulnerability of preimplantation embryos to toxicants exposure such as irradiation and CPA (Barton et al., 2007; Toyoshima, 2009). We elucidated the activation of important DDR mechanisms against CPA damaged spermatozoon in the early embryo and followed their expression during the development of cleavage stage embryos.

The first mark of DNA damage detected in embryos sired by CPA treated males was DNA DSBs, measured by the formation of γH2AX foci in early pre-pronuclear zygotes. Paternal exposure to CPA during spermiogenesis induced the formation of DNA damage that was recognized in the early zygote during spermatozoon chromatin decondensation (Grenier et al., 2010). The altered spermatozoon chromatin structure induced earlier and enhanced DNA DSBs detection by γH2AX; this was accompanied by accelerated spermatozoon chromatin decondensation in pre-pronuclear zygotes sired by CPA exposed males (Figure 5.1) (Grenier et al., 2010). The DNA damage assessed as DNA DSBs could either be resolved in two-cell embryos or disguised by the dynamic chromatin remodeling and processing during the first zygotic mitotic division and minor zygotic transcriptional activation. DNA damage detected by γH2AX peaks again at the eight-cell stage; this may represent accumulation of unrepaired DNA or newly formed DNA breaks (Grenier et al., 2012).

As a second DDR marker, we measured PARP1 activity with PAR product to detect DNA SSBs and DNA repair induction in embryonic cleavage stages. We noticed a significant decrease in PARP1 activity visualized by the reduced PAR nuclear localization in eight cell embryos from the CPA treated group compared to the control group (Figure 5.1) (Grenier et al., 2012). As a result, decreased

PARylation of histone and DNA binding proteins may condense the chromatin, preventing nuclear epigenetic modifications or protein access to the site of damage, thus preventing DNA damage repair.

The use of DDR markers to assess embryonic quality and developmental competence in reproductive medicine and clinical settings is controversial since they can be indicators of DNA repair or cell death. The differentiation between the fundamental roles of γH2AX and PARylation as biomarkers of DNA damage repair or indicators of cell death needs to be elucidated.

The assessment of DNA repair mediators as opposed to DNA damage recognition markers may provide a way to specifically target their repair role following DNA damage (Figure 1.5). As a first attempt to differentiate between the fundamental roles of DDR markers, we assessed the expression of a mediator of DNA repair, 53BP1. 53BP1 gets recruited to sites of γH2AX and PAR accumulation in cleavage stage embryos. Our results suggested that paternal exposure to CPA did not have any impact on the recruitment of 53BP1 repair protein in cleavage stage embryos (Grenier et al., 2012). These results suggest that paternal exposure to CPA does not activate a 53BP1 mediated maternal response but might be activating other mediators of DNA damage repair.

As future directions, we could assess the expression of the murine double minute MDM2/MDMX complex and RAD51 protein, due to their crucial roles in DNA damage repair and embryonic development. The phosphorylation and activation of MDM2 in early two-cell embryos mediate survival signaling through the transcription of prosurvival effectors and the degradation of P53 (O'Neill et al., 2012). Knock in mice expressing a mutation in the MDM2/MDMX complex are embryonic lethal as a result of p53 mediated apoptosis and decreased cell proliferation (Huang et al., 2011). RAD51 is a DNA repair protein involved in the repair of DNA DSBs in mitotically dividing cells in order to maintain genomic integrity against DNA damaging insults. Mice deficient in RAD51 are embryonic lethal, they exhibit chromosomal instabilities and elevated levels of p53 following DNA damaging agents exposures (Smiraldo et al., 2005; Tian et al., 2010). The

exact expression level and acquisition of DNA repair mediators are not well characterized during preimplantation development. In addition to the assessment of these candidates in embryonic cleavage stages, we could measure them in later compacted morula or blastocyst stages in order to understand how embryos respond to damage and acquire different defense mechanisms.

As a second approach to differentiate between the two fundamental roles of γH2AX and PARylation as indicators of cell death, we could assess the expression and activation of p21 and p53 or annexin V immunoreactivities in our male-mediated developmental toxicity model. The expression and activation of p21 and p53 in early embryos is tightly regulated in a stage specific manner to assure genomic integrity and DDR during preimplantation development as reviewed in Toyoshima, 2009. Sperm-irradiated mouse preimplantation embryos are protected by p53 dependent S-phase checkpoint in the zygote, p21 cleavage arrest at morula/blastocyst stages and apoptosis in damaged cells of inner cell mass at the blastocyst stage (Toyoshima, 2009; Zhang et al., 2011). Annexin V immunoreactivity is used to differentiate between permeable cell membrane and phosphatidylserine binding sites on the cell surface as features of necrosis and apoptosis respectively. Mouse and human early embryos treated with chemicals inducing developmental arrest, DNA fragmentation and apoptosis, resulted mostly in propidium iodide positive versus annexin V positive blastomeres in cleavage and blastocyst stage embryos (Fabian et al., 2009; Chi et al., 2011).

Thus, we propose the assessment of DNA repair mediators as well as cell death markers as future directions for this project to improve the selection of embryos with highest developmental competence and chances of survival in our male-mediated developmental toxicity model.

5.3 The Incidence of Micronuclei in Cleavage Stage Embryos; a Cell Death Sentence?

MNs are extra nuclear pieces of chromosomes or whole chromosome that are formed during cellular division. Although MNs are very similar to the

nucleus, composed of DNA, histones and numerous DNA binding proteins, MNs can be differentiated by the type of chromosomes they contain. Fluorescence in situ hybridisation probes are used to characterize which chromosome(s) is (are) present in MNs. There are human probes against chromosomes most likely to be associated with an abnormal chromosome karyotype or aneuploidy such as chromosomes 13, 15, 16, 18, 21, 22, X and Y (Zhang et al., 2010). In the rat, there are only two available fluorescent in situ hybridisation probes, for chromosomes 4 and Y, which limits our accessibility to this technique. The impact of an abnormal chromosome karyotype on the general health of the embryo depends on the kind of aneuploidy and which chromosome is duplicated or absent from the main genome.

There are several limitations to working with fluorescent in situ hybridisation probes in rat embryos. Work previously published in the lab using probes against chromosomes 4 and Y in spermatozoa exposed to 9 weeks of CPA treatment reported an increase in the incidence of chromosome 4 disomy and nullisomy compared to control spermatozoa (Barton et al., 2003). Thousands of spermatozoa had to be analyzed to find a significant induction of chromosomal abnormalities following CPA treatment. Knowing this, it makes this experiment very labor intensive to do with embryos, considering that the average number of embryos per female is between 12 and 15. The second limitation with these probes is that they target a specific region of the chromosome increasing the chance of obtaining false negative data. The third limitation with these probes is that they do not give any information about the clastogenic, pieces of chromosomes, or aneugenic, whole chromosome, effects of CPA exposure if they do not target the centromere region of the chromosome. The difficulty with the detection of centromeres is their omnipresence during mitosis as reviewed in Craig and Choo, 2005. Centromeres are only detectable during metaphase and anaphase making their detection extremely difficult in a limited quantity of embryos. Furthermore, MN have to be actively dividing to be able to detect centromeres; this is not a problem in two-cell embryos but is a problem in eight-cell embryos since they progressively lose their capacity to divide (Grenier et al.,

2011). The availability of additional rat fluorescent in situ hybridisation probes and the detection of centromeres would provide more information on the MN chromatin content and allow us to differentiate between a clastogenic or aneugenic effect of CPA respectively.

The chromatin composition of MN can also be differentiated from the main nucleus based on their epigenetic signature: DNA methylation and post-translational histone modifications. There is a well documented epigenetic asymmetry between the maternal and paternal chromatin in pronuclear zygotes and early two-cell embryos; DNA and histones are hypermethylated in the maternal chromatin while DNA is hypomethylated and histones are acetylated in the paternal chromatin. Taking advantage of this parental epigenetic signature, our data demonstrating the absence of maternal specific epigenetic histone H3K9me3 suggested that MNs originated from the damaged paternal genome (Grenier et al., 2011).

Lastly, MNs can be characterized by their chromatin content; structural components and DNA binding proteins involved in DDR may reveal important information on their possible functions. The presence of nucleoli in MNs suggests the possibility to synthesize rRNA due to the presence of a specific chromosome region. The capacity of MNs to efficiently synthesize rRNA also depends on the presence of rRNA synthesizing machinery; this remains to be tested in our model. The capacity of MNs to synthesize DNA depends on the presence of DNA synthesizing machinery and specific DNA sequences. CPA induced MNs have the capacity to synthesize DNA in two-cell embryos but this ability is gradually lost as they progress to the eight-cell stage (Grenier et al., 2011). The formation of the micronucleolar membrane and pores provides proper protein exchange between the MN, cytoplasm and nucleus by cytoplasmic microtubules. CPA induced MNs have incomplete membrane formation, as indicated with lamin B1 staining, implying improper communication of the MN within the blastomere (Grenier et al., 2011). Moreover CPA induced MNs are enriched with all DDR proteins used in the study: γH2AX foci, 53BP1 protein and PAR products, compared to the

main nucleus. The purpose of this specific micronuclear localization of DDR proteins remains inconclusive since they may either target MNs for repair or cell death. Similar to the characterization of DDR in embryos sired by CPA treated males, additional markers of DNA repair mediators and, more specifically, cell death markers must be used to differentiate the fate of CPA induced MNs during preimplantation development.

Still very controversial is the fate of the MN and the embryos bearing them. Our data suggest an eventual degradation of CPA induced MNs due to their loss of function and enrichment with DDR proteins (Grenier et al., 2011; 2012). As for the fate of embryos bearing MNs, the incidence of MNs seems to be linked to the embryonic developmental delay (Grenier et al., 2011) and the high incidence of early post-implantation loss (Trasler et al., 1987). Nevertheless, are MNs a trigger for death of its original blastomere or of the whole embryo? If MNs induce cell death of the blastomere associated with them, can the rest of the embryo survive such an insult? Can MNs be repaired, expulsed or degraded without affecting the survival of the whole embryo? The incidence and number of MNs did not increase as the embryo divided, implying that MNs are not being degraded or the mechanisms of degradation are not yet active in the developmental stages studied (Grenier et al., 2011). The chromosomal signature of MNs greatly impact the fate of embryos bearing them (Biancotti and Benvenisty, 2011). These questions are crucial in the field of reproductive toxicology and assisted reproduction clinics since the fate of embryos bearing MNs is associated with a decreased chance of survival (Farfalli et al., 2007; Rubio et al., 2007; Ambroggio et al., 2011). What if early embryos were able to repair the damage or expulse MNs and continue to divide, implant and give rise to viable offspring? We need to determine the capacity of the embryo to target cells with MNs for repair or death and determine the fate of the embryos with MNs in later stages of development (Figure 5.1). These are some of the problems related to the incidence and impact of MNs during preimplantation development.

In our male-mediated developmental toxicity model, our questions related to the fate of MNs and embryos bearing them remain unanswered. We were not able to differentiate embryos with MNs from embryos free of MNs nor were we able to distinguish blastomeres with MNs from blastomeres free of MNs with markers used in these studies. As future directions, we would like to select embryos with the highest chances of successful implantation with specific DDR markers able to identify embryos with the least amount of DNA damage, highest DNA repair capacity and lowest incidence of MNs. We expect DNA damaged spermatozoa to have a higher incidence of MNs in early embryos with limited DDR capacity. We also expect embryos bearing MNs to be more damage and susceptible to peri-implantation loss. To test our hypotheses, we could determine the immunoreactivity of these biomarkers, γH2AX, 53BP1 and PAR, in later cleavage stage embryos in addition to the proposed mediators of DNA repair and cell death markers.

5.4 Assisted Reproduction Techniques, ARTs

5.4.1 Increased Use of ARTs and their Safety

As a result of chemotherapeutic treatment, male cancer survivors often face subfertility issues and have to depend on the use of assisted reproduction techniques (ARTs) in order to conceive. In vitro fertilization (IVF) and intra-cytoplasmic sperm injection (ICSI) are two routinely performed ARTs in fertility clinics (Figure 5.1). Common to both techniques is the hormonal stimulation of ovulation followed by ultrasound guided egg retrieval and fertilization outside the body by mature spermatozoa in culture media. During the ICSI procedures, a single mature spermatozoon is injected inside the oocyte, bypassing the oocyte's natural barrier against "unqualified" spermatozoa as opposed to the unselected spermatozoon fertilizing the oocyte during IVF techniques. ICSI procedures are usually performed in cases of proven female subfertility factors such as maternal age, genetic predisposition or ovulation problems or in cases of proven male subfertility factors such as sperm motility issues or low sperm counts. Successful fertilizations are noted a few hours after the ART procedure by the appearance of

two PN corresponding to the early zygotic stage. Embryos mature and divide *in vitro* until the developmental stage required for a regulated single embryo replacement in the patient's uterus.

Increased incidence of chromosomal abnormality and aneuploidy in embryos conceived by ARTs raise concerns about the safety of these procedures (Hansen et al., 2002). Moreover, there is an increase in epigenetic disorders in children born following ART procedures (Lucifero et al., 2004; Kobayashi et al., 2009; Manipalviratn et al., 2009). Epigenetic disorders may be due to superovulation as well as the composition of culture media deregulating DNA methylation at imprinted loci in blastocysts grown *in vitro* compared to blastocysts grown *in vivo* (Market-Velker et al., 2010a; 2010b). They might also be due to the altered DNA methylation programming of imprinted genes reported in men with abnormal semen parameters (Marques et al., 2004) and in oligospermic men (Filipponi and Feil, 2009). Reports on the epigenetic effects and their relationship to ICSI in humans are very limited compared to what has been reported for animal studies in which altered DNA methylation patterns in the male germ line were subsequently transmitted to the next four generations (Anway et al., 2005). The increased incidence of peri-implantation loss and abnormal pregnancy outcome associated with the increased uses of ARTs reinforces the importance of improving sperm selection methods for male germ cell quality (Figure 5.1) (Sakkas et al., 2007; Wright et al., 2008; Said and Land, 2011).

5.4.2 Sperm Selection Methods

The current sperm selection methods performed in infertility clinics are the swim up and density gradient centrifugation assays. The swim up assay select spermatozoa with greatest motility while the density gradient centrifugation technique separates the poorly condensed chromomycin A3 positive and nicked DNA spermatozoa from healthy ones (Le Lannou and Blanchard, 1988; Larson et al., 2000; Virro et al., 2004). The more advanced sperm selection methods are developed to improve the selection of mature, structurally intact and non-

apoptotic spermatozoa with high DNA integrity based on apoptosis, DNA integrity, membrane maturation and ultrastructure spermatozoa factors. The characterization of spermatozoa based on these factors is crucial to improve ART outcomes.

The detection of structural chromosomal aberrations in spermatozoa by fluorescent *in situ* hybridization assays is a good predictor of potential genotoxic effects on spermatogenic stem cells (Wyrobek et al., 2007). Fluorescent *in situ* hybridization assays join aneuploidy assays, DNA fragmentation assays, and chromosome breakage assays as good predictors of abnormal pregnancy and progeny outcomes in animal models. The predictive power of sperm selection based on spermatozoa nuclear DNA integrity, sperm chromatin structure assay and terminal deoxynucleotidyl transferase-mediated dUTP nick end labelling tests, on pregnancy outcomes in human is controversial (Spano et al., 2005; Niu et al., 2011). The DNA fragmentation index measured by the sperm chromatin structure assay seems to be a test of choice in human infertility and urology clinics for the assessment of sperm DNA quality and associated risk for infertility, spontaneous miscarriages and abnormal pregnancy outcome (Greco et al., 2005; Evenson and Wixon, 2007:).

In research undertaken for this thesis, we observed in pre-pronuclear zygotes that the genome of decondensing spermatozoa exposed to CPA was heavily damaged compared to that of control spermatozoa, and that the rate of sperm chromatin decondensation was accelerated (Grenier et al., 2010). Our data confirm previously published data by Codrington et al., 2004 stating that mature spermatozoa exposed to CPA are more damaged than control unexposed spermatozoa. Scientists in the field observed severe adverse consequences in offspring conceived by ICSI procedures when DNA damaged spermatozoa are used as a treatment of male infertility in ARTs (Aitken and De Iuliis, 2007; Barroso et al., 2009). Abnormal ART outcomes reinforce the need of more advanced sperm selection methods.

Figure 5.1. Reproductive medicine relevance of the CPA male mediated developmental toxicity model. Time dependent events activated as a consequence of paternal exposure to CPA are timely matched with ARTs screening methods illustrating the importance of detailed DDR to improve diagnosis of early embryos.

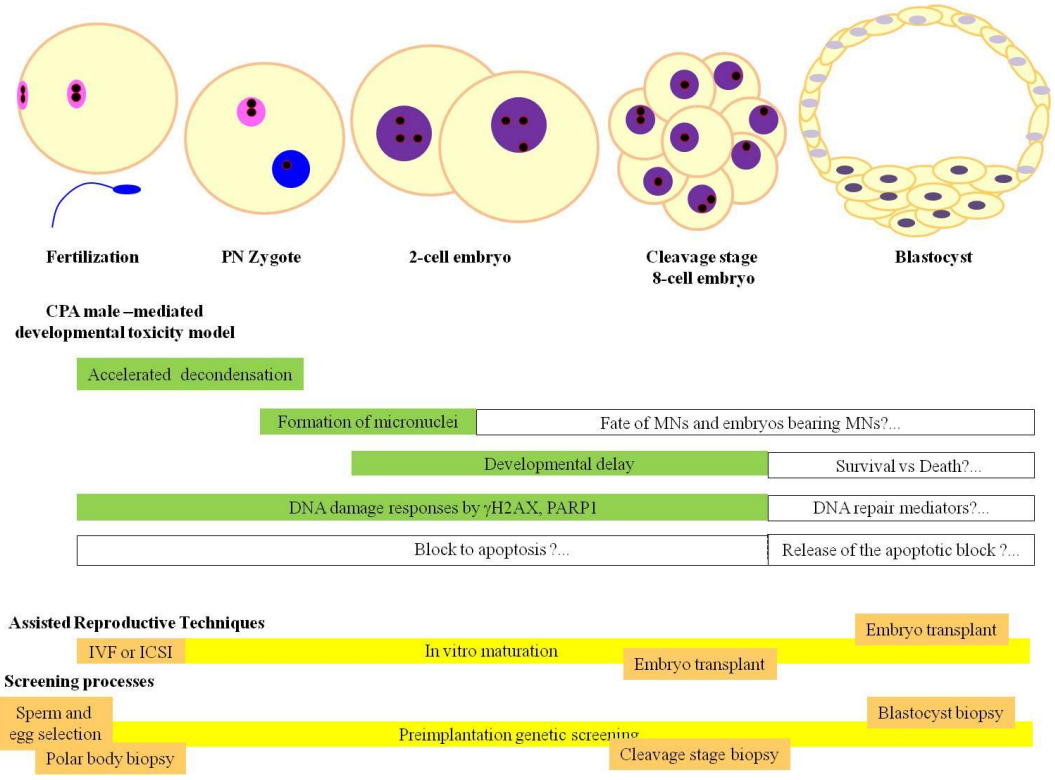
Fertilization
PN Zygote
2-cell embryo
Cleavage stage
8-cell embryo
Blastocyst
CPA male –mediated
developmental toxicity model
Accelerated decondensation
Formation of micronuclei
Fate of MNs and embryos bearing MNs?...
Developmental delay
Survival vs Death?...
DNA damage responses by γH2AX, PARP1
DNA repair mediators?...
Block to apoptosis ?...
Release of the apoptotic block ?...
Assisted Reproductive Techniques
Embryo transplant
IVF or ICSI
In vitro maturation
Embryo transplant
Screening processes
Blastocyst biopsy
Sperm and
egg selection
Preimplantation genetic screening
Polar body biopsy
Cleavage stage biopsy

There are four non routine ART advance sperm selection methods with proven fertilization and pregnancy rate improvements. The first promising sperm selection method to improve ART outcome is based on the detection of apoptosis using a magnetic cell sorting and glass wool apparatus. This test detects phosphatidylserine on the outer surface of the sperm membrane using Annexin-V-conjugated paramagnetic microbeads. Apoptotic sperm in the ejaculate are separated using a magnetic-activated cell sorting system and non-apoptotic sperm are isolated from the sample using density gradient centrifugation assay (Said et al., 2008). This method selects spermatozoa with highest motility and mitochondrial membrane potential (Grunewald et al., 2006; 2008).

The second promising sperm selection method is based on real time motile sperm organelle morphology examination at a magnification of x6300 prior to ICSI procedures (Bartoov et al., 2001; 2002). This method assesses six sperm organelles: acrosome, postacrosomal lamina, neck, tail, mitochondria and nucleus for both its shape and presence of vacuole. The beneficial effects from this method remain to be proven in human using ICSI procedures since detrimental effects of toxicant exposure on spermatozoal morphology are very limited.

The third promising sperm selection method is based on sperm surface charge differences and measured by an electrophoresis isolation technique. It is used to generate a suspension rich in morphologically normal size, viable sperm with low levels of DNA damage, normally differentiated and capacitated CD52 expressing spermatozoa (Giuliani et al., 2004; Ainsworth et al., 2005).

Sperm selection method based on sperm membrane maturity using a hyaluronic acid binding assay represent the fourth sperm selection method. Sperm binding to hyaluronic acid is proposed to reduce the incidence of chromosomal abnormality and trisomy by selecting only mature spermatozoa (Huszar et al., 1997; 2003).

Despite their labor intensity protocols and risk of sperm loss, the safety and efficacy of these new advance sperm selection methods remain to be proven

in clinical settings. Their beneficial effects on ART outcome are encouraging but their recommendation as routine tests in ART is still premature (Said and Land, 2011).

5.4.3 Preimplantation Genetic Diagnosis, PGD

Multiple pregnancy rates from ARTs are associated with numerous medical complications. In order to improve pregnancy outcomes of ARTs, single-embryo transfer is becoming the preferred treatment of infertility. As a result, embryonic screening methods are being developed to select embryos with the greatest expected developmental competence and chances of survival (Figure 5.1). Routine embryonic screening methods in ARTs are based on morphological parameters; embryos are examined every day during cleavage stages and scored on the number, size, cell-shape and fragmentation rate of the embryo blastomeres (Ebner et al, 2003). More advanced embryonic developmental stages are scored on their degree of compaction while blastocysts are evaluated on the quality and degree of expansion of the trophectoderm and inner cell mass.

Preimplantation genetic diagnosis (PGD) is a more invasive procedure performed on blastomeres to screen for specific genetic defects that could lead to pregnancy termination, diseases or cancer predisposition, to match a sibling human leukocyte antigen as a ″savior sibling″ and for sex selection before implantation (Fechner and McGovern, 2011). As opposed to PGD, preimplantation genetic screening (PGS) is most commonly used for patients with unexplained infertility, recurrent pregnancy loss and repetitive IVF failures to increase the chances of successful ART cycle (Fechner and McGovern, 2011).

5.4.3.1 Embryo Biopsy

Experts in the field have developed embryonic biopsy methods to improve the selection of the “best” embryo for transplantation. Embryonic biopsies can be done at three specific developmental stages (Figure 5.1). The first type of embryo biopsy is performed on the polar body of the oocyte following egg retrieval or on the zygote following fertilization (Geraedts et al., 2010). Advantages of this

technique are the absence of chromosomal mosaicism between nucleus and the abstraction from the reduction of the embryo nuclear and cytoplasmic volume during a biopsy. The analysis of polar bodies only gives information on the maternal genotype and is often associated with diagnostic error due to the degradation of the polar body material during meiosis.

The second and most common type of embryo biopsy is performed on cleavage stage embryos at the eight-cell stage by the removal of one blastomere for diagnosis (de Vos et al., 2009). Advantages to this technique are: the possible determination of the maternal and paternal genetic contributions to the embryo, the totipotency of blastomeres at this stage and the fact that you have enough time to perform this technique and obtain the diagnostic results before the transfer day.

The third type of embryo biopsy is performed on blastocysts on the fifth day following fertilization and provides a larger amount of trophectoderm cells for analysis. Major limitations to this technique are: the limited number of embryos that survive to the blastocyst stage and leaving insufficient time to complete the diagnosis before the embryo has to be transferred in the patient's uterus. Vitrification and cryopreservation of the blastocyst improve the survival of these embryos (Zhang et al., 2009).

Major concerns exist about the beneficial effects of single blastomere biopsy which may not represent the whole embryo due to chromosomal mosaicism (Fechner and McGovern, 2011). As a result of chromosomal mosaicism, embryo biopsy often results in false negatives or positive results, leading to the acceptance of an embryo carrying an abnormal karyotype or the destruction of a normal one. Out of the successful pregnancies, leaders in the field have reported no differences in developmental growth and live births in offspring born from biopsied embryos compared to ICSI alone (Ao et al., 2006; Desmyttere et al., 2009; Liebaers et al., 2010). Embryo biopsies are in their infancy; long term health consequences on offspring born from these techniques are unknown. The need of more advance embryonic selection methods with proven safety and

efficacy is crucial before the implementation of these techniques as routine tests in ART clinics.

5.4.3.2 Embryo Selection Methods

More sophisticated techniques to select most competent oocytes and embryos are based on genomics, transcriptomics, metabolomics and proteomics. Genomic tests consist of fluorescent *in situ* hybridization probes against chromosomes to screen for aneuploidy and to determine chromosome makeup while polymerase chain reaction is performed to identify single-gene disorders (Rechitsky et al., 2002; Colls et al., 2009; Yan et al., 2009).

The study of granulosa and cumulus cells transcriptomic profiles is a non invasive method of selection used to predict oocyte quality, embryo competence and pregnancy outcomes (McKenzie et al., 2004; Montfoort et al., 2008; Assou et al., 2008; Hamel et al., 2008; 2010). Granulosa and cumulus cells are the "nursing cells" of oocytes and early embryos (Anderson et al., 2009). The selection method is based on reverse transcription polymerase chain reaction and DNA microarrays expression levels of candidate genes predicting embryonic quality and developmental competence (Assou et al., 2010).

Secretory profiles of embryos measured in culture medium can be correlated to their cellular function and reproductive outcome (Katz-Jaffe and Gardner, 2008). Protein secretory profiles of embryos vary in response to *in vitro* fertilization, culture conditions and cryopreservation techniques. The identification of biomarkers associated with successful implantation by mass spectrometry and protein microarrays can be used to select embryos with highest development competence (Katz-Jaffe et al., 2006; Domínguez et al., 2008).

Metabolomic profiles of the follicular fluid and embryonic culture medium are used to select embryos with highest developmental competence based on the presence of specific amino acids. This method is based on the detection of candidate markers by high-resolution vibrational and nuclear magnetic resonance

spectroscopic techniques which reflect the global physiologic and metabolic health of an oocyte and embryo (Seli et al., 2007; 2008).

These newly developed embryo selection methods have great potential in ARTs promoting single-embryo over multiple embryo transfer as reviewed in Fechner and McGovern, 2011.

5.5 Significance, Implication and Relevance of the Project to ARTs Outcomes

Additional studies are required to understand how embryos are able to respond to DNA damage as a result of genotoxic or epigenetic toxicant exposure. There are two goals to improve embryonic selection methods. The first obvious one is to improve the selection of embryos associated with increased developmental competence and survival following ARTs. The second goal is to minimize the false positive and negative results from preimplantation genetic screening in order to prevent the transfer of abnormal embryos and to prevent the wastage of healthy ones. Therefore all efforts in the field of PGS are directed towards these three questions: 1- how can we select the best quality embryo? 2- how early during development can we make this selection? 3- how can we minimize chromosomal mosaicism?

Based on the results obtained in this research project, we suggest that the most appropriate time during preimplantation development to assess embryonic competence is at the eight-cell stage (Figure 5.1). According to our results, the first visible DNA damage mark in early embryos is the formation of MN in two-cell embryos; MN can be observed using a high definition light microscope. The second visible impact of paternal exposure to CPA is the delayed embryonic developmental progression in four- and eight-cell embryos.

The remaining embryonic developmental effects of paternal exposure to CPA require more invasive embryonic selection methods. The first effect of paternal exposure to CPA is the acceleration of decondensation of the spermatozoa and the detection of increased DNA damage in pre-PN zygotes

(Figure 5.1). We expect that these effects can be attenuated with the previous uses of sperm selection methods using DNA fragmentation tests and sperm chromatin compaction assays promoting the selection of best suited spermatozoa population for fertilization.

The second impact of paternal exposure to CPA is the activation of DNA damage responses by the recognition of DNA damage with γH2AX and DNA repair responses by PAR in eight-cell embryos (Figure 5.1). During preimplantation development, the embryo gradually acquires DDR proteins, demonstrating its capacity to respond to an insult. At the cleavage stage, it is possible to perform a single blastomere biopsy without affecting the survival of the remaining blastomeres. Therefore, a proteomic analysis of DNA damage response proteins, such as γH2AX and PAR polymers, in addition to an evaluation of the genomic integrity at the chromosome level may enhance the selection of eight-cell embryos associated with the greatest chance of survival.

These results have important clinical relevance since embryonic selection is commonly made in cleavage stage embryos at the eight-cell stage as reviewed in Fechner and McGovern, 2011. Additional reasons supporting the diagnosis of cleavage stage embryos, as opposed to later stages of development, is the effect of *in vitro* environment and culture medium on the quality of embryonic development (Rienzi et al., 2011). It has been shown that the duration of *in vitro* maturation and the composition of culture medium are contributing factors to embryonic loss and increased incidence of adult onset diseases as reviewed in Fechner and McGovern, 2011. Concerns with preimplantation genetic screening techniques in the field of human reproductive medicine reinforce the importance and relevance of performing these experiments in animals to improve the efficacy of selection methods and embryonic developmental outcomes.

5.6 The Possible Existence of a Block to Apoptosis in Cleavage Stage Embryos

Cell fate depends on the balance between pro-apoptotic and survival signals. As opposed to the activation of cell death in response to DNA damage in somatic cells, the blastomeres of the early preimplantation embryo have developed mechanisms by which they are able to resist pro-apoptotic signals as shown in bovine embryos (Hardy, 1999; Brison, 2000; Paula-Lopes and Hansen, 2002a; Krininger III et al., 2003; Soto et al., 2003; de Castro e Paula and Hansen, 2008). This evolutionary resistance to apoptosis comes from pro-apoptotic cues generated as part of the developmental process (Hansen and Fear, 2011). Fertilization induces oscillations in Ca^{2+} in the fertilized oocyte; this Ca^{2+} comes from the endoplasmic reticulum (Ajduk et al., 2008) and promotes mitochondrial permeabilization and induction of apoptosis (Lemasters et al., 2009; Rizzuto et al., 2009). Apoptosis is mediated by the selective activation of caspase 3 in damaged blastomeres, allowing the survival of the remaining healthy blastomeres (Paula-Lopes and Hansen, 2002b; Jousan and Hansen, 2007). Signs of apoptosis, such as the presence of DNA stand breaks between nucleosomes, only become visible following genome activation through transcriptionally-dependent processes in the cleavage stage embryo (Men et al., 2003; Roth and Hansen, 2004; Soto and Smith, 2009). The establishment of an apoptosis-resistance state in the early two-cell embryo is due to a combination of mitochondrial and nuclear epigenetic modifications as reviewed in Hansen and Fear, 2011.

5.6.1 Apoptotic Block at the level of Mitochondria

The failure of pro-apoptotic signals comes partially from the resistance of mitochondria to depolarization rather than from the absence of caspase-9 and caspase-3 activation. Both caspases can be activated by chemical depolarization of mitochondria with carbonyl cyanide 3-chlorophenylhydrazone in two-cell embryos (Brad et al., 2007). Before visible signs of cell death are observed, such as DNA fragmentation and chromatin condensation, the expression of genes involved in cell death is upregulated while the expression of cell survival genes is downregulated (Jurisicova et al., 1998). The developmental acquisition of mitochondrial responsiveness to pro-apoptotic signals coincides with changes in

BCL2 and BAX protein concentrations. The inhibition of mitochondrial depolarization in two-cell embryos is due to the high concentration of survival protein BCL2 compared to the low concentration of pro-apoptotic BAX. Cleavage stage embryos accumulate BAX proteins and reduce BCL2 proteins enabling mitochondrial pore formation in response to pro-apoptotic signals (Fear and Hansen, 2011).

5.6.2 Apoptotic Block at the Epigenetic Level

The condensed chromatin structure of two-cell embryos is enriched with DNA methylation as opposed to the chromatin of eight-cell embryos which becomes progressively less methylated (Dean et al., 2001; Hou et al., 2007; Maalouf et al., 2008). The condensed chromatin structure of two-cell embryos prevents the degradation of the linker DNA between nucleosomes by caspase activated DNAses while the decondensed chromatin structure of eight-cell embryos is more accessible to activated DNAses. The role of histone acetylation in the regulation of the apoptotic block is specific to histone and acetylated lysine residues (Wu et al., 2011). Evidence for the involvement of epigenetic modifications in repressing apoptosis comes from experiments using an inhibitor of DNA methylation (5-aza-2'-deoxycytidine) or an inhibitor of histone deacetylation (trichostatin-A). These inhibitors open up the chromatin, allowing DNAse accessibility to internucleosomal linker DNA only in two-cell embryos that are simultaneously treated with a mitochondrial depolarization chemical (carbonyl cyanide 3-chlorophenylhydrazone) (Carambula et al., 2009).

According to these findings, the two-cell block to apoptosis is the result of mitochondrial impermeable membrane and condensed epigenetic regulation. In response to toxicant exposure, both levels of apoptotic repression have to be relieved for apoptosis to occur in two-cell embryos. Paternal exposure to CPA disrupts the epigenetic regulation of early embryonic developmental events, promoting an open chromatin structure (Barton et al., 2005; 2007; Grenier et al., 2010; 2012). The existence of an apoptotic block at the level of mitochondria could explain the lack of responsiveness to DNA damage introduced at

fertilization by spermatozoa in early two-cell embryos. The epigenetic disruption in early embryo sired by CPA treated males could alter the expression of BCL2 and BAX proteins, relieving the mitochondrial block in cleavage stage embryos compared to control embryos. To test this hypothesis, we could determine the concentrations of BCL2 and BAX proteins, the activation of caspases 3 and 9 and the apoptosis inducible effect of treatment with a mitochondrial depolarization chemical in our CPA male-mediated developmental toxicity model. The permeabilization of mitochondrial membrane and decondensation of chromatin structure would relieve apoptotic block and allow early DNA damaged cleavage stage embryos to undergo cell death. These experiments would provide a possible mechanism by which DNA damaged embryos survive preimplantation development.

5.7 Future Directions

Mitochondria are the energy source for the development of embryos, for the activation of DDR mechanisms, and are partially responsible for the apoptotic block. Determination of the mitochondrial energy balance between energy production and energy consumption would be valuable as a general assessment of embryonic health, DDR capacity and the competence of embryos sired by CPA exposed males to survive. Mito Tracker Green and MitoSox Red probes are used to detect functional mitochondria. These probes do not measure the level of energy production or consumption during the development of cleavage stage embryos. We should like to pursue our evaluation of the early embryo energy store to determine if there could be a link between early cleavage stage delay and energy depletion due to the activation of DNA damage responses as a consequence of paternal exposure to cyclophosphamide.

We propose the use of a sensor of mitochondrial potential, 5,5’,6,6’-tetrachloro-1,1’,3,3’ tetraethylbenzimidazolylcarbocyanine iodide (JC-1), to measure the mitochondrial membrane potentials and differentiate between hyperpolarized energy rich and hypopolarized energy depleted mitochondria. The dynamic distribution of energy rich and poor mitochondria is crucial for the

proper progression of embryos during preimplantation development as reviewed in van Blerkom, 2011.

In response to any type of insult, a shift towards mitochondrial depolarization is considered as an early sign of apoptosis. In our model, mitochondria depolarization in embryos sired by CPA treated males may explain the developmental delay, dampened DDR observed with PARP1 and could be linked to the repression of apoptotic block during cleavage stage development. As a consequence of the mitochondrial depolarization and relieve of the apoptotic block, the assessment of mitochondrial pore formation by the release of Ca2+ ions and the activation of caspases are interesting leads to pursue. These future leads would provide valuable insight into the effects of paternal exposure to CPA on the acquisition and activation of diverse DDR mechanisms affecting the progression and regulation of developmental events in cleavage stage embryos.

Together, these studies in this thesis provide mechanisms by which a DNA damaged spermatozoon can alter embryonic outcome and may serve as a starting point for the development of molecular markers to improve the selection of embryos with higher developmental competence for use in reproductive medicine and infertility clinics.

ORIGINAL CONTRIBUTIONS

1. A subclassification of type *a* partially decondensed spermatozoa chromatin structure was characterized in pre-pronuclear zygotes according to the specific order of chromatin decondensation. The chromatin of spermatozoa decondensed first at the posterior end (type *a*1-2), then at the tip (type *a*3) and finally on ventral sides (type *a*4). The chromocenter was the last chromatin region to decondense, indicating that specific chromatin binding proteins and/or a paternal epigenetic signature play a role in the orderly regulation of early zygotic post-fertilization events.

2. Chronic paternal exposure to cyclophosphamide altered the progression of pre-pronuclear zygotes, accelerating the progression of sperm decondensation stages to type *c* sperm nuclei without having any impact on the pattern of sperm chromatin remodelling, assessed with histones H4K12ac and H3S10ph. These studies provide evidence that in pre-pronuclear zygotes sired by cyclophosphamide exposed males, the maternal stored proteins are prepared to react to the altered rate of spermatozoon decondensation.

3. Independent of drug treatment, spermatozoon chromatin remodelling, assessed with histones H4K12ac and H3S10ph, followed the same order of sperm decondensation within type *a* sperm nuclei and displayed distinct patterns of chromatin remodelling in type *b* and *c* sperm nuclei.

4. Chronic paternal exposure to cyclophosphamide led to an earlier and enhanced detection of DNA double strand breaks in the decondensing male genome in pre-pronuclear zygotes. An even distribution of small γH2AX foci was detected in type *a*2 and *a*3 sperm nuclei while larger γH2AX foci were observed in type *b* and *c* sperm nuclei. Within the sub classification of type *a* sperm nuclei, the detection of small γH2AX foci

suggests the extent of DNA damage induced by paternal exposure to cyclophosphamide. The recruitment of γH2AX as larger foci in decondensed sperm chromatin is indicative of DNA damage recognition and DNA repair protein recruitment.

5. Chronic paternal exposure to cyclophosphamide delayed the timing of the first zygotic division in embryos matured *in vitro* without affecting their capacity to divide. Simultaneously, we observed the formation of micronuclei initially visible as lagging pieces of chromosomes at metaphase during the first zygotic division. Micronuclear formation did not prevent the progression of embryos during preimplantation development but slowed down the rate of embryonic development.

6. Micronuclei induced by chronic paternal exposure to cyclophosphamide were of paternal chromatin origin as suggested by the absence of maternal specific H3K9me3 epigenetic marks. The zygote expels part of the damaged paternal genome in the form of micronuclei during the first zygotic division as a response to DNA damage.

7. Chronic paternal exposure to cyclophosphamide induced the formation of functional micronuclei capable of synthesizing newly replicated DNA. Micronuclei in two-cell embryos incorporated EdU Click-iT molecular probe; their capacity to replicate DNA was decreased by the eight-cell stage. Furthermore, studies with lamin B1 revealed the incomplete formation of micronuclear membranes, suggesting a disrupted nuclear and micronuclear communication during development.

8. Chronic paternal exposure to cyclophosphamide selectively activated DNA damage responses in eight-cell embryos as indicated by the induction of large γH2AX foci and decreased nuclear PARylation.

Paternal exposure to cyclophosphamide had no effect on 53BP1 repair protein intensity or localization or on selective mitochondrial MitoTracker Green and MitoTracker Red Sox probes. We are suggesting γH2AX and PAR products as potential biomarkers of embryonic developmental competence after exposure to genotoxic or epigenetic toxicants.

9. Micronuclei induced by chronic paternal exposure to cyclophosphamide were enriched with DNA damage response markers, with large γH2AX foci, 53BP1 and PAR products, compared to the main nucleus. These data support the paternal origin of micronuclei as the most DNA damaged chromatin, recognized and expulsed during the first zygotic division. The role of the enrichment of DNA damage response markers in micronuclei remains elusive; one possibility is that they target the blastomere or whole embryo for DNA repair and or cell death.

10. The presence of micronuclei and a delay in developmental progression had no impact on the activation of DNA damage responses at any of the cleavage stages in embryos sired by cyclophosphamide exposed males. The biomarkers used in these studies: γH2AX, 53BP1, PAR products and MitoTrackers, are not good indicators of embryos with micronuclei.

REFERENCES

Ajduk A, Malagocki A, Maleszewski M. (2008). Cytoplasmic maturation of mammalian oocytes: development of a mechanism responsible for sperm-induced Ca2+ oscillations. Reprod Biology 8, 3-22.

Ainsworth C, Nixon B, Aitken RJ. (2005). Development of a novel electrophoretic system for the isolation of human spermatozoa. Human Reproduction 20, 2261-2270.

Aitken RJ, De Iuliis GN. (2007). Origins and consequences of DNA damage in male germ cells. Reprod Biomed Online 16, 727-733.

Ambroggio J, Gindoff PR, Dayal MB, Khaldi R, Peak D, Frankfurter D, Dubey AK. (2011). Multinucleation of a sibling blastomere on day 2 suggests unsuitability for embryo transfer in IVF-preimplantation genetic screening cycles. Fertil Steril. 96, 856-859.

Anderson RA, Sciorio R, Kinnell H, Bayne RA, Thong KJ, de Sousa PA, Pickering S. (2009). Cumulus gene expression as a predictor of human oocyte fertilisation, embryo development and competence to establish a pregnancy. Reproduction 138, 629-637.

Ao A, Jin S, Rao D, Son WY, Chian RC, Tan SL. (2006). First successful pregnancy outcome after preimplantation genetic diagnosis for aneuploidy screening in embryos generated from natural-cycle in vitro fertilization combined with an in vitro maturation procedure. Fertil Steril. 85, 1510.e9-11.

Assou S, Haouzi D, De Vos J, Hamamah S. (2010). Human cumulus cells as biomarkers for embryo and pregnancy outcomes. Mol Hum Reprod. 16, 531-538.

Assou S, Haouzi D, Mahmoud K, Aouacheria A, Guillemin Y, Pantesco V, Rème T, Dechaud H, De Vos J, Hamamah S. (2008). A non-invasive test for assessing embryo potential by gene expression profiles of human cumulus cells: a proof of concept study. Mol Hum Reprod. 14, 711-719.

Barroso G, Valdespin C, Vega E, Kershenovich R, Avila R, Avendano C, Oehninger S. (2009). Developmental sperm contributions: fertilization and beyond. Fertil Steril. 92, 835-848.

Barton TS, Wyrobek AJ, Hill FS, Robaire B, Hales BF. (2003). Numerical chromosomal abnormalities in rat epididymal spermatozoa following chronic cyclophosphamide exposure. Biol Reprod. 69, 1150-1157.

Bartoov B, Berkovitz A, Eltes F. (2001). Selection of spermatozoa with normal nuclei to improve the pregnancy rate with intracytoplasmic sperm injection. National England Journal of Medicine 345, 1067-1068.

Bartoov B, Berkovitz A, Eltes F, Kogosowski A, Menezo Y, Barak Y. (2002). Real-time fine morphology of motile human sperm cells is associated with IVF-ICSI outcome. J Androl. 23, 1-8.

Biancotti JC, Benvenisty N. (2011). Aneuploid human embryonic stem cells: origins and potential for modeling chromosomal disorders. Regen Med. 6, 493-503.

Brad AM, Hendricks KEM, Hansen PJ. (2007). The block to apoptosis in bovine two-cell embryos involves inhibition of caspase-9 activation and caspase-mediated DNA damage. Reproduction 134, 789-797.

Brison DR. (2000). Apoptosis in mammalian preimplantation embryos: regulation by survival factors. Human Fertility (Cambridge) 3, 36-47.

Carambula SF, Oliveira LJ, Hansen PJ. (2009). Repression of induced apoptosis in the 2-cell bovine embryo involves DNA methylation and histone deacetylation. Biochem. Biophys Res Commun. 388, 418-421.

Chi HJ, Koo JJ, Choi SY, Jeong HJ, Roh SI. (2011). Fragmentation of embryos is associated with both necrosis and apoptosis. Fertil Steril. 96, 187-192.

Colls P, Goodall N, Zheng X, Munné S. (2009). Increased efficiency of preimplantation genetic diagnosis for aneuploidy by testing 12 chromosomes. Reprod Biomed Online 19, 532-538.

Craig JM, Choo KH. (2005). Kiss and break up- -a safe passage to anaphase in mitosis and meiosis. Chromosoma 114, 252-262.

Domínguez F, Gadea B, Esteban FJ, Horcajadas JA, Pellicer A, Simón C. (2008). Comparative protein-profile analysis of implanted versus non-implanted human blastocysts. Hum Reprod. 23, 1993-2000.

de Castro e Paula LA, Hansen PJ. (2008). Ceramide inhibits development, cytokinesis, induces apoptosis in preimplantation bovine embryos. Molecular Reproductive Development 75, 1063-1070.

de Vos A, Staessen C, De Rycke M, Verpoest W, Haentjens P, Devroey P, Liebaers I, Van de Velde H. (2009). Impact of cleavage-stage embryo biopsy in view of PGD on human blastocyst implantation: a prospective cohort of single embryo transfer. Hum Reprod. 24, 2988-2996.

Dean W, Santos F, Stojkovic M, Zakhartchenki V, Walter J, Wolf E, Reik W. (2001). Conservation of methylation reprogramming in mammalian development: aberrant reprogramming in cloned embryos. Proc Natl Acad Sci USA 98, 13734-13738.

Delbès G, Hales BF, Robaire B. (2010). Toxicants and human sperm chromatin integrity. Mol Hum Reprod. 16, 14-22.

Desmyttere S, Bonduelle M, Nekkebroeck J, Roelants M, Liebaers I, De Schepper J. (2009). Growth and health outcome of 102 2-year-old children conceived after preimplantation genetic diagnosis of screening. Early Hum Dev. 85, 755-759.

Ebner T, Moser M, Sommergruber M, Tews G. (2003). Selection based on morphological assessment of oocytes and embryos at different stages of preimplantation development: a review. Hum Reprod Update 9, 251-262.

Evenson DP, Wixon RL. Use of the sperm chromatin structure assay (SCSA®) as a diagnostic tool in the human infertility clinic. In: Anderson D, Brinkworth MH (eds), Male-Mediated Developmental Toxicity, vol 1, 1st ed. Cambridge: RSC Publishing; 2007: 77-84.

Fabian D, Bukovská A, Juhás, Koppel J. (2009). Apoptotic processes and DNA cytosine methylation in mouse embryos arrested at the 2-cell stage. Zygote 17, 269-279.

Farfalli VI, Magli MC, Ferraretti AP, Gianaroli L. (2007). Role of aneuploidy on embryo implantation. Gynecol Obstet Invest. 64, 161-165.

Fear JM, Hansen PJ. (2011). Developmental changes in expression of genes involved in regulation of apoptosis in the bovine preimplantation embryo. Biology of Reproduction 84, 43-51.

Fechner AJ, McGovern PG. (2011). The state of the art of in vitro fertilization. Front Biosci (Elite Ed). 3, 264-278.

Filipponi D, Feil R. (2009). Perturbation of genomic imprinting in oligozoospermia. Epigenetics 4, 27-30.

Geraedts J, Collins J, Gianaroli L, Goossens V, Handyside A, Harper J, Montag M, Repping S, Schmutzler A. (201). What next for preimplantation genetic screening? A polar body approach! Hum Reprod. 25, 575-577.

Giuliani V, Pandolfi C, Santucci R, Pelliccione F, Marcerola B, Focarelli R, Rosati F, Della Giovampaola C, Francavilla F, Francavilla S. (2004). Expression of gp20, a human sperm antigen of epididymal origin, is reduced in spermatozoa from subfertile men. Mol Reprod Dev. 69, 235-240.

Greco E, Scarselli F, Iacobelli M, Rienzi L, Ubaldi F, Ferrero S, Franco G, Anniballo N, Mendoza C, Tesarik J. (2005). Efficient treatment of infertility due to sperm DNA damage by ICSI with testicular spermatozoa. Hum Reprod. 20, 226-230.

Grunewald S, Paasch U, Said TM, Rasch M, Agarwal A, Glander HJ. (2006). Magnetic-activated cell sorting before cryopreservation preserves mitochondrial integrity in human spermatozoa. Cell Tissue Bank 6, 99-104.

Grunewald S, Said TM, Paasch U, Glander HJ, Agarwal A. (2008). Relationship between sperm apoptosis signalling and oocyte penetration capacity. Int J Androl. 31, 325-330.

Hamel M, Dufort I, Robert C, Gravel C, Leveille MC, Leader A, Sirard MA. (2008). Identification of differentially expressed markers in human follicular cells associated with competent oocytes. Hum Reprod. 23, 1118-1127.

Hamel M, Dufort I, Robert C, Léveillé MC, Leader A, Sirard MA. (2010). Genomic assessment of follicular marker genes as pregnancy predictors for human IVF. Mol Hum Reprod. 16, 87-96.

Hansen M, Kurinczuk JJ, Bower C, Webb S. (2002). The risk of major birth defects after intracytoplasmic sperm injection and in vitro fertilization. National England Journal of Medicine 346, 725-730.

Hansen PJ, Fear JM. (2011). Cheating death at the dawn of life: Developmental control of apoptotic repression in the preimplantation embryo. Biochemical and Biophysical Research Communications 413, 155-158.

Hardy K. (1999). Apoptosis in the human embryo. Rev Reprod. 4, 125-134.

Hou J, Liu L, Lei T, cui X, An X, Chen Y. (2007). Genomic DNA methylation patterns in bovine preimplantation embryos derived from in vitro fertilization. Sci China C Life Sci. 50, 56-61.

Huang L, Yan Z, Liao X, Li Y, Yang J, Wang ZG, Zuo Y, Kawai H, Shadfan M, Ganapathy S, Yuan ZM. (2011). The p53 inhibitors MDM2/MDMX complex is required for control of p53 activity in vivo. Proc Natl Acad Sci U S A 108, 12001-12006.

Huszar G, Ozenci CC, Cayli S, Zavaczki Z, Hansch E, Vigue L. (2003). Hyaluronic acid binding by human sperm indicates cellular maturity, viability, and unreacted acrosomal status. Fertil Steril. 79, 1616-1624.

Huszar G, Sbracia M, Vigue L, Miller DJ, Shur BD. (1997). Sperm plasma membrane remodelling during spermiogenesis maturation in men: relationship among plasma membrane beta 1,4-galactosyltransferase, cytoplasmic creatine phosphokinase, and phosphokinase isoform ratios. Biol Reprod. 56, 1020-1024.

Jousan FD, Hansen PJ. (2007). Insulin-like growth factor-1 promotes resistance of bovine preimplantation embryos to heat shock through actions independent of its anti-apoptotic actions requiring PI3K signalling. Mol Reprod Dev. 74, 189-196.

Jurewicz J, Hanke W, Radwan M, Bonde JP. (2009). Environmental factors and semen quality. Int J Occup Med Environ Health 22, 305-329.

Jurisicova A, Latham KE, Casper RF, Varmuza SL. (1998). Expression and regulation of genes associated with cell death during murine preimplantation embryo development. Mol Reprod Dev. 51, 243-253.

Katz-Jaffe MG, Gardner DK. (2008). Symposium: innovative techniques in human embryo viability assessment. Can proteomics help to shape the future of human assisted conception? Reprod Biomed Online 17, 497-501.

Katz-Jaffe MG, Gardner DK, Schoolcraft WB. (2006). Proteomic analysis of individual human embryos to identify novel biomarkers of development and viability. Fertil Steril. 85, 101-107.

Kobayashi H, Hiura H, John RM, Sato A, Otsu E, Kobayashi N, Suzuki R, Suzuki F, Hayashi C, Utsunomiya T, Yaegashi N, Arima T. (2009). DNA methylation errors at imprinted loci after assisted conception originate in the parental sperm. Eur J Hum Genet. 17, 1582-1591.

Krininger III CE, Stephens SH, Hansen PJ. (2003). Developmental changes in inhibitory effects of arsenic and heat shock on growth of preimplantation bovine embryos. Mol Reprod Dev. 63, 335-340.

Larson KL, DeJonge CJ, Barnes AM, Jost LK, Evenson DP. (2000). Sperm chromatin structure assay parameters as predictors of failed pregnancy following assisted reproductive techniques. Hum Reprod. 15, 1717-1722.

Le Lannou D, Blanchard Y. (1988). Nuclear maturity and morphology of human spermatozoa selected by Percoll density gradient centrifugation of swim-up procedure. J Reprod Fertil. 84, 551-556.

Lemasters JJ, Theruvath TP, Zhong Z, Nieminen AL. (2009). Mitochondrial calcium, the permeability transition in cell death. Biochim Biophys Acta 1787, 1395-1401.

Liebaers I, Desmyttere S, Verpoest W, De Rycke M, Staessen C, Sermon K, Devroey P, Haentjens P, Bonduelle M. (2010). Report on a consecutive series of 581 children born after blastomere biopsy for preimplantation genetic diagnosis. Hum Reprod. 25, 275-282.

Lucifero D, Chaillet JR, Trasler JM. (2004). Potential significance of genomic imprinting defects for reproduction and assisted reproductive technology. Hum Reprod Update. 10, 3-18.

Maalouf WE, Alberio R, Campbell KH. (2008). Differential acetylation of histone H4 lysine during development of in vitro fertilized cloned and parthenogenetically activated bovine embryos. Epigenetics 3, 199-209.

Manipalviratn S, DeCherney A, Segars J. (2009). Imprinting disorders and assisted reproductive technology. Fertil Steril. 91, 305-315.

Market-Velker BA, Fernandes AD, Mann MR. (2010b). Side-by-side comparison of five commercial media systems in a mouse model: suboptimal in vitro culture interferes with imprint maintenance. Biol Reprod. 83, 938-950.

Market-Velker BA, Zhang L, Magri LS, Bonvissuto AC, Mann MR. (2010a). Dual effects of superovulation: loss of maternal and paternal imprinted methylation in dose-dependent manner. Hum Mol Genet. 19, 36-51.

Marques CJ, Carvalho F, Sousa M, Barros A. (2004). Genomic imprinting in disruptive spermatogenesis. Lancet 363, 1700-1702.

McKenzie LJ, Pangas SA, Carson SA, Kovanci E, Cisneros P, Buster JE, Amato P, Matzuk MM. (2004). Human cumulus granulosa cell gene expression: a predictor of fertilization and embryo selection in women undergoing IVF. Hum Reprod. 19, 2869-2874.

Men H, Monson RL, Parrish JJ, Rutledge JJ. (2003). Degeneration of cryopreserved bovine oocytes via apoptosis during subsequent culture. Cryobiology 47, 73-81.

Niu ZH, Shi HJ, Zhang HQ, Zhang AJ, Sun YJ, Feng Y. (2011). Sperm chromatin structure assay results after swim-up are related only to embryo quality but not to fertilization and pregnangy rates following IVF. Asian J Androl. 13, 862-866.

O'Neill C, Li Y, Jin XL. (2012). Survival signaling in the preimplantation embryo. Theriogenology 77, 773-784.

Pacey AA. (2010). Environmental and lifestyle factors associated with sperm DNA damage. Hum Fertil. (camb) 13, 189-193.

Paula-Lopes FF, Hansen PJ. (2002a). Apoptosis is an adaptive response in bovine preimplantation embryos that facilitates survival after heat shock. Biochem Biophys Res Commun. 295, 37-42.

Paula-Lopes FF, Hansen PJ. (2002b). Heath-shock induced apoptosis in preimplantation bovine embryos is a developmentally-regulated phenomenon. Biol Reprod. 66, 1169-1177.

Rechitsky S, Verlinsky O, Chistokhina A, Sharapova T, Ozen S, Masciangelo C, Kuliev A, Verlinsky Y. (2002). Preimplantation genetic diagnosis for cancer predisposition. Reprod Biomed Online 5, 148-155.

Rienzi L, Vajta G, Ubaldi F. (2011). New culture devices in ART. Placenta 32 Suppl 3, S248-251.

Rizzuto R, Marchi s, Bonora M, Aguiari P, Bononi A, De Stefani D, Giorgi C, Leo S, Rimessi A, Siviero R, Zecchini S, Pinton P. (2009). Ca^{2+} transfer from the ER to mitochondria: when how and why. Biochim Biophys Acta 1787, 1342-1351.

Roth Z, Hansen PJ. (2004). Involvement of apoptosis in disruption of oocyte competence by heat shock in cattle. Biol Reprod. 71, 1898-1906.

Rubio C, Rodrigo L, Mercader A, Mateu E, Buendía P, Pehlivan T, Viloria T, De los Santos MJ, Simón C, Remohí J, Pellicer A. (2007). Impact of chromosomal abnormalities on preimplantation embryo development. Prenat Diagn. 27, 748-756.

Said TM, Agarwal A, Zborowski M, Grunewald S, Glander HJ, Paasch U. (2008). Utility of magnetic cell separation as a molecular sperm preparation technique. J Androl. 29, 134-142.

Said TM, Land JA. (2011). Effects of advanced selection methods on sperm quality and ART outcome: a systematic review. Hum Reprod Update 17, 719-733.

Sakkas D, Seli E, Bizzaro D, Manicardi GC, Jakab A, Huszar G. Safety of sperm for use in intra-cytoplasmic sperm injection. In: Anderson D, Brinkworth MH (eds), Male-Mediated Developmental Toxicity, vol 1, 1st ed. Cambridge: RSC Publishing; 2007: 85-93.

Seli E, Botros L, Sakkas D, Burns DH. (2008). Noninvasive metabolomic profiling of embryo culture media using proton nuclear magnetic resonance correlates with reproductive potential of embryos in women undergoing in vitro fertilization. Fertil Steril. 90, 2183-2189.

Seli E, Sakkas D, Scott R, Kwok SC, Rosendahl SM, Burns DH. (2007). Noninvasive metabolomic profiling of embryo culture media using Raman and near-infrared spectroscopy correlates with reproductive potential of embryos in women undergoing in vitro fertilization. Fertil Steril. 88, 1350-1370.

Smiraldo PG, Gruver AM, Osborn JC, Pittman DL. (2005). Extensive chromosomal instability in Rad51d-deficient mouse cells. Cancer Res. 65, 2089-2096.

Soto P, Natzke RP, Hansen PJ. (2003). Actions of tumor necrosis factor-á on oocyte maturation and embryonic development in cattle. Am J Reprod Immunol. 50, 380-388.

Soto P, Smith LC. (2009). BH4 peptide derived from Bcl-xL and Bax-inhibitor peptide suppresses apoptotic mitochondrial changes in heat stressed bovine oocytes. Mol Reprod Dev. 76, 637-646.

Spano M, Seli E, Bizzaro D, Manicardi GC, Sakkas D. (2005). The significance of sperm nuclear DNA strand breaks on reproductive outcome. Curr Opin Obstet Gynecol. 17, 255-260.

Tamburrino L, Marchiani S, Montoya M, Elia Marino F, Natali I, Cambi M, Forti G, Baldi E, Muratori M. (2012). Mechanisms and clinical correlates of sperm DNA damage. Asian J Androl. 14, 24-31.

Tian L, Peng G, Parrant JM, Leventaki V, Drakos E, Zhang Q, Parker-Thornburg J, Shackleford TJ, Dai H, Lin SY, Lozano G, Rassidakis GZ, Claret FX. (2010).

Essential roles of Jab1 in cell survival, spontaneous DNA damage and DNA repair. Oncogene 29, 6125-6137.

Toyoshima M. (2009). Analysis of p53 dependent damage response in sperm-irradiated mouse embryos. J Radiat Res. 50, 11-17.

Van Montfoort AT, Geraedts JP, Dumoulin JC, Stassen AP, Evers JL, Ayoubi TA. (2008). Differential gene expression in cumulus cells as a prognostic indicator of embryo viability: a microarray analysis. Mol Hum Reprod. 14, 157-168.

Virro MR, Larson-Cook KL, Evenson DP. (2004). Sperm chromatin structure assay (SCSA) parameters are related to fertilization, blastocyst development, and ongoing pregnancy in in vitro fertilization and intracytoplasmic sperm injection cycles. Fertil Steril. 81, 1289-1295.

Wright VC, Chang J, Jeng G, Macaluso M. (2005). Assisted reproductive technology surveillance-United States, 2005. MMWR Surveill Summ. 57, 1-23.

Wu X, Li Y, Xue L, Wang L, yue Y, Li K, Bou S, Li GP, Yu H. (2011). Multiple histone site epigenetic modifications in nuclear transfer, in vitro fertilized bovine embryos. Zygote 19, 31-45.

Wyrobek AJ, Schmid TE, Bishop J, Marchetti F. Advances in the direct measurements of partial chromosomal duplication, deletions and breaks in human and murine sperm by sperm FISH In: Anderson D, Brinkworth MH (eds), Male-Mediated Developmental Toxicity, vol 1, 1st ed. Cambridge: RSC Publishing; 2007: 210-223.

Yamauchi Y, Riel JM, Ward MA. (2012). Paternal DNA damage resulting from various sperm treatments persists after fertilization and is similar before and after DNA replication. J Androl. 33, 229-238.

Yan LY, Qiao J, Chen Y, Huang J, Liu P, Sun QY. (2009). Application of three-dimensional fluorescence in situ hybridization to human preimplantation genetic diagnosis. Fertil Steril. 92, 1492-1495.

Zhang X, Trokoudes KM, Pavlides C. (2009). Vitrification of biopsied embryos at cleavage, morula and blastocyst stage. Reprod Biomed Online 19, 526-531.

Zhang XP, Liu F, Wang W. (2011). Two-phase dynamics of p53 in the DNA damage response. Proc Natl Acad Sci U S A 108, 8990-8995.

Zhang XY, Ata B, Son WY, Buckett WM, Tan SL, Ao A. (2010). Chromosome abnormality rates in human embryos obtained from in-vitro maturation and IVF treatment cycles. Reprod Biomed Online 21, 552-559.